FTD-HT-23-95-68

FOREIGN TECHNOLOGY DIVISION

HYDROGEN BRITTLENESS IN NONFERROUS METALS

by

B. A. Kolachev

FTD-HT-23-95-68

EDITED TRANSLATION

HYDROGEN BRITTLENESS IN NONFERROUS METALS

By: B. A. Kolachev

Translated under: Contract F33657-68-D-0865

THIS TRANSLATION IS A RENDITION OF THE ORIGINAL FOREIGN TEXT WITHOUT ANY ANALYTICAL OR EDITORIAL COMMENT. STATEMENTS OR THEORIES ADVOCATED OR IMPLIED ARE THOSE OF THE SOURCE AND DO NOT NECESSARILY REFLECT THE POSITION OR OPINION OF THE FOREIGN TECHNOLOGY DIVISION.	PREPARED BY: TRANSLATION DIVISION FOREIGN TECHNOLOGY DIVISION WP-AFB, OHIO.

FTD-HT-23-95-68

Date 19 68

B. A. Kolachev

VODORODNAYA KHRUPKOST' TSVETNYKH METALLOV

Izdatel'stvo "Metallurgiya"
Moskva 1966

256 pages

DATA HANDLING PAGE

01-ACCESSION NO.	09-DOCUMENT LOC	20-TOPIC TAGS
TM8001318		brittleness, solid mechanical property, titanium alloy

04-TITLE HYDROGEN BRITTLENESS IN NONFERROUS METALS

47-SUBJECT AREA
11

42-AUTHOR/CO-AUTHORS KOLACHEV, B. A.

10-DATE OF INFO -----66

43-SOURCE VODORODNAYA KHRUPKOST' TSVETNYKH METALLOV. MOSCOW, IZD-VO METALLURGIYA (RUSSIAN)

09-DOCUMENT NO. FTD-HT-23-95-68

08-PROJECT NO. 72301-78

63-SECURITY AND DOWNGRADING INFORMATION	64-CONTROL MARKINGS	97-HEADER CLASN
UNCL, 0	NONE	UNCL

76-REEL/FRAME NO.	77-SUPERSEDES	78-CHANGES	40-GEOGRAPHICAL AREA	NO. OF PAGES
1886 0308			UR	239

CONTRACT NO.	I REP ACC. NO.	PUBLISHING DATE	TYPE PRODUCT	REVISION FREQ
F33657-68-D-0865	65-AM6026330	94-00	Translation	NONE

SUBJ CODE 02-UR/0000/66/000/000/0001/0256

ACCESSION NO.

ABSTRACT This book is intended for use by metallurgists, technologists and engineers as well as by students doing advanced or graduate work. The book is devoted to problems concerning the interaction of hydrogen with metals, and the harmful effects this has on the properties of the metal. Considerable attention is given to processes that take place during the hydrogen-metal interaction, the state of hydrogen in liquid and solid solution, and the interaction of hydrogen with dislocations and other structural imperfections of metals. The effect of hydrogen on the structure and properties of the following metals are discussed: Be, Mg, Al, U, Ti, Zr, V, Nb, Ta, Cr, Mo. W. Fe, Cu, Ag, Au. Special attention is devoted to the hydrogen brittleness of Ti alloys.

TABLE OF CONTENTS [Abridged]:

1. Introduction 1

Part One. Interaction of Metals with Hydrogen and Structural Peculiarities of Metal-Hydrogen Systems

Chapter 1. General Relationships in the Interaction of Metals with Hydrogen..... 3

Chapter 2. The sState of Hydrogen in Metals 14

Part Two. General Problems of the Influence of Hydrogen on the Mechanical Properties of Metals

Chapter 1. Classification of Types of Hydrogen Brittleness in Metals 38

Chapter 2. Hydrogen Brittleness of the First Kind... 41

Chapter 3. Hydrogen Brittleness of the Second Kind...55

Chapter 4. Influence of Hydrogen on Creep, Fatigue Strength, and Weldability 109

Part Three. Influence of Hydrogen on the Structure and Properties of Metals and Their Alloys

Chapter 1. Beryllium, Magnesium, and Aluminum 115

Chapter 2. Uranium.....135

Chapter 3. Titanium and its Alloys 136

Chapter 4. Zirconium and its Alloys 173

Chapter 5. Vanadium, Niobium, and Tantalum 183

Chapter 6. Chromium, Molybdenum and Tungsten.....198

Chapter 7. Nickel, Palladium and Platinum.....203

Chapter 8. Copper, Silver and Gold 209

References 214

TABLE OF CONTENTS

Foreword 1

Part One. Interaction of Metals with Hydrogen and Structural Peculiarities of Metal-Hydrogen Systems

Chapter 1. General Relationships in the Interaction of Metals with Hydrogen 3

1. Diffusion of Hydrogen in Metals 3
2. Absorption of Hydrogen by Metals 5
3. Metal-Gas Diagrams of State 8
4. Sources of Hydrogenation 10

Chapter 2. The State of Hydrogen in Metals 14

1. The State of Hydrogen in Metallic Solid Solutions 14
2. Interaction of Hydrogen with Defects in the Crystalline Structure of Metals 17
3. Experimental Data on the Interaction of Hydrogen with Imperfections in the Crystal Structure of Metals 21
4. Adsorption of Hydrogen on Internal Interfaces 28
5. Chemical Nature of the Phases Formed on Interaction of Metals with Hydrogen 30
6. Peculiarities of the Interaction of Hydrogen with Heterophase Alloys 34

Part Two. General Problems of the Influence of Hydrogen on the Mechanical Properties of Metals

Chapter 1. Classification of Types of Hydrogen Brittleness in Metals 38

Chapter 2. Hydrogen Brittleness of the First Kind 41

1. Hydrogen Embrittlement of Metals 41
2. Brittleness Due to Molecular Hydrogen 41
3. Hydride Hydrogen Brittleness 48
4. Cold Shortness Due to Dissolved Hydrogen 52

Chapter 3. Hydrogen Brittleness of the Second Kind 55

1. Irreversible Brittleness of the Second Kind 55
2. General Conceptions of the Mechanism of Reversible Hydrogen Brittleness of the Second Kind 58
3. Influence of Hydrogen on Crack Propagation in Metals 64
4. Analysis of Theories of Reversible Hydrogen Brittleness that Have Been Proposed for Metals that Absorb Hydrogen Endothermically 69
5. Analysis of Theories of Reversible Hydrogen Brittleness for Metals that Absorb Hydrogen Exothermically 73
6. Dislocation Theory of Reversible Hydrogen Brittleness of Metals 77

7. General Mechanism of the Influence of Hydrogen on Germination and Propagation of Cracks 89
8. Mechanism of Crack Germination and Propagation in Metals that Absorb Hydrogen Endothermically 94
9. Peculiarities of the Mechanism of Crack Germination and Propagation in Metals that Absorb Hydrogen Exothermically 96
10. Possibility of Reversible Brittleness due to Interstitial Impurities Other Than Hydrogen 98
11. Static Hydrogen Fatigue 100

Chapter 4. Influence of Hydrogen on Creep, Fatigue Strength, and Weldability 109

1. Influence of Hydrogen on the Creep of Metals 109
2. Influence of Hydrogen on the Fatigue Strength of Metals 110
3. Influence of Hydrogen on the Properties of Welded Joints 111

Part Three. Influence of Hydrogen on the Structure and Properties of Metals and Their Alloys

Chapter 1. Beryllium, Magnesium, and Aluminum 115

1. Interaction of Beryllium, Magnesium and Aluminum with Hydrogen 115
2. Influence of Hydrogen on the Properties of Beryllium 121
3. Influence of Hydrogen on the Properties of Magnesium 123
4. Influence of Hydrogen on the Properties of Aluminum 128

Chapter 2. Uranium 135

1. Interaction of Uranium with Hydrogen 135
2. Influence of Hydrogen on the Properties of Uranium 136

Chapter 3. Titanium and its Alloys 136

1. Kinetics of Interaction of Titanium and its Alloys with Hydrogen 141
2. Diagram of State of the Titanium-Hydrogen System 144
3. Influence of Hydrogen on the Structure and Properties of Titanium 147
4. Influence of Alpha-Stabilizers on the Tendency of Titanium to Hydrogen Brittleness 151
5. Influence of Hydrogen on the Structure and Properties of Industrial Alpha-Alloys 152
6. Influence of Beta-Stabilizers on the Tendency of Titanium to Hydrogen Brittleness 155
7. Hydrogen Brittleness of Industrial (Alpha + Beta) Alloys in the Annealed State 159
8. Influence of Heat Treatment on the Hydrogen Brittleness of (Alpha + Beta) Alloys 161
9. Influence of Hydrogen on the Long-Term Strength and Thermal Stability of (Alpha + Beta) Alloys 164
10. Hydrogen Brittleness of the Beta-Alloys 167
11. Maximum Permissible Hydrogen Concentrations in Titanium and its Alloys 171

Chapter 4. Zirconium and its Alloys 173

1. Kinetics of Interaction of Zirconium with Hydrogen 173
2. Diagram of State of the Hydrogen-Zirconium System 174

3. Influence of Hydrogen on the Structure and Properties of Zirconium and its Alloys 176

Chapter 5. Vanadium, Niobium, and Tantalum 183

1. Interaction of Metals of Subgroup VB with Hydrogen 183
2. Influence of Hydrogen on the Properties of Vanadium 187
3. Influence of Hydrogen on the Properties of Niobium 189
4. Hydrogen Brittleness of Vanadium-Niobium Alloys 192
5. Influence of Hydrogen on the Properties of Tantalum 195

Chapter 6. Chromium, Molybdenum and Tungsten 198

1. Interaction of Chromium, Molybdenum and Tungsten with Hydrogen 198
2. Influence of Hydrogen on the Properties of Chromium, Molybdenum and Tungsten 199

Chapter 7. Nickel, Palladium and Platinum 203

1. Interaction of Nickel, Palladium and Platinum with Hydrogen 203
2. Influence of Hydrogen on the Properties of Nickel, Palladium and Platinum 205

Chapter 8. Copper, Silver and Gold 209

1. Interaction of Copper, Silver and Gold with Hydrogen 209
2. Influence of Hydrogen on the Properties of Copper, Silver and Gold 209

References 214

FOREWORD

Hydrogen brittleness of metals has attracted more and more attention in studies conducted in recent years. It has been found that under certain conditions, negligibly small concentrations of hydrogen may result in the formation of cracks in the metal and premature failure of manufactured parts.

This problem has become particularly acute for high-strength steels and a number of new metals and alloys of them that have come to be used in modern engineering.

Many original papers and monographs have been devoted to study of the interaction of metals with hydrogen. In most of the monographs, however, attention is focused on the kinetics of interaction of the metals with hydrogen and the nature of the interaction between the phases that are formed. Only in certain monographs [5-8] are problems of the interaction of metals with hydrogen and the influence of hydrogen on their structure and properties given as much attention. However, the influence of hydrogen on the structure and properties of new metals such as zirconium, niobium and vanadium, and a number of others, is left out of consideration.

The recently published translation of Cottrell's survey article entitled "The Hydrogen Brittleness of Metals" [9] briefly discusses the results of research into the hydrogen brittleness of the new metals. However, this survey does not reflect any of the extensive work done by Soviet researchers on this topic. Cottrell's survey makes no mention of a single steel or a single alloy developed in the USSR. For this reason, practical utilization of the material given in the survey by our designers and production engineers is very difficult.

The present book makes an attempt to generalize recently published periodical literature of a fundamentally important nature on the hydrogen brittleness of the new structural metals: titanium, zirconium, vanadium and niobium. It also presents results obtained in our own investigations.

A striking uniformity is to be observed in the influence exerted by hydrogen on the mechanical properties of metals: without exception, hydrogen lowers plasticity. This consistency relates to certain common structural features of metal-hydrogen systems and the behavior of hydrogen during deformation of the metal. Hence the influence of hydrogen on the properties of metals can be described with certain general principles as a point of departure.

The character assumed by hydrogen brittleness is related to the nature of the phases formed on interaction of the metals with hydrogen and with the changes that occur in the structure of these phases during subsequent heat treatment. For this reason, it is difficult in many cases to foresee how hydrogen brittleness will be manifested in a given metal and project ways to eliminate it. It is therefore natural that Part One of the monograph is devoted to general relationships obtaining in the interaction of hydrogen with metals.

Part Two considers contemporary conceptions of the mechanism of hydrogen brittleness in metals. Particular attention is given the influence of hydrogen on long-term strength, creep, fatigue strength, static fatigue and tracking in welded joints. Finally, Part Three examines the influence of hydrogen on the structure and properties of the individual metals.

The monograph covers all of the basic structural metals except iron and its alloys, the influence of hydrogen on whose structure and properties has been quite exhaustively described in recently published monographs [6, 8]. In the discussion of the general relationships, however, the authors have often turned to data obtained for iron and its alloys in order to establish a more complete picture of the phenomenon as a whole.

Certain errors and omissions may have been admitted in the description and discussion of the data presented in this monograph, and the author will be grateful to readers for pointing them out.

The author expresses his heartfelt gratitude to A.A. Bukhanova, V.S. Lyasotskaya, N.Ya. Gusel'nikov, V.V. Shevchenko, L.N. Zhuravlev, M.A. Vershkov and I.V. Kashkin, who were of great assistance in the conduct of the original experiments and in preparing the manuscript for printing. The author is indebted to V.I. Dobatkin, N.F. Anoshkin, A.A. Alov and A.P. Gudchenko, whose remarks resulted in substantial improvement of the book's content. Particular acknowledgment is due to V.A. Livanov for the friendly assistance that he rendered throughout the entire project.

Part One

INTERACTION OF METALS WITH HYDROGEN AND STRUCTURAL PECULIARITIES OF METAL-HYDROGEN SYSTEMS

Chapter 1

GENERAL RELATIONSHIPS IN THE INTERACTION OF METALS WITH HYDROGEN

1. DIFFUSION OF HYDROGEN IN METALS

Hydrogen interacts to one degree or another with practically all metals. On contact of metals with hydrogen, a thin layer of the adsorbed gas first forms on their surfaces. This superficial or physical adsorption is supplanted by activated adsorption or chemosorption. Activated adsorption is, in turn, a preliminary stage in the diffusion process of hydrogen in metals. During activated adsorption, the hydrogen molecules decompose into atoms, which then diffuse into the interior of the metal. In this case, the displacement of the atoms of the gas in the solid is facilitated considerably.

The atomic nature of hydrogen diffusion in metals has been confirmed experimentally in investigations of diffusion of a mixture of hydrogen with deuterium.

A hypothesis advanced in [81] states that the diffusion of hydrogen in metals depends on the size of the gaps between the positive ions of the metal lattice. If the gaps between the positive ions are larger than the effective diameter of the hydrogen atom, hydrogen diffuses easily in the metal. Such metals include Al, Pb, Pd, Ir, Pt, Mo, Ta, W (α-modification), Zr, Be, Ti, Re and Os. Otherwise, the diffusion of hydrogen is difficult; the metals in this case include Cu, Ag, Au, Li, Na, K, Rb, Cs, Ba, Cr (α-modification). Experimental data do not contradict this hypothesis.

The published data on the diffusion coefficients of hydrogen in metals have been determined basically for rather high temperatures (Table 1). There is almost no information available on the diffusion rates of hydrogen in metals at temperatures around room temperature, except for the iron-hydrogen system. Published data on the diffusion of hydrogen in iron at low temperatures are quite contradictory. The values given for the hydrogen diffusion coefficient at 298°K vary from 10^{-9} to 10^{-5} cm^2/sec. In spite of the contradictory quantitative results, there is one thing that all of these data have in common: below 473°K, the diffusion coefficients of hydrogen in steel are quite far below the values extrapolated from the high-temperature data.

Thus, for example, according to [12], the temperature depend-

TABLE 1

Coefficients of Diffusion of Hydrogen in Metals

Metal	Temperature range °K	D_0 cm²/sec	Q cal/mole	Q j/mole	Literature source
Titanium	773—1073 (α)	$1,8 \cdot 10^{-2}$	12380	51800	[55]
	773—1373 (β)	$1,95 \cdot 10^{-3}$	6640	27800	
	α-phase	$4,8 \cdot 10^{-3}$	10080	42200	[56]
	β-phase	$5,7 \cdot 10^{-3}$	8700	36450	
Zirconium	1143—1383 (β)	$7,37 \cdot 10^{-3}$	8540	35800	[59]
	1033—1283 (β)	$5,32 \cdot 10^{-3}$	8320	34900	[60]
	333—523 (α)	$1,09 \cdot 10^{-3}$	11400	47800	[445]
	578—883 (α)	$0,7 \cdot 10^{-3}$	7100	29700	[69]
Niobium	873—973	0,0215	9370	39300	[338]
Molybdenum	848—1253	0,059	14700	61600	[390]
Uranium	663—903 (α)	$1,4 \cdot 10^{-3}$	8400	26850	[456]
Iron	473—1053	$1,4 \cdot 10^{-3}$	3200	13400	
	298—473	0,12	7820	32750	[451]
	673—1173	0,0022	2900	12150	[446]
	673—1173	0,00076	2300	9640	[447]
	673—1173	0,0012	2900	12150	[448]
	283—373	0,0165	9200	38550	[449]
	293—353	0,011	8740	36600	[449]
	673—1173	0,0017	6800	28500	[450]
	423—1173	0,00089	3050	12780	[448]
	298—1063	0,0014	3200	13400	[451]
	499—966	0,000387	1080	4520	[452]
Nickel	473—823	0,017	10800	45200	[76]
	751—1071	0,0011	8400	35200	[77]
	653—873	0,015	10600	94400	[78]
	358—438	0,002	8700	36450	[79]
	523—673	0,023	10800	45200	[80]
	673—873	0,001	5500	23050	[58]
	653—1259	0,0045	8600	36050	[82]
	673—973	0,0076	9880	41400	[83]
	476—769	0,0107	10125	42500	[84]
	703—1123	0,0095	10300	43100	[85]
	576—969	0,0042	8400	35200	[203]
	1243—1593	0,0055	8920	37900	[427]
Copper		$9,7 \cdot 10^{-4}$	5580	23400	[58]
Aluminum	673—933	$1,2 \cdot 10^{-5}$	33500	140500	[83]
	673—933	0,21	10900	45400	[86]
	633—873	0,11	9780	40700	[17]

ence of the hydrogen diffusion coefficient in α-iron can be expressed by two equations:
above 473°K:

$$D = 1,4 \cdot 10^{-3} \exp\left(-\frac{3200}{RT}\right) \text{ cm}^2/\text{sec},$$

below 473°K:

$$D = 0{,}12 \exp\left(-\frac{7820}{RT}\right) \text{ cm}^2/\text{sec}.$$

It follows from these data that the bond strengths of hydrogen in iron below and above 473°K would appear to be substantially different. It is shown in this same source that work-hardening lowers the diffusion rate of hydrogen in iron.

R.A. Ryabov, P.V. Gel'd, and V.A. Gol'tsov [67] arrived at a similar conclusion in a study of the hydrogen permeability of nickel and manganese steels. They showed that with increasing phase hardening in alloyed austenite, the activation energy of hydrogen diffusion increases. The authors conclude that the metal's lattice defects are, in a sense, traps for hydrogen atoms. The mobility of hydrogen atoms is sharply reduced on an increase in dislocation density and refinement of the mosaic blocks.

A quite commonly held opinion is that diffusion along grain boundaries does not play a substantial role in metal-hydrogen systems. This is explained in terms of ionization of hydrogen in metals to protons, which, possessing very small size, are able to move as easily in the volume of a grain as along its boundaries.

Experimental facts indicate that this law is not always observed. It appears that the influence of the grain boundaries on diffusion becomes stronger the lower the degree of ionization of the hydrogen to protons and the lower the temperature. Thus, for example, the coefficient of diffusion of hydrogen in an iron single crystal is practically the same in the temperature range from 686-1050°K as it is for diffusion in a specimen composed of fine crystals [1]. At 518°K, however, the diffusion coefficient of hydrogen for the iron single crystal is only half the value for the fine-crystalline specimen.

The above is confirmed by data on the reaction kinetics of hydrogen with fine- and coarse-grained titanium [7]. At 973°K, a fine-grained titanium specimen absorbs hydrogen 6 times as rapidly as a coarse-grained specimen. Further considerations in favor of the above hypotheses are given in [13].

2. ABSORPTION OF HYDROGEN BY METALS

A gas that has diffused in some manner into the interior of a metal is distributed among the metal atoms forming the crystal lattice. This phenomenon is known as absorption. The terms "solution" and "occlusion" are used as equivalents to the term "absorption." "Occlusion" is fully consistent with the definition of absorption given above, but "solution," in our opinion, does not quite correspond to the essence of the phenomena that take place as gas penetrates metal.

It would seem to us more correct to use the term "solution" only for processes that result in the formation of liquid and solid solutions of hydrogen in the metal. However, not only solution proper, but also formation of chemical compounds with specific properties in some cases may take place as the gas penetrates into the metal. Thus, for example, on absorption of hydro-

gen by titanium at 573°K, the first to form is a solid solution of hydrogen in α-titanium. When the hydrogen content reaches approximately 0.15% (by mass), the solution of hydrogen in α-titanium has been saturated, and a hydride phase is segregated as more hydrogen is introduced into the metal from the supersaturated solution. As the content rises above the solubility limit, the new hydrogen is not dissolved, but is consumed in formation of the hydride phase. In sum, the total quantity of absorbed hydrogen will be larger than the quantity of dissolved hydrogen.

We distinguish between endothermic and exothermic absorption according to the sign of the heat effect. Endothermic absorption takes place with absorption of heat, and therefore the quantity of absorbed hydrogen increases with increasing temperature. The temperature dependence of the amount C of absorbed hydrogen in these metals is described by the equation

$$C = Ke^{-\frac{Q}{2RT}}, \qquad (1)$$

where Q is the heat of absorption of 1 mole of gas; K is a constant; R is the gas constant; T is the absolute temperature. Taking logarithms, we bring Eq. (1) to the form

$$\ln C = \ln K - \frac{Q}{2RT}$$

and, consequently, it is represented graphically in the coordinates $\ln C$-$(1/T)$ by a straight line from whose slope the heat of absorption Q can easily be found.

The heat of absorption of hydrogen in these metals is positive and quite large in absolute magnitude. In endothermic absorption, the hydrides are not formed in direct reaction of the metal with molecular hydrogen, so that the concepts of "absorption" and "solution" are identical over the entire hydrogen concentration range. At constant temperature, solubility is described as a function of the hydrogen pressure p by the equation

$$C = K\sqrt{p}, \qquad (2)$$

where K is a constant for a given temperature.

This law, which has come to be known as Sieverts' law, is a consequence of dissociation of the hydrogen molecules into atoms during solution: $H_2 \rightleftarrows 2H$. Combination of Eqs. (1) and (2) gives

$$C = ap^{1/2}e^{-\frac{Q}{2RT}}$$

or

$$\ln C = \ln a - \frac{Q}{2RT} + \frac{1}{2}\ln p. \qquad (3)$$

The solubility of hydrogen increases rapidly as these metals go from the solid to the liquid state. A similar but smaller stepwise change in solubility takes place in allotropic transformations. The solubility of hydrogen in liquid metals increases only

up to a certain temperature, and when the temperature is raised further, it decreases, reaching zero at the metal's boiling point [466, 467].

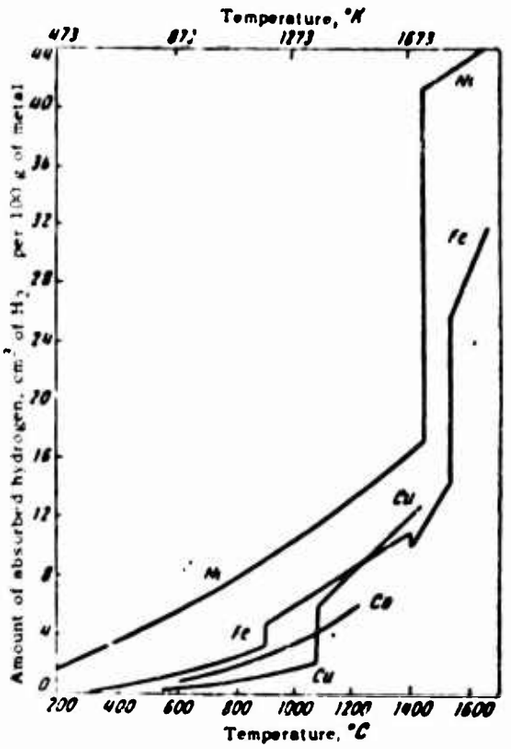

Fig. 1. Hydrogen absorption isobars for nickel, iron, cobalt and copper at 1 atmosphere (0.1 Mn/m^2).

The above-described character of the interaction is dominant in iron, nickel, cobalt, copper, aluminum, platinum, silver, tin and magnesium (Fig. 1).

Exothermic absorption takes place with liberation of heat, and as a result the hydrogen content in the metal at a given pressure decreases with increasing temperature. This kind of hydrogen absorption is observed in palladium, vanadium, tantalum, titanium, zirconium, niobium, cerium, and thorium. Typical hydrogen absorption isobars for certain metals of this group are given in Fig. 2. Hydrides are formed in these systems if the hydrogen concentration is high enough, by its direct interaction with the metals.

Dissociation of the molecules into atoms also precedes hydrogen absorption in these metals, but the amount of absorbed hydrogen in these metals at constant temperature is directly proportional to the square root of pressure only within the limits of solubility of hydrogen in the metal.

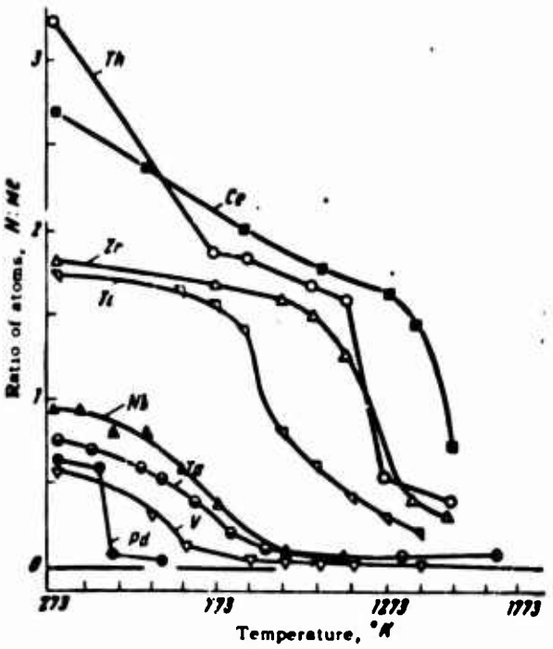

Fig. 2. Hydrogen absorption isobars of palladium, vanadium, niobium, tantalum, titanium, zirconium, cerium and thorium.

3. METAL-GAS DIAGRAMS OF STATE

Like other heterogeneous equilibrium systems, metal-gas systems are subject to the phase rule and can be described by means of diagrams of state, which, however, have a number of specific peculiarities. These arise from the need to take into account the hydrogen pressure in the equilibrium metal-hydrogen system, while the vapor pressure can be disregarded for most metallic systems. Accordingly, the phase rule for metal-hydrogen systems should be used in the form

$$C = K - \Phi + 2,$$

where C is the number of degrees of freedom of the system; K is the number of system components; Φ is the number of phases present at equilibrium.

Metal-hydrogen systems have diagrams of state that are superficially similar to those of metallic systems. However, when these diagrams are used to analyze the state of the system, hydrogen pressure must be taken into account, since the equilibrium concentration of hydrogen in the metal is related to the partial pressure.

It is advisable to indicate hydrogen pressure isobars on the diagrams of state of metal-hydrogen systems, since without them it is difficult to appraise the equilibrium state of the system

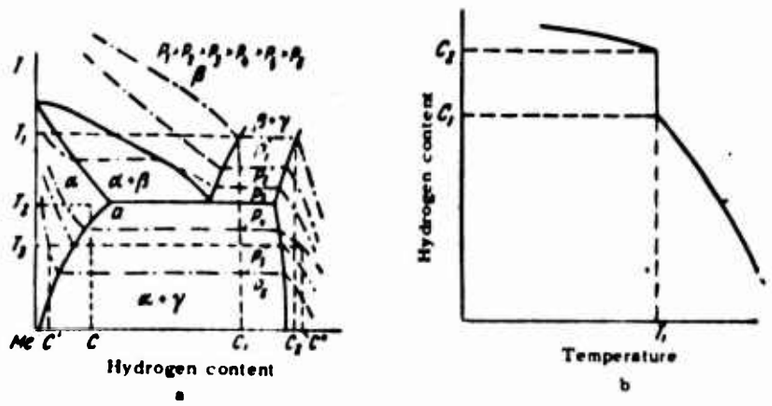

Fig. 3. Scheme of diagram of state of metal-hydrogen system for metals that absorb hydrogen exothermically.

in a given case.

Figure 3a presents a schematic diagram of state of a metal-hydrogen system for the case in which hydrogen stabilizes a high-temperature modification of a metal that absorbs hydrogen exothermically.

Isobars have also been entered on the diagram. For metals that absorb hydrogen exothermically, the temperature at which a given equilibrium pressure p is established diminishes with increasing hydrogen content. If the hydrogen content is sufficient, the single-phase region is replaced by a two-phase region. In this region, the temperature at which a given hydrogen pressure is established remains constant in accordance with the phase rule. On further introduction of hydrogen, the amount of the second phase gradually rises, and, finally, the two-phase region is supplanted by one phase. In this concentration range, the temperature corresponding to a given equilibrium hydrogen pressure decreases as the hydrogen content in the metal rises. Thus the isobars are closely related to the equilibrium metal-hydrogen diagram. This relation is illustrated in Fig. 3b.

Let us see how the equilibrium conditions of the system can be evaluated from the metal-hydrogen diagram of state. Assume that a metal with hydrogen concentration C has been heated to a temperature T_3. At this temperature, the alloy of composition C will have an equilibrium $\alpha + \gamma$ structure only at a fully defined (equilibrium) external hydrogen pressure P_5. If a lower hydrogen pressure P_6 is maintained in the system, hydrogen will be eliminated from the metal until its concentration has been lowered to C'. As a result, the alloy will have acquired a single-phased structure represented by phase α. If a pressure higher than equilibrium, for example, P_4, is maintained in the system, the metal will be saturated with hydrogen until the hydrogen concentration in it reaches the value C''. As a result, the metal will have acquired a single-phase structure represented by phase γ.

In this case, when the metal is heated in a closed space, hydrogen will be driven out of it until the hydrogen concentration in the metal and its pressure in the system correspond to equilibrium conditions. Naturally, these conditions depend not only on temperature, but also on the volume of the system.

Thus, it is a considerably more complex task to determine the phase composition of a hydrogen-saturated metal from the metal-hydrogen diagram of state than it is for metallic systems. It must be noted, however, that for metals that absorb hydrogen exothermically, such as titanium and zirconium, the equilibrium hydrogen pressure at temperatures around room temperature and lower is negligibly small, and the diffusion of the hydrogen takes place slowly. Hence the hydrogen-concentration change in such metals with time can be disregarded, and the metal-hydrogen state diagram can be used to determine the phase composition of the alloys at low temperatures, just as for metallic systems.

4. SOURCES OF HYDROGENATION

Hydrogen can penetrate into metals during casting of ingots, pressworking, heat treatment, welding, etching, application of electrolytic coatings, and during the use of finished products.

On extraction from their ores, many metals (titanium, zirconium, high-melting metals) are obtained in the form of a powder or sponge with a highly developed surface, which adsorbs large quantities of gases, including hydrogen and water vapor. During smelting, hydrogen is transferred from the powder or sponge into the ingot, and this process even takes place during vacuum remelting, although to a lesser degree. Naturally, the better the vacuum, the greater the percentage of the hydrogen that will be eliminated from the smelter and the smaller the amount that will transfer into the metal.

Water vapor that has been adsorbed by the sponge and moisture that has entered the furnace when it is charged, react with the metal to form oxides on its surface or solutions of oxygen in the surface layer and hydrogen distributed between the gaseous phase and the metal in accordance with Sieverts' law.

At temperatures below 1500-2000°K, when thermal decomposition of water vapor does not take place to any marked degree, contamination of metals by hydrogen is a result of reduction or dissociation of water vapor on the surface of the metal. The net reaction of water vapor with the metal can be described by the following scheme:

$$Me + H_2O \rightarrow Me_nO_m + [H]_{Me} + H_2,$$

where $[H]_{Me}$ is hydrogen dissolved in the metal.

The temperature beginning at which this reaction takes place to an appreciable degree depends on the nature of the metal and the atmosphere. The more developed the surface of the metal, the lower will be the temperature at which chemical reaction begins between the metal and water vapor. Thus, for example, compact ti-

tanium acts with water vapor only above 873°K, while titanium sponge begins to decompose the vapor above 623°K. As a rule, liquid metals decompose water vapor and are contaminated by the hydrogen formed on this decomposition.

In the general case, hydrogen is distributed nonuniformly in metals. This nonuniformity results not from zone liquation, as it might seem at first glance, but from thermal segregation of hydrogen. The diffusion rate of hydrogen is so high at high temperatures that neither zone nor intradendritic liquation of hydrogen can occur.

Hydrogen segregation arises during slow cooling of the ingot after freezing. The surface layers of the ingot cool more rapidly than its center. In metals that absorb hydrogen endothermically, the solubility of the hydrogen decreases with decreasing temperature, so that the hydrogen will have a tendency to escape from the cooler surface layers into the hotter core. The reverse is observed for metals that absorb hydrogen exothermically.

During arc smelting in an inert-gas atmosphere, the average hydrogen content does not change, but there is a marked redistribution of the hydrogen due to the variation of its solubility with temperature. In the case of exothermic absorption, hydrogen moves from hot to cold zones during the melting process. In melting with a consumable electrode, hydrogen will transfer from the lower, hotter part of the electrode to its top, and the concentration at the top of the electrode will rise. The result will be an ingot with hydrogen content varying along its length, higher at the beginning and lower at the end.

In vacuum arc melting of metals with a consumable electrode, the hydrogen content should be uniform over the length of the ingot once the process has been stabilized. However, the bottom of the ingot will be more heavily contaminated by hydrogen, since the water vapor adsorbed by the inner walls of the furnace will be liberated at the beginning of melting. In ingots of metals that absorb hydrogen exothermically, the top of the ingot is also enriched in it when the arc is extinguished and the cooling metal acts as a getter.

The above-described nonuniformity in the distribution of hydrogen in ingots obtained by arc melting will be reversed for endothermic hydrogen absorption.

Hydrogenation also takes place during heating for pressworking and during heat treatment. This hydrogenation is promoted by water vapor, reducing atmospheres, and the presence of atomic hydrogen, which is formed on quenching in water. For metals that absorb hydrogen exothermically, prolonged heating before pressworking, prolonged high-temperature heat treatment, and slow cooling tend to promote hydrogenation.

The least hydrogen contamination is observed on heating in electric furnaces, in which an oxidizing atmosphere is inevitably established. During heating in a fuel-oil-fired furnace, hydrogen saturation takes place more rapidly than in an electric furnace,

even with an oxidizing atmosphere. Reducing atmospheres are totally inadmissible during heating of metals that absorb hydrogen exothermically. The metal must be protected from direct contact with the furnace flame and combustion products, particularly when steam is used to atomize the fuel.

Metals are even more heavily contaminated with hydrogen during heating in gas-fired furnaces. However, experience gained under industrial conditions indicates that heating takes place more rapidly in the gas furnace than in the electric or fuel-oil-fired furnace because of the high heating ability of the gas. Hence the time to heat ingots is shortened substantially. Shortening the holding times and lowering the heating temperature, measures that lower the rate of diffusion of hydrogen in the metal, make it possible to hold the hydrogen content in the products below the maximum permissible limit provided that its content in the original ingot was low enough.

To lower the hydrogen content in the metal, it is also recommended that heating for pressworking or high-temperature heat treatment be conducted in an inert-gas atmosphere. Even nitrogen can be used as such an inert environment for titanium and its alloys.

If the hydrogen content exceeds the maximum permissible value, vacuum annealing is used. Titanium and its alloys are vacuum-annealed at temperatures of 973-1073°K at a pressure of 10^{-4} mm Hg (0.013 n/m^2) [7]. The optimum temperature range for niobium is 1973-2273°K at the same pressure [51]. It must be noted, however, that vacuum annealing is not the most efficient of countering hydrogen embrittlement. Firstly, it is an expensive operation, since it requires expensive equipment. Secondly, a decrease in the plasticity of vacuum-annealed metals has been observed in a number of cases during the process of aging at room temperature. Metals that have been vacuum-annealed have highly active surfaces and absorb hydrogen from water vapor even at room temperature, with the result that a thin brittle layer forms on the surfaces of products.

The most expedient way to secure a low hydrogen content is to adjust the process of extracting the sponge, smelting the metal, and treating it with this goal in mind, rather than using vacuum annealing.

The state of affairs described above is typical for all metals that absorb hydrogen exothermically. The picture observed for metals that absorb hydrogen endothermically, in which solubility decreases with temperature, is less clear-cut. It appears that under the conditions being considered, such metals may be hydrogenated even if the hydrogen content in the cast metal is very low. If the hydrogen content exceeds the solubility limit under pressworking or heat-treatment conditions, the hydrogen is driven out. It is eliminated first from the surface layers of the ingot; concurrently with this process, the hydrogen content is diffusion-equalized through the cross section of the ingot. As a final result, the average hydrogen content in forgings is lower than in the melt. Removal of hydrogen is more complete if cooling

is slow. Heat-treatment formulas can be worked out for such metals to lower hydrogen content effectively in the products and thereby eliminate hydrogen brittleness.

Metals are also hydrogenated during welding, due to hygroscopic moisture and the water of crystallization present in electrode coatings and fluxes [26, 28, 46, 142]. Such high-temperature-active metals as titanium and zirconium are arc-welded in an atmosphere of protective inert gases – helium and argon – or under a special oxygen-free flux [47, 48]. To prevent hydrogenation during welding, even the inert gases and oxygen-free fluxes must be purified of moisture quite thoroughly. The electrodes or rod material (in welding with nonmelting electrode) must contain the smallest possible amount of hydrogen. Hydrogen content must also be minimized in weldable titanium workpieces.

Hydrogen can also enter the metal from the etchants used to improve sheet surface quality and eliminate a surface layer contaminated by gaseous impurities. Thus, it has been observed that the acids that dissolve titanium (hydrofluoric, hydrochloric, sulfuric, phosphoric) cause severe hydrogenation of titanium and thus give rise to hydrogen brittleness. To prevent hydrogenation, oxidizers that bind the atomic hydrogen liberated during etching must be added to the etching solution. Thus, the addition of 10% nitric acid to hydrofluoric solution reduces the amount of hydrogen adsorbed by titanium by a factor of ten.

Quite often, metals that are inert to hydrogen on direct exposure to it in molecular form absorb it well in an electrochemical reaction at the cathode. Electrolytically deposited metals always contain considerable quantities of hydrogen. Chromium, manganese, iron, nickel, cobalt, and palladium absorb particularly large amounts of hydrogen during electroplating.

And, finally, hydrogenation may occur during use of finished products under exposure to steam or a humid atmosphere, in the synthesis of various types of hydrocarbons, in the hydrogenation of petroleum products, and so forth. Some of the related problems (for example, hydrogen embrittlement and hydrogen corrosion) will be examined below.

Chapter 2

THE STATE OF HYDROGEN IN METALS

Hydrogen that has been absorbed by a metal may be present in it in various states:

a) dissolved in the metal;

b) segregated on crystal-structure defects;

c) adsorbed on the surfaces of microcavities and second-phase particles;

d) accumulated in microcavities in molecular form;

e) having formed hydrides with the basic metal;

f) reacting with second phases.

Which of the above states, and, very often, which states predominate depends on the nature of the metal. These states are not independent; dynamic equilibrium obtains between them. Thus, for example, the equilibrium between hydrogen in solid solution and molecular hydrogen in microcavities is determined by the Sieverts equation.

1. THE STATE OF HYDROGEN IN METALLIC SOLID SOLUTIONS

Hydrogen is at least partially ionized in a metal. Ionization of the hydrogen may be of various kinds and culminates in extreme cases in the formation of either a positively charged ion, a proton, or a negatively charged H^- ion.

Ionization of the hydrogen atom to the negative H^- ion takes place on its reaction with alkali and alkaline-earth elements. In other metals, hydrogen is at least partially ionized to the proton, yielding its electron to the shared electron gas. The idea that the hydrogen atom is ionized on solution in metals to the proton was first advanced by I.A. Krasnikov [15]. Subsequently, he confirmed this hypothesis experimentally for elements of the first long period from manganese to zinc [16]. The positive hydrogen ion has no affinity to any of the ions of other elements, and the aggregate of protons in a metal is called a proton gas, by analogy with the electron gas.

Recently, conceptions of the ionization of hydrogen to the proton in metals have undergone certain modifications [6, 12, 23].

A free proton could hardly exist in an aggregate comprising an enormous number of electrons; it is partially screened by electrons, with the result that a kind of electron shell is formed. This shell is not a single-electron cloud, like that on the free hydrogen atom, but a kind of aggregation of external electrons that are entrained by the proton as it moves in the metal.

The radii of interstices for various metals and the radius of the hydrogen electron cloud were calculated in [81]. The electron-cloud radius of hydrogen was calculated by the Thomas-Fermi method. The radius at which the electrons fully screen the charge of the proton was taken as the limit of the hydrogen electron shell. The dimensions r_1 and r_2 of the interstitial spaces and the average value of the hydrogen electron shell radius are listed in Table 2.

Some (if not all) of the electron-screened protons are apparently positioned in interstices. In this case, in accordance with the principle of minimum free energy, they should be at the interstices that conform most closely to their size. Values of the degree of nonconformity between the effective diameter of the hydrogen and the interstice that it will occupy with the greatest probability, $\varepsilon = \frac{r_{1,2} - r_{cp}}{r_{1,2}}$, are given in Table 2.

Positive ionization of hydrogen in metals has been demonstrated by direct experiment for a number of metal-hydrogen systems by V.N. Yavoyskiy and G.N. Batalin [18]. They found that in molten metals (aluminum, copper, low-carbon steel, YalT), hydrogen is displaced toward the negative pole under the influence of even a relatively weak constant electric field. V.N. Yavoyskiy and D.F. Chernegi [19] showed that in steels, hydrogen is displaced toward the cathode even in the solid state.

TABLE 2

Dimensions of Interstitial Spaces and Effective Radius of Hydrogen Ion

Element	r_1 Å	r_2 Å	r_{cp} Å	ε	Element	r_1 Å	r_2 Å	r_{cp} Å	ε
Be	0,977	1,272	0,845	—	Cu	0,58	0,822	1,118	0,36
Mg	1,11	1,523	1,162	0,047	α-Zr	1,047	1,465	0,954	—0,089
Al	1,18	1,451	0,942	—0,202	β-Zr	0,988	1,2	0,954	—0,0344
α-Ti	1,065	1,455	0,859	—0,193	Mo	1,06	1,262	0,72	—0,322
V	1,108	1,285	0,759	—0,31	Pd	1,037	1,297	0,818	—0,21
α-Cr	0,799	0,968	0,835	—	Ag	0,632	0,905	1,241	0,372
β-Cr	0,932	1,284	0,850	—	Ta	0,912	1,097	0,811	—0,11
α-Fe	0,821	0,996	0,823	0,0025	α-W	0,928	1,114	0,720	—0,224
γ-Fe	0,903	1,147	0,819	—0,093	Pt	1,019	1,276	0,818	—0,197
Ni	0,778	1,013	0,918	0,0935	Au	0,386	0,66	1,145	0,735

A similar phenomenon was observed in solutions of hydrogen in palladium [20].

Data recently obtained indicate impressively that both positive and negative hydrogen ions coexist in metals. After passage of direct current through a steel rod 8 mm in diameter and 400 mm long for 100 hours, Yu.A. Klyachko, T.A. Izmanova and L.L. Kunin [24] observed an elevated hydrogen content in the cathodic and anodic zones of the rod. Consequently, hydrogen may be displaced in the solid not only toward the cathode, but also toward the anode. The existence of positive and negative ions in solid and liquid steel has also been demonstrated experimentally by V.I. Lakomskiy [14].

Directional migration of hydrogen in metals is observed not only on application of an electric field, but also when there is a temperature gradient or a stressed state in the lattice. Redistribution of protons can apparently also take place between two zones of differing chemical composition, either in the case of a liquational inhomogeneity in a solid solution or for two phases with different compositions.

The degree of ionization of the hydrogen in a metal is a highly essential factor in determining the nature of the metal-gas system. However, there are very few experimental data available in this connection. Quantitative data on the degree of ionization of hydrogen have been obtained only for palladium.

Duhm [431], measuring the mobility of hydrogen atoms in palladium in the presence of a steady electric field and the hydrogen diffusion coefficient, found that the effective charge on the hydrogen ion ranges 1/500 to 1/600 of an elementary charge, i.e., that the proton is almost completely screened by electrons of the metal.

Ubbelohde [432] came to the conclusion that the degree of ionization of hydrogen in palladium does not exceed 90%. The data of Wagner and Heller [11], who studied electrotransfer in dilute solutions of hydrogen in palladium and found that the effective charge of the protons was +0.5 e, are considered most reliable.

In conclusion, we should discuss certain terminological problems related to the structural peculiarities of metal-hydrogen systems. In the opinion of certain investigators [2, 4, 8], solid solutions of hydrogen in a number of metals have such a unique structure that the term "solid solution" is totally inapplicable to metal-hydrogen systems in the ordinary sense.

Thus, for example, N.A. Galaktionova [4] indicates that for a whole series of systems (for example, hydrogen-iron, hydrogen-nickel and others), the concept of the solid solution in the generally accepted sense is totally inapplicable, since the hydrogen, which is present in substantial quantities and exerts a marked influence on the properties of the metal, is present in atomic form neither at lattice points nor in interstices, where it would have to be if the system were a substitutional or interstitial solid solution. A similar view is taken by G.V. Karpenko and R.I. Krip-

yakevich [8].

It seems to us that two concepts have been confused in the above cases: that of the solid solution and that of the type of solid solution. A solid solution means phases in which the proportions of the components can change without affecting its homogeneity. Now do solutions of hydrogen in metals conform to this definition? Definitely, yes! The crystal lattice of the metals and their metallic properties are preserved on solution of hydrogen in metals within the homogeneity range.

The other question is to what type do solid solutions of hydrogen in metals belong? Actually, the concept of the interstitial solid solution would hardly be useful for description of solutions of hydrogen in metals if the hydrogen is ionized to the proton.

Smith [2], N.A. Galaktionova [4], G.V. Karpenko and R.I. Kripyakevich [8] found a way out of the dilemma by negating the existence of solid solutions of hydrogen in metals for this case. It appears to us to be more logical to retain the solid-solution concept, but since it differs in structure from interstitial and substitutional solid solutions, it should be classified as a new type of solid solution, for example, the proton solid solution.

2. INTERACTION OF HYDROGEN WITH DEFECTS IN THE CRYSTALLINE STRUCTURE OF METALS

Various types of interactions may take place between dissolved hydrogen atoms and dislocations in the general case: elastic, electrical and chemical.

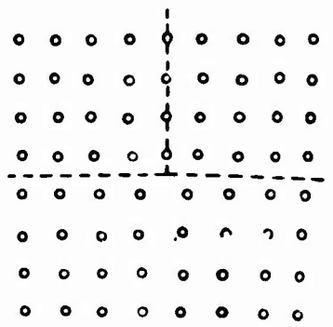

Fig. 4. Diagram of crystal lattice of a metal in section perpendicular to line of dislocation.

The elastic interaction is governed by the presence of a field of elastic stresses around the dissolved atom and around the dislocation. The nature of this interaction can be explained as follows with reference to the example of a positive edge dislocation (Fig. 4). In the part of the crystal above the dislocation, the interatomic distances are smaller than equilibrium, i.e., this zone of the lattice is compressed and displaces interstitial atoms into zones in which the interstitial spaces are larger. In the part of the crystal below the dislocation, the interatomic distances are greater than equilibrium, i.e., the lattice is expanded in this region. If interstitial atoms diffuse into this region, the elastic stresses are to some extent relieved and the energy of the crystal is lowered.

These considerations lead us to the conclusion that elements that form interstitial solid solutions must be concentrated below dislocations. This kind of accumulation of solute atoms around a dislocation has come to be known as an impurity cloud (atmosphere)

or Cottrell cloud (atmosphere).

Cottrell and Bilby [27] showed that in an interstitial solid solution, the maximum energy of elastic interaction of impurity atoms U_0 with edge dislocations is determined by the equation

$$U_0 = -\frac{A}{d}, \qquad (4)$$

where d is the effective width of the dislocation.

For interstitial impurities, the coefficient A is defined by the relation

$$A = -4Gb\varepsilon r_0^3, \qquad (5)$$

where G is the shear modulus; b is the Burgers vector; r_0 is the radius of the largest rigid sphere that does not cause volume distortions on introduction into the interstice; ε is the relative difference between the radius r_1 of the impurity atom and the radius r_0, defined as $\frac{r_1 - r_0}{r_0}$.

At high enough temperatures, the Cottrell atmosphere is thermodynamically unstable, and the concentration of impurity atoms is the same throughout the volume of the metal. As the temperature is lowered, the impurity atoms begin to draw toward the dislocations.

At a temperature below T_K, the impurity atmospheres become saturated; at this point, the interstitial atoms occupy all possible positions below the dislocation line, so that the free volume below the dislocation is utilized to the maximum. The saturation temperature T_K of the Cottrell atmosphere is determined by the equation

$$T_K = \frac{U_0}{k \ln 1/C_0}, \qquad (6)$$

where C_0 is the average impurity concentration in the metal.

In the case of Cottrell-atmosphere saturation, an interstitial impurity atom will be found below each atom of the basic metal lying on the dislocation line. If the interaction energy is large enough, several rows of impurity atoms may be formed along the dislocation line. The temperature of impurity saturation of the Cottrell atmospheres rises with increasing bonding energy and concentration of the impurities.

If hydrogen is ionized to the proton in metals, we should hardly expect a substantial energy of elastic interaction of hydrogen atoms with dislocations. However, this energy should increase with diminishing degree of ionization of the hydrogen atom and reach values of the order of 0.1 ev for the unionized hydrogen atom. The energy of interaction should be even larger for the negatively ionized atom. As a result of quantitative estimates of

the elastic-interaction energy between hydrogen atoms and dislocations by the equations given above, with consideration of the effective radii of the hydrogen ions according to [81], we obtain values of 0.055, 0.0055 and 0.375 ev for magnesium, iron and nickel, respectively. We have assumed in the calculations that the hydrogen is located in interstices whose dimensions are closest to the radius of the proton electron shell.

In many transition metals, the dimensions of the interstitial spaces are larger than the diameter of the hydrogen atom. As a result, the nonconformity $\varepsilon = \frac{r_{i.s} - r_0}{r_0}$ between the impurity and metal atoms is found to be negative. This means that the hydrogen atoms will tend to locate not in the expanded part of the crystal, but in the compressed part. The interesting ideas developed by Yu.V. Grdina [34] are applicable in this case. He assumes that a cloud of hydrogen atoms (protons) forms in the compressed part. Inside the cloud, the forces drawing the atoms toward dislocations are offset by pressure forces, which create forces of repulsion between hydrogen atoms. Analyzing this model, Yu.V. Grdina arrives at the conclusion that the hydrogen atmosphere takes the form of a cylinder of radius $R_a = \frac{A \sin \alpha}{3\,kT}$ along the dislocation with an average hydrogen atom concentration in the atmosphere four times the average concentration in the volume of the metal. According to the proposed model, the radius of the hydrogen atmosphere should diminish with temperature. When its radius becomes smaller than the interatomic distance d, the atmosphere ceases to exist for all practical purposes. This critical temperature is determined by the equation

$$T_{кр} = \frac{A}{3kd}. \qquad (7)$$

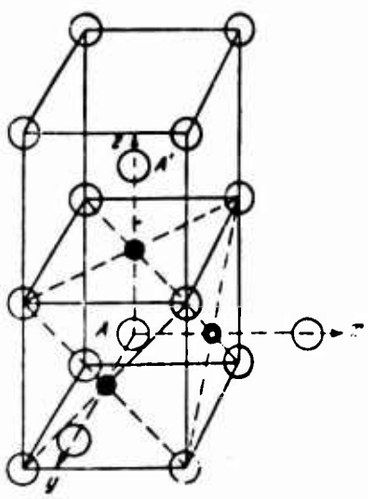

Fig. 5. Interstitial octahedral spaces in body-centered cubic lattice.

In an analysis of internal friction in iron, Snoek [33] proposed another possible mechanism for the interaction of impurity atoms with dislocations. The interstitial spaces are nonsymmetrical in metals with a body-centered structure (Fig. 5). The distances between atoms situated at the centers (A-A') of elementary cells are smaller than the distances between atoms in the baselines. Hence an interstitial atom in an octahedral space creates tetragonal distortions, with the result that interaction arises between interstitial atoms and dislocations. As a result of this interaction, the interstitial atoms are arranged in an orderly fashion around the dislocation, occupying those interstices that ensure the lowest free energy in the dislocation field. This ordered arrangement of the interstitial atoms has come to be known as the Snoek atmosphere.

Suzuki [32] showed that chemical interaction may occur between dislocations and impurity atoms in metals with face-centered crystal structures. In these metals, the dislocations usually split into partial dislocations with a packing defect between them. The atomic layers forming the packing defect have hexagonal rather than cubic structure. In metals with hexagonal close-packed structure, the dislocations also split into subdislocations separated by a lattice defect having a cubic structure.

Impurity atoms may have different solubilities inside the packing defect and outside of it. The dimensions and shape of the interstitial spaces are the same in hexagonal dense-packed and face-centered cubic lattices, so that the solubility difference is unrelated to the difference in elastic-interaction energies, and is thermochemical in nature. This interaction is described formally as the effective energy of bonding between the impurity atoms and the stretched dislocation.

Electrical interaction takes place between hydrogen atoms and dislocations, in addition to the elastic and chemical interactions. The appearance of an edge dislocation in the structure of the crystal results in a change in ionic density around it. If we assume that the electron-gas density does not change appreciably around a dislocation, local disturbances of electrical neutrality should arise in this zone. A local positive charge appears in the compressed part of the lattice and a negative charge in the expanded part, i.e., we have a kind of "linear dipole." An attempt was made in [31] to evaluate the energy of interaction between a charged impurity ion, which was represented in the form of a point charge carrier, and the electric field around a dislocation. For an impurity ion with an effective charge q, this energy was found to be

$$U_{el} = \frac{1}{30} \frac{h^2}{2m\lambda^2} q, \qquad (8)$$

where λ is the wavelength of the electrons of the electron gas; m is the mass of the electron; h is Planck's constant.

If we assume that in transition metals, the hydrogen atom is completely ionized to the proton and, consequently, that $q = +1$, while the electron-gas electron wavelength is close to the interatomic distance ($\sim$2.7 A), we find that $U_{el} = 0.69$ ev.

Actually, the effective charge of the proton should be smaller due to its screening by electrons, and, consequently, the energy of electrical interaction between protons and dislocations will also be smaller. Although the effective charge of the proton is known only for palladium ($q = +0.5$), we may nevertheless assume that the energy of electrical interaction of dislocations with protons must be no smaller in most transition metals than the energy of elastic interaction of unionized hydrogen atoms with them.

3. EXPERIMENTAL DATA ON THE INTERACTION OF HYDROGEN WITH IMPERFECTIONS IN THE CRYSTAL STRUCTURE OF METALS

The interaction of hydrogen with defects in the crystalline structure of metals can be judged from the influence of hydrogen on the internal friction of the metals. Weiner and Gensamer [35] found two internal-friction peaks in iron with hydrogen: one at 50°K and another at 105°K. In their opinion, the internal-friction peak at 50°K is a result of hydrogen diffusion due to a stress gradient, and is analogous to the Snoek peak, which arises on redistribution of carbon and nitrogen atoms in interstices.

As was indicated above, interstitial atoms in a body-centered lattice create tetragonal distortions, with the result that Snoek atmospheres appear at the dislocations. In the absence of an external stress, interstitial atoms that are not bound into the Snoek atmospheres are distributed uniformly along the three short axes x, y and z of the spaces. The application of external stresses, for example along the z-axis, increases the distance between atoms A and A' and thereby increases the size of the interstitial z-space. Hence interstitial atoms in the z-spaces will distort the lattice to a lesser degree than those in x- or y-spaces. For this reason, atoms will transfer to z-spaces from x- and y-spaces. Redistribution of the interstitial atoms in the interstices results in an internal-friction peak from which the impurity's diffusion coefficient can be found. The hydrogen-connected low-temperature peak in iron was also observed in [435, 436].

Heller [42] showed that the low-temperature internal-friction peak in a hydrogen-saturated iron wire is observed at 29°K rather than 50°K [35]. The internal-friction peak appears at 35°K in deuterium-saturated wire. The rise in the temperature of the peak is greater than might be expected on the basis of the isotope-mass difference.

However, Heller notes that the peak that he observed cannot be explained in terms of relaxation effects, which Snoek postulated in the case of nitrogen and carbon in iron. If we assume that diffusion at temperatures close to absolute zero takes place with the same activation energy as at room temperature, then the hydrogen peak would be observed at 45°K or even higher at a frequency of 1 Hz instead of the experimentally found value of 29°K. Hence the activation energy of the observed phenomenon is lower. Heller accounts for the transition of the hydrogen atom from one interstice to another under applied stresses in terms of a tunnel effect that makes it possible to cross potential barriers with a lower activation energy, and confirms this hypothesis by calculations which he carried out for a quantum-mechanical model of the phenomenon observed.

Weiner and Gensamer [35] explain the second internal-friction peak at 105-120°K in terms of entrainment of the hydrogen atmospheres by oscillating dislocations during the internal-friction measurement. The second peak does not appear if the tests are made immediately after hydrogenation. But if specimens are held at room temperature for 24 hours and the tests are then conducted

at subzero temperatures, the second internal-friction peak appears. The hypothesis offered by the authors for this effect was that the hydrogen-atmosphere density rises in the specimens after hydrogenation, so that the internal-friction peak rises accordingly. Since hydrogen drifts toward dislocations from solid solution, the first peak (at 50°K) then subsides. After four days, the first peak vanishes again and the second reaches its maximum. On further aging, the 105°K peak declines, to vanish completely after 10 days, since the degree of saturation of the hydrogen atmospheres becomes so high that the motion of dislocations stops at the stress level corresponding to the test technique adopted.

Heller [42] also obtained an internal-friction peak at 105°K, but he did not study it in detail and, in essence, offered no explanation of his own for this peak, apparently having accepted the interpretation of Weiner and Gensamer. At the same time, the explanation that he gives for the second peak is not quite correct. The most dependable value of the hydrogen diffusion coefficient in iron at room temperature is 10^{-7} cm^2/sec. It follows from this that 0.1 sec and not 4 days, as found by the authors of [35], is necessary for diffusion of hydrogen from solution to dislocations. Four days are required for diffusion of carbon and nitrogen to dislocations.

Rogers showed that spurious internal-friction effects may be caused by redistribution of carbon and nitrogen due to unintentional deformation of the specimens when they are saturated with hydrogen. The internal stresses that inevitably arise in specimens when they are saturated with hydrogen also cause redistribution of carbon and nitrogen. However, this hypothesis is contradicted by the conclusion at which Weiner and Gensamer arrived. They found that the internal-friction peaks at 50 and 105°K do not depend on the method by which the hydrogen is introduced. On electrolytic introduction of hydrogen into steel and in hydrogenation in an atmosphere of molecular hydrogen under high pressure, identical internal-friction figures were obtained.

Hewitt [439] obtained completely different results in a study of internal friction in low-alloy steels. In this study, the specimens were annealed in a hydrogen atmosphere at 1073-1273°K at a pressure of 1 atmosphere gauge (0.1 Mn/m^2) or at 983-973°K under a pressure of 64 atmospheres gauge (6.4 Mn/m^2), followed by quenching in water. Gas analysis showed that the hydrogen content in the steel after such treatment varied from 1 to 6 cm^3 to 100 g of metal. Internal friction was studied on a very sensitive machine that operated in the frequency range from 10 to 90 kHz, at temperatures ranging up from 20°K (the temperature of liquid hydrogen). No internal-friction peak associated with the presence of hydrogen in the specimen was observed in this study.

The author concludes that in the temperature range investigated, hydrogen does not form an interstitial solid solution in the lattice of α-iron. An appreciable hydrogen concentration in interstitial solid solution appears at temperatures above 400°K. Below this temperature, hydrogen is segregated from the solid solution and concentrates along dislocation lines, from which it gradually migrates at a rate substantially lower than that of true

diffusion.

The method used to study internal friction in Hewitt's work differs from that used in the studies cited earlier in that, firstly, internal friction was studied on quenched and not on annealed specimens and, secondly, the frequency of the vibrations was higher by a factor of approximately 10^3-10^4 than in the other studies.

The internal friction of hydrogenated tantalum specimens was studied in [459]. The investigations were made on wire 0.76 and 1 mm in diameter at frequencies of 75 and 270 Hz. Internal friction was measured during continuous cooling of specimens at a rate of 2 deg/min from 473 to 77°K and subsequent heating to 523°K at the same rate. Six relaxation peaks were detected (at 103, 190, 274, 309, 327, and 483°K). The peaks at 103, 190 and 274°K appear only at hydrogen concentrations above 33.3 atoms, and their amplitude rises with increasing hydrogen content.

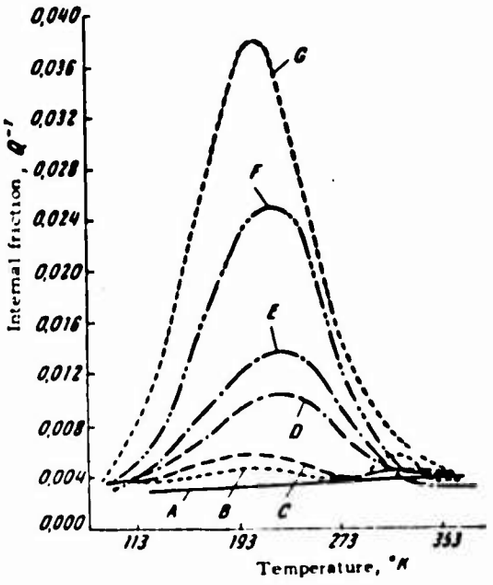

Fig. 6. Internal friction in hydrogenated vanadium specimens as a function of temperature at a frequency of 270 Hz and the following H_2 contents in % (atomic): A) 0.0; B) 1.2; C) 2.7; D) 5; E) 7.6; F) 10.4; G) 14.1.

Beginning at this hydrogen concentration, the amplitude of the oxygen peak diminishes with increasing hydrogen content. On this basis, the authors conclude that at hydrogen concentrations above 33.3% (atomic), the hydrogen atoms in the hydride Ta_2H are located not only in octahedral, but also in tetrahedral interstices, from which they displace oxygen atoms. The peak at 274°K is due to ordering of hydrogen atoms in octahedral spaces with an activation energy of 12.5 kcal/mole (52.4 kj/mole), while the peak at 190°K is due to tetrahedral ordering with an activation energy of 8.5 kcal/mole (35.6 kj/mole). The authors explain the

peaks at 309 and 327°K in terms of establishment of long-range and short-range order in the tantalum hydride, and that at 103°K by the Bordoni effect. The authors stress specifically that they did not succeed in detecting a peak due to ordering of hydrogen atoms in interstices in the solid solution of hydrogen in tantalum. This peak should appear at 138°K with an activation energy of 6 kcal/mole (25 kj/mole). The absence of this peak can be related either to the low solubility of hydrogen in tantalum or to almost complete ionization of the hydrogen atom to the proton.

The internal friction of vanadium alloys with 1.2-14.7% (atomic) of H_2 in the temperature range from 83°K to 483°K was measured in [418] on wire specimens with diameters of 0.625 and 1.375 mm at frequencies of 75 and 270 Hz, respectively. It was found that hydrogen produces relaxation peaks whose heights depend on the hydrogen concentration in the vanadium (Fig. 6). One relaxation peak appears on the cooling curve, while the heating curve has a more complex nature. The height of the peaks decreases when the specimens are held at temperature after hydrogenation. Peak height is proportional to hydrogen concentration, except for the alloy with 10.4% (atomic) H_2.

A stable peak appears at 190°K and a frequency of 175 Hz; its activation energy amounts to 8.5 kcal/g-atom (35.5 kj/g-atom).

After five days' holding, which promotes more uniform distribution of the hydrogen, a peak is observed at 198°K and its activation energy is 9050 cal/g-atom (38,000 j/g-atom). The authors conclude that this relaxation peak in the vanadium-hydrogen system is due to ordering of hydrogen atoms at tetrahedral interstitial positions in the lattice of V_2H.

Convincing data on the interaction of hydrogen with dislocations were obtained in none of the works cited above. In principle, inferences can be drawn concerning such interaction from boundary friction, but no methodically correct studies in this direction have been published.

Data on the interaction of hydrogen with dislocations have been obtained by x-ray structural analysis. Analyzing the results of x-ray structural investigations of iron, Bastien [23] concludes that hydrogen atoms do react with dislocations. Broadening of the {110}, {112} and {123} lines was observed on x-ray diffraction patterns from polycrystalline specimens that had been electrolytically polished and electrolytically saturated with hydrogen. Degassing in a vacuum at 473°K for 7 hours, followed by three minutes of holding at 373°K, eliminated the line broadening. Broadening of the {112} lines was observed in hydrogen-saturated single crystals.

In Bastien's opinion, the line broadening on the x-ray patterns is due to preferential accumulation of hydrogen along the {112} planes in tetrahedral spaces, and especially along the dislocations associated with these planes.

The most convincing data in favor of the existence of interaction of hydrogen with dislocations were obtained in studies of

mechanical properties. Thus, for example, Rogers [36, 37] showed that like C and N, hydrogen may produce a flow peak. This peak appears below 153°K and is related to condensation of hydrogen on dislocations.

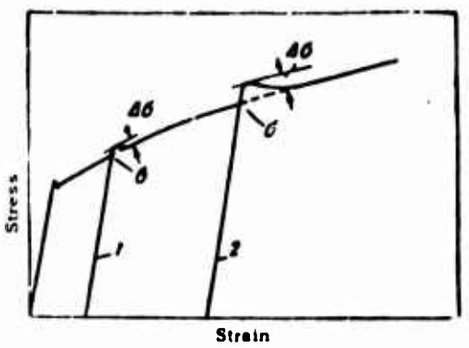

Fig. 7. Diagram of change in nature of tension curve on removal of load and reloading. 1) Immediate reloading; 2) reloading after aging.

Interesting data on the interaction of hydrogen atoms with dislocations in nickel were obtained in [102]. At temperatures below 153°K, a flow peak appears on the tension curves for hydrogen-saturated nickel specimens. If tension is interrupted at a given point in time, the load removed, and then the specimen reloaded, an increase in toughness over the original tension curve is observed in the initial stage of reloading. If tension is reapplied immediately after unloading of the specimen, the relative toughening is small, and is independent of the preceding deformation. If, however, a certain time is allowed to elapse before reloading the specimen, the relative toughness increase rises, and to a greater degree the longer the pause between loadings (Fig. 7). This effect is known as strain aging.

It is due to the fact that in the first loading, the dislocations are freed of the hydrogen atmospheres surrounding them and the atmospheres do not retard their motion if reloading follows immediately. With aging of the specimens after unloading, the atmospheres reform around the dislocations, which produces the flow peak.

According to Cottrell and Bilby [27], the kinetics of impurity-atmosphere formation on dislocations can be described in the early stages of aging by the equation

$$n(t) = 3\left(\frac{\pi}{2}\right)^{1/3} n_0 \left(\frac{ADt}{kT}\right)^{1/3}, \qquad (9)$$

where n_0 is the total number of dissolved atoms per unit volume; $n(t)$ is the number of atoms that settle on a unit length of the dislocation in a time t.

If we assume that the relative toughening $\Delta\sigma/\sigma$ is propor-

tional to $n(t)$, a linear relation should obtain between $\Delta\sigma/\sigma$ and $t^{2/3}$.

Figure 8 shows $\Delta\sigma/\sigma$ as a function of $t^{2/3}$ for nickel with and without hydrogen. For the specimens without hydrogen, the relative strength increase does not depend on aging time after unloading. For hydrogen-saturated specimens, the toughening ratio increases with aging time, with a linear relationship obtaining between $\Delta\sigma/\sigma$ and $t^{2/3}$. This is testimony to the effect that interaction of hydrogen atoms with dislocations is the cause of the toughening.

If it is remembered that $D \sim D_0 e^{-Q/RT}$, the following relation should be observed for $\Delta\sigma/\sigma = \text{const}$ [$n(t) = \text{const}$]:

$$\ln \frac{t}{T} = \ln A - \frac{Q}{RT},$$

where A is a constant.

It is seen from Fig. 8 that a linear relation actually is observed between $\ln t/T$ and $1/T$, with an activation energy Q of 9.3 kcal/g-atom (38.9 kj/g-atom), which agrees rather closely with the average activation energy for diffusion of hydrogen in nickel. Thus, the relative strengthening on aging of hydrogenated nickel specimens is undoubtedly due to the interaction of hydrogen atoms with dislocations.

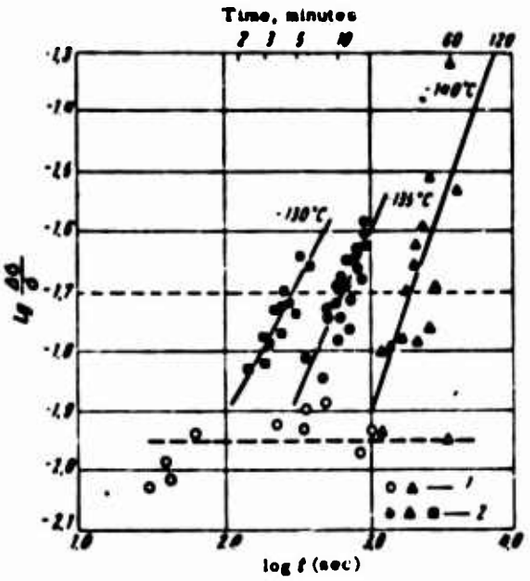

Fig. 8. Strain-hardening ratio in strain aging as a function of t for nickel. 1) Specimens without hydrogen; 2) specimens with hydrogen.

Reference [354] presents convincing data on dislocation blocking by hydrogen atoms in niobium. Here the change in properties during strain aging of technically pure niobium that had been smelted out in an arc furnace was studied in the initial state and after hydrogenation. The aging curve was determined from flow-peak recovery and from the change in the dynamic elastic modulus.

Tension tests were carried out at 223°K on a Baldwin-Emery rigid-type machine, at a strain rate of 0.005 min^{-1}. The specimens were stretched until a yield-point plateau appeared, and were then unloaded and aged at 394-533°K for various times. It was established that after short aging, no flow peak appears on the tension curves on reloading. If, however, the aging time was above a certain critical value, the flow peak returns. The critical aging time t necessary for return of the flow peak is represented by a straight line in the coordinates $\ln\frac{1}{t} - \frac{1}{T}$ as a function of the absolute temperature T; from the slope of this line we can determine the activation energy of the process responsible for the strain aging. This energy is found to be 10.5 kcal/g-atom (44 kJ/g-atom), i.e., smaller by a factor of 2-3 than the activation energy in diffusion of carbon, nitrogen and oxygen in niobium, and almost the same as the activation energy of diffusion of hydrogen in niobium (9.37 kcal/atom). It follows from this that the strain aging studied in [354] is due to the interaction of hydrogen atoms with dislocations.

The elastic modulus also recovers during aging of deformed niobium specimens, with an activation energy of 8080[sic]-9.92 kcal/g-atom (36-41.5 kJ/g-atom), which is also close to the activation energy for hydrogen diffusion.

Not all investigators agree that the hydrogen atom interacts with dislocations in metal [12, 38].

The contradictory opinions among various authors concerning the interaction of hydrogen with dislocations in metal arise from the fact that hydrogen atoms may be neutral or either positively or negatively ionized in the same metal. The positive ions may be responsible for one phenomenon, and the negative ones for others; the neutral atoms, on the other hand, play an intermediate role.

Moreover, impurities that interact with the dislocations more strongly than does hydrogen are always present in metals. These include, for example, oxygen, carbon and nitrogen. The temperatures at which they condense on dislocations are considerably higher than for hydrogen, and during slow cooling they form Cottrell atmospheres. It can easily be shown that total saturation of impurity atmospheres in annealed metals is achieved at an extremely small impurity content, of the order of 10^{-4}-10^{-5}% (atomic). During slow cooling, therefore, when the temperature has dropped to a value at which formation of hydrogen atmospheres is possible, all points under dislocations have already been occupied by other impurity atoms. In this case, hydrogen can condense on dislocations, but its distribution over the dislocations, the bonding energy, and the condensation temperature must now be

different, since the basic stimulus to this process is not elastic, but chemical interaction, due to the differing electrochemical natures of the hydrogen atoms on the one hand and the oxygens, nitrogens and carbons on the other. To study the interaction of hydrogen with available dislocations, it is necessary to cool the metals rapidly in the temperature range in which formation of impurity atmospheres composed of oxygen, nitrogen and carbon atoms is possible. Beginning at a certain temperature at which the diffusion rate of these impurities has become so small that it is practically impossible for the atmospheres to form, the specimens must be cooled slowly. The diffusion rate of hydrogen in metals at temperatures around room temperature is 10^8-10^{10} times those of other interstitial impurities, and the mobility of hydrogen atoms is sufficient to form atmospheres even at comparatively low temperatures. This has not been taken into account in experimental studies, and this may be the reason for the contradictory opinions advanced by various investigators concerning the interaction of hydrogen atoms with dislocations.

Few data have been published on the interaction of hydrogen with packing defects. A reference to a private communication of Nutting is found in [169], to the effect that hydrogen lowers the energy of packing defects and therefore expands them. The influence of hydrogen on the probability of packing defects in spectroscopically pure (99.999%) copper was studied in [25]. The probability of the presence of packing defects was determined by x-ray diffraction studies, from the shift of the diffraction lines of specimens that had been degassed in high vacuum at a pressure of $5 \cdot 10^{-7}$ mm Hg ($6.6 \cdot 10^{-5}$ n/m^2) and then annealed in a hydrogen atmosphere at 900, 1000 and 1100°K. It was found in this study that the probability of packing defects increases with increasing hydrogen content in copper [from $3.0 \cdot 10^{-3}$ in pure copper to $7 \cdot 10^{-3}$ in copper with $1.7 \cdot 10^{-5}$% (by mass) of H_2 (0.02 cm^3/100 g)].

4. ADSORPTION OF HYDROGEN ON INTERNAL INTERFACES

In the general case, hydrogen in solid solution must be distributed nonuniformly. The hydrogen concentration at grain boundaries may differ substantially from the average. Hydrogen appears to be a horophilic impurity with respect to many metals, i.e., it lowers their surface energy [39]. For this reason, hydrogen accumulates at grain boundaries.

Segregation on grain boundaries is also possible for purely geometric reasons. Accumulation of vacancies and other defects is observed along grain boundaries, with the result that the packing density of the atoms is lower at boundaries than in the bulk of the grain. For metallic atoms, these purely geometric factors are not dominant, but for ases this may be a basic cause of their segregation at boundaries [40].

In addition to segregation of hydrogen on grain boundaries, hydrogen may accumulate at interfaces inside the grain, for example, along those planes at which shear has occurred during plastic deformation. Werner and Davis [41] established that the amount of hydrogen absorbed by cold-rolled steel from the gaseous medium at a pressure of 710 mm Hg increases as the temperature rises from

room to 523°K, reaches a maximum at this temperature, and then decreases, reaching a minimum at 675°K. When the temperature is increased further, the amount of absorbed hydrogen increases again. The authors explain this type of dependence of the amount of absorbed hydrogen on temperature in terms of a dual, endothermic and exothermic, nature of hydrogen absorption by steel in the temperature range from 473 to 673°K.

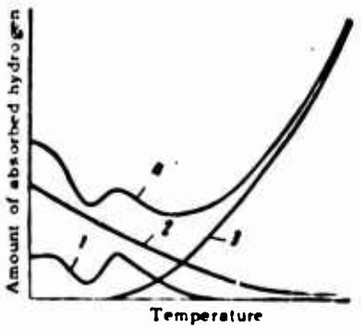

Fig. 9. Change in amount of hydrogen absorbed by various mechanisms as a function of temperature for metals that absorb hydrogen endothermically. 1) Adsorption, chemosorption, adsorption on internal interfaces; 2) molecular hydrogen in pores; 3) hydrogen in solution; 4) total quantity of absorbed hydrogen.

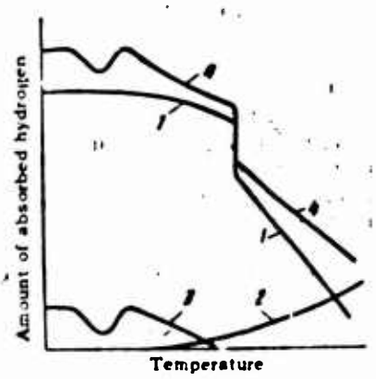

Fig. 10. Curve of variation of amount of hydrogen absorbed by various mechanisms with temperature for metals that absorb hydrogen exothermically. 1) Hydrogen dissolved in metal and bound into hydrides; 2) molecular hydrogen in pores; 3) adsorption, chemosorption, adsorption on internal interfaces; 4) total sorption.

Analysis of the experimental data showed that endothermic absorption is solution of hydrogen in the ferrite lattice, and, in accordance with the general relationships, the amount of hydrogen absorbed by this mechanism increases with rising temperature. Exothermic absorption consists in chemosorption of atomic hydrogen on internal interfaces.

Since exothermic absorption does not occur in annealed steels, chemosorption would appear to take place at those inter-

faces that form during cold plastic deformation. At 523°K, the amount of hydrogen absorbed by this mechanism is 20-25 times greater than the amount absorbed by annealed steel.

The dual nature of absorption should be characteristic for all deformed metals in which solution of hydrogen is an endothermic process. In this case the amount of absorbed hydrogen should be the sum of the quantity of endothermically absorbed hydrogen, which increases with rising temperature, and the amount of exothermically absorbed hydrogen, which diminishes with temperature in accordance with the scheme shown in Fig. 9. Molecular hydrogen, which can accumulate in cavities, should be added to the total amount. The amount of molecular hydrogen should decrease with temperature because of the increase in its solubility.

For metals that absorb hydrogen endothermically, we observe the opposite type of temperature dependence of the amount of hydrogen absorbed by the bulk of the metal and the amount of molecular hydrogen in microcavities (Fig. 10). In these metals, the amount of hydrogen in microcavities is extremely small. While the pressure of molecular hydrogen in metals of the first group sometimes reaches tens of thousands of atmospheres, in metals of the second group, it is, as a rule, millionths of a millimeter of mercury or less. In metals that absorb hydrogen endothermically, its pressure can rise above atmospheric only at temperatures near the melting point at the concentration usually encountered.

And, finally, hydrogen may be adsorbed on the surfaces of internal cracks, with the amount adsorbed diminishing with increasing temperature for all metals. Published data on the adsorption of hydrogen on internal-crack surfaces in aluminum [64] and steel [65, 66] confirm this conclusion.

5. CHEMICAL NATURE OF THE PHASES FORMED ON INTERACTION OF METALS WITH HYDROGEN

The final products of the reaction of hydrogen with metals may be either chemical compounds (hydrides) or solid solutions, or, in a certain range of temperatures and pressures, a two-phase mixture represented by solid solutions and hydrides. The nature of the reaction products depends on the nature of the metal. A number of classifications has been proposed for the products of interaction of hydrogen with the elements [2, 3, 441], and, in our opinion, the most successful among them is that submitted by Herd.

Herd classifies hydrides into four groups: ionic, transition-metal, intermediate and covalent. Each of these groups corresponds to a certain position of the elements in the Mendeleyev Periodic Table (Fig. 11).

If we adopt Herd's hydride classification, it is necessary to distinguish solid solutions of hydrogen in metals from chemical compounds of metals with hydrogen (hydrides). In transition metals of Groups IIIB-VB, solid solutions and hydrides are obtained on direct interaction with hydrogen, while in metals of Groups VIB-VIIIB, the result consists solely of solid solutions,

which cannot quite properly be called metal-like hydrides. True hydrides of a number of metals of Groups VIB-VIII can be obtained indirectly.

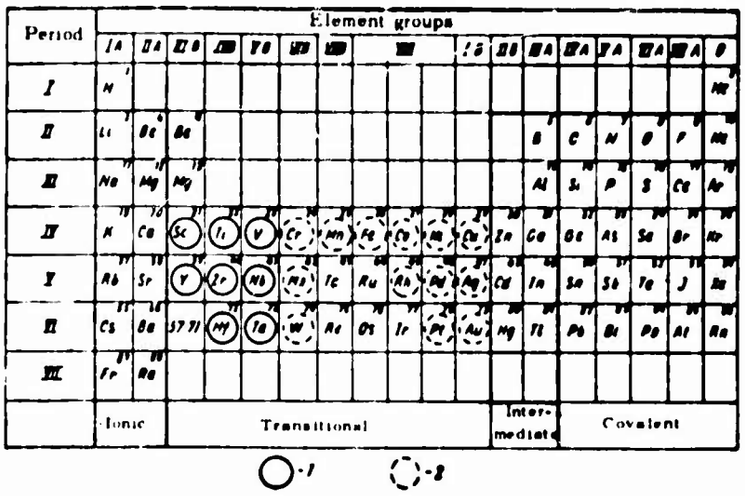

Fig. 11. Relation of nature of hydrogen interaction with metals to their position in the Mendeleyev Periodic Table. 1) Exothermic absorption; 2) endothermic absorption.

The hydrides of transition metals exhibit metallic properties, and their nature can be explained on the basis of the metallic-bond theory. The external electrons of transition elements are classified as bonding electrons, which are responsible for cohesive forces in metals, and atomic electrons, which cause ferromagnetism under certain conditions. According to Pauling, the number of bonding electrons increases in transition metals from zero in the inert gases to 5.78 in Group VI elements and those that follow. Thus, the largest number of bonding electrons in transition metals is 5.78 per atom. If we assume that hydrogen atoms yield their electrons completely to the free-electron gas, all states in the bonding-electron band in Groups IIIB, IVB and VB elements will be filled at 2.73, 1.78 and 0.78 atoms of hydrogen per metal atom.

It is interesting to note in the above connection that under ordinary conditions, transition-metal hydrides exist only at excess concentrations of the metal atoms over the stoichiometric compositions MeH_3; MeH_2; MeH. On direct interaction of titanium, zirconium, and vanadium with molecular hydrogen, it is quite easy to obtain preparations of the compositions $TiH_{1.70}$ — $TiH_{1.75}$; $ZrH_{1.92}$; $VH_{0.7}$ — $VH_{0.9}$, but further introduction of hydrogen involves colossal difficulties.

These facts indicate that the structure of the transitional hydrides actually is determined by the number of free states in the bonding-electron band and, consequently, the theoretical for-

mulas for Group IIIB-VB hydrides should not be MeH_3, MeH_2 and MeH, but $MeH_{2,78}$, $MeH_{1,78}$ and $MeH_{0,78}$.

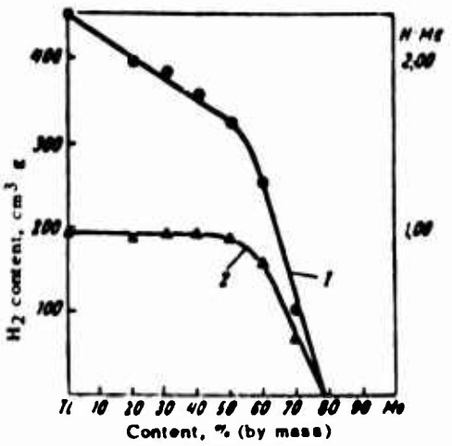

Fig. 12. Amount of absorbed hydrogen as a function of composition of titanium-molybdenum alloys. 1) H_2 content; 2) ratio of number of H atoms to number of metal atoms.

The hypothesis advanced concerning the nature of the transitional hydrides makes it possible to explain why hydrides are not formed in elements of Groups VIB-VIIB on direct reaction between them and hydrogen: these metals have no free states in the bonding-electron band. As we pass from metals of Group VB to metals of Groups VIB-VIIIB, the type of absorption also changes. Transitional elements of Groups IIIB-VB absorb hydrogen exothermically, while Group VIB-VIIIB elements (except palladium) absorb it endothermically.

The hypothesis that free states in the bonding-electron band are decisive in exothermic absorption is confirmed by data obtained in study of the interaction of titanium-molybdenum alloys with hydrogen. With increasing molybdenum content in the alloys, the amount of absorbed hydrogen diminishes and becomes negligibly small in alloys containing more than 80% (atomic) of Mo (Fig. 12). In the alloy of Ti + 75% (atomic) Mo, the number of bonding electrons is 5.5 per atom, i.e., very close to the value at which, according to Pauling, the bonding-electron band is completely filled.

Exothermic absorption is suppressed in metals of Group VIB, and endothermic absorption has not yet developed to an adequate degree, so that these metals absorb an exceedingly small quantity of hydrogen. It is indicated in [442] that not only hydrogen, but also other interstitial impurities, such as oxygen, nitrogen, and carbon, exhibit their solubility minimum at the electron concentration of 5.78.

While the tendency of metals to exothermic absorption is determined by the number of unoccupied states in the bonding-electron band, it appears that endothermic absorption is governed by

the tendency of the metal to fill the atomic-electron band with hydrogen electrons. This tendency is manifested only weakly in elements of Group VIB, since the atomic electron band is practically unfilled. With increasing atomic number of the element, the atomic-electron band is filled to an increasing degree, and one would expect that the tendency to capture hydrogen electrons and, consequently, the tendency to absorb, would increase. Unfortunately, experimental data on the hydrogen interaction of most Group VI-VIII elements are highly unreliable. In transitional elements directly adjacent to the metals of Group IB, and particularly in nickel and palladium, rather stable hydrides are formed. The composition of these hydrides is determined by the number of unoccupied states in the metal's *d*-band. Indeed, it was shown in [434] by neutron diffraction that in the β-phase of the Pd-H system, the hydrogen atoms are situated in octahedral spaces in the palladium lattice. If the geometric factor were decisive, palladium hydride would have the structure PdH. At a hydrogen pressure of 1 atmosphere excess (0.1 Mn/m^2), however, palladium is saturated only to the composition $PdH_{0.7}$.

Palladium is a paramagnetic metal, because of the presence in its structure of unfilled sublevels in the *d*-band of the electron gas. When silver, which yields its electrons to the *d*-band, is dissolved in palladium, the paramagnetism decreases and vanishes altogether at 70%; we find that the *d*-band is completely filled. On solution of hydrogen, the paramagnetism of palladium also decreases, to vanish [21, 22] at a 0.5-0.6 ratio of hydrogen to palladium atoms. Mott and Jones [433] explain this in terms of hydrogen behaving like a metal in palladium, yielding its electrons to the *d*-band of the electron gas and thereby reducing the number of unfilled states in the *d*-band. In alloys of palladium containing more than 70% of Ag, hydrogen does not dissolve. From this it follows that the asymmetry of hydrogen to palladium is determined by the presence of vacant places in its *d*-band. Total saturation of the *d*-band occurs at the composition $PdH_{0.7}$.

The structure of nickel hydride is also determined by its electronic structure, and here we observe a certain similarity in the structures of nickel and palladium hydrides, despite the fact that their heats of absorption are of opposite signs (palladium absorbs hydrogen exothermically and nickel endothermically).

The hydrides of transition metals are distinguished by very simple crystal structures, of the type that has come to be known as interstitial. In the hydrides, the metal atoms form either a face-centered cubic lattice with a coordination number of 12 or a body-centered cubic lattice with a coordination number of 8, or a close-packed hexagonal lattice with a coordination number of 12. As a rule, the crystal lattices of hydrides show little distortion.

The hydrogen atoms in the hydrides occupy interstices. Since they are small, they frequently occupy not the larger spaces in the structure, but those that conform more closely to them in size. In close-packed structures, for example, the hydrogen is found not at octahedral, but at tetrahedral spaces.

Transition-metal hydrides have low densities. As a rule, volume increases by 10-20% on formation of a hydride. For this reason, hydride formation on saturation of compact metals with hydrogen is accompanied by the appearance of large tensile stresses around them. Hydrides are friable brittle powders with low mechanical strength.

6. PECULIARITIES OF THE INTERACTION OF HYDROGEN WITH HETEROPHASE ALLOYS

Hydrogen absorption continues until an equilibrium pressure has been established in the system – that corresponding to the vapor pressure of hydrogen above the hydrogen alloy of the metal obtained as a result of concentration saturation. The hydrogen equilibrium pressure increases with increasing concentration of hydrogen in the metal. The relation between hydrogen equilibrium pressure, hydrogen concentration and temperature can be described by the following equation for low-concentration solid solutions of hydrogen in metals:

$$p = \psi C^2 e^{\frac{Q}{RT}}, \qquad (10)$$

where p is the equilibrium hydrogen pressure; C is the hydrogen concentration in solution; T is the absolute temperature; R is the gas constant; Q is the heat of solution of hydrogen in the metal; ψ is a coefficient that depends on entropy.

In first approximation, the quantities Q and ψ are independent of temperature, but depend essentially on the concentration of the impurities and alloying elements dissolved in the metals.

In a heterophase alloy, the hydrogen concentrations are different in the different phases. In the alloy, the hydrogen is redistributed between the phases until thermodynamic equilibrium is arrived at in the system. Under equilibrium conditions, the partial pressures of hydrogen above the individual phases may be equal to one another, from which, in accordance with (10), we have for a system composed of two phases α and β

$$\frac{C_\beta}{C_\alpha} = \sqrt{\frac{\psi_\alpha}{\psi_\beta}} e^{\frac{Q_\alpha - Q_\beta}{2RT}}. \qquad (11)$$

The hydrogen concentration in the β-phase will be higher than that in the α-phase when

$$\sqrt{\frac{\psi_\alpha}{\psi_\beta}} e^{\frac{Q_\alpha - Q_\beta}{2RT}} > 1.$$

The ratio between the hydrogen concentrations in the phases should change with temperature. The hydrogen concentrations in the α- and β-phases will be equal to one another at a certain temperature T_r:

$$T_r = \frac{Q_\alpha - Q_\beta}{2R \ln \sqrt{\frac{\psi_\beta}{\psi_\alpha}}}. \qquad (12)$$

It follows from (11) that when $Q_\alpha > Q_\beta$ and ψ_α/ψ_β is not too small, the hydrogen concentration in the β-phase will be higher than the hydrogen concentration in the α-phase at low temperatures. With increasing temperature, the ratio C_β/C_α should decrease and become equal to unity at the temperature T_r. At higher temperatures, the hydrogen concentration in the β-phase will be smaller than that in the α-phase, and the ratio C_β/C_α should decrease with rising temperature. It should be noted that the temperature T_r can lie outside the two-phase region α + β and will then be fictitious.

If the entropy factors are closely similar for the phases, the ratio of their hydrogen concentrations is determined by the heat of solution of the hydrogen, i.e., the concentration in the β-phase is higher than that in the α-phase if $Q_\beta < Q_\alpha$. Consequently, the hydrogen concentration will be higher in the phase for which the heat of solution is lower (taking the sign into consideration). This concentration difference will be particularly large when one of the phases absorbs hydrogen with absorption of heat (Q positive), while the other absorbs it with liberation of heat (Q negative).

The solubility difference between the phases can be utilized for internal degasification of one of the phases at the expense of the other. The composition of the alloy should be adjusted in such a way that the heat effect of hydrogen absorption by the second phase will be much smaller (with consideration of sign) than for the basic phase. In this case, a small quantity of the second phase is sufficient to degasify the basic phase almost completely. It appears that this method might be used to obtain substantial plasticity improvement in high-melting metals, which, as a rule, have body-centered cubic structure. Metals with this structure are particularly sensitive to contamination by interstitial impurities.

The same principle can be used as a basis for degasification of liquid metals by substances that do not react (or react very little) with them but have a strong affinity to hydrogen.

It is quite easy to estimate the amount of degasifier that must be introduced into the melt to reduce its hydrogen concentration by a given factor (n). Let the hydrogen concentration in the melt before degasification be C_0. If the weight of the melt is G, the weight of hydrogen in it will be C_0G. After degasification, the hydrogen concentration in the melt is to be $C_r = C_0/n$ and that in the degasifier C_d. If there are no losses of hydrogen to the atmosphere,

where G_1 is the weight of the degasifier.

$$C_p G + C_A G_1 = C_0 G.$$

From this we find

$$G_1 = \frac{n-1}{n} \frac{C_0}{C_A} G$$

or

$$G_1 = (n-1) \frac{C_p}{C_A} G. \qquad (13)$$

If the hydrogen concentration in the melt and in the degasifier are not very high, so that (11) applies, Eq. (13) assumes the form

$$G_1 = (n-1) G \sqrt{\frac{\psi_p}{\psi_A}} e^{\frac{Q_p - Q_A}{2RT}}. \qquad (14)$$

Equation (13) is more generally applicable than (14). Thus, for example, (14) would hardly be applicable to the liquid aluminum/solid titanium system, since for small amounts of titanium, the hydrogen is concentrated so strongly in the degasifier that (10) no longer holds.

At the ratio between the hydrogen concentrations in the phases that is characteristic for the solid titanium/liquid aluminum system, the theoretical amount of degasifier will be determined simply by the quantity of hydrogen C_d that each gram of titanium can absorb at the degasification temperature. To determine the amount of degasifier in this case, Eq. (13) should be used.

For the temperature 973°K C_d = 1% (by mass), and hence to reduce the hydrogen concentration by half in aluminum containing 0.3 cm^3/100 g [$2.7 \cdot 10^{-5}$% (by mass)], we need $1.35 \cdot 10^{-5} G$ of titanium, i.e., 13.5 g per ton. In reality, however, it will be necessary to introduce several times that amount of titanium, in view of the nonideal degasification conditions (the time required for diffusion of hydrogen to the degasifier, inhibition of absorption as the degasifier approaches saturation, etc.)

It has also been assumed in the calculations that the titanium does not react with molten aluminum, something that is not absolutely true. The amount of titanium that dissolves must be taken into account in calculating the amount of degasifier. If, however, very little titanium dissolves, it should be placed in a filtering shell that does not react with the melt or degasifier, but is capable of passing hydrogen.

What is essential, however, is that a comparatively small amount of titanium is necessary for effective degasification of molten aluminum. In a trial run, 25 g of titanium in the form of a 14 × 14 mm rod was introduced at 973°K into a 5-kg charge of molten aluminum. After one hour of holding at this temperature, the hydrogen concentration in the aluminum had fallen from 0.32 to 0.22 cm^3/100 g.

The second phase in the alloy can also react chemically with diffusing hydrogen, producing gaseous chemical compounds in some cases. For example, reaction of hydrogen with oxides included inside the metal may result in the formation of steam, whose pressure may be considerable.

Manuscript Page No.	Transliterated Symbols
15	ср = sr = sredniy = average
18	к = k = Kottrell = Cottrell
19	кр = kr = kriticheskiy = critical
20	эл = el = elektricheskiy = electrical
34	р = r = ravnyy = equal
35	р = r = rasplav = melt
35	д = d = degazator = degasifier

Part Two

GENERAL PROBLEMS OF THE INFLUENCE OF HYDROGEN ON THE MECHANICAL PROPERTIES OF METALS

Chapter 1

CLASSIFICATION OF TYPES OF HYDROGEN BRITTLENESS IN METALS

As follows from the data given in Part One, interaction of metals with hydrogen may result in formation of solid solutions of hydrogen in the metal, hydrides, gaseous products formed on reaction of hydrogen with the phases composing an alloy, or molecular hydrogen in various types of gaps in the structure. In all cases, hydrogen has a detrimental influence on the properties of the metals, but the brittle-fracture mechanisms of metals due to various types of hydrogen interaction must be distinguished clearly, since the countermeasures against brittleness will be specific in accordance with the various factors causing it.

Numerous studies made by Soviet and foreign investigators have shown that there are two kinds of hydrogen brittleness in metals. Brittleness of the first kind increases with increasing rate of deformation, while brittleness of the second kind, on the other hand, decreases with increasing deformation rate and vanishes completely at a high enough rate of deformation. The difference between these types of hydrogen brittleness is illustrated by Fig. 13, which shows the influence of rate of extension on the necking of technically pure titanium with 0.05% H_2 and the (α + β) titanium alloy VT3-1 with 0.15% H_2. Hydrogen brittleness of the first kind may be due primarily to gaseous products formed inside the metal on reaction of diffusing hydrogen with impurities or alloying elements. Thus, for example, in nickel, copper, and silver, hydrogen reacts with oxides, which, as a rule, are always present in one or another quantity along the grain boundaries, with the result that steam forms under high pressure. The steam weakens the cohesive forces between the granules and therefore promotes brittle failure. This phenomenon has come to be known as hydrogen embrittlement.

Brittleness of the first kind may also be due to molecular hydrogen present in structural gaps under high pressure. This brittleness is developed in its most characteristic form in steels at rather high hydrogen contents.

In a number of metals that absorb hydrogen exothermically (titanium, zirconium), brittleness of the first kind is governed by laminar segregations of hydrides, which act essentially as internal notches in the metal and promote the germination and propagation of cracks. Like that of ordinary notches, the detrimental influence of hydrides increases with increasing deformation rate.

In a number of metals, e.g., in niobium, hydrogen dissolves

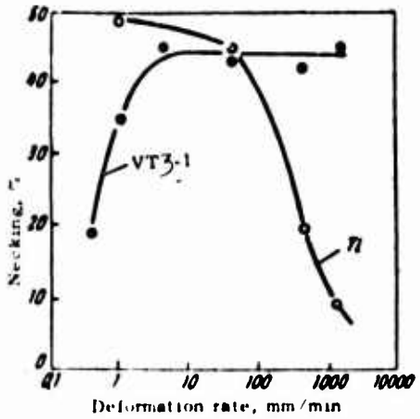

Fig. 13. Influence of deformation rate on necking of technically pure titanium with 0.05% H_2 and VT3-1 alloy with 0.15% (by mass) of H_2.

in large quantities, to form hydrides or other embrittling phases. The hydrogen pressure in cavities in niobium is negligibly small, but the hydrogen nevertheless converts the metal to a brittle state. This brittleness can be explained in terms of the hydrogen's distorting the niobium lattice to effect a change from plastic to brittle. It is similar to the cold shortness caused by oxygen, nitrogen, and phosphorus dissolved in metals.

Hydrogen brittleness of the second kind appears at low deformation rates. This type of brittleness develops primarily in hardened metals and alloys with hydrogen contents exceeding the solubility limit at the test temperature. In this case, the hardening process "fixes" hydrogen-supersaturated solid solutions, which decay on long-term application of stresses, with formation of finely dispersed laminar hydride segregations or with liberation of molecular hydrogen, which results in a sharp drop in the plasticity of the alloys.

The hydrogen embrittlement due to decay processes that develop during deformation might be called irreversible brittleness of the second kind in the sense that if the load is removed after prolonged action of stresses, the plasticity of the alloys is not recovered, and brittle failure is observed in subsequent tests at high rates, no matter how much time has elapsed after removal of the load.

The nature of the hydrogen brittleness that develops in metals at low deformation rates when the hydrogen content is below the solubility limit at the test temperature is most complex. In its most characteristic form, this brittleness is developed in steels and typical ($\alpha + \beta$) titanium alloys. Brittleness of this kind might be called reversible brittleness of the second kind. If, for example, an ($\alpha + \beta$) titanium alloy that has been saturated by hydrogen is subjected to long-term stressing, sources of

hydrogen brittleness form in it and we observe low plasticity immediately after removal of the stresses of high-speed mechanical testing. However, the plasticity of the ($\alpha + \beta$) alloy is almost completely recovered during aging after removal of the stresses first applied. Thus, after removal of the preliminary stresses, the hydrogen-brittleness sources are destroyed with the passage of time and their embrittling effect is eliminated.

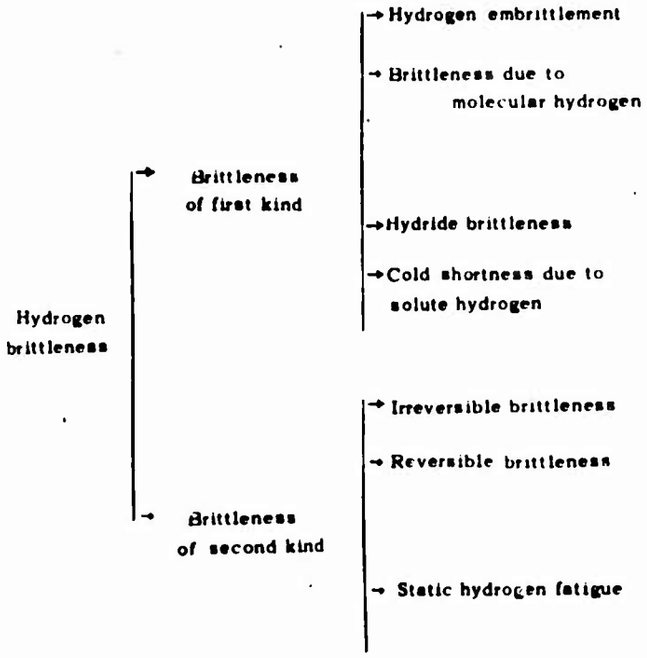

It should be noted that the conceptions of reversible and irreversible hydrogen embrittlement were first introduced in application to steel in the work of L.S. Moroz and T.E. Mingin [98, 99].

An independent form of irreversible hydrogen brittleness is found in the premature failure of hydrogen-saturated specimens under static load (static hydrogen fatigue).

The mutual relationships between the various forms of hydrogen brittleness can be represented by the scheme shown above.

Below we shall examine the possible mechanisms of hydrogen brittleness in metals, devoting our basic attention to reversible hydrogen brittleness of the second kind. General laws are illustrated by data obtained for specific metals.

Chapter 2

HYDROGEN BRITTLENESS OF THE FIRST KIND

1. HYDROGEN EMBRITTLEMENT OF METALS

On reaction of metals with hydrogen, one of the phases forming the alloy may react with the hydrogen to produce gaseous products that accumulate inside the metal and cause it to become brittle. This phenomenon, which has come to be known as hydrogen embrittlement, is observed in silver, copper and nickel. At a temperature above a certain limit, the oxygen that is always present in these metals in one or another amount as an impurity usually reacts with the hydrogen. The temperatures beginning at which the hydrogen reacts to an appreciable degree with oxides are 773, 773, and 1073°K for copper, silver and nickel, respectively.

A directional flow of hydrogen is set up in the metals, from the hydrogen source at the surface toward the oxides in the interior of the metal. The water vapor formed at the metal-oxide interface creates conditions favorable to the formation of submicroscopic and microscopic structural discontinuities, i.e., it causes irreversible changes in the structure and properties of the metals. The process will continue until dynamic equilibrium is established in the system, when the amount of hydrogen diffusing from the surface has become equal to the amount of hydrogen diffusing away from the discontinuities toward the surface.

In the above-named metals, the oxygen is concentrated along grain boundaries, and hence it is precisely here that the water vapor formed on the reaction of hydrogen with oxygen accumulates, resulting in intergranular cracking and brittle failure.

In steels, the carbides usually react with hydrogen, forming methane [43]. This reaction, which is sometimes called hydrogen corrosion, develops at rather high pressures and temperatures above 473-573°K, and also takes place basically along grain boundaries, where, as a consequence, a high-pressure gas accumulates, causing brittle failure on application of an external load. Since carbon diffuses quite rapidly at high temperatures, it is continuously fed into the grain boundaries from the interior of the grains and reacts with hydrogen, with the result that the steel becomes decarburized. Its structure becomes loose and the steel loses plasticity.

2. BRITTLENESS DUE TO MOLECULAR HYDROGEN

In metals that absorb hydrogen endothermically (iron, alu-

minum, magnesium, etc.), the most detrimental effect of hydrogen is associated with formation of porosity. The development of porosity is determined by the hydrogen content in the metals, the rate and nature of the alloy's crystallization, the magnitude of the external pressure, and the magnitude of the equilibrium hydrogen partial pressure and the tendency of the alloys to form supersaturated hydrogen solutions. Porosity is associated with decreasing solubility of hydrogen in the metal as it cools, with the result that the hydrogen attempts to leave the solution. A.P. Gudchenko [276] notes the following possible characteristic cases of liberation of dissolved hydrogen from a metal during the process of its cooling:

1) evolution of hydrogen from the melt during cooling, up to the time of freezing,

2) evolution of hydrogen taking place directly at the crystallization front as it develops,

3) evolution of hydrogen from the supersaturated solid solution when the latter is not in contact with the liquid phase.

Hydrogen is released from a liquid melt in the form of bubbles when the equilibrium partial pressure of the dissolved hydrogen exceeds the total external pressure on the zone of liquid metal under consideration.

In frontal crystallization, any zone of the molten metal will be exposed to atmospheric and hydrostatic pressure right up to the time of freezing, so that for hydrogen bubbles to form in the liquid, its internal pressure must exceed 1 atmosphere (0.1 Mn/m^2).

In volume crystallization, the branches of dendrites merge at a certain stage in freezing, and isolated cavities that are no longer acted upon by the atmospheric pressure are formed between them. As the melt freezes, these cavities fill up, shrinkage occurs, and, as a result, a vacuum that facilitates escape of hydrogen from the melt is created. Under these conditions, hydrogen bubbles may form at hydrogen partial pressures smaller than 1 atm (0.1 Mn/m^2).

Porosity due to lowering of the solubility of hydrogen in the molten metal during its cooling is not observed at very low or very high rates of crystallization.

The absence of porosity in castings at very low crystallization rates is due to diffusive elimination of hydrogen from the melt [283, 285]. Crystallization of the metal begins from the mold walls and proceeds in the direction toward the center of the casting. Since the solubility of hydrogen is lower in the solid metal than in the liquid metal, the hydrogen will be forced into the melt until its pressure has reached a critical value at which bubble formation becomes possible. Solubility in the liquid metal increases with increasing temperature, so that a flow of hydrogen from the basic body of the casting into the deadhead is set up. The casting may be found to be free of gas porosity even when there is a considerable hydrogen content in the melt if the hydro-

gen is eliminated from the melt by diffusion through its surface into the environment. As a result, the permeability of oxide films on the surface of the molten metal becomes particularly important.

The oxide films on molten aluminum are particularly difficult for hydrogen to permeate. Hence diffusive elimination of hydrogen from molten aluminum is very difficult or even totally impossible unless the oxide film is broken up in some way or its low permeability is modified.

Thus, it is reported in [186, 284] that the introduction of sodium into aluminum and aluminum alloys changes the properties of the oxide film on the melt surface, with the result that it becomes permeable to hydrogen. As a result, aluminum and aluminum alloys are effectively degasified in the seasoning process after injection of sodium.

With rapid cooling, the hydrogen forms supersaturated solid solutions, and porosity is again absent.

Liberation of hydrogen directly at the interface between solid and liquid phases is associated with the lower solubility of hydrogen in the solid phase. Passage of hydrogen from the solid to the liquid phase takes place by diffusion, and hence the higher the rate of advance of the crystallization front and the smaller the crysallization surface area, the less complete will be the transfer of hydrogen from the solid to the liquid phase and the lower will be the porosity.

In many respects, the development of porosity depends on the shape and dimensions of the liquid-solid transitional region. The larger the area of the interface between solid and liquid, and the slower the rate of growth of the solid phase, the more effectively will hydrogen be transferred from the solid to the liquid phase and the greater will be the gaseous porosity.

The transition region also contributes in a purely mechanical fashion to the development of gas-shrinkage porosity. The highly ramified dendrites make it difficult for the bubbles formed in the liquid to float upward and promote the development of porosity.

The nature of crystallization depends substantially on alloy composition. Alloys with a narrow temperature range of crystallization crystallize frontally and have little tendency to gas porosity. Alloys with a broad temperature range of crystallization crystallize in volume and have a strong tendency to gas porosity.

Gas bubbles form as a result of formation of seeds and subsequent growth. The critical size r_0 of a spontaneous gas bubble is determined by the Gibbs equation:

$$\frac{2\gamma}{r_0} = p + kTN \ln \frac{c}{c_0}, \qquad (15)$$

where γ is the specific surface energy; k is Boltzmann's constant; N is the number of atoms per unit volume; T is the absolute tem-

perature; C is the actual concentration of hydrogen in the metal; C_0 is the equilibrium concentration; p is the pressure.

It follows from this equation that with increasing supersaturation of the melt with hydrogen, spontaneous formation of gas bubbles is made easier. At the initial point in time, the hydrogen pressure in the bubble is very high, and it increases in dimensions until the equilibrium pressure p has been established in it in accordance with Sieverts' law $C = K\sqrt{p}$. The dimensions r of the equilibrium bubble are determined by

$$p = p_{ат} + p_{гидр} + \frac{2\gamma}{r}, \qquad (16)$$

where p_{at} is the pressure of the surrounding gaseous medium; p_{gidr} is the hydrostatic pressure.

Relation (16) is sometimes taken as a criterion for spontaneous seeding. Actually, this relation links the gas pressure in the bubble to its radius, and there is no direct relation to gas-bubble seeding. It simply indicates that the pressure in a small bubble is very high.

Spontaneous formation of critical seed bubbles due to statistical heterophase fluctuations is improbable, and hence any factor that facilitates seeding will promote porosity strongly. Phase interfaces may be such factors. Thus, for example, due to their high capillarity and limited wettability, solid surfaces almost always have pores that are unfilled by liquid. Bubbles form in these pores and gradually grow to a certain size governed by the crystallization conditions. Subsequently, they may tear away from the capillary on which they were germinated and float to the surface.

If there is much hydrogen in the metal, the hydrogen pressure in pores and cavities may be quite high. Since the strength of the metal is very low at high temperatures, the hydrogen may, under certain conditions, cause hot cracking in castings. G.A. Korol'kov and I.I. Novikov [440] showed, however, that hydrogen can lower the tendency of metals to hot shortness if it reduces linear shrinkage.

Hydrogen pores can form not only in the melt, but also in the solid metal, if the supersaturation is high enough.

According to a hypothesis of Talbot and Granger [419], this porosity might be called secondary porosity, to distinguish it from interdendritic porosity. Secondary porosity has been detected, for example, in aluminum [419]. If the hydrogen content in the molten aluminum or aluminum alloy is low enough, for example lower than 0.15 cm^3 per 100 g of metal, ingots poured by the continuous method are free of coarse interdendritic porosity. However, "secondary pores" with diameters of about 1 μ are observed in the cast metal. These pores are seeded immediately after freezing on imperfections and foreign inclusions or when the cast metal is heated. Their increase to the sizes observed in the

cast metal is due to supersaturation by vacancies. These pores are finally stabilized by hydrogen being forced out of the solid metal.

Secondary porosity also occurs when metals that dissolve little hydrogen in the solid state are bombarded by protons, e.g., on proton bombardment of beryllium or aluminum. Due to the low solubility of hydrogen in these metals, the solid solution is greatly oversaturated with hydrogen, with the result that gas pores form around any suitable seed. Since the supersaturation (C/C_0) is very great, it follows from the Gibbs equation (15), which applies not only to formation of bubbles in the liquid metal, but also to the solid metal, that the radius of the critical seeds may be exceedingly small. It was shown in [463] that the seeds of these pores may be accumulations of vacancies even smaller than 100 Å in diameter, dislocation loops formed during bombardment, or even grain boundaries. The pores grow until they have established an equilibrium pressure determined, on the one hand, by Sieverts' law, and, on the other, by the relation

$$p = \frac{2\gamma}{r}, \qquad (17)$$

where γ is the specific surface energy; r is the pore radius.

The pores grow as a result of vacancy diffusion into them. This process can take place only at rather high temperatures.

Pores may also be seeded without vacancies, in the motion of dislocations that are generated by Frank-Read sources that have been activated by supersaturation stresses. For growth of pores by this mechanism, it is necessary that

$$p - \frac{2\gamma}{r} > \frac{Gb}{r}, \qquad (18)$$

where p is the pressure; γ is the specific surface energy; G is the shear modulus; r is the pore radius; b is the Burgers vector.

It follows from this condition that formation of pores is possible for aluminum if $p \approx 6\left(\frac{2\gamma}{r}\right)$. This pressure, which is equal to 10^2 Mn/m^2 in a pore of 0.1-mm radius, is developed in aluminum at 373°K with a (mass) H_2 content of only 10^{-11}% ($\sim 10^{-7}$ cm^3/100 g). Thus, if hydrogen diffuses adequately into aluminum, pores have no difficulty in forming and growing.

In some cases, cast or annealed metal shows no secondary pores, because it has been difficult for them to seed. Heating the metal results in the appearance of secondary porosity. On subsequent heating of the metal, the pore volume increases, since the hydrogen enclosed in them is expanding. The pressure is lowered, and since the gas is distributed between the pores and the solid solution in accordance with Sieverts' law, the fraction of the total hydrogen content in the pores rises.

Local equilibrium between the gas pressure inside the pore

and the surface-tension forces acting upon it is maintained for each pore. Hence the steady-state pressure varies from pore to pore, depending on radius. Since the gas pressure is higher in small pores than in larger ones, smaller pores are unstable with respect to larger pores. Since hydrogen can diffuse easily in metal, the porosity is progressively concentrated into a smaller number of larger pores. The excessive porosity is generated inside the metal, and does not enter it from its exposed surface. It follows from the analogy with other problems that this process is associated with generation of vacancies on suitable sources. This factor complicates the behavior of the pores on heating. If a pore is located next to a working source of vacancies, it will be expanded readily. But if it is far from such a source, its growth will be impeded.

In some metals of high purity, pores expand much more rapidly on the basic grain boundaries than inside the grains. This is due to the fact that vacancies can form more easily at grain boundaries than from potential sources located inside grains, for example, from dislocation lines. There are a number of preferred positions for pores even inside the grains, and these are apparently related to secondary vacancy sources at subgrain boundaries or on submicroscopic particles of the second phase.

As the pores at the grain boundaries expand, the smaller pores inside the grains become unstable with respect to them. They become smaller, and the hydrogen in them diffuses into the pores on the grain boundaries. If the hydrogen content is high enough, the pores at the grain boundaries join to form cracks.

The situation is different in technically pure metals. In the less pure material, the influence of the main grain boundaries is not dominant, and is suppressed by branched interphase boundaries associated with numerous disperse particles of high phases.

Theoretical calculation of the behavior of pores on heating is quite complex, since a rise in temperature produces a number of effects that act in different directions:

1) the gas pressure in the pores rises in accordance with the gas laws;

2) the equilibrium internal hydrogen pressure in solution decreases;

3) the diffusion rate of the hydrogen increases;

4) vacancy sources are activated;

5) the rate of elimination of hydrogen from the specimens into the atmosphere rises;

6) the strength of the metal and, consequently, its resistance to increase in the size of the pores decrease.

Enlargement of the pores is due to the system's tendency to lower its free energy. Greenwood and Boltax [307] showed that the

rate of pore growth at constant temperature can be expressed by

$$\frac{dr}{dt} = DK\left(\frac{1}{r_{sr}^{1/3}} - \frac{1}{r^{1/3}}\right), \qquad (19)$$

where r and r_{sr} are the radius of the pore and the average pore size at a given time t; D is the diffusion coefficient; K is the constant in the Sieverts equation.

This equation was derived on the assumption that hydrogen is not eliminated from the specimen. This is not actually the case; in aluminum, for example, hydrogen is eliminated effectively from the specimen at temperatures above 573°K. Elimination of hydrogen from the specimen results in resorption and disappearance of pores. Small pores are resorbed first, since the rate of resorption of the pores is inversely proportional to the cube of their radii [308]. At high bombardment temperatures, no pores are formed at all, because the rate of diffusion of hydrogen is high and it is eliminated from the specimens into the atmosphere.

Similarly, secondary porosity is a hazard in the cast metal only in large-section ingots.

The molecular hydrogen pressure in structural discontinuities reaches extremely high values in electrolytic hydrogenation of metals that absorb hydrogen endothermically. In electrolytic hydrogenation, hydrogen ions are liberated at the surface of the metal. At certain electrolyte concentrations and current densities, the hydrogen-ion concentration at the cathode is equivalent to a hydrogen pressure of thousands of atmospheres at room temperature or at very high temperature and normal pressure. Solubility in these metals is relatively low at room temperature, so that the limit of solubility is reached rapidly. Hydrogenation does not stop with attainment of solubility in the metals. Diffusing through the metal, hydrogen ions move out of the metal lattice toward phase boundary surfaces, on the surfaces of microcavities, nonmetallic occlusions, or other collectors. Escaping from the metallic lattice into these collectors, hydrogen ions and atoms recombine to form hydrogen molecules. In sum, the hydrogen is, as it were, in a trap, since it can diffuse in the metal only in the atomic state; hydrogen molecules are not capable of diffusion.

As a result of the "trap effect," the pressure in gaps may reach several thousands and even tens of thousands of atmospheres, which results in blisters in the surface layer of the metal and cracks inside it.

Hydrogen present in pores under high pressure facilitates the formation and propagation of cracks on application of external stresses, and this promotes brittle fracture. The theoretical aspects of the development of this kind of brittleness are examined in the work of L.S. Moroz and T.E. Mingin [98, 99] in application to steel.

To explain the crack-germination mechanism, the authors in-

vestigate the stressed state near the surface of a pore under an internal hydrogen pressure and show that the stressed state that arises around a pore causes intensification of plastic-deformation inhomogeneity, leading to premature failure.

The embrittling effect of hydrogen due to its high pressure should manifest more strongly if the pores are wedge-shaped instead of spherical. Such cavities may form in plastic deformation of metals. L.S. Moroz and T.E. Mingin [131] did in fact observe that steel that was hydrogenated electrolytically after strain-hardening by 8-10% extension was considerably more inclined to irreversible hydrogen brittleness than was undeformed steel.

In metals that absorb hydrogen exothermically, this type of brittleness is not observed, since the internal hydrogen pressure is extremely small, even when its contents in the metal are high. Thus, the hydrogen pressure in collectors in titanium at 293°C will be 0.1 Mn/m^2 only at a 3.5% by mass content of H_2. At the same time, at considerably lower concentrations, of the order of 0.01% by mass of H_2, brittleness does result from this cause.

3. HYDRIDE HYDROGEN BRITTLENESS

Metals that absorb hydrogen exothermically form hydrides with them. The solubility of hydrides in these metals is rather high at elevated temperatures. With decreasing temperature, the solubility of the hydrides decreases, to become negligibly small at room temperature. Thus, the solubility limit for hydrogen at room temperature is 0.002% (by mass) for titanium [68], 0.0008 (by mass) for zirconium [69, 70] and $0.6 \cdot 10^{-7}$% (by mass) for uranium (at 373°K [71]). Since the solubility of hydrogen in these metals is negligible at room temperature, secondary hydride segregations are formed in them at very low hydrogen concentrations.

As a rule, hydrides are segregated in the form of thin lamellae during slow cooling and in the form of highly dispersed particles during quenching. Laminar segregations of the hydride phase frequently form along slip and twinning planes, although other orientations of the hydrides with respect to the matrix are also encountered. Thus, in titanium and α-titanium alloys [72], hydrides separate preferentially along the planes of the $\{10\bar{1}0\}$ and $\{10\bar{1}1\}$ systems, which are preferred slip planes at room temperature.

Segregation of hydrides results in hydrogen brittleness in metals. The following peculiarities are typical for brittleness of this kind.

Over a broad range of hydrogen concentrations, hydride inclusions do not influence the strength and plastic properties of metals when the tests are run at testing-machine crossbar speeds smaller than 10-20 mm/min. In other words, brittle failure does not appear if the tensile tests are run under the standard conditions of production practice.

The tendency to hydride brittleness rises with increasing rate of deformation, with notching, and with lowering of the test temperature. Hydride brittleness lowers impact strength most of

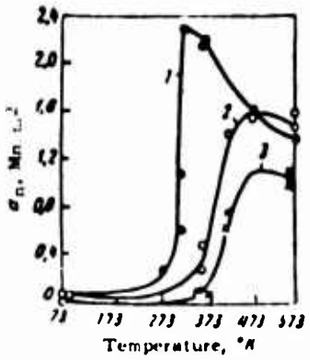

Fig. 14. Change in impact strength of titanium containing 0.035% (by mass) of H_2 as a function of test temperature [422]. 1) Smooth specimens; 2) notch radius 5 mm; 3) notch radius 2 mm.

all. Figure 14 shows, by way of example, data illustrating the variation of the impact strength of titanium containing 0.035% (by mass) of H_2 as a function of test temperature. The tests were conducted on cylindrical specimens 7 mm in diameter with circular notches 1.5 mm deep and radii of 5, 2 and 0.5 mm at the base of the notch. The data obtained in [422] indicate that lowering the test temperature embrittles titanium containing 0.035% (by mass) of H_2, and that the temperature of the plastic-to-brittle transition rises with increasing sharpness of the notch. The sharp drop in impact strength is accompanied by a change in the nature of the fracture. The fracture surfaces in brittle specimens indicate clearly that failure has propagated along interfaces between the hydride phase and the matrix. Thus, hydride lamellae in the microstructure are sources of Griffiths cracks, which develop on application of stresses due to the weak cohesion between the segregation and the ground phase and as a result of differences in their elastic and plastic properties. During deformation of hydrogen-saturated metals, the formation and propagation of cracks that form around hydrides is facilitated by internal tensile stresses, which arise at the ends of the hydride segregations due to the larger specific volume of the hydrides by comparison with the basic metal.

The stronger tendency of metals to hydride brittleness under the influence of notching, increased deformation rate, and lower temperature can be explained by positing that the hydrides have a certain plasticity but rather low tensile strength [45]. In tensile tests on smooth specimens, the normal stresses do not exceed the tensile strength, and the influence of hydrogen does not manifest under these conditions. Notching and raising the rate of deformation increase the normal stresses, leading to brittle failure. In addition, at high deformation rates, considerable stress concentration may arise in zones adjacent to ductile hydride segregations. On slow application of the load, there is time for the stresses to redistribute as a result of plastic deformation, and, as a result, no substantial stress concentration occurs.

The shape and manner of distribution of the hydrides in the metal has substantial influence on its plastic properties. It was shown in [7] that prolonged annealing of hydrogen-saturated titanium at 423°K converts the segregated titanium hydride to a more compact form, with the result that impact strength rises.

Thin lamellar segregations of titanium hydride, on the other hand, create considerably greater stress concentrations under tension, especially when the tests are run at high machine-crossbar speeds.

The shape of hydride segregations depends essentially on the size and shape of the macro- and microscopic grain structures, as well as on the rate of cooling [73]. With a fine-grained equilibrium structure, hydrides are segregated basically along grain boundaries in the form of highly compact and frequently irregularly shaped inclusions with a high thickness-to-length ratio. At low hydrogen concentrations, the compact hydrides along the grain boundaries do not form a continuous network of segregations, and in this case there is no distinct hydrogen embrittlement. At high hydrogen concentrations, the hydrides form an almost continuous network of segregations along the grain boundaries and, consequently, form more or less continuous lines for the advance of fracture, which results in a strong embrittling effect – one that is sharper than in the case of disordered segregations throughout the entire structure [74].

In a fine-grained structure, the hydrides are segregated in the form of extremely thin lamellae along certain crystallographic directions. Such lamellae are effective stress concentrators, and for this reason brittleness is more acutely in evidence than in the case of compact hydride segregations present in the same quantity.

It was shown in [7] that the impact strength of coarse-grained titanium with lamellar hydride segregations drops sharply when even thousandths of a percent of hydrogen are introduced. The impact strength of fine-granular titanium with compact hydrides remains practically constant up to 0.015% (by mass) of H_2, after which it drops off sharply.

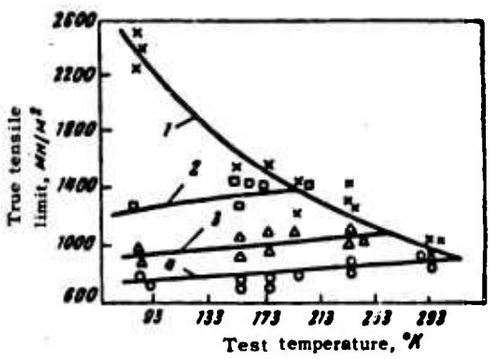

Fig. 15. True ultimate strength of titanium with various hydrogen contents, in % (by mass), as a function of test temperature. 1) Annealing in vacuum; 2) 0.012; 3) 0.035; 4) 0.060.

As we indicated earlier, the tendency to hydride brittleness increases with diminishing temperature. According to A.F. Ioffe's scheme, this effect is due to the fact that the tensile limit shows almost no change with diminishing temperature, while the shear limit rises sharply. At a low enough temperature, therefore, the tensile limit will be reached before the shear limit.

A.F. Ioffe's diagram was constructed from test results for the failure of rock salt at various temperatures. However, attempts to verify this scheme experimentally for metals encountered a number of difficulties related to obtaining an ideal brittle fracture in metals. The experimental data obtained by B.B. Chechulin and M.B. Bodunova [422] for hydrogen-saturated titanium confirm A.F. Ioffe's conception with high accuracy. Figure 15, which is based on their data, shows the variation of true tensile strength with temperature for titanium with various hydrogen contents. The strength of vacuum-annealed titanium rises steadily as the temperature is lowered to 77°K. The strength of hydrogenated titanium increases only until a certain temperature is reached, at which the tensile limit intervenes. On further lowering of the temperature, failure takes place by parting rather than shear, and, in accordance with the ideas of A.F. Ioffe, the tensile limit is virtually independent of temperature.

The experimental data obtained by B.B. Chechulin and M.B. Bodunova indicate that the tensile limit is lowered with increasing hydrogen content, so that the temperature of the plastic-to-brittle transition is raised.

Lenning, Spretnak and Jaffee [234] explain the increased tendency of titanium to hydride brittleness with diminishing temperature in terms of a change in the nature of deformation with temperature and the crystallographic correspondence of hydride segregations and slip and twinning planes. They submit that the hydrides apparently influence either the slip mechanism or the twinning mechanism, or both simultaneously. Since hydrogen embrittlement is particularly distinct at temperatures below 373°K, when twinning begins to play a major role in plastic deformation, it is possible that titanium hydrides have a stronger influence on the twinning mechanism than on slip.

The influence of interstitial impurities, including hydrogen, on twinning in niobium single crystals was studied in detail in [430]. Various quantities of nitrogen, oxygen, carbon and hydrogen were injected into the single crystals by diffusion.

The crystals were deformed by compression at the temperature of liquid nitrogen, with slow application of the load (from $0.85 \cdot 10^{-4}$ to $1.7 \cdot 10^{-4}$ sec^{-1}) or by impact. It was found that oxygen, carbon and nitrogen inhibit twinning. At concentrations from 0.03 to 0.1% (by mass), hydrogen, to the contrary, influences neither the critical twinning stress nor the frequency of twinning. In some specimens with higher hydrogen contents, lamellar segregations of niobium hydride were detected. It was shown in a supplementary series of experiments that niobium with 0.0681% H_2 has a single-phased structure at room temperature and a two-phased structure at 77°K, the latter represented by a solution of hydro-

gen in niobium and by segregations of niobium hydride. Fine cracks were detected at the joints between the twins and hydride lamellae. Thus, hydrogen in solid solution has little effect on the twinning mechanism, but in the form of hydrides it facilitates cracking and thereby contributes to brittle failure.

An analogous phenomenon was observed in hydrogen-saturated zirconium [313].

4. COLD SHORTNESS DUE TO DISSOLVED HYDROGEN

In some metals that absorb hydrogen exothermically, hydrides are formed at very high hydrogen concentrations, and brittleness arises in them not because of hydride segregations, but at lower hydrogen concentrations, due to the lattice distortions caused by interstitial hydrogens. This brittleness appears at high rates of deformation.

The nature of this brittleness should be the same as that of the cold-shortness of metals for which such interstitial impurities as oxygen, nitrogen, and phosphorus are responsible.

The most important experimental results of recent studies devoted to the problem of cold shortness is the definitely established fact that marked plastic deformation always precedes brittle failure, at least in zones near the failure. In any event, failure takes place by germination of cracks as a result of merging of several dislocations that have become blocked on some obstacle, and its propagation in the metal.

The difference consists in the fact that viscous fracture is determined by the propagation of cracks, and brittle fracture by their germination. In brittle fracture, the first crack to be germinated propagates throughout the entire volume of the metal, causing one piece of the specimen to break away from the other.

In viscous failure, the development of the crack is inhibited by plastic deformation of the metal at its head. The elastic energy that causes the crack to grow will then be scattered by plastic flow over secondary slip planes. Any factor that inhibits secondary slip will promote spalling. In hexagonal-lattice metals having one slip plane, secondary slip is excluded, so that scattering of elastic energy is made difficult; it is this that accounts for the strong tendency of such metals to brittle failure.

A different and more complex picture is observed in metals with the cubic structure, which have many slip planes.

Studies of recent years have shown that all metals with the cubic structure, including the body-centered ones, are not in themselves inclined to cold shortness; they are made cold-short by interstitial impurities. The difference between face-centered and body-centered cubic metals consists in a difference in sensitivity to the detrimental influence of these impurities. The interstitial pores in metals with the face-centered cubic structure are larger in size than those in body-centered metals, and for this reason the former are less sensitive to contamination by in-

terstitial impurities. For body-centered metals to be ductile at low temperatures, they must be purified of impurities more thoroughly than metals with the face-centered structure. If the impurity content in these metals is small enough, they will, like metals with the face-centered lattice, retain plasticity to temperatures near absolute zero. Thus, for example, iron that has been purified by zone melting was found to be plastic even at 4.2°K.

If the temperature of the metal is below a certain critical temperature, the impurities, forming Cottrell atmospheres, will block dislocations. As the temperature is lowered, the dislocations will be slowed down still further by the blocking atmospheres. When external stresses are applied to the metal, the dislocation sources will tend to break free of the impurity atmospheres. They are not released simultaneously, but a dislocation source that has broken away from the inhibiting action of an impurity cloud generates a somewhat larger number of dislocations, which may accumulate sufficiently in front of an obstacle to germinate a crack if no adjacent impurity-blocked dislocation source goes into operation and scatters elastic energy at the head of the accumulation.

Temperature fluctuations assist in freeing dislocations from impurity atmospheres. As the temperature decreases, the fluctuations become smaller and, finally, they become so insignificant that the time required to liberate the neighboring dislocation source will be greater than the time necessary for germination of a crack from a first accumulation. Brittle failure intervenes in such cases.

It appears that hydrogen brittleness of this type is observed in niobium and tantalum at room temperature. The first hydride-phase segregations in these metals, at least at room temperature, appear at hydrogen concentrations considerably higher than those that produce brittleness at high deformation rates.

Brittleness of this kind is observed in the β-titanium alloy VT15. The impact strength of this alloy at room temperature drops sharply at a content of about 0.25% H_2, although there are no traces of hydride-phase segregation in the structure of the alloy even at 0.5% (by mass) of H_2.

Unfortunately, there have been no detailed studies devoted specifically to cold shortness due to dissolved hydrogen, and the statements advanced above are hypothetical. But there is no doubt that brittleness of this kind is no serious danger. Lattice distortions due to solution of hydrogen are so insignificant that the cold shortness caused by the dissolved hydrogen appears at hydrogen concentrations far above those encountered under production conditions.

Manuscript Page No.	Transliterated Symbols
44	ат = at = atmosfernyy = atmospheric
44	гидр = gidr = gidridnyy = hydride
47	ср = sr = sredniy = average

Chapter 3

HYDROGEN BRITTLENESS OF THE SECOND KIND

1. IRREVERSIBLE BRITTLENESS OF THE SECOND KIND

The hydrogen brittleness that develops at low deformation rates may be due to decay processes taking place in hydrogen-supersaturated solid solutions under the influence of applied stresses. Brittleness of this kind may be observed in metals that form hydrides with hydrogen. In these systems, the solubility of the hydrides in the metal falls off sharply as temperature is lowered, as is shown schematically in Fig. 3a (see page 9). At hydrogen concentrations above the solubility limit, the structure of the alloy is represented at equilibrium by a solid solution of hydrogen in the metal and by hydride segregations. These hydride segregations lead to the hydride brittleness considered in the preceding section, which appears at high deformation rates.

When the hydrogen concentration in the metal does not exceed the maximum solubility (see point a on Fig. 3a), the metal can be heated to a temperature, for example to T_1, at which the hydrogen will be in solid solution. Generally speaking, heating should be carried out in a closed space, with the hydrogen pressure in it maintained at the level corresponding to equilibrium at the hydrogen concentration in question; the pressure must therefore be varied with temperature. If hydrogen losses through the specimen surface are excluded and the equilibrium pressure is not too high, these precautionary measures are taken automatically.

If the hydrogen concentration in the metal is not too high, a solid solution saturated with hydrogen is fixed in the specimens during quenching. In this state, the metal is not inclined to hydrogen brittleness at high deformation rates, but if plastic deformation takes place slowly, the solid solutions decay, with formation of thin lamellar hydride segregations. Subsequently, the mechanism of this decay is similar to that of hydride brittleness of the first kind, as described above.

Since hydrogen diffusion takes place at high rates in metals, the hydride may be partially segregated from the solid solution even at hydrogen concentrations below the maximum solubility a during quenching from the single-phase region, e.g., from temperature T_1. In this case we observe hydrogen brittleness even at high and low deformation rates.

The excess hydride segregations, which are, as a rule, in the lamellar form, are a cause of hydrogen brittleness in metals at

high deformation rates, while the hydrogen-supersaturated solid solution causes brittleness at low deformation rates.

The possibility is not excluded that processes resulting in hydrogen brittleness even without formation of hydride-phase segregations may advance concurrently with the hydride brittleness that appears at low deformation rates.

For example, hydride brittleness is observed in α-titanium alloys at low deformation rates. By way of example, Fig. 16 shows the influence of hydrogen on the mechanical properties of VT5-1 alloy after quenching from 873°K and after slow cooling from the same temperature with the furnace. The necking ratio of alloy VT5-1 in the annealed state drops sharply with introduction of hydrogen when tensile tests are conducted at high speed, while it shows practically no change in slow tests. The necking of alloy VT5-1 in the quenched state, on the other hand, diminishes very slightly after introduction of hydrogen in fast tests, but it drops sharply in low-speed tests if the hydrogen content exceeds 0.015% (by mass).

Thus, in the quenched state, the α-titanium alloy VT5-1 is more inclined to hydrogen brittleness at slow tensile-machine-crossbar speeds than at high speeds. This kind of brittleness can also be observed in other metals, notably zirconium.

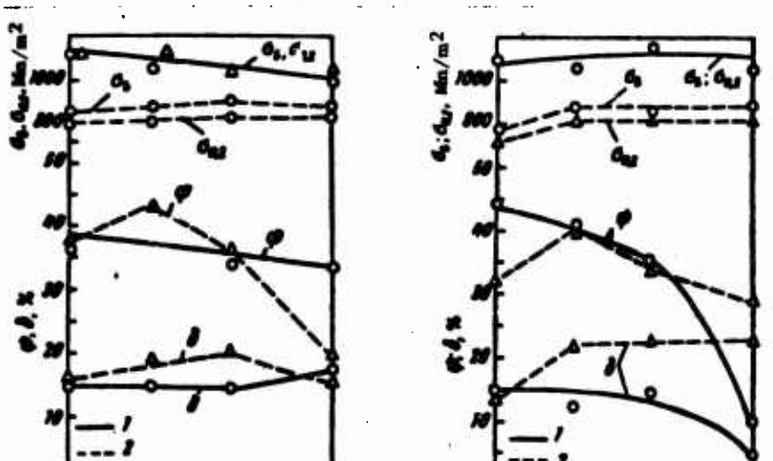

Fig. 16. Influence of hydrogen on the mechanical properties of the α-titanium alloy VT5-1 after quenching (a) and after cooling with the furnace (b) in tests with various deformation rates in mm/min: 1) 20; 2) 0.4.

Investigation of the microstructure of annealed and quenched specimens of VT5-1 alloy after failure showed that the hydrides are oriented at random in annealed specimens for any deformation rate and in quenched specimens tested at high deformation rates. In quenched specimens tested at slow speeds, a considerable quan-

tity of hydrides oriented perpendicular to the axis of tension was detected near the failure surface. The same type of oriented hydride segregation had been observed in [391-393].

Marshall and Louthan [391] showed that in zirconium and zirconium alloys acted upon by external stresses, hydrogen is liberated from supersaturated solution in the form of lamellae that are oriented in a definite manner with respect to the operating stresses. The hydride lamellae have a tendency to orient perpendicular to tensile stresses; they extend parallel to compressive stresses. Such orientation of the hydrides is more favorable from an energy standpoint. The density of zirconium hydride is lower than that of zirconium. Hence the segregation of hydride lamellae perpendicular to the tensile stresses relieves stresses in the matrix and thereby lowers the system's free energy.

They also showed that in tensile tests, hydride lamellae perpendicular to the tension axis embrittle Zircalloy-2 sharply, while lamellae oriented parallel to tensile stresses have little influence on its properties under the conditions of tension.

Hydride segregations oriented with respect to acting stresses are observed when the stresses exceed a certain critical value. This critical value depends on the technology used in making the specimens and on their orientation with respect to the direction of action of the stresses.

We may assume that stress-oriented decay of supersaturated solutions of hydrogen in zircalloys is an activated process, and that the critical stress is determined by the activation energy of this process. Louthan [393] showed that hydride segregations oriented with respect to stresses are also observed in titanium.

Since hydrides are segregated along quite definite planes of the habit, we can control the texture of the material to change its sensitivity to operating-stress-oriented hydride segregation. The material will be most sensitive to oriented decay if the texture in it is such that the planes of the hydride habit are perpendicular to the operating tensile stresses. Conversely, the material will have little tendency to oriented hydride segregation if the habit planes are oriented at small angles to the direction of action of the tensile stresses.

It was shown experimentally in [457] that the orientation of hydrides in zircalloys is influenced not only by the position of the specimen with respect to the external loads, but also by aspects of the process by which the material was prepared. Past deformation of the alloy by rolling, forging, drawing or stretching results in the appearance of a preferential orientation of the hydride habit planes. Hence the hydrides are forced to segregate not perpendicular to the tensile stresses, but along existing planes of the habit. Thus, a well-directed technology for obtaining semifinished pieces from zircalloy and manufacturing the elements of the finished structures may alleviate the detrimental influence of oriented hydride segregation.

Similar stress-oriented hydride segregations can be observed

in any system in which hydrides are formed.

Moreover, stress-oriented segregations of second phases are possible in any system in which the specific volumes of the phases differ.

2. GENERAL CONCEPTIONS OF THE MECHANISM OF REVERSIBLE HYDROGEN BRITTLENESS OF THE SECOND KIND

Of all of the forms of hydrogen brittleness in metals, that of greatest scientific interest is the brittleness that appears at low rates of plastic deformation with hydrogen concentrations

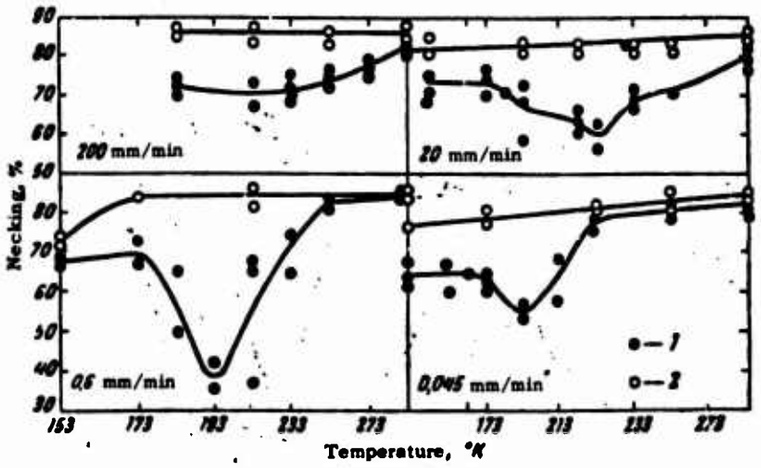

Fig. 17. Influence of temperature and test speed on plasticity of alloy of iron with 0.5% Cr, saturated with hydrogen (1) and with no hydrogen (2) [101].

that are rather high but not higher than the solubility limit at the temperature of the experiment. This brittleness is governed by processes that unfold during plastic deformation in solid solutions of hydrogen in the metal.

This type of brittleness was first observed in steels.

The basic laws governing reversible hydrogen brittleness in steels can be illustrated by data for a steel with 0.5% Cr (Fig. 17). These studies were made on specimens 3 mm in diameter with a gauge length of 75 mm, into which 2 cm^3 of H_2 had been injected electrolytically for each 100 g of metal.

The results obtained by V.Ya. Yagunova and K.V. Popov confirm the data of earlier investigations, which indicated that the hydrogen brittleness of steel appears only in a certain temperature range. The plasticity minimum of steels with chromium is shifted toward higher temperatures as the deformation rate increases. It is interesting to note that the hydrogen brittleness of a steel with 0.5% Cr is more distinct at a deformation rate of 0.6 mm/min

than at 0.045 mm/min.

Hydrogen brittleness of this type was observed more recently in (α + β) titanium alloys [61, 254-257]. The hydrogen brittleness of (α + β) titanium alloys, like that of steels, appears only at low deformation rates. In [238, 239, 248, 256, 261], this relationship was confirmed on Soviet (α + β) titanium alloys.

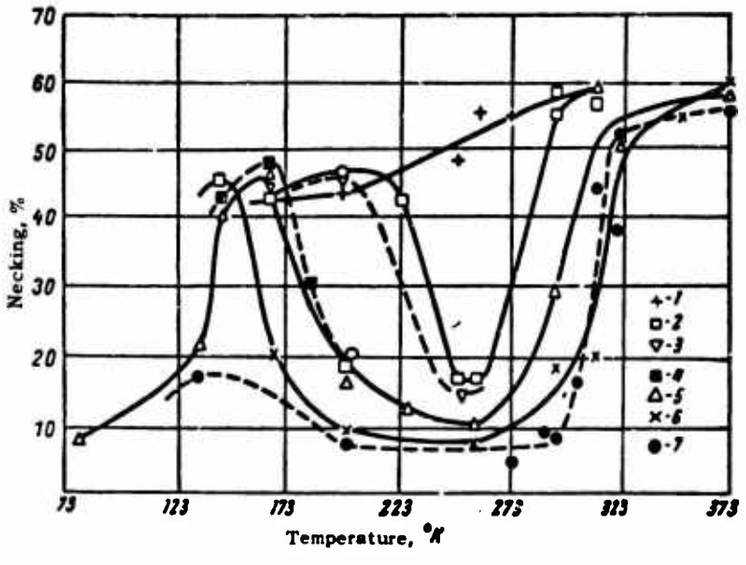

Fig. 18. Influence of temperature on necking of alloy Ti-140A with 0.0375% H_2 in mechanical tensile testing at various deformation rates, mm/min: 1) 25.4; 2) 12.7; 3) 6.35; 4) 2.54; 5) 1.27; 6) 0.64; 7) 0.13.

The influence of temperature on the hydrogen brittleness of (α + β) alloys was studied by Kotfila and Erbin [139] and somewhat later by Ripling [255], who detected restoration of plasticity of hydrogen-saturated (α + β) alloys during tests at relatively low temperatures. This phenomenon was investigated in detail by Schwartzberg, Williams and Jaffee [264] on the alloy Ti-140A (2% Cr, 2% Mo, 2% Fe, rest Ti) with a stabilized (α + β) structure.

The results of mechanical tests run on smooth specimens at various stretching speeds and various temperatures indicated that the necking of the vacuum-annealed alloy diminishes smoothly with decreasing temperature, with practically identical curves corresponding to the various stretching speeds.

A completely different picture is observed for the alloy containing 0.0375% H_2 (Fig. 18). At high stretching speed (of the order of 25.4 mm/min), no embrittlement is observed anywhere in the temperature range. Embrittlement is observed at lower stretching speeds, and is the more distinct the lower the rate of deformation. This brittleness is found in a certain temperature range, and is developed most strongly at temperatures of the order of 223°K.

At lower test temperatures, the necking increases sharply and

reaches values practically equal to or even higher than those that are characteristic for the vacuum-annealed alloy at the same deformation speeds. The temperature of plasticity recovery is lower the lower the stretching speed; only at a stretching rate of 0.13 mm/min are the properties recovered very poorly.

Somewhat different relationships were observed for the (α + + β) titanium alloy VTZ-1. Tests were run on forged material obtained from a production ingot that was subjected to double annealing after hydrogenation: 870°C for 1 hour, cooling in air to 650°C, 1 hour of holding, cooling in air. The tensile test was run on smooth specimens on a mechanically driven machine. The hydrogen content in the specimens varied from 0.002 to 0.1% (by mass).

By way of example, Fig. 19 shows the effect of test temperature on the mechanical properties of VTZ-1 alloy with 0.05% H_2 at various stretching speeds. As these data show, necking drops sharply at a stretching speed of 0.4 mm/min from 35% at 295°K to 4% at 255°K. As the temperature is lowered further to about 233°K, the necking remains unchanged, of the order of 5%, and at still lower temperatures it rises slightly, to reach 9% at 203°K. At a deformation rate of 4 mm/min, the necking varies with temperature in approximately the same way as at the 0.4-mm/min speed. The only difference is that the temperature at which necking begins to decrease sharply and the temperature corresponding to the plasticity minimum are shifted toward higher values, 285 and 267°K, respectively. At a stretching rate of 20 mm/min, the necking decreases in a very narrow temperature range from 233 to 273°K.

Elongation is approximately the same for all three speeds in the temperature range from 293 to 230°K, and decreases slightly at lower temperatures.

It was at first assumed that hydrogen embrittleness at low deformation rates was characteristic only for (α + β) titanium alloys, but later experiments showed that both α- and β-titanium alloys are inclined to this kind of brittleness. By way of example, Fig. 20 shows the influence of hydrogen on the mechanical properties of the Soviet β-titanium alloy VT15 after quenching in water from 780°C.

At a high deformation rate, of the order of 20 mm/min, the plasticity of the quenched VT15 alloy remains high over the entire temperature range from 213 to 293°K. At a low deformation rate, of the order of 0.4 mm/min, necking decreases sharply at first as the temperature is lowered. This decrease takes place in a narrow temperature range. If we take the point at which necking has decreased by half as the upper temperature of the appearance of hydrogen brittleness, these temperatures are 281, 275 and 265°K for hydrogen concentrations of 0.05, 0.03 and 0.015% (by mass), respectively. Thus, with increasing hydrogen content, the upper limit of the onset of hydrogen brittleness rises. At temperatures around 243°K, the plasticity of the hydrogenated specimens is restored. At temperatures from 243 to 213°K, the necking of VT15 alloy amounts to approximately 40-50% for all of the hydrogen concentrations studied.

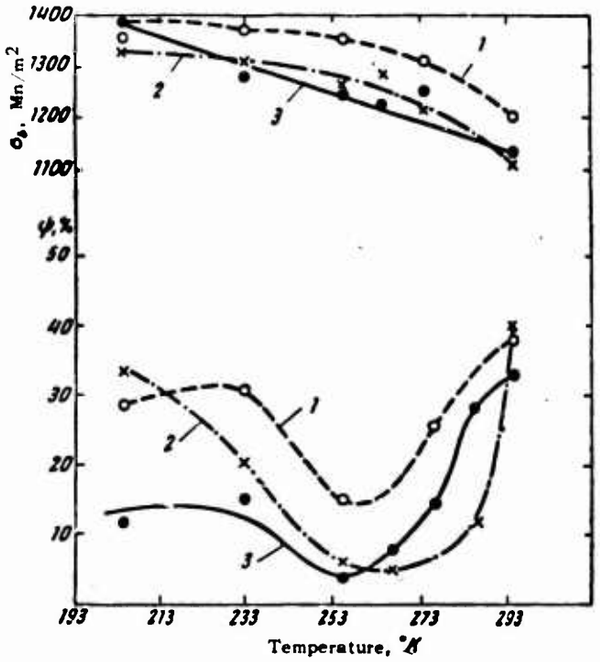

Fig. 19. Influence of temperature on the mechanical properties of the (α + β) titanium alloy VT3-I with 0.03% H_2 in tests at various speeds, in mm/min: 1) 20; 2) 4; 3) 0.4.

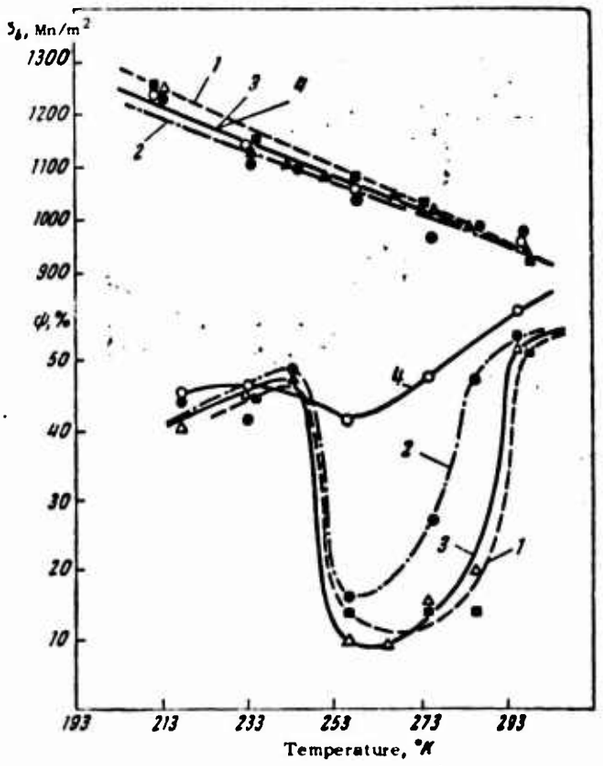

Fig. 20. Influence of temperature on the mechanical properties of the β-titanium alloy VT15 with the following H_2 contents, in %: 1) 0.05; 2) 0.015; 3) 0.03; 4) 0.002.

It is a quite commonly held opinion that metals with the face-centered lattice and, in particular, nickel, are not inclined to hydrogen brittleness at low deformation rates. Thus, for example, we read in Cotterill's paper [9]: "...we may not expect that a low deformation speed will produce a hydrogen-embrittlement effect (of the type observed in steel) in any metals that have either a close-packed hexagonal or a face-centered lattice (with the possible exception of beryllium)." This is not actually the case. As was first shown by Troiano et al. [95] and later by Boniszewski and Smith [102], nickel and its alloys are inclined to hydrogen brittleness in slow deformation, although perhaps to a lesser degree. To illustrate the tendency of nickel to hydrogen brittleness, Fig. 21 shows the effect of test temperature on the mechanical properties of electrolytically hydrogenated nickel for two stretching speeds for comparison with the properties of nickel not containing hydrogen.

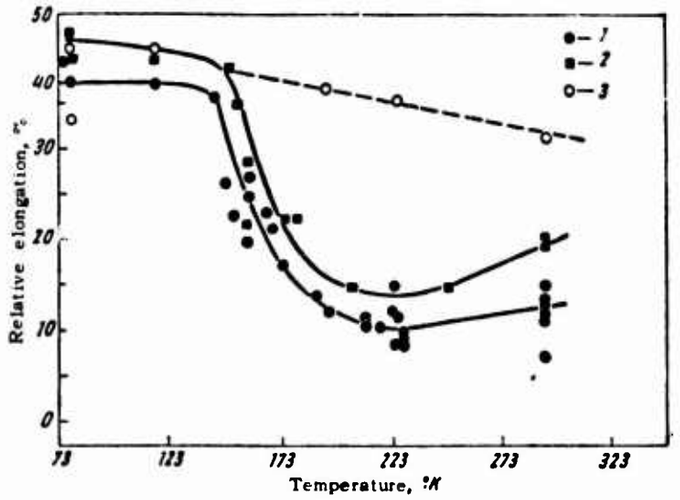

Fig. 21. Influence of temperature on the mechanical properties of unhydrogenated and electrolytically hydrogenated nickel at the following deformation rates, sec^{-1}: 1) $3.33 \cdot 10^{-4}$; 2) $1.67 \cdot 10^{-3}$; 3) nickel without hydrogen.

Reversible hydrogen brittleness has been detected in many transition metals in recent years. In all cases, the following relationships are characteristic for reversible hydrogen brittleness of the second kind:

1. This kind of brittleness appears in a certain temperature range, which depends on the rate of deformation, the nature of the alloys, and their chemical composition.

2. With increasing rate of deformation, the temperature range of plasticity decrease becomes narrower, the plastic characteristics improve, and if the speed exceeds a certain limit, brittleness is not observed.

3. The temperature of the transition from viscous to brittle

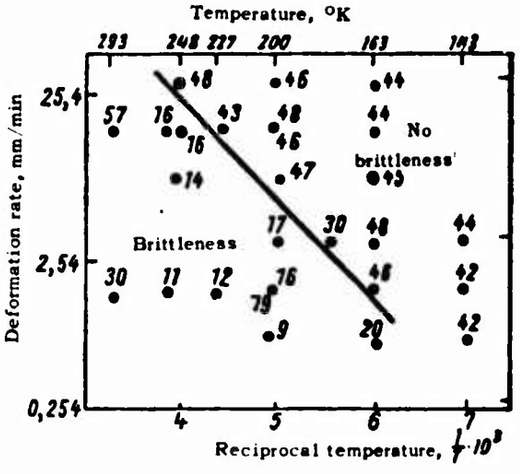

Fig. 22. Necking (numerals on figure) as a function of experimental conditions for Ti-140A alloy with 0.0375% H_2.

failure rises with increasing hydrogen content.

4. Failure takes place along grain boundaries at low deformation speeds.

5. Hydrogen has little influence on yield point and elongation until the neck is formed, and inhibits necking very strongly.

Analysis of experimental data for a number of metals indicates convincingly that reversible hydrogen brittleness is controlled by hydrogen diffusion.

The decisive role of hydrogen diffusion in the development of reversible hydrogen brittleness of the second kind is confirmed by the fact that the activation energy of plasticity recovery at low temperatures is identical for many metals with the activation energy of thermal diffusion of hydrogen. On comparison of these two processes, however, difficulties arise in connection with the fact that hydrogen diffusion has been studied only at high temperatures for many metals. But recent studies have shown that extrapolation of the high-temperature diffusion data to low temperatures is not quite admissible, since imperfections of crystal structure may have a substantial influence on hydrogen diffusion at low temperatures.

These difficulties can be appreciated from data obtained for the (α + β) titanium alloy Ti-140. The experimental data shown for it in Fig. 18 can be presented somewhat differently, with the logarithm of stretching speed and the reciprocal of absolute temperature as coordinates, as has been done in Fig. 22. Points corresponding to the experimental conditions have been entered on this diagram, next to numerals that indicate the necking values obtained under these conditions. The region with high values of

necking is separated by a straight line from the region with low values. The slope of this line gives the activation energy of the plasticity-recovery process. This energy is found equal to about 3 kcal/g-atom (12.6 kj/mole) for all of the hydrogen concentrations investigated. Thus, the plasticity-recovery process is determined not by hydrogen concentration, but by diffusion processes.

It is interesting to compare the activation energy obtained with the activation energy for the diffusion of hydrogen. Wasilewski and Kehl [55] found that in the 923-1153°K range, the activation energy for diffusion of hydrogen in the unalloyed α-phase is 12.4 kcal/g-atom (52 kj/g-atom), while for diffusion in the unalloyed β-phase, it is 6.64 kcal/g-atom (28 kj/g-atom). Maringer found by the internal-friction method that at 100°K the activation energy for diffusion of hydrogen in the β-phase of the alloy Ti + + 8% Mn is around 6 kcal/g-atom (25 kj/g-atom). There are no other data concerning the hydrogen activation energy in α- and β-phases.

The discrepancy between the activation energies for diffusion and recovery of plasticity can be explained in two ways. Firstly, the diffusion rate of hydrogen in the β-phase of alloy Ti-140A may differ substantially from the diffusion rate in the β-phase of the alloy Ti + 8 Mn. Secondly, at low temperatures, the diffusion of hydrogen in titanium and its alloys may, in contrast to high temperatures, depend substantially on structural factors.

If we assume that the diffusion of hydrogen in the β-phase of titanium at low temperatures is determined by the same equation as at high temperatures, then substitution of 3 kcal/g-atom (12.6 kj/mole) for the activation energy given by Wasilewski and Kehl results in a diffusion coefficient 10^4 times larger than with an activation energy of 6.6 kcal/g-atom. In other words, the processes that lead to plasticity recovery take place 10^4 times more rapidly than the diffusion of hydrogen in the β-phase as calculated from the equation obtained at high temperatures. It is quite possible that fixation of nonequilibrium vacancies takes place in titanium alloys, resulting in a substantially higher rate of diffusion.

The reverse has been observed in steel. The activation energy of thermal diffusion of hydrogen at low temperatures is considerably higher than at high temperatures, so that the rate of diffusion at temperatures below 473°K is found to be substantially lower than the values extrapolated on the basis of high-temperature data. It is difficult to judge at the present time whether the difference in the behavior of steel and Ti-140A alloy is a consequence of different kinds of hydrogen absorption or of other factors. There is no doubt that more detailed study of the low-temperature hydrogen-diffusion coefficients and the activation energies of the processes that result in hydrogen brittleness would be very useful in solving this problem.

3. INFLUENCE OF HYDROGEN ON CRACK PROPAGATION IN METALS

A number of studies of steel, titanium and titanium alloys

have shown that hydrogen facilitates the germination and propagation of cracks in metals.

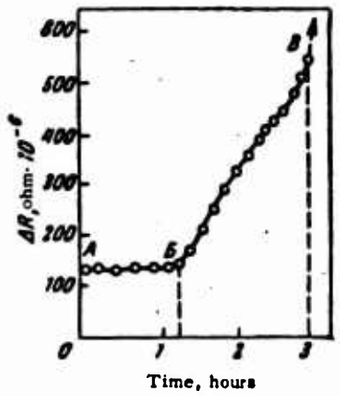

Fig. 23. Change in resistance of hydrogenated notched specimen of SAE4340 steel as a function of loading time at room temperature.

Circumstantial investigations of the germination and propagation of cracks in steel were conducted by Troiano [88-90] by measuring the resistance of a specimen as it was loaded. These studies showed that the failure process of hydrogenated specimens consists of three stages: a) an incubation period, b) germination of the crack and its comparatively slow propagation and c) rapid propagation of the crack across the remaining impact section of the specimen.

By way of example, Fig. 23 shows the variation of resistance in a hydrogenated steel specimen as a function of loading time in tests conducted at room temperature. These data indicate that on application of a static load, the resistance of the specimen rises to the value indicated by point A. This resistance increase is due to the elastic and plastic deformation of the specimen due to the actual application of the load. At first, the specimen's resistance does not change with increasing loaded time (segment АБ). The processes leading during the incubation period to germination of the cracks take place within solid solutions of hydrogen in the metal, without disturbing the continuity of the metal.

At the time corresponding to point Б, the crack germinates and propagates slowly across the section of the specimen, with a concurrent comparatively slow but steady increase in resistance. At point В, the slow propagation of the crack is supplanted by rapid propagation over the entire remaining cross section of the specimen, at a rate comparable with the speed of propagation of elastic waves.

The incubation period is a very important characteristic, one that determines the conditions of appearance of hydrogen brittleness. At the same time, it enables us to appraise the combination of load and hydrogen content that will not lead to any harmful disturbances in the metal's structure if the product's working time does not exceed the incubation period.

The length of the incubation period depends primarily on the applied stresses. At stresses higher than the short-term strength limit, the specimen breaks practically instantaneously, and the incubation period is zero. With decreasing magnitude of the applied stresses, the incubation period becomes longer.

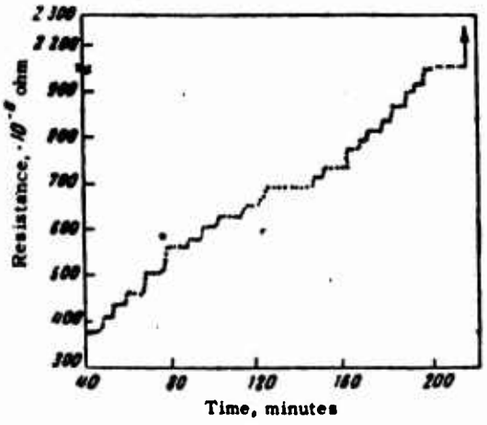

Fig. 24. Increase in resistance of hydrogenated specimens of alloy Ni + 20% Cu + 2% Al as a function of time of action of constant load.

The incubation period decreases sharply with increasing hydrogen content in the steel. The crack germinated at the end of incubation begins to propagate spontaneously, without any increase in the external stresses. The rate of propagation of the crack in the second stage increases with increasing hydrogen content in the specimens.

Careful study [89] showed that the second-stage crack develops stepwise. Curves illustrating the dependence of resistance in hydrogenated specimens on time of stress application resemble staircases (Fig. 24). Throughout the second stage, therefore, the crack grows in alternating incubation periods and times of almost instantaneous growth by a certain finite increment. The same type of crack growth in hydrogenated steel specimens was reported by Ya.M. Potak and O.P. Breslavtseva [91].

Analysis of the experimental data shows that the processes resulting in premature failure of hydrogenated specimens under static load are diffusive in nature. This conclusion is confirmed by the following experimental fact [89]. Steel specimens were held for 20 min under the load at which the incubation period was 30 min. Then the specimens were unloaded and held at room temperature for a day. This operation was repeated four times on the same specimens, but resistance measurements showed that no cracks had been germinated in them. Consequently, the total incubation period was 80 min. This indicates reversibility of the processes leading to failure. Under the influence of applied stresses, hydrogen diffuses to points at which germination of a crack is possible, and if its local concentration exceeds the tolerable values, the crack opens. If, on the other hand, the stresses are re-

moved before the crack has formed, thermal motion eliminates the segregation at the potential point of crack germination.

An investigation conducted in [266] of the germination and propagation of cracks in ($\alpha + \beta$) titanium alloys on the basis of the resistance increase of the specimens indicated that under static load, like steel, these materials fail by germination of a crack and its controllable growth. The changes that take place in the materials under constant static load before formation of the crack are reversible as long as there is no marked plastic deformation – indicating hydrogen diffusion controlled by the applied stresses.

In [87], the influence of hydrogen on the tendency of titanium to crack propagation was evaluated on the basis of the work done in propagating it. The ability of a crack to propagate increases as the work expended on its propagation decreases. This work was determined graphically from a plot of load vs. deflection obtained in static bending tests on notched specimens. The work necessary for propagation of the crack was quantitatively equal to the area of the region of the diagram traced after formation of the crack.

Figure 25 presents test results for notched titanium specimens with various hydrogen contents and steel SKhL4 according to L.S. Moroz et al. [87]. It follows from these data that low-strength titanium ($\sigma_{0.2} < 450$ Mn/m^2) with a small hydrogen content [less than 0.01% (by mass)] is somewhat inferior as regards this characteristic to alloy steels of the same strength at temperatures above 253°K but superior to them at low temperatures. However, the injection of small quantities of hydrogen facilitates crack propagation substantially in titanium.

In [137, 138], the time to appearance of cracks was used as a basis for judging the influence of hydrogen on the tendency of titanium alloys to form cracks under static long-term bending. Study of the tendency of metals to cracking by the static-bending method is based on the acceleration of the cracking process in metal under the influence of long-acting tensile stresses. Creation of tensile stresses promotes the germination and propagation of cracks in three ways:

a) such a stressed state in itself promotes opening of cracks;

b) stresses cause decay of supersaturated solutions, with segregation of embrittling phases;

c) directional diffusion of hydrogen from compression to tension regions arises.

The tests were run by bending specimens lying on two open supports with a force applied at the center of the specimen. The tests were conducted at first in three variants. In the first, the specimens were given a deflection corresponding to stresses in the tension layer of the specimen equal to 0.8 of the alloy's yield point in bending. In the second and third variants, a de-

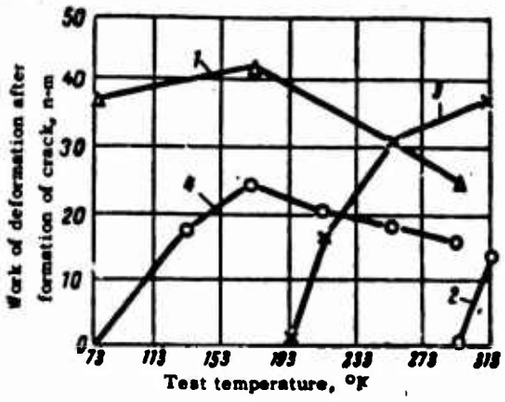

Fig. 25. Influence of static-bending test temperature on work of deformation after formation of cracks: 1) titanium with $\sigma_{0.2}$ = = 440 Mn/m^2; 0.004% H_2; 2) titanium with $\sigma_{0.2}$ = 560 Mn/m^2; 0.0125% H_2; 3) same as 2, after vacuum annealing at 1173°K; 4) steel SKhL4; $\sigma_{0.2}$ = 560 Mn/m^2.

flection corresponding to tension-layer stresses of 0.5 of the yield point was created at first, and then the deflection was increased by 0.1 mm every 5 days in the second variant and by 0.2 mm daily in the third. If failure had not occurred after 40 days in the third-variant tests, the deflection was not increased further, and the specimens were held to failure at the deflection that had been established at 40 days. All specimens were inspected daily with a binocular magnifier to determine the time of appearance of a crack at the surface.

The initial deflection was determined by the formula

$$f_0 = \frac{K\sigma_{\tau\,(изг)}\,l^2}{6Eh},$$

where K = 0.8 and 0.5 for tests by the first, second and third variants, respectively; $\sigma_{t(izg)}$ is the yield point in bending; l is the specimen gauge length; E is the elastic modulus; h is the specimen thickness.

It was found that tests by the second and third variants are more sensitive and take less time than those by the first; they were therefore taken as the basic test method.

Tests carried out by the method adopted indicated that hydrogen promotes formation of cracks in titanium and its alloys. Titanium alloys with both the α and the (α + β) structure fail prematurely at hydrogen contents above a certain critical value [of the order of 0.01 + 0.015% (by mass)]. In static bending, diffusion processes take place in the course of time in all titanium alloys containing high hydrogen concentrations and lower the metal's ultimate strength.

It is very important that the presence of a hydride phase or hydride segregation is not the decisive cause of premature failure under the influence of applied stresses under these loading conditions. Not only in ($\alpha + \beta$) titanium alloys, but also in α-alloys, comparatively speedy germination and propagation of cracks can be observed even in the absence of a hydride phase.

The level of the metal's plastic properties has a strong influence on the tendency of titanium and its alloys to form cracks in static bending. Increasing the nitrogen and oxygen contents in these alloys contributes to the formation of cold cracks by lowering plasticity and increasing strength.

4. ANALYSIS OF THEORIES OF REVERSIBLE HYDROGEN BRITTLENESS THAT HAVE BEEN PROPOSED FOR METALS THAT ABSORB HYDROGEN ENDOTHERMICALLY

A number of theories of hydrogen brittleness have been proposed to explain the relationships described above. As a rule, these theories have been elaborated for a single quite specific metal, although they were based on assumptions that made it possible to extend them to other similar metals. Thus, for example, theories proposed for steel can be extended to a number of metals that absorb hydrogen endothermically.

The hydrogen-brittleness theories that have been proposed for steel can be classified into three groups [8]:

1) theories of molecular pressure,

2) adsorption theories,

3) maximum-triaxial-stress theories.

A theory of hydrogen brittleness based on the pressure of molecular hydrogen was first proposed by Zappfe and Sims [103, 104]. In their opinion, the hydrogen brittleness of steel is related to the pressure of molecular hydrogen that has accumulated in collectors, which may be so high (of the order of several tens of thousands of atmospheres) that the tensile stresses that they produce exceed the elastic limit of the steel, leading to deformation of the metal and, in the final analysis, formation of cracks.

The decrease in the tendency of steel to hydrogen brittleness with increasing deformation rate and decreasing temperature is explained as follows. In plastic deformation, the dimensions of submicroscopic pores increase, with the result that the hydrogen pressure in them diminishes. If deformation is slow, the hydrogen has time to diffuse from the metal into microcavities and maintain high pressure in them until failure occurs. If, however, deformation is fast, the hydrogen does not have time to maintain high pressure in the micropores and hydrogen brittleness vanishes. As the test temperature is lowered, the diffusion rate of the hydrogen atoms decreases and, finally, becomes so low that it cannot sustain high pressure in the pores; brittleness disappears.

The molecular-hydrogen theory was subsequently refuted by the

critiques of a number of authors. Thus, for example, the hypothesis that pore hydrogen pressure is a decisive factor in the tension process is negated by data obtained in the study of Ya.M. Potak and O.P. Breslavtseva [91].

V.A. Yagunova and K.V. Popov [101] also note that the molecular-pressure theory cannot satisfactorily explain the increase in the plasticity of hydrogenated steel at temperatures above a certain critical limit. The plasticity increase with rising test temperature could be explained from the premises of this theory if the hydrogen had time to escape from the steel into the atmosphere during stretching at temperatures above the critical limit as a result of acceleration of diffusion processes. However, experiments indicate that the hydrogen content in specimens undergoes no marked change during a time considerably longer than that of the test.

Ya.M. Potak and O.P. Breslavtseva [91] present another argument against this theory. According to the work of Ludwig, N.N. Davidenkov, et al., rendering a ductile metal brittle requires creating triaxial tension capable of raising the yield point to the level of the tensile limit. The internal hydrogen pressure in submicroscopic pores creates in the metal surrounding them a stressed state that can be characterized as a combination of radial compression and biaxial tension.

The considerations given above are strictly valid for a spherical pore. If the pore had sharp ends, like those of cracks germinated by a dislocation mechanism, a triaxial stressed state would arise at a certain distance from it.

Theories of high molecular hydrogen pressure cannot satisfactorily account for a number of fine details of reversible hydrogen brittleness, for example, the type of fracture in hydrogenated steel under static load.

It must not be concluded on the basis of the above critical remarks that molecular hydrogen pressure plays no part whatsoever in the development of hydrogen brittleness. First of all, as stated above, irreversible hydrogen brittleness may develop at a high enough internal hydrogen pressure. In addition, high molecular hydrogen pressure must be an essential, if not a decisive factor in any mechanism of reversible hydrogen brittleness.

The theory of molecular hydrogen pressure was subsequently improved. According to recent conceptions [117, 118], protons form Cottrell atmospheres on dislocations, and these are entrained by moving dislocations during plastic deformation. If a dislocation with a Cottrell cloud reaches a collector, some of the protons will penetrate into the collector and be converted there into molecular hydrogen, raising the pressure in the collector. In this case the hydrogen pressure in the collectors will be higher than would follow from Sieverts' law.

In [121], P.V. Sklyuyev, L.I. Kvator and V.Ye. Shapiro link reversible hydrogen brittleness with accelerated diffusion of atomic hydrogen during the plastic-deformation process toward slip

planes, where it is converted to the molecular form. The molecular hydrogen is under high pressure and therefore produces triaxial stresses that make plastic deformation difficult and lower plasticity.

In view of the difficulties encountered in elaborating a correct theory of reversible hydrogen brittleness on the basis of conceptions revolving around high molecular hydrogen pressure, Ya.M. Potak [91, 96] and N. Petch et al. [113, 127] proposed what have come to be known as adsorption theories. As was first shown by P.A. Rebinder [122, 123], adsorption of surface-active substances on the surface of a solid may lower its strength and plasticity substantially as a result of a decrease in surface energy. Thus, for example, many ductile metals show brittle failure under the influence of low-melting liquid metals. References [124, 125] present numerous examples indicating that certain relationships observed in brittleness under exposure to liquid metals are in many respects at least formally similar to those observed for hydrogen brittleness.

Carrying Rebinder's ideas further, Ya.M. Potak [96] advanced the hypothesis that the hydrogen brittleness of steel is governed by the action of hydrogen as a surface-active substance. Adsorption of hydrogen at the surface lowers the surface energy of steel and, consequently, strengthens its tendency to brittle failure.

Hydrogen adsorbed on the initial surface promotes only the germination of cracks, and not their development. Continuous diffusion of hydrogen from the interior of the metal toward its surface is necessary for propagation of a destructive crack. Hence all factors that reduce the amount of hydrogen diffusion toward the crack inhibit the development of hydrogen brittleness. Thus, for example, an increase in the rate of deformation shortens the time available for hydrogen to diffuse to a germinating crack and thereby alleviates hydrogen brittleness. Lowering the temperature has a similar effect. At low enough temperatures, practically no hydrogen diffusion occurs, and hence hydrogen brittleness is not observed. The amount of hydrogen adsorbed on the surface of a crack depends not only on the rate of diffusion of hydrogen from the interior of the metal, but also on the rate of its desorption from the crack surface. Desorption occurs as a result of conversion of hydrogen adsorbed on the surface into molecular hydrogen. The desorption rate increases with rising temperature; at a high enough temperature, the desorption rate from the crack surface is greater than the rate of diffusion, and hydrogen brittleness is arrested.

Petch and Stables [127] relate the adsorption mechanism of reversible hydrogen brittleness in steel to dislocation theory, proposing that hydrogen lowers surface energy, thus facilitating the formation and propagation of cracks that form in accordance with the dislocation mechanism.

However, the adsorption theories are not quite correct. According to contemporary conceptions of the failure mechanism in metals, the Griffiths criterion, which determines spontaneous de-

velopment of cracks that lead to failure, should be taken in the form

$$\sigma \geqslant \left[\frac{2E(A+\gamma)}{\pi l}\right]^{1/2}, \qquad (20)$$

where γ is the crack surface energy; A is the work of plastic deformation of the metal associated with propagation of the crack; E is the elastic modulus; l is the length of the crack; σ is the stress necessary for development of the crack.

In ductile metals, the work of plastic deformation A is thousands of times the surface energy γ, so that if the hydrogen were to lower the surface energy of the crack even to zero, this would introduce no substantial changes into the nature of crack germination and propagation.

A decrease in crack surface energy due to adsorption of hydrogen on its surfaces is not the decisive cause of hydrogen brittleness. This does not mean that adsorption of hydrogen by the surface of a crack is not important at all. Brittle failure must be due to factors that lower the work of plastic deformation A in germination and propagation of cracks, but as soon as this work has been lowered to values comparable with the surface energy, adsorption of hydrogen begins to play a very important role.

According to Petch and Stables [127], the breaking stress σ_r may be expressed as

$$\sigma_p = \sigma_0 + Kd^{-1/2}, \qquad (21)$$

where σ_0 is a stress that does not depend on grain size; d is the diameter of the grain; the coefficient K is related to the crack surface energy by the relationship

$$K = \left(\frac{6\pi G\gamma}{1-\mu}\right)^{1/2},$$

where G is the shear modulus; μ is the Poisson bracket.

Consequently, the breaking stress σ_r plotted as a function of $d^{-\frac{1}{2}}$ must be a straight line from whose inclination to the axis of abscissas we can find K and, consequently, the surface energy γ.

Petch [113] showed that this relationship is indeed observed for unhydrogenated 1 and hydrogenated 2 steels (Fig. 26). It follows from Fig. 26 that the surface energy of a crack in a steel without hydrogen is approximately 2 j/m^2, while in hydrogenated steel it is about 0.5 j/m^2, i.e., smaller by a factor of 4. The surface-energy value of iron in the presence of hydrogen agrees closely with values calculated from the Langmuir isotherms for adsorption of hydrogen on steel [0.65 j/m^2 at a 10^{-3}% (atomic) hydrogen content].

When the work of plastic deformation is sharply reduced, the germination and propagation of cracks in hydrogen brittleness may

be made easier by a decrease in cohesive forces due to solution of hydrogen, as noted by Troiano and Blanchard for nickel [95].

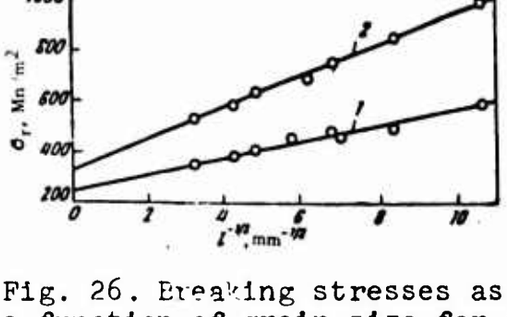

Fig. 26. Breaking stresses as a function of grain size for a low-carbon steel at 291°K [113].

A maximum-stress theory was proposed by Morlet, Johnson and Troiano [128] to explain the highly complex nature of the plasticity change in previously hydrogenated and then deformed steel, and was later refined and detailed by G.V. Karpenko and R.I. Kripyakevich [97]. They start with the proposition that internal hydrogen collectors serve as potential stress concentrators. Under the combined action of internal pressure and external forces, a three-dimensional stressed state that is difficult to evaluate in quantitative terms is created in the lattice of the metal. There is no doubt, however, that with a nonspherical collector a region of maximum triaxial tension may arise in its vicinity. During deformation of the steel, the hydrogen is redistributed, since it has a tendency to diffuse toward points with excess free energy, especially in a region of maximum triaxial tension. Thus, the hydrogen concentrates in the zone of maximum triaxial tension, i.e., where germination of a crack is most probable by virtue of the very nature of the stressed state. Inhibiting plastic deformation in the zone of the triaxial stressed state due to local strain-hardening of microvclumes, weakening interatomic bonds, and lowering the surface energy of the steel, the hydrogen promotes opening of the crack. It lowers strength only in microvolumes, and not throughout the entire cross section of the specimen. Consequently, propagation of the crack requires diffusion of hydrogen to its extremity. As is shown in [8], this theory enables us to explain many minute details of reversible hydrogen brittleness in steel.

5. ANALYSIS OF THEORIES OF REVERSIBLE HYDROGEN BRITTLENESS FOR METALS THAT ABSORB HYDROGEN EXOTHERMICALLY

As was stated above, the behavior of (α + β) titanium alloys is similar to that of steel; (α + β) titanium alloys, like steels, are most sensitive to hydrogen brittleness at slow stretching speeds. On this basis, Ripling [255] postulated that the hydrogen brittleness mechanisms of (α + β) titanium alloys and steel are the same. In his opinion, therefore, the hydrogen embrittlement of (α + β) titanium alloys can be explained on the basis of the

theories proposed to explain the hydrogen brittleness of steel, for example, on the basis of competing diffusion and deformation rates proposed by Zappfe and Sims [103]. However, this analogy did not withstand criticism because the molecular hydrogen pressure is negligibly small in titanium and large in steel.

At one time, considerable recognition was accorded to a theory of the hydrogen brittleness of (α + β) alloys proposed in its most complete form by Jaffee, Lenning and Craighead [258]. In elaborating their theory, these authors proceeded from the premise that β-alloys are not embrittled even at high hydrogen concentrations (∿0.2%) and therefore concluded that the hydrogen brittleness observed in (α + β) titanium alloys at comparatively low concentrations cannot be due to processes that take place only inside the β-phase. On the other hand, they consider that the hydrogen embrittlement of (α + β) alloys cannot be governed by processes taking place solely in the α-phase. In this case, embrittlement would be intensified instead of reduced with increasing testing speed. From this they concluded that the hydrogen embrittlement of (α + β) alloys must be related to processes taking place at the interface between the α and β-phases.

In (α + β) titanium alloys, the hydrogen is concentrated in the β-phase. Jaffee, Lenning and Craighead [258] assume that at slow stretching speeds, the hydrogen in the β-phase migrates in proton form toward the interface of the α- and β-phases. The hydrogen interacts with the α-phase and, in the final result, hydride segregations are formed at the boundary of the α- and β-phases and cause embrittlement. The motive force of this reaction is displacement of β-phase hydrogen by the stresses that arise in it on application of a load. This force should increase with diminishing temperature. In addition, ordinary thermal diffusion operates in the opposite direction, tending to equalize concentration through the volume of the β-phase. As we know, diffusion rate increases with increasing temperature. We should therefore observe viscous failure at high temperatures and brittle failure at low temperatures.

The assumptions on which the hypothesis of Jaffee, Lenning and Craighead were based were not subsequently confirmed by experiment.

Burte [257] failed to observe any traces of a third phase in all but one of his studies of (α + β) alloys at the hydrogen concentrations that cause brittleness. Burte therefore assumes that hydrogen-enriched microvolumes are formed during plastic deformation, without disturbance of homogeneity in the solid solutions. These microvolumes are created as a result of the tendency of hydrogen to accumulate at dislocations, vacancies and grain boundaries. If the hydrogen concentration at these places exceeds a certain value, microcracks may be germinated in these microvolumes, and will then develop and lead to failure. Since diffusion of hydrogen is necessary to form these hydrogen-enriched places, hydrogen brittleness appears only at low stretching speeds.

It has also been noted that both α- and β-titanium alloys [251, 290] are inclined to reversible hydrogen brittleness in a

certain temperature range. The assumptions on which the hypothesis under consideration was based are not entirely correct, first of all because the composition of the β-phase in the (α + β) alloys in which hydrogen brittleness was observed at room temperature was not the same as the composition of the β-alloys investigated. It is quite possible that hydrogen brittleness would be observed at room temperature in β-titanium alloys with the same composition as the β-phase of the investigated (α + β) titanium alloys.

Thus, for example, the composition of the β-phase in alloy VT3-1 is almost the same as the composition of the single-phase β-alloy VT15. The average composition of VT15 alloy is 3% Al, 11% Cr, and 7% Mo, while that of the β-phase in alloy VT3-1 after isothermal annealing is 2% Al, 11% Cr, 10% Mo [249-250]. Accordingly, hydrogen brittleness is observed in VT3-1 alloy in practically the same temperature range as in VT15.

The coincidence of the hydrogen-brittleness ranges for VT15 and VT3-1 alloys, although imperfect, indicates that interfaces between the α- and β-phases are not responsible for the brittleness of (α + β) titanium alloys. The intergranular nature of fracture in hydrogen brittleness is due not to the specific nature of the processes taking place at the boundaries between two different phases, but to the properties of the grain boundaries as such.

In view of the experimental facts noted above, the hypothesis of Jaffee, Lenning and Craighead cannot be regarded as satisfactory.

Let us now turn to another hypothesis of hydrogen brittleness, which was proposed in [248, 256, 261, 272] and is to a certain extent the direct opposite of that examined above. The second hypothesis is based on redistribution of alloying elements between the β- and α-phases to bring them close to their equilibrium state, with the result that the β-phase is enriched in β-stabilizers and hydrogen. On this basis, the authors assume that the hydrogen embrittlement of (α + β) alloys is governed by enrichment of the β-phase by hydrogen in the process of plastic deformation, with subsequent segregation of finely dispersed hydrides or intermetallide inclusions in it, or by embrittlement of the β-phase itself. However, it is difficult to explain the entire aggregate of experimental facts on the hydrogen brittleness of (α + β) alloys with this theory – in particular, the recovery of plasticity of the (α + β) alloys during aging after removal of applied stresses; fracture of hydrogenated (α + β) alloys along grain boundaries and not through the body of the β-grain, and the like.

Williams [275] assumes that the solubility of hydrogen in the α- and β-phases diminishes sharply with decreasing temperature. In his opinion, therefore, the hydrogen brittleness that develops at low deformation rates in titanium alloys differs from that which appears at high deformation rates only in the kinetics of hydride segregation.

If the conditions of manufacture and heat treatment are such that massive segregations of a hydride phase appear, we observe brittleness of the first kind. If, on the other hand, hydrides are

not segregated in the cooling process, the solution is supersaturated with hydrogen. Application of stresses may cause segregation of hydrides from the supersaturated solution and result in brittleness of the second kind.

The brittleness due to supersaturation should appear in a definite temperature range. The upper temperature limit of this brittleness will be the temperature corresponding to the solubility limit at the given hydrogen content in the metal, while the lower limit will be the temperature below which the rate of diffusion of hydrogen is so low that hydride formation is practically impossible.

Williams assumes that the decisive factor in the development of this brittleness is nevertheless not the diffusion of hydrogen and not supersaturation, but the process in which seeds of the hydride phase are formed. If the experimental conditions are such that no hydride-phase seeds form, hydrogen brittleness will not arise even when the limiting solubility is exceeded and the hydrogen diffusion rate is quite adequate.

The theory submitted by Williams is based on the assumption that germination of hydrides in titanium alloys is difficult, especially in the β-phase. It is assumed that seeding depends on deformation, i.e., seeds do not form until a critical stress level is reached.

The influence of deformation rate on the sensitivity of titanium alloys to hydrogen brittleness is explained by the action of two factors: the diffusion-controlled growth rate of hydrides and the rate at which failure of the specimen intervenes.

At high deformation rates and low temperatures, hydrides either do not have sufficient time to form at all during deformation or do not reach sizes adequate for participation in the failure process. Brittle failure occurs only at stresses that are adequate for germination, but not so high that plastic deformation occurs before the hydrides have reached the size necessary to bring about failure.

The weakest point in the Williams hypothesis is the assumption that the critical stress below which hydrides do not form is higher than the yield point. This assumption requires rigorous experimental proof.

Williams assumes that his hypothesis of hydrogen brittleness is valid for all (α + β) titanium alloys. It appears to us that the ideas that he advances explain only hydride brittleness of the second kind, which we examined earlier (see page 55), when the solubility of hydrogen is indeed above the limit.

Experimental data obtained in a number of studies indicate convincingly that hydrogen brittleness develops in (α + β) titanium alloys even at hydrogen concentrations below its solubility limit at the temperature of the experiment. This conclusion is confirmed, for example, by the results obtained in [251] from investigation of the influence of prestressing on hydrogen embrit-

tlement of the (α + β) alloy VT3-1. Specimens of alloy VT3-1 with 0.002 and 0.05% (by mass) of H_2 were stretched at slow speed until a neck appeared; the load was then removed and the specimens held at room temperature for various times, after which they were broken at high testing-machine speeds. It was found that with a short pause between tests, the specimens showed brittle fracture, while the failure was plastic if the interval was longer.

It follows from these data that prestressing accelerates hydrogen embrittlement, but subsequent prolonged holding at room or elevated temperature eliminates the stimulating effect of preliminary stresses.

This effect can be accounted for in terms of formation of hydrogen-atom segregations during preliminary loading, without disturbance to the continuity of the metal. Prolonged holding after preloading desorbs these accumulations and restores plasticity.

6. DISLOCATION THEORY OF REVERSIBLE HYDROGEN BRITTLENESS OF METALS

It has now been established that reversible hydrogen brittleness is observed in many transit'on metals irrespective of their crystal structure. It is detected in metals with body-centered lattices: iron, niobium, varadium, tantalum [9], nickel [95, 102, 366, 395], austenitic steels [359, 461], which have a face-centered cubic structure, in α-titanium alloys with close-packed hexagonal structure [239, 241, 251]. This brittleness is observed in metals that absorb hydrogen endothermically, for example in iron and nickel, as well as in exothermically absorbing metals such as titanium, vanadium, niobium, and tantalum. In metals of the former group, hydrogen can develop enormous internal pressures, while in the latter group this pressure is negligibly small. The basic qualitative laws of reversible hydrogen brittleness are the same for all metals irrespective of whether hydrides form in them or not.

Thus the hydrogen-brittleness mechanism of metals must embody some common factor that depends neither on their crystal structure, nor on internal hydrogen pressure, nor on the presence of hydrides, although these factors undoubtedly have substantial influence on the details of this mechanism. What is common to the processes leading to hydrogen brittleness of metals is the dislocation nature of the plastic-deformation mechanism and the failure process. Consequently, hydrogen brittleness must be governed by the specific influence exerted by hydrogen on the motion of dislocations in plastic deformation and on the seeding and propagation of the cracks that lead to failure.

An attempt is made in [231] to explain the basic relationships in reversible hydrogen brittleness from the premises of dislocation theory. It is supposed that if the temperature is below a certain critical temperature T_0, hydrogen forms Cottrell atmospheres on dislocations. If deformation is slow and the temperature is not too low, so that the mobility of the hydrogen atoms is comparable to the speed of the dislocations, the atmospheres will accompany the dislocations, lagging a certain distance behind them.

Since the dislocation is then acted upon by a force that drives it backward toward its initial position at the center of the atmosphere, the resistance to plastic deformation is increased by a certain amount. Plastic deformation is accomplished basically as a result of generation of new dislocations by some source under the action of applied stresses and their migration in slip planes. Under these conditions, newly formed dislocations will also be overgrown by hydrogen atmospheres.

Moving under the influence of applied stresses, the dislocations will reach grain boundaries with their hydrogen atmospheres and form pileups. In view of the fact that as many as a hundred or more dislocations may move along a single operating slip plane, we should expect considerable segregation of hydrogen at the grain boundaries. If the operating stresses are large enough, a crack will germinate at the juncture of grain boundaries or at the point of a pileup, with the hydrogen facilitating not only germination of the crack, but also its subsequent propagation.

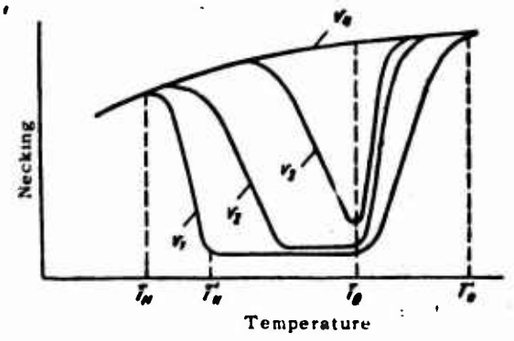

Fig. 27. Scheme of influence of test temperature and deformation speed on necking of hydrogen-saturated titanium alloys: $v_1 < v_2 < v_3 < v_4$.

The reversible nature of this brittleness can be explained as follows: if the load is removed before cracks appear, thermal diffusion will gradually equalize the hydrogen concentration through the volume of the metal and at least partially eliminate segregation of hydrogen at the grain boundaries.

In principle, dislocation pileups may occur not only at a grain boundary, but also inside a grain. Hydrogen brittleness has actually been observed in single crystals of ferrosilicon [462]. In polycrystalline material, however, these pileups are not a decisive factor in the development of hydrogen brittleness. Thus, the crucial idea in the proposed hydrogen brittleness theory is the assumption that under certain conditions dislocations move to grain boundaries together with the hydrogen atmospheres surrounding them and progressive segregation of hydrogen leads to premature failure.

The type of interaction between hydrogen atoms and moving

dislocations depends essentially on deformation temperature. If the temperature is too low, the mobility of the hydrogen atoms will be so small that even at a relatively moderate deformation rate v_1 (Fig. 27) the dislocations will not take hydrogen atmospheres into tow, but will break out of them and move freely in the metal. In this case, a creep tooth will appear on the tension curve, so that the yield point is raised, but the plasticity will remain high for two reasons: a) motion of the dislocations is not retarded by hydrogen clouds; b) the dislocations do not deliver hydrogen atoms to the grain boundaries.

With rising temperature, the mobility of hydrogen atoms increases, and at a certain temperature T_n it becomes comparable with the velocity of motion of the dislocations at the same deformation rate v_1. At this temperature, the dislocations begin to entrain some hydrogen atmospheres, with the result that plasticity is lowered. At a certain temperature T'_n, the dislocations have entrained complete hydrogen atmospheres.

If the deformation rate is left unchanged, again at v_1, a further increase in temperature should have no substantial effect on plasticity. Indeed, it follows from the equation linking the deformation rate $\dot{\varepsilon}$ with the speed v of the dislocations, the dislocation density ρ, and the Burgers vector b [4]:

$$\dot{\varepsilon} = v\rho b, \qquad (22)$$

that under the conditions indicated ($\dot{\varepsilon}$ = const), the number of dislocations arriving at the boundary remains in first approximation unchanged. Although the resistance to motion of dislocations on the part of the atmospheres accompanying them must decrease somewhat with rising temperature, the amount of hydrogen delivered by the dislocations to the grain boundary will be the same as at temperature T'_n. As a result, the specimens will fail at temperatures above T'_n in almost as brittle a fashion as at T'_n.

Finally, the temperature becomes so high (T_0) that the Cottrell atmospheres begin to break up under thermal motion. The hydrogen-atmosphere density decreases and they offer less resistance to the motion of dislocations. In addition, each dislocation delivers fewer hydrogen atoms to the grain boundary than at lower temperatures. Ultimately, beginning at T_0, plasticity increases sharply, and when the Cottrell atmospheres have been completely destroyed hydrogen brittleness vanishes.

If the deformation rate is higher than v_1, say v_2, the drop in plasticity begins at a higher temperature, since the mobility of the hydrogen atoms should be higher at the higher dislocation velocity and enable them to interact with the moving dislocation and trail it. Finally, at a certain deformation rate v_3, the temperature (T'_n) beginning at which the Cottrell atmospheres are fully entrained by moving dislocations is the same as temperature T_0, above which the Cottrell atmospheres are unstable, and then a sharp minimum appears on the plasticity-temperature curve.

It appears that the temperature of full plasticity recovery (T'_0) depends on rate of deformation. As was indicated earlier, the Cottrell atmospheres become unstable at temperatures above T_0 and are gradually broken up by thermal motion. If it is taken into account that the moving dislocation is dissipating its energy along the path of its motion and hence nearby atoms acquire, in addition to their thermal energy, a dissipated energy that increases with increasing dislocation speed, we should expect a decrease in the temperature of full plasticity recovery with increasing deformation speed.

At high enough deformation rates, of the order of v_4, the dislocations are torn away from the hydrogen atmospheres surrounding them over the entire temperature range in which they exist.

Let us now turn to a mathematical analysis of the picture that we have drawn. The critical velocity v_{kr} at which the atmospheres are entrained by moving dislocations is determined by the equation [30]:

$$v_{кр} = \frac{4D}{l},$$

where l is the characteristic length; D is the impurity diffusion coefficient.

The characteristic length l can be found from the equation

$$l = \frac{A}{kT} = \frac{4Gber^3}{kT}, \qquad (23)$$

where G is the shear modulus; ε is the stress caused by the dissolved atom; r is the radius of the impurity atom; k is Boltzmann's constant; T is the absolute temperature.

Then, according to (22), the critical deformation rate can be expressed by

$$\dot{e} = v_{кр}\rho b = \frac{4D\rho bkT}{A}.$$

Assuming that $D = D_0 e^{-\frac{Q}{RT}}$, where Q is the activation energy for diffusion of hydrogen in the metal, we find

$$\dot{e} = \frac{4D_0\rho b}{A} kTe^{-\frac{Q}{RT}}. \qquad (24)$$

In accordance with the general premises set forth above, therefore, the critical deformation rate beginning at which the dislocations entrain hydrogen atmospheres increases with rising temperature. It is essential, however, that this velocity is independent of the alloy's hydrogen content.

The temperature at which plasticity recovery begins (T_0), on the other hand, depends strongly on the average hydrogen concen-

tration C_0 in accordance with Eq. (6):

$$T_0 = \frac{U_0}{k \ln \frac{1}{C_0}},$$

where U_0 is the maximum bonding energy of the hydrogen atom.

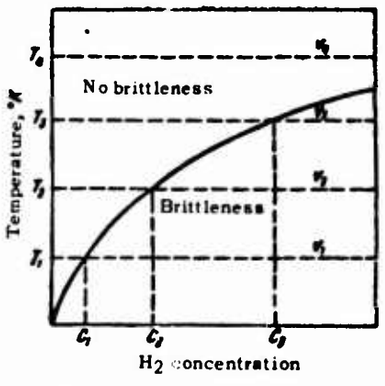

Fig. 28. Diagram of temperature range of hydrogen brittleness in titanium alloys as a function of hydrogen content.

This equation is represented graphically by the diagram shown in Fig. 28. This figure shows the temperatures (T_1, T_2, T_3 and T_4) determined by (24), below which hydrogen brittleness is not developed in tests at the speeds v_1, v_2, v_3 and v_4 because the speed of the dislocations is considerably higher than the mobility of the atoms. Thus, the temperature interval in which hydrogen brittleness can develop is bounded above by the breakdown temperature of the Cottrell atmospheres (T_0) and below by the temperature (T_n) below which the dislocations tear away from the Cottrell atmospheres. The point of intersection of the curves characterizing these temperatures determines the maximum permissible hydrogen concentration, below which hydrogen brittleness does not develop at the given deformation speed. Thus, for example, for deformation speed v_1, hydrogen brittleness does not appear over the entire temperature range if the hydrogen content is below C_1.

If the hydrogen concentration is higher than C_1, the temperature range of hydrogen brittleness increases with rising hydrogen content. As the deformation rate is increased, the hydrogen concentration beginning at which hydrogen brittleness is observed rises, while the brittleness temperature interval decreases.

Such are the basic propositions of the dislocation theory of hydrogen brittleness. The question arises as to the extent to which they agree with experimental data. Figure 18 showed the variation of necking in Ti-140A alloy (2% Cr, 2% Fe, 2% Mo) contain-

ing 0.0375% (by mass) of H_2 as a function of test temperature for various speeds of the testing-machine crossbar [264]. There is no doubt as to the qualitative agreement of the behavior of hydrogen-saturated titanium alloys that proceeds from the dislocation theory with the experimental data.

These same data enable us to make at least an approximate quantitative check of the proposed theory. If we assume that the energy bonding hydrogen atoms to dislocations in titanium is around 0.1 ev ($1.6 \cdot 10^{-20}$ j) and $d = 3 \cdot 10^{-10}$ m, then $A = 5.0 \cdot 10^{-30}$ j·m. The dislocation density ρ in the annealed metals is of the order of 10^7-10^8 cm^{-2}. It follows from [264] that the activation energy for diffusion of hydrogen in the β-phase of alloy Ti-140A is approximately 3 kcal/g-atom (12.5 kj/g-atom) in the temperature range from 135 to 323°K. Assuming that the diffusion coefficient of hydrogen in the β-phase of Ti-140A alloy at room temperature is the same as that for Ti-4Al-4Mn alloy, i.e., $1.9 \cdot 10^{-9}$ cm^2/cm [50], we find D_0 and obtain for the critical relative deformation rate

$$\dot{\varepsilon} = 3{,}8 \cdot 10^{-8} \rho T \exp\left(-\frac{1500}{T}\right) \text{ min}^{-1} .$$

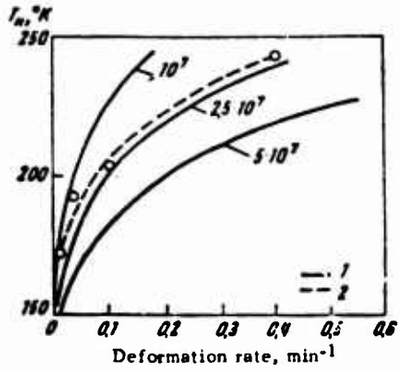

Fig. 29. Temperature of onset of plasticity drop (T_n) as a function of deformation rate for Ti-140A alloy. 1) Calculated curve; 2) experimental curve. The numerals beside the curves indicate dislocation density in cm^{-2}.

This equation is represented graphically in Fig. 29 for dislocation densities of 10^7, $2.5 \cdot 10^7$ and $5 \cdot 10^7$ cm^{-2}. The same diagram shows temperatures T_n for Ti-140A alloy at various deformation speeds.

Figure 30 shows the Cottrell atmosphere condensation temperature, calculated by (6), as a function of hydrogen content for various bonding-energy values, together with the temperatures corresponding to the sharp minimum on the necking-test temperature curves for alloy Ti-140A with various hydrogen contents.

Considering that we have a highly approximate calculation

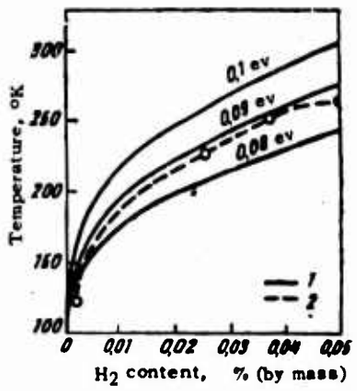

Fig. 30. Temperature of onset of plasticity recovery (T_0) as a function of hydrogen content for Ti-140A alloy. 1) Calculated curves; 2) experimental curve.

with a number of assumptions, stemming, in particular, from the fact that not all of the physical quantities are known in the temperature range of interest to us, it must be conceded that the that the agreement between the proposed mechanism of reversible hydrogen brittleness of the second kind and experimental data is quite satisfactory.

The true picture must be more complex. Thermal diffusion tends to distribute hydrogen uniformly throughout the volume of the grain. If the deformation rate is not too low, the segregations of hydrogen due to transport of hydrogen atoms by dislocations to an obstacle will not be appreciably disturbed by thermal diffusion. If, on the other hand, the deformation rate is extremely low, thermal diffusion will predominate over hydrogen segregation in the pileup zone, and the metal will not be supersaturated with hydrogen.

Thus, plasticity should be recovered not only at very low test temperatures, but also at very low deformation speeds. In other words, hydrogen brittleness of the type considered should be observed not only in a certain temperature range, but also in a certain range of deformation speeds. The experimental data cited above in describing the basic qualitative laws characteristic of reversible hydrogen brittleness confirm this conclusion. Thus, for example, the experimental data presented above for alloy VT3-1 (see Fig. 19) can be presented for each test temperature with properties and deformation rate as coordinates. Figure 31 shows such curves for two test temperatures: 285 and 233°K. These data indicate that at 285°K, hydrogen brittleness does indeed appear in a definite deformation-speed range in VT3-1 alloy. At 233°K, however, plasticity is not recovered at a deformation speed of 0.4 mm/min, since thermal diffusion takes place very weakly at this temperature. We should expect recovery of plasticity at this temperature at much lower deformation speeds. A similar pattern is also observed for steel with 0.5% Cr (see Fig. 17).

If thermal destruction of hydrogen segregations in the tension process is an essential factor, the curves illustrating the variation of necking with temperature (see Fig. 27) should be modified.

An increase in plasticity may intervene in slow deformation not because of destruction of Cottrell atmospheres, but at lower temperatures, due to thermal destruction of segregations at the head of the pileups. The lower the deformation rate, the longer will thermal desorption operate, and hence the more completely will brittle-failure sources be eliminated. Consequently, the plasticity minimum should be shifted toward lower temperatures as the deformation rate is lowered (Fig. 32).

In real alloys, hydrogen brittleness can be described in approximation by one or another scheme, depending on the experimental conditions, and in particular, on hydrogen content. If the hydrogen content in the alloy is close to the solubility limit, but lower than this limit, the tendency to thermal desorption of segregations will be weak and the variation of plasticity with temperature should be described by the scheme shown in Fig. 27. If the hydrogen content is considerably lower than the solubility limit, the plasticity should vary with test temperature in accordance with the scheme shown in Fig. 32.

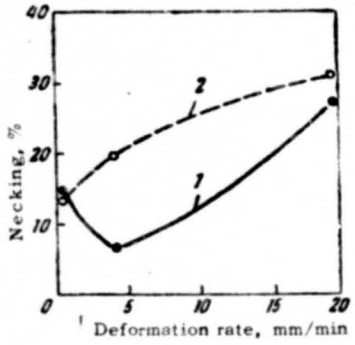

Fig. 31. Influence of deformation rate on mechanical properties of VT3-1 alloy with 0.05% (by mass) of H_2 in tension tests at 285 (1) and 233 (2) °K.

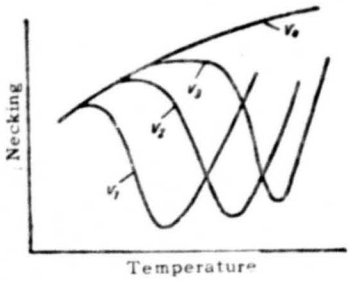

Fig. 32. Diagram showing effect of test temperature on necking of titanium alloys at various deformation speeds with consideration of thermal desorption of segregated hydrogen: $v_1 < v_2 < v_3 < v_4$

In the above discussion, we have not taken into account the fact that in deformation the dislocation density increases sharply, often by 2-3 orders. This inaccuracy does not affect the results of the discussion when the deformation rate is below critical at the dislocation densities characteristic for annealed metals (of the order of 10^7-10^8), i.e., in the range T'_n-T_0 (see Fig. 27). Actually, it follows from (22), which links deformation rate with dislocation density ρ and the speed of the dislocations v, that the velocity of the dislocations should diminish in deformation at constant speed, since $\dot{\varepsilon}$ and b remain constant, while ρ increases. Hence if hydrogen atoms are entrained by dislocations at the initial dislocation density, this will be even more so at higher densities.

If the true rate of deformation at the beginning of tension is somewhat higher than critical, the interaction of dislocations with impurity atoms may result in stepwise deformation. To the extent that the deformation rate is above critical, the dislocations are torn away from the atmospheres surrounding them at the initial phase of stretching. Under these conditions, the liberated dislocation sources operate dynamically and generate a large number of dislocations. To the extent that the dislocation density increases and the rate of deformation is held constant, the velocity of their motion diminishes and becomes comparable to the mobility of the hydrogen atoms. This is equivalent to raising the critical rate of deformation. The dislocations are overgrown by hydrogen atmospheres and the resistance offered plastic deformation increases. On an increase in external stresses, the dislocations are again torn out of their surrounding atmospheres, and the Frank-Read sources again go into dynamic operation. The result of multiple repetition of this effect is a sawtooth-shaped tension curve.

With increasing temperature, the diffusion coefficient of the hydrogen increases and, consequently, so does the critical deformation rate. Finally, the critical deformation rate comes to be higher than the selected speed at the dislocation density characteristic of annealed metals. Under these conditions we do not observe stepwise deformation. Even at the dislocation density typical for the annealed state, the rate of motion of the dislocations becomes comparable with the hydrogen-atom mobility. Obviously, stepwise formation should be observed on the tension curve at temperatures from T_n to T'_n (see Fig. 27). The lower limit of this effect will be the temperature T_n at which the drop in plasticity begins, and the upper limit will be the temperature T'_n, at which minimum plasticity is reached. It follows from the above that the upper temperature limit of stepwise deformation can be described by (24) at the dislocation density characteristic for annealed metal (10^7-10^8 cm^{-2}).

Generally speaking, (24) is strictly valid only for metals with a body-centered structure. In metals with face-centered and close-packed hexagonal structures, hydrogen can form Suzuki atmospheres on packing defects of stretched dislocations. For such metals, therefore, the upper temperature of stepwise plastic flow

must be related to the appearance of "viscous" motion of stretched dislocations together with Suzuki atmospheres as a result of the increase in the hydrogen atom diffusion rate with increasing temperature.

The upper limit of stepwise deformation for metals with the most densely packed structures was determined in [140]. To estimate the initial temperatures of viscous motion of dislocations together with Suzuki atmospheres, the authors of that study arbitrarily represented the stretched dislocation as consisting of two rigidly interconnected subdislocations with a packing defect between them. On displacement of the stretched dislocation over a distance considerably smaller than its width, a packing-defect strip with a solute-atom concentration C_0 corresponding to that of the matrix is formed behind the first subdislocation. A strip of the same width without the packing defect but with the solute atom concentration peculiar to the packing defect remains behind the second subdislocation.

The stretched dislocation will advance together with its Suzuki atmosphere if the atmosphere has time to form during the motion of the dislocations at the front of the packing defect and to resorb behind it. Analysis of this scheme results in the following formula for the maximum deformation rate $\dot{\varepsilon}$ at which viscous motion of a Suzuki atmosphere is possible for a given temperature T:

$$\dot{\varepsilon} = \frac{\pi^2 (1-\mu) D_0 e^{-\frac{Q}{RT}}}{60 G^2 b^3 \Delta\sigma_{max}}, \qquad (25)$$

where μ is the Poisson bracket; $D_0 e^{-\frac{Q}{RT}}$ is the diffusion coefficient of the impurity; G is the shear modulus; b is the Burgers vector; $\Delta\sigma_{max}$ is the parting stress of the dislocations, which is equal to the maximum height of the flow threshold.

The authors of papers devoted to hydrogen brittleness in titanium alloys make no mention of stepwise deformation. However, this phenomenon has been observed distinctly in investigations of hydrogen brittleness in steel [37, 105, 107-109], nickel [102], and niobium [465]. The link between stepwise deformation and hydrogen brittleness has been most thoroughly investigated for nickel [102]. At low enough temperatures, tension curves for electrolytically hydrogenated nickel specimens are smooth and show a flow peak, although it is not as distinct as in steel (Fig. 33). The difference between the upper and lower flow limits is only about 2 Mn/m^2. There is no flow peak on the tension curves of unhydrogenated specimens. At these temperatures, the tension curves of hydrogenated specimens are almost identical to those of specimens without hydrogen, and both types of specimens break at almost the same elongation and necking.

As the test temperature rises, the tension curves of hydrogenated specimens become sawtoothed, while those of specimens not containing hydrogen remain smooth (Fig. 33). This temperature corresponds to the lower critical temperature of stepwise deformation.

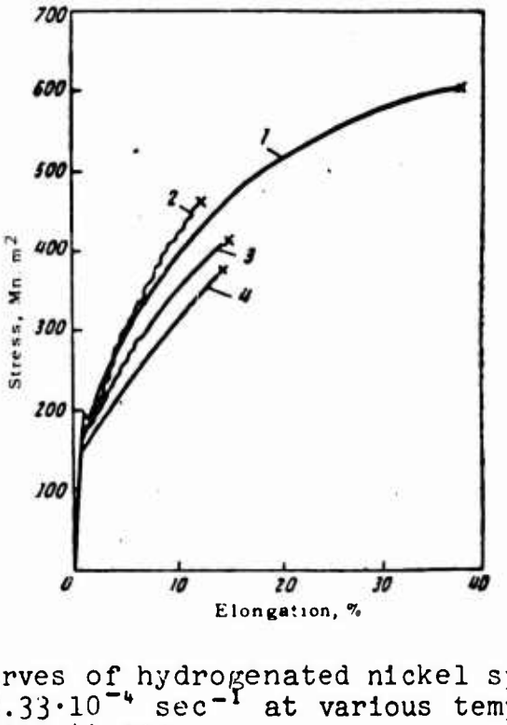

Fig. 33. Tension curves of hydrogenated nickel specimens in tests (deformation rate $3.33 \cdot 10^{-4}$ sec^{-1} at various temperatures, °K): 1) 77; 2) 193; 3) 223; 4) 293.

TABLE 3

Critical Temperatures of Stepwise Deformation for Nickel Containing 40 cm^3/100 g of H_2

Rate of deformation, sec^{-1}	Critical temperatures, [°K]		
	lower	upper	
	experimental	experimental	calculated
$3,33 \cdot 10^{-4}$	153	228	212
$8,33 \cdot 10^{-4}$	157	243	222
$1,67 \cdot 10^{-3}$	163	251	229
$2,5 \cdot 10^{-3}$	—	256	233

As the temperature is raised further, the tension curve becomes smooth over a larger and larger part of its length and, finally, the tension curve is no longer sawtoothed at a certain temperature. This temperature corresponds to the upper critical temperature of stepwise deformation. The upper and lower temperatures depend on deformation rate. This relationship is illustrated by Table 3, which lists critical temperatures for nickel containing 40 cm^3/100 g of H_2.

It is interesting to evaluate the agreement of the critical points with (24), which determines the critical deformation rate. Let us take $\rho = 10^8$ cm^{-2} for annealed nickel. It follows from Table 1 that the average value of activation energy for diffusion of hydrogen in nickel is close to 9.2 kcal/g-atom (38.55 kj/mole), while $D_0 = 0.01$. The Burgers vector may be set equal to 2.544 Å.

According to [102], the energy bonding hydrogen atoms to dislocations is 0.08 ev, which implies a coefficient $A = 3.3 \cdot 10^{-30}$ j·m.

In this case, Eq. (24) for the critical deformation rate assumes the form $\dot{\varepsilon} = 4{,}25 \cdot 10^{3} \cdot T \cdot \exp\left(-\frac{4600}{T}\right) \text{min}^{-1}$. Table 2 presents upper temperatures of stepwise deformation calculated from this equation. The agreement between the experimental and calculated values is obvious.

If we evaluate the upper limit of stepwise deformation by (25), we obtain substantial discrepancies between the experimental and theoretical values.

At a given stretching temperature, the real velocities at which stepwise deformation is observed are found to be three orders below the calculated values. This result can be regarded as proof that hydrogen does not form Suzuki atmospheres in nickel. The hydrogen brittleness of nickel is governed by Cottrell atmospheres.

The lower-limit temperature can be estimated on the basis of the notion of dynamic interaction between hydrogen atoms and dislocations [101]. After the dislocations have been torn out of the surrounding atmospheres as a result of the operation of applied stresses, they again begin to interact with hydrogen atoms dissolved in the metal. If the temperature is low and the deformation rate is not too low, the time of this interaction will be adequate for secondary capture of the hydrogen atoms by the dislocations. In this case no hydrogen brittleness develops. The probability of secondary capture of hydrogen atoms increases with rising temperature as a result of the increasing diffusion rate of the hydrogen and, beginning at a certain temperature T_n, exerts a marked influence on the properties of the metal.

The initial temperature of secondary impurity-atom capture by dislocations was calculated by V.G. Savitskiy and K.V. Popov [130] in estimating the temperature dependence of the yield point in steel. In a later study [101], the ideas advanced are extended to the hydrogen brittleness of steel.

However, the basic notions on which [130] was based are not entirely correct. The authors assume that the deceleration of moving dislocations on dislocations that have been blocked by clouds of foreign atoms occurs when the foreign atoms have time to approach the dislocations and form a cloud of sufficient density around them during the time necessary for attainment of the yield point. Actually, elastic deformation is the principal process during attainment of the yield point, practically no new dislocations form, and the old dislocations have already been overgrown, to the extent that it is possible, by impurity atmospheres – even before deformation. Secondary capture occurs after dynamic operation of Frank-Read sources, when the speed of motion of the generated dislocations drops off sharply.

As we noted earlier, hydrogen brittleness may be governed,

in principle, by two factors: transport of hydrogen atoms to grain boundaries and retardation of dislocations by atmospheres. The hypothesis set forth above is based on the assumption that the former process is decisive in the development of hydrogen brittleness. It is assumed in [101], on the other hand, that the basic cause of hydrogen brittleness is to be found in obstacles to the motion of slipping dislocations, which are created as a result of secondary capture of dislocations by hydrogen atoms.

Dislocations whose motion has been stopped at obstacles are overgrown by hydrogen atmospheres and effectively inhibit the motion of free dislocations, thus rendering plastic deformation difficult.

With rising temperature, the stability of obstacles blocked by hydrogen atoms will diminish as a result of the fact that the dislocations begin to move together with the hydrogen atmospheres surrounding them. Plasticity begins to recover as the temperature rises, when the increase in secondary hydrogen-atom captures by dislocations will be compensated by a more rapid increase in the number of dislocations set in motion together with their clouds. This relationship has not been confirmed experimentally.

We have considered above only the aspects observed generally for metals in the presence of hydrogen, irrespective of their nature, namely, transport of hydrogen to grain boundaries and other obstacles around which dislocation pileups form. Formally, the dislocation mechanism of reversible hydrogen brittleness reduces to the attainment around the obstacles, as a result of dislocation transport of hydrogen atoms, of a hydrogen concentration at which the development of hydrogen brittleness of the first kind becomes possible in microvolumes at some point in time. The influence of hydrogen on the dislocation mechanism of crack germination must, on the other hand, be different for different metals. It may be related either to the high pressure of the molecular hydrogen in microvolumes that have been enriched in hydrogen, or to the formation of hydrides in them, or to blocking of plastic deformation along secondary slip planes due to lattice distortions caused by solute hydrogen.

7. GENERAL MECHANISM OF THE INFLUENCE OF HYDROGEN ON GERMINATION AND PROPAGATION OF CRACKS

The general nature of the influence of hydrogen concentrated in a dislocation-pileup zone on germination and propagation of cracks may be evaluated by examining those parameters of the dislocation theories of metal failure that may change in the presence of hydrogen.

Several dislocation models of crack germination have been proposed, but we shall dwell on the Cottrell scheme, since the influence of hydrogen on crack germination has already been analyzed for it by Blanchard and Troiano [95], with the solution of the problem given in the most general form, without dependence on the nature of the hydrogen solutions formed in the metal. The method of solving this problem can also be extended to other models of crack germination with essentially the same conclusions as

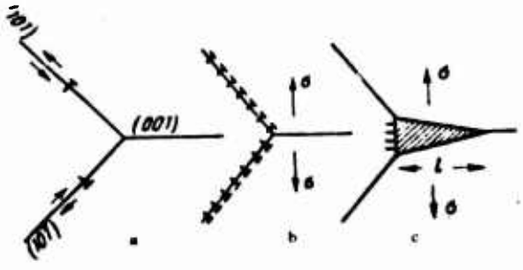

Fig. 34. Diagram illustrating derivation of the energy of a crack formed on merging of dislocations sliding in two intersecting slip planes.

to the nature of the effect of hydrogen on this process.

As a result of coagulation of dislocations sliding in two intersecting slip planes (Fig. 34, a and b), according to Cottrell, a crack opens along cleavage planes perpendicular to the applied stress σ (Fig. 34c). Such a crack can be interpreted formally as a pileup of n edge dislocations, each with a Burgers vector b. The energy of the pileup that has been formed per unit length in the direction perpendicular to the drawing in Fig. 34 is

$$W = \frac{Gn^2b^2}{4\pi(1-\mu)} \ln \frac{4R}{l},$$

where G is the shear modulus; nb is the maximum separation of the crack surfaces; μ is the Poisson bracket; R is the radius of the stress field.

To this energy, it is necessary to add the free energy of the crack surface, which is equal to the product of the crack-surface area ($2l$) by the surface energy γ. In addition, formation of the crack is accompanied by a decrease in the field of the applied stresses by an amount $\frac{\pi(1-\mu)\sigma^2 l^2}{8G}$.

And, finally, it is necessary to consider the work performed by the applied stress as the volume of the opening crack increases:

$$-\frac{\sigma nbl}{2}.$$

Thus, the energy W_t associated with formation of the crack has four components:

$$W_t = \frac{Gn^2b^2}{4\pi(1-\mu)} \ln \frac{4R}{l} + 2\gamma l - \frac{\pi(1-\mu)\sigma^2 l^2}{8G} - \frac{\sigma nbl}{2}. \qquad (26)$$

This equation can be presented in the form

$$W_t = 2\gamma\left[C_1 \ln\frac{4R}{l} + l - \frac{l^2}{C_2} - 2\left(\frac{C_1}{C_2}\right)^{1/2} l\right], \qquad (27)$$

where

and

$$\left.\begin{aligned} C_1 &= \frac{Gn^2b^2}{8\pi(1-\mu)\gamma} \\ C_2 &= \frac{8G\gamma}{\pi(1-\mu)\sigma^2} \end{aligned}\right\}. \qquad (28)$$

Spontaneous propagation of the crack and, consequently, total failure will occur if the energy W_t decreases continuously with increasing l. In actuality, W_t passes through a minimum at a certain crack length if the stresses are not too large. The variation of the energy W_t as a function of crack size is shown graphically in Fig. 35.

The extreme crack dimensions are determined from the condition

$$\frac{\partial W_t}{\partial l} = 0.$$

After differentiating the energy W_t with respect to l and performing simple transpositions, we obtain the following second-degree equation:

$$l^2 - \left[1 - 2\left(\frac{C_1}{C_2}\right)^{1/2}\right] C_2 l + C_1 C_2 = 0. \qquad (29)$$

The smaller root l' of this equation corresponds to the energy minimum (M_1), and the larger, l'', to the maximum (M_2). As the tensile stresses σ increase – which corresponds to a decrease in C_2 – the extreme values of crack length move closer together, and with the condition

$$\sigma nb = 2\gamma \qquad (30)$$

they merge. At higher stresses, Eq. (29) has no real roots, and the increase in the dimensions of the crack results in continuous growth of the crack, since its energy is decreasing continuously with increasing l. Condition (30) is the condition of spontaneous crack propagation.

Blanchard and Troiano [95] postulated that the change in the free energy of a metal due to hydrogen can be expressed by

$$f(l) = \frac{A}{l^m}. \qquad (31)$$

where A is a constant that depends on the hydrogen concentration in the metal but does not depend on crack length. If A is positive, the energy f decreases continuously with increasing crack dimensions (Fig. 35, curve 2).

In this case, the energy W_H associated with the crack is the

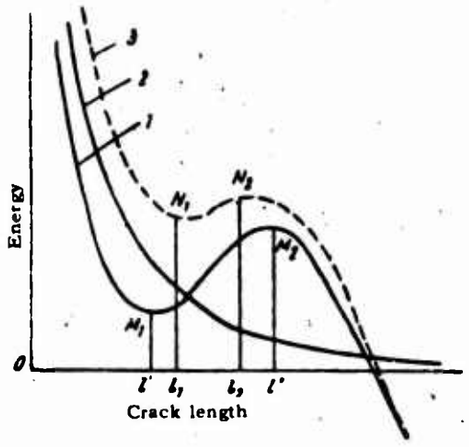

Fig. 35. Influence of hydrogen on change in crack energy as a function of its length. 1) Crack energy for metal without hydrogen; 2) additional crack energy due to hydrogen; 3) total crack energy for a metal with hydrogen.

sum of the energies

$$W_H = W_m + f(l).$$

The energy W_k is shown in Fig. 35 (curve 3) as a function of crack length. Like the energy W_t, the curve of W_H also has a minimum N_1 and a maximum N_2, although these are closer to one another than in the case of a hydrogen-free metal. With increasing hydrogen content, the inclination of the $f(l)$ curve to the axis of abscissas increases, so that the points of the maximum and minimum move toward one another. These points meet at a certain critical hydrogen concentration. At this concentration, the first crack germinated propagates without hindrance and brittle failure occurs. Thus an increase in hydrogen content has an effect similar to that of increasing external stresses.

Mathematical analysis of the picture described above enables us to find the critical value of A, which leads to brittle failure at a given tensile-stress level:

$$A = \frac{2\gamma G^{m+1} n^{m+1} b^{m+1}}{m\pi^{m+1}(1-\mu)^{m+1}} \frac{1}{\sigma^{m+1}} \left(1 - \frac{\sigma n b}{2\gamma}\right). \qquad (32)$$

The breaking stress σ can be evaluated as a function of hydrogen content from this equation. Since the analytical expression for the function A is unknown, only qualitative analysis of (32) is possible. Blanchard and Troiano postulate that if the hydrogen content in the metal is below the solubility limit for normal conditions, A will be negative. In this case the additional energy associated with the hydrogen will increase with prolongation of the crack and, consequently, hydrogen will not contribute

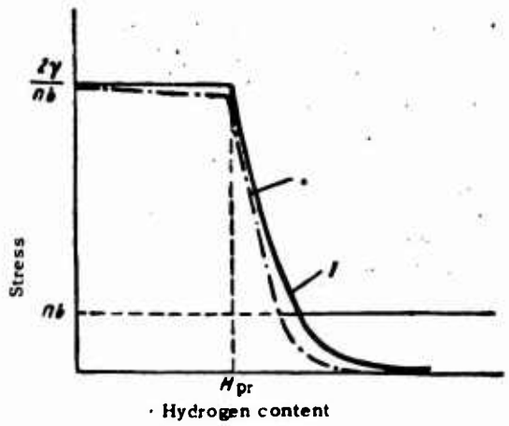

Fig. 36. Stress at failure as a function of hydrogen concentration. 1) Cohesive forces independent of hydrogen content, change in crack surface energy due to adsorption of hydrogen by its surface not taken into account; 2) same as 1, with change in surface energy considered.

to propagation of the crack. Below the solubility limit (H_{pr}), therefore, the breaking stress does not depend on hydrogen concentration unless the hydrogen influences cohesive forces in the metals (Fig. 36).

When the hydrogen concentration reaches the solubility limit, $A = 0$. In this case, the breaking stress for hydrogen-saturated metals is the same as that for unsaturated metals, i.e., $\sigma = \frac{2\gamma}{nb}$. On a further increase in hydrogen content, the breaking stress drops sharply.

It has been assumed in the above discussion that the surface energy of the metal is independent of hydrogen content. Since hydrogen is a horophilic impurity in most metals, we may expect the surface energy to decrease with increasing hydrogen content, so that the dependence of breaking stress on the hydrogen content would be described not by the solid curve but by the dot-dash curve.

The ideas of Blanchard and Troiano explain the germination of cracks and, at best, their propagation within a single grain. On reaching grain boundaries the crack stops. Further propagation of the main crack may occur as a result of merging of cracks that have formed independently with the participation of hydrogen in adjacent grains, or by penetration of the main crack into adjacent grains. However, experiments indicate that the brittle failure of metals in the presence of hydrogen takes place preferentially along grain boundaries. This is no doubt due to the transport of hydrogen to grain boundaries not only along the slip plane in which the crack was germinated, but also along many others. The net result is that the hydrogen concentration adequate to stimulate intergranular failure is formed along the grain boundaries.

Thus, the ideas of Troiano and Blanchard should be regarded as only a first approximation in solution of the problem posed. Its more or less complete solution will require study of the influence of hydrogen on the mechanism of intergranular failure.

8. MECHANISM OF CRACK GERMINATION AND PROPAGATION IN METALS THAT ABSORB HYDROGEN ENDOTHERMICALLY

Blanchard and Troiano examined only the general scheme of the effect of hydrogen on crack germination and propagation. This picture can be filled in for metals that absorb hydrogen in different ways.

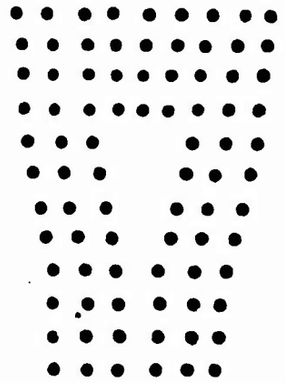

Fig. 37. Initial stage in genesis of a crack by compacting of dislocations in a single slip plane.

In metals that absorb hydrogen endothermically, the hydrogen partial pressure is quite high even at relatively low concentrations in solution. In such metals, a considerable internal pressure may arise inside the cavity of the crack. The influence of internal pressure on the growth of a disk-shaped crack was studied by Kacinczy [110, 111]. However, he disregarded the influence of the pressure on the elastic energy and volume of the crack for a fixed crack radius. A more rigorous solution of the problem is given in [112]. Although the influence of hydrogen on the stability of microcracks in iron and steels was examined in [110, 111], the conclusions drawn there are valid for all metals that absorb hydrogen endothermically.

In analyzing the influence of hydrogen on the stability of microcracks in metals, the authors begin with the model proposed by Stroh [62, 63] for the formation of microcracks. According to this scheme, the crack forms at the head of a dislocation pileup when the stresses have become large enough to compact the dislocations. Figure 37 shows the initial stage in the formation of such a crack, when three edge dislocations with Burgers vector b have met.

Garofalo et al. first examined a hypothetical case in which

a Stroh crack exists in the metal without external load, with only the internal hydrogen pressure acting on it.

The equation that they obtained is quite consistent with the expression for the Cottrell cracking energy with the external stress σ replaced by the hydrogen pressure p.

Stable microcrack dimensions correspond to a minimum of system energy. System energy will be lowest if the first derivative of the energy is zero and the second is larger than zero. We can easily find from this condition that a crack will be stable if the condition

$$pl < \frac{n'bG}{\pi(1-\mu)} \tag{33}$$

is observed.

If this condition is not satisfied, however, the total microcrack energy will not have a minimum and the crack will propagate unhindered. The internal pressure corresponding to this critical transition is determined by the relationship

$$p_{кр} = \frac{2\gamma}{n'b}. \tag{34}$$

Thus, if a Stroh crack has formed, it can propagate at high enough internal pressures only under the influence of these pressures, even in the absence of external stresses.

For quantitative evaluation of the critical pressure, let us apply the formula for surface energy as a function of hydrogen pressure:

$$\gamma = \gamma_0 - 2\Gamma_s kT \ln[1 + (A_1 f)^{1/2}], \tag{35}$$

where Γ_s is the number of hydrogen molecules adsorbed per unit area of the crack at saturation; A_1 is a constant; f is the fugacity.

According to Phragmen, fugacity can be expressed by

$$f^{1/2} = A_2 C \exp\frac{Q}{RT}, \tag{36}$$

where C is the hydrogen concentration, which depends on hydrogen temperature and pressure in accordance with the equation

$$C = B_1 p^{1/2} \exp\left(-\frac{Q + B_2 p}{RT}\right). \tag{37}$$

From (34-37), we obtain the following equation, from which the critical pressure can be found:

$$p_{кр} = \frac{2}{n'b}\left\{\gamma_0 - 2\Gamma_s kT\left[\ln\left(1 + A_1^{1/2} A_2 B_1 p_{кр}^{1/2} \exp\frac{B_2 p_{кр}}{RT}\right)\right]\right\}.$$

According to Stroh, the number of dislocations n' forming the crack cannot exceed 6. For α-iron, the critical pressure at room temperature is found to be $1.53 \cdot 10^5$ Mn/m^2 for $n' = 5$ and $2.2 \cdot 10^5$ Mn/m^2 for $n' = 3$. It follows from the Sieverts relation that this pressure will obtain if the hydrogen concentrations in the α-iron are 2.5 cm^3/100 g and 13.5 cm^3/100 g, respectively. Actually, it has been observed that internal cracks form rapidly at these hydrogen concentrations unless measures are taken to eliminate thermal stresses.

Similar calculations for the case of combined action of internal pressure and external stresses result in the following expression for the critical crack length:

$$l_{кр} = \frac{4\gamma G}{\pi(1-\mu)}[0{,}186\sigma_p^2 + p^2 + (0{,}186\sigma_p^2 + p^2)^{1/2}(0{,}175\sigma_p + p)]^{-1}, \quad (38)$$

where σ_p is the magnitude of the external breaking stresses. From this equation, the authors calculated the critical crack length on the basis of Petch's experimental data [113]. The calculated critical crack sizes for hydrogenated specimens ($\sim 10^{-7}$ cm) was found to be two to three orders lower than for unhydrogenated specimens ($\sim 10^{-4}$ cm). For the hydrogen concentration studied (10 cm^3/100 g), the critical crack dimensions do not depend on grain size, which implies that in this case the internal pressure was high enough to stimulate the development of newly formed Stroh cracks without a considerable increase in the external stresses.

To simplify their calculations, the authors of the cited paper adopted a number of assumptions that are not always satisfied. Thus, for example, they left out of account the possible segregation of hydrogen atoms on dislocations, and also assumed that there is no appreciable plastic deformation prior to formation of the microcracks.

It is also assumed in this study that the hydrogen pressure in the cavity of the crack can be described by a Sieverts equation obtained under conditions different from those observed in the vicinity of the crack. It is assumed further that the pressure inside the crack remains constant as it develops.

Recent studies [12] have shown that the equilibrium hydrogen pressure in steel is appreciably lower than that indicated by the Sieverts equation, thus giving rise to doubt as to whether this pressure is sufficient for the development of hydrogen brittleness. If the basic process promoting the development of reversible hydrogen brittleness is dislocation transport of hydrogen atoms, then in the pileup region that gives rise to the crack, the hydrogen concentration would be tens of times, and the internal pressure hundreds of times, higher than their average values in the volume of the metal, so that these fears are unjustified.

9. PECULIARITIES OF THE MECHANISM OF CRACK GERMINATION AND PROPAGATION IN METALS THAT ABSORB HYDROGEN EXOTHERMICALLY

In metals that absorb hydrogen exothermically, the internal

pressure is very low and cannot stimulate the formation and development of cracks. As was shown above, neither can a decrease in surface energy resulting from hydrogen adsorption on the crack surfaces be the basic factor facilitating development and propagation of cracks.

It should be noted, however, that all metals that absorb hydrogen exothermically form hydrides with it. It may be assumed that it is precisely the formation of hydrides at hydrogen segregation points that is responsible for hydrogen brittleness in these metals. Reversible hydrogen brittleness of the second kind develops in these metals at average hydrogen concentrations below the solubility limit. In a certain temperature range, however, segregations form at the heads of dislocation pileups at low deformation speeds, and here the hydrogen concentration is many times the average concentration in the metal. When the hydrogen concentration in these segregations exceeds the solubility limit, hydrides are segregated. Hydride segregations may be highly dispersed and even coherently bound to the metal lattice.

As was noted above, hydrides are formed in metals for the most part along cleavage planes. Since the densities of hydrides are considerably lower than that of the basic metal, hydride segregation results in substantial tensile stresses along the cleavage planes and thereby facilitates germination of cracks. It appears that hydrides may also be precipitated along secondary slip planes, rendering plastic deformation at the apex of the crack difficult.

The germinated crack propagates rapidly and soon stops, since its point has entered a zone that is not enriched in hydrogen. Further diffusion of hydrogen to the end of the crack is necessary for its further development. This is why the crack develops in a stepwise fashion.

The reversible nature of hydrogen brittleness of this type can be explained by the escape of hydrogen from these segregations by thermal diffusion after removal of the load, so that there is a trend to more uniform distribution throughout the metal. Since the average hydrogen concentration is below the solubility limit, submicroscopic hydride segregations in pileup regions will be dissolved and will soon disappear. In view of the small dimensions of the hydride segregations and the high rate of diffusion of hydrogen, even at relatively low temperatures, we should expect this process to take place very rapidly.

In this case, the conditions of brittle failure may be evaluated as follows. Let us assume in first approximation that hydrogen delivered to a pileup by dislocations forms a cylindrical cloud of uniform density[1] and radius $R = \alpha nb$, where n is the number of dislocations in the pileup and α is a coefficient larger than unity. If we disregard the average concentration in the pileup volume and assume that each atom of the metal presents one hydrogen atom at the edge of the missing half-plane, the number of hydrogen atoms in this cylinder, converted to a single atomic plane, will be n. The number of metal atoms inside this cylinder,

[1]/108

converted to a single atomic plane, is $\frac{\pi A^2}{4a^2}$, where a is the atomic diameter. Then the hydrogen concentration in the cylinder will be

$$C = \frac{4a^3n}{\pi R^2}.$$

Considering that $a \approx b$ and $R = \alpha n b$, we get

$$C = \frac{4}{\pi a^3 n}.$$

A crack will be germinated when $C > C_n$, where C_n is the solubility limit of hydrogen in the metal.

If, following Blanchard and Troiano, we assume that at the hydrogen concentration equal to the solubility limit $A \approx 0$ and $\sigma = \frac{2\gamma}{nb}$, then the condition of brittle failure will assume the form

$$\sigma \geqslant \frac{1}{2}\gamma\alpha^2\pi C_n.$$

Thus, as would be expected, the trend to reversible hydrogen brittleness of the second kind should increase with diminishing solubility limit of the hydrogen in the metal.

It appears that in a number of metals that adsorb hydrogen exothermically, it may stimulate the development of reversible hydrogen brittleness even without the formation of hydrides, as a result of the high internal stresses. As we indicated above, the β-titanium alloy VT15 and niobium show brittle failure even under impact loading at high hydrogen concentrations, although the latter are still below the solubility limit at room temperature. Similarly, a crack may appear in a microvolume enriched in hydrogen at low deformation speed because of high internal stresses and not because of hydride segregation.

10. POSSIBILITY OF REVERSIBLE BRITTLENESS DUE TO INTERSTITIAL IMPURITIES OTHER THAN HYDROGEN

Dislocations can be transported to obstacles not only by hydrogen atoms, but also by atoms of other interstitial impurities: carbon, nitrogen, oxygen and others. We may therefore expect to find not only reversible hydrogen brittleness in metals, but also nitrogen, oxygen, and other brittlenesses. They would be subject to the same qualitative relationships as reversible hydrogen brittleness, and, in particular, they should appear in a definite temperature interval.

Unlike hydrogen brittleness, the reversible brittleness due to dislocation transport of oxygen, carbon or nitrogen atoms should, under comparable experimental conditions, appear at higher temperatures, since the diffusion coefficients of these elements are considerably smaller than those of hydrogen and the Cottrell

atmosphere condensation temperatures are higher.

Actually, we observe high-temperature plasticity collapse in almost all metals. A.L. Presnyakov [465] assumes that these plasticity collapses are due to defects that form in plastic deformation either due to the deformation process itself or because of secondary diffusion (diffusion related to certain structural transformations that accompany deformation). If both types of distortion simply add, plasticity will be reduced; if they tend to cancel one another, plasticity will rise.

It appears possible to us that the high-temperature plasticity troughs observed in many cases are related to reversible brittleness governed by interstitial impurities other than hydrogen. By way of example, Fig. 38 shows the influence of test temperature on the mechanical properties of titanium that had been thoroughly degasified in vacuum for various deformation rates. These data indicate that the high-temperature plasticity trough shifts toward higher temperatures with increasing deformation speed. Qualitatively, the variation of the plasticity of titanium with temperature at various deformation speeds is in good agreement with Fig. 32. In contrast to hydrogen brittleness, the high-temperature plasticity drop has a stronger influence on relative elongation than on necking.

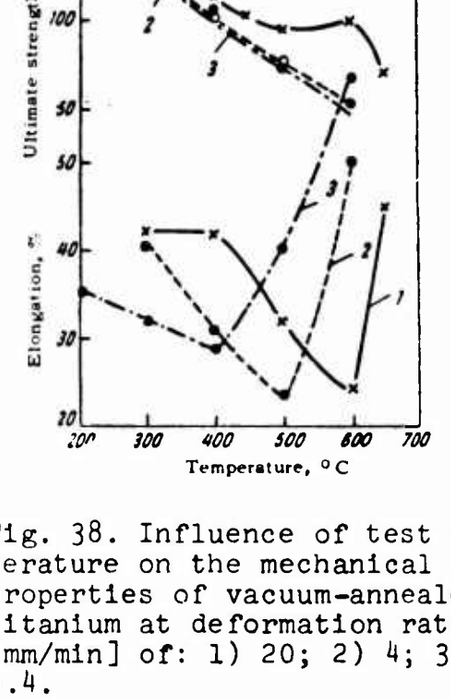

Fig. 38. Influence of test temperature on the mechanical properties of vacuum-annealed titanium at deformation rates [mm/min] of: 1) 20; 2) 4; 3) 0.4.

The plasticity trough is not associated with the segregation of stable phases; even in iodide titanium, this trough appears

just as conspicuously as in technical titanium. On this basis, the opinion has been advanced that the plasticity trough is unrelated to interstitial impurities. Actually, a very small impurity content is sufficient for the formation of saturated Cottrell atmospheres – a content considerably lower than that present in iodide titanium. Transport of impurity atoms to grain boundaries or other obstacles can also take place in iodide titanium.

A sharp increase in plasticity at high deformation speed is observed at temperatures above 873°K, and hence the temperature at which Cottrell atmospheres begin to decay must be above this value.

According to [119], the interaction energy of interstitial atoms with dislocations in titanium is 0.15-0.4 ev. If an impurity with an interaction energy of 0.4 ev is responsible for this plasticity trough, it follows from (13) that its concentration in the solution must be 0.45% (atomic). In titanium of the melt investigated, the oxygen content was close to this value: 0.4% (atomic).

In vanadium, a plasticity trough is observed at 573-723°K [120]. It is shown in [54] that this effect is related to strain aging due to the interaction of oxygen atoms with dislocations. It is interesting to note that as in hydrogenated nickel specimens, we observe stepwise flow in plastic deformation of vanadium at temperatures somewhat above the plasticity minimum.

Stepwise plastic deformation has also been observed in steel in the blue-shortness range [106]. These data indicate that the plasticity troughs due to various interstitial impurities have something in common.

In most cases, dislocations could hardly transport substitutional atoms to grain boundaries or other obstacles. The energy bonding substitutional atoms to dislocations is usually small, so that the Cottrell atmosphere decay temperature is below room temperature. At these temperatures, the mobility of substitutional atoms is so small that at ordinary deformation rates reversible brittleness would hardly be observed. Interstitial atoms, such as nitrogen, oxygen, and carbon, on the other hand, have large energies of bonding to dislocations, and the Cottrell atmosphere breakdown temperature is in close agreement with the range in which high-temperature brittleness develops.

Thus, reversible hydrogen brittleness is not some special sort of phenomenon; it is one of the aspects, and perhaps the most interesting one, of the over-all problem of brittle failure in metals.

11. STATIC HYDROGEN FATIGUE

In recent years, a great deal of attention has been devoted to the influence of hydrogen on the mechanical properties of metal under the action of static loads. If the external stresses are above a certain critical value, cracks form and develop in the metal if they act for long periods, leading ultimately to brittle failure of the article. This phenomenon has come to be known as

static fatigue. A quantitative measure of the resistance of a metal to static fatigue is its long-term strength, which characterizes the maximum stress that the metal can withstand for a given time without failing.

Numerous studies have shown that hydrogen lowers the ability of metals to withstand static loads, leading to premature failure at a given stress level as compared with unhydrogenated specimens. In other words, hydrogen lowers long-term strength. This phenomenon was given the name static hydrogen fatigue by G.V. Karp nko and R.I. Kripyakevich.

This brittleness is most dangerous from a practical standpoint, since it appears suddenly in many cases, after the finished product has operated for a long time at stresses that are not only lower than the ultimate strength, but even lower than the yield point. Moreover, no appreciable plastic deformation precedes brittle failure in static fatigue. Static hydrogen fatigue appears at hydrogen concentrations so minute that they cause no marked change in mechanical properties in static tensile tests [88, 92]. The tendency of metals to static hydrogen fatigue cannot be brought out in any of the short-term tests that have been developed thus far. Long-term strength or static-bending tests represent satisfactory methods of evaluating the tendency of metals to brittleness of this kind.

Long-term strength depends on the ultimate strength of the alloy and its structure, on the concentration and distribution of hydrogen in the specimens and parts, and on stress concentration.

In general, we observe a tendency to increased susceptibility to static hydrogen brittleness with increasing strength of the alloy. Thus, for example, static hydrogen fatigue is not observed in steels with ultimate strengths below 1250 Mn/m^2 [88]. However, this relationship is not without exceptions, particularly when we compare alloys with different metallic bases.

Long-term strength diminishes to a greater degree the higher the hydrogen content. A decrease in long-term strength is observed basically on notched specimens. With increasing notch radius of curvature, the long-term strength of hydrogenated specimens rises, and in the total absence of the notch it would apparently be the same for hydrogenated and unhydrogenated specimens. Under real conditions, however, there are always stress concentrators (machining tracks, cracks, cross-section changes, and the like) on the surface of the part (or specimen). Thus conditions for the appearance of static hydrogen fatigue always exist.

Research has shown [94] that the plasticity of previously hydrogenated steel specimens is recovered in tests of particularly long duration. It is assumed [8, 94] that the recovery of plasticity in steels in very long tests is associated with desorption of hydrogen in the testing process.

Microscopic investigations of crack-germination points made on longitudinal ground sections of specimens at various test stages showed that the crack is germinated at the very apex of a

sharp notch but at a certain distance from the apex of a blunter notch. It is known [8, 125] that the zone of maximum triaxial stress is at the apex of a very acute notch and at a certain distance from the apex of a blunt notch, and that this distance increases with increasing notch radius. It follows from this that in static hydrogen fatigue, the crack is germinated in the region of maximum tensile stresses.

The above description of the influence of hydrogen on the long-term strength of steel is apparently characteristic for all metals that absorb hydrogen endothermically. The relationships characteristic for metals that absorb it exothermically have been most thoroughly studied for the (α + β) titanium alloy Ti-4Al-4Mn [266].

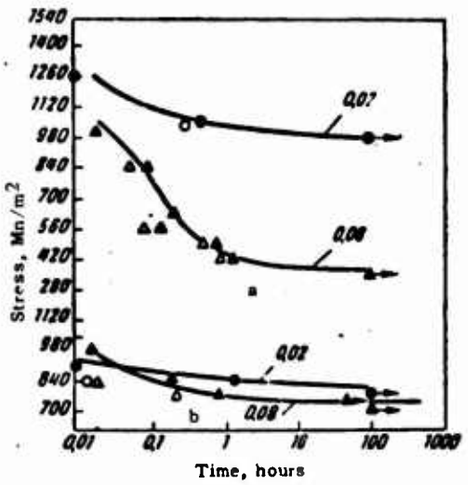

Fig. 39. Long-term-strength curves for (α + β) titanium alloy Ti + 4% Al + 4% Mn. a) After aging; b) after quenching.

These tests, which were made on notched specimens, indicated that hydrogen weakens the ability of titanium alloys to resist static fatigue and thus lowers long-term strength. Like steels, titanium alloys fail in static hydrogen fatigue by germination of a crack and its progressive growth. As a rule, the crack appears at the apex of the notch and progressively advances into the specimen until the cross section of the specimen has been weakened to the point at which it propagates instantaneously through the rest of the intact section. The studies showed that germination of the crack is accelerated if the hydrogen content is above a certain critical level.

In titanium alloys, the phenomena are complicated by creep, which appears at unusually low temperatures. Appreciable plastic deformation may occur as a result of creep at room temperature and result in a narrow range of retarded failure in unnotched specimens, irrespective of whether or not they contain hydrogen. True hydrogen static fatigue can be isolated from the phenomena

associated with creep by measuring electrical resistance during the loading process and correcting it with consideration of the change in specimen cross section during creep.

Premature hydrogen failure of (α + β) titanium alloys under static load is sensitive to structure. The varying sensitivities of (α + β) titanium alloys in various states to static hydrogen fatigue is illustrated by Fig. 39, which shows the relation between the time to failure of notched specimens and applied stress for the alloy Ti-4Al-4Mn.

These data indicate that (α + β) titanium alloys in the as-quenched state are less sensitive to static hydrogen failure than in the aged or annealed state. The varying tendency of the (α + β) titanium alloy Ti-4Al-4Mn to static hydrogen fatigue after various types of heat treatment can be explained primarily in terms of the differences in the amount of β-phase in the structure: 45% in the quenched alloy, 35% in the quenched and aged alloy, and 25% in the annealed alloy. In titanium alloys, hydrogen concentrates in the β-phase, since the heat of solution of hydrogen in that phase is lower (with consideration of sign) than in the α-phase. Hence the less there is of the β-phase in the alloy, the greater the degree to which this phase will be saturated with hydrogen at a given average hydrogen concentration, and the more readily will it form cracks.

It appears that the nature of the alloy's base also exerts substantial influence. In the annealed and aged states, the α-phase forms the matrix of the alloy, while in the quenched state there is no continuous contact between grains of the α-phase. In (α + β) titanium alloys that are simultaneously alloyed with α- and β-stabilizers, the α- and β-phases are strengthened to approximately the same degree, but by virtue of its hexagonal structure the α-phase is less plastic and therefore inhibits propagation of cracks that have formed to a lesser degree. In general, transition from the α-matrix to a β-matrix should increase resistance to static hydrogen fatigue.

In all three states (quenched, aged and annealed), the length of the incubation period and the time to failure decrease with increasing hydrogen content. Failure of alloy Ti-4Al-4Mn in the annealed state under applied stresses of 112 kg/mm^2 (1100 Mn/m^2) occurs after 0.01 sec at 0.08% (by mass), 1 hour at 0.045% (by mass) and after more than 100 hours at 0.005% (by mass) of H_2.

The authors conclude that the aged alloy, which possesses high strength, is more inclined to static hydrogen fatigue than the alloy in the quenched state with its lower strength. The hardening brought about by heat treatment strengthens the tendency of titanium alloys to premature failure under static loading if their hydrogen contents exceed the tolerable value.

Static hydrogen fatigue of titanium alloys appears in a certain temperature range. Thus, for example, hydrogen lowers the long-term strength of quenched and aged Ti-4Al-4Mn alloy only at test temperatures from 77 to 541°K (Fig. 40). At excessively high temperatures, hydrogen has no detrimental influence on static fa-

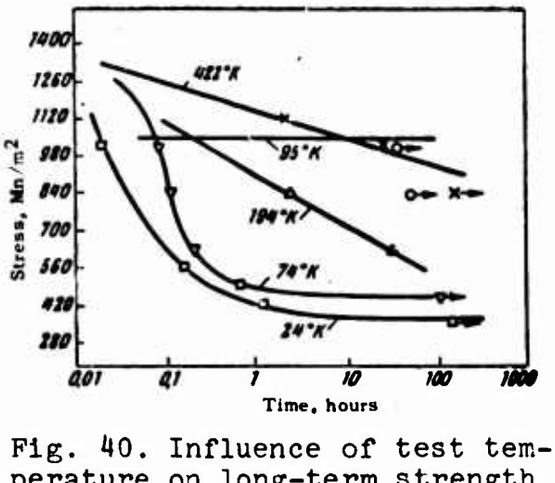

Fig. 40. Influence of test temperature on long-term strength of the (α + β) titanium alloy Ti + 4% Al + 4% Mn in the aged state.

tigue. Failure occurs at room temperature at smaller applied stresses than at higher or lower temperatures. At a given external-stress level, the time to failure becomes shorter as the temperature is lowered from 421°K to room temperature, but it rises again at lower temperatures. These data, plotted with the logarithm of time and reciprocal absolute temperature as coordinates, indicate that this phenomena cannot be described by a single energy of activation. Below room temperature, the activation energy is positive and closely similar in absolute magnitude to the activation energy for diffusion of hydrogen in β-titanium. This dependence indicates that static hydrogen fatigue is determined in this temperature range by diffusion of hydrogen, and that the increase in time to failure is due to lowering of hydrogen-atom mobility with decreasing temperature.

Williams [275] showed on the example of alloy Ti-4Al-4Mn that the detrimental influence of hydrogen on the static fatigue of (α + β) titanium alloys appears in a very narrow range of applied stresses. The results that he obtained for the alloy Ti-4Al-4Mn containing 0.02% H_2 in static long-term strength tests on smooth specimens at room temperature are presented in Fig. 41. At stresses of the order of 1120-1160 Mn/m^2, failure occurs quickly and plastically. At stresses below 1080 Mn/m^2, failure occurs only after prolonged operation of the stresses (more than 100 hr), but still plastically. Only in a very narrow stress range from 1120 to 1080 Mn/m^2, when failure occurs within 2-50 hours after application of the load, is brittleness observed.

It was found in [457] that zirconium and the alloy Zircalloy-2 are not inclined to accelerated static fatigue in the presence of hydrogen up to 0.05% by weight. In these materials, premature failure under static load intervenes only at stresses near the ultimate strength. On the other hand, the alloys Zr + 1,25 Al + 1,0% Sn + + 1,0% Mo and Zr + 2,5% Nb are very sensitive to notching and to the de-

velopment of accelerated failure under static loading.

These data indicate how important the plasticity of the matrix is in the development of premature failure. In zirconium and the alloy Zircalloy-2, there are hydrides at 0.05% (by mass) of

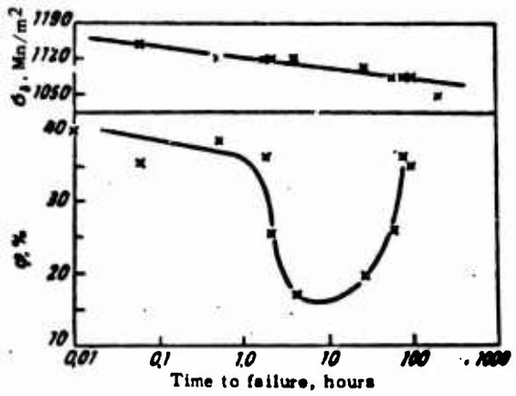

Fig. 41. Influence of level of applied stresses on time to failure for the alloy Ti + 4% Al + 4% Mn with 0.02% H_2.

H_2, but the matrix is highly plastic and premature failure does not occur in the presence of hydrogen. In the alloy of Zr + 2.5% Nb, there are considerably fewer hydride segregations than in zirconium and Zircalloy-2, but the matrix has low plasticity and the alloy is very strongly inclined to static hydrogen fatigue. Thus, tendency to static fatigue is closely related to the work of plastic deformation in formation of a crack and its propagation: the smaller this work, the lower the long-term strength.

The alloy Zr + 1.25% Al + 1% Sn + 1% Mo has no hydride segregations, but it is nevertheless strongly inclined to premature failure in the presence of hydrogen. As in titanium, this failure may be governed by directional diffusion of hydrogen to the interfaces between the α- and β-phases and by the development of brittleness at these points. The authors of [457] assume that the premature failure of the (α + β) alloy Zr + 1.25% Al + 1% Sn + 1% Mo is due to local hydride segregation at the point of failure under the action of stresses, since porosity was observed in this region. Forscher [458] showed that porosity in the fracture is observed only when the microstructure shows hydride segregation; such porosity is not to be detected if the hydrogen is in solid solution.

The mechanism of development of hydrogen brittleness under static tension, at least with high applied stresses, appears to be similar with the mechanism of brittleness under continuous stretching. Actually, all of the basic phenomena of static hydrogen fatigue and, in particular, its development in a definite temperature and stress range, can be explained from the standpoint of the dislocation theory of hydrogen brittleness set forth

above.

It should, however, be noted that in many cases the harmful influence of hydrogen on static fatigue strength has been observed at stresses below the yield point. At these stresses, motion of dislocations and formation of dislocation pileups sufficient to give rise to destructive cracks are excluded. What may be operating in this case is the failure mechanism [129, 132-135] elaborated to explain the formation of cold cracks in steels and titanium alloys under static loading on the basis of conceptions involving a lowering of the shear strength of grain boundaries below the shear strength of the body of the grain and the capacity of the metal for elastoviscous slip along grain boundaries under the conditions of deformation at low speeds. This peculiarity of polycrystalline solids is related to the lack of coordination between the crystal lattices of contacting grains at the interface between them, at which a high concentration of stresses and defects is created as a result. In this case, microcracks form as a result of directional diffusion of vacancies toward grain boundaries and their coalescence.

In hydrogen-saturated metal, the appearance of stress-field inhomogeneities at the grain boundaries should also stimulate directional diffusion of hydrogen to grain boundaries. This migration of hydrogen toward grain boundaries is brought about not by the motion of dislocations together with Cottrell atmospheres, as in reversible hydrogen brittleness, but as a result of upward diffusion. There is no doubt that this type of diffusion is dominant in premature failure under static bending.

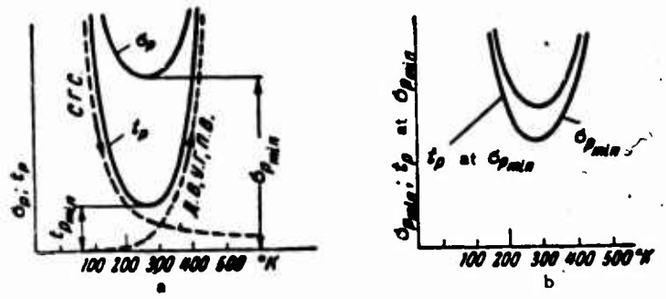

Fig. 42. Diagram showing influence of temperature on breaking stress σ_r, time to failure t_r (a) and minimum critical breaking stress ($\sigma_{r_{min}}$) (b).

In accordance with the ideas developed in [129], lowered static fatigue should be observed in a certain temperature range irrespective of whether or not there is hydrogen in the metal. This is explained by the fact that two groups of processes that influence failure in opposite directions develop in the metal as the temperature rises: 1) a lowering of boundary shear strength (С.Г.С.) and thermal activation of vacancy motion (Д.В.); 2) or-

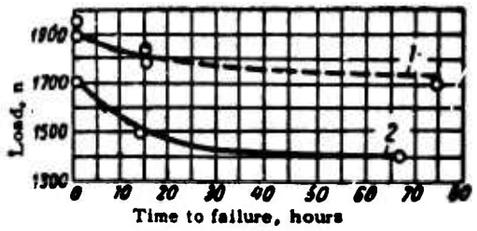

Fig. 43. Influence of load on time to complete failure of notched titanium specimens in static bending. 1) 0.01% H_2; 2) 0.07-0.08% H_2.

dering of boundary structure (у.г.) and stilling of vacancies (п.в.) (Fig. 42a). The first group of processes promotes the premature development of static fatigue, while the second inhibits it. The net result is that at very low temperatures, the long-term strength for a given time σ_r and the time to failure at a given applied-stress level (t_r) are large, because the boundary shear resistance is high and diffusion of vacancies toward grain boundaries is difficult. With increasing temperature, the shear resistance of the boundaries decreases and the diffusion rate of the vacancies rises, thus contributing to premature static fatigue. At high enough temperatures, however, the second group of processes develops rapidly, causing a kind of "relaxation." As a result, lowered static fatigue is observed in a definite temperature range (Fig. 42b).

Thus, it follows from [129] that the existence of a definite temperature range of static hydrogen fatigue is not a phenomenon governed by hydrogen. The role of hydrogen reduces to enhancement of this relationship. Its behavior is similar to that of vacancies: combined diffusion of hydrogen atoms and vacancies to the grain boundaries lowers long-term strength more sharply than does diffusion of vacancies alone.

The cases of premature failure of hydrogenated specimens under static loading that were considered above pertained to materials or hydrogen concentrations with which segregations of a hydride phase do not form. Actually, hydrogen also lowers long-term strength when hydride segregations are present in the structure of the material, the more so as they are precipitated from hydrogen-supersaturated solutions under the action of applied load. In this case the brittleness is irreversible.

Figure 43 presents curves characterizing the influence of load on time to total failure for notched titanium specimens with various hydrogen contents under static bending, according to L.S. Moroz et al. [229]. These data indicate that hydrogen causes a sharper drop in breaking stress as a function of loading time, i.e., it lowers the long-term strength of titanium by a substantial margin.

It is indicated in [129] that hydrogen must greatly reduce the time to failure of quenched or rapidly cooled titanium specimens under static loading. In this case, hydride segregation should promote the development of cracks that is due to coagulation of vacancies at grain boundaries. In view of the fact that the hydride transformation in titanium has a large volume effect (three times that of the martensite transformation in steel), hydrogen lowers long-term strength substantially even when the number of hydride segregations is small.

It is interesting to note that static fatigue failure always develops along grain boundaries in steel but quite often along cleavage boundaries in titanium. The authors of [129] conclude that this difference is due to the fact that only elastoviscous flow along grain boundaries develops in steel in static fatigue, while the flow is elastoplastic in titanium. Actually, the failure along cleavage planes in titanium may be governed by segregation of hydrides, which, as a rule, form along cleavage planes.

Manuscript Page No.

Footnote

97 [1]Actually, the cloud is not cylindrical; it is elongated along the slip plane and has a nonuniform hydrogen-atom distribution.

Transliterated Symbols

68 т = t = tekuchest' = yield, flow

68 изг = izg = izgib = bending

72 р = r = razrusheniye = breaking, failure

78 н = n = nachal'nyy = initial

80 кр = kr = kriticheskiy = critical

90 т = t = treshchina = crack

93 пр = pr = predel'nyy = limiting

Chapter 4

INFLUENCE OF HYDROGEN ON CREEP, FATIGUE STRENGTH AND WELDABILITY

1. INFLUENCE OF HYDROGEN ON THE CREEP OF METALS

There are very few data on the influence of hydrogen on the creep of metals. Such work as has been done has been devoted for the most part to the effect of hydrogen on the creep strength of titanium and titanium alloys. It was observed in [45] that when the load is first applied, hydrogen increases the absolute amount of deformation and the creep rate. However, the authors indicate that as the stress rises above the yield point, admixture of hydrogen has no substantial influence on creep. It was found in [270] that hydrogen raises the creep rate of alloys in the titanium-molybdenum and titanium-chromium systems. On the other hand, Zwicker [114] reports that at concentrations below 0.1% (by mass), hydrogen increases the creep resistance of notched specimens at room temperature.

A quite detailed study of the influence of hydrogen on the creep rate of the ($\alpha + \beta$) titanium alloy Ti-2Al-2Mn was made in [268]. It was observed that for the vacuum-annealed alloy, the initial creep rate is lower at all test temperatures than for hydrogenated specimens. However, the data for hydrogenated specimens are so contradictory that it is impossible to establish any general relationship linking creep rate with hydrogen concentration. It was observed in the same study that the initial creep rate depends very strongly on grain size: with an equiaxial fine granular structure, the initial creep rate is higher than for a coarse lamellar structure.

We have observed in a study of the influence of hydrogen on the properties of titanium in the 573-873°K temperature range that hydrogen lowers creep rate at temperatures above 773°K. At lower temperatures, reversible hydrogen brittleness may develop in titanium during the creep tests. The rate of its development depends essentially on speed of deformation and hydrogen content, so that the over-all picture obtained is quite complex.

In [299], the influence of hydrogen on the creep of Zircalloy-2 and the zirconium alloys Zr — 2% Nb and Zr + 3% Nb + 1% Sn was studied at 848°K. It was found that hydrogen raises the creep rate of Zircalloy-2 at applied stresses of 60 Mn/m^2.

At higher stresses, 110 Mn/m^2, hydrogen lowers the creep rate

of this alloy substantially at concentrations greater than 0.05% (by mass). In the alloy Zr + 3% Nb + 1% Sn, hydrogen has little influence on creep rate at a stress of 120 Mn/m^2, but at higher stresses it also reduces creep sharply. A somewhat different picture is observed for the alloy of Zr + 2% Nb. At stresses of 90 and 110 Mn/m^2, hydrogen increases creep rate. The creep curves for this alloy are quite similar for the stresses chosen.

It appears probable that at low stresses and temperatures, hydrogen accelerates creep. With increasing applied stresses and rising temperature, hydrogen has a tendency to lower creep rate.

The decrease in creep rate on injection of hydrogen into metals may result from an influence that it exerts on the vacancy mechanism of creep. The work of V.N. Gulyayev [273] is of great interest in this respect.

V.N. Gulyayev assumes that interstitial impurities can heal vacancies, especially if the dimensions of the interstitial atoms are close to the critical ratio r_x/r_0 (r_x is the radius of the interstitial atom and r_0 is the radius of the basic metal), which is 0.59. The author explains the lowering of creep rate when steel is alloyed with boron, nitrogen and oxygen by the formation of Cottrell atmospheres around dislocations of these atoms and healing of the vacancies by passage of the impurity atom from the interstitial position to a substitutional position.

2. INFLUENCE OF HYDROGEN ON FATIGUE STRENGTH OF METALS

The influence of hydrogen on fatigue strength has been studied only for steels, titanium and titanium alloys. The results obtained by various authors are to a certain degree contradictory. In some studies, a lowering of endurance limit is noted on saturation of the metals with hydrogen, in others no appreciable influence of hydrogen on the resistance of the metal to cyclic loading is observed, and in still others the fatigue strength was found to rise on introduction of hydrogen. It is possible that these contradictions are due to differences in the technique of specimen preparation and testing.

Despite the sharp increase in the sensitivity of titanium to notching in the presence of hydrogen in single-pass tensile or impact tests, hydrogen has practically no influence on the sensitivity of titanium to stress concentrators under the conditions of sign-alternating cyclic loading [215].

The influence of hydrogen on the fatigue strength of technically pure titanium was investigated in Berger's study [216]. The tests were run on smooth and notched specimens with a 3.0 theoretical stress concentration coefficient. The specimens were subjected to alternating-sign bending as they rotated at 10^5 cycles per minute. It was found that the fatigue limit of notched specimens containing 0.039% H_2 was the same as for those containing 0.0018% H_2.

It was found in the recently published study [235] that raising the hydrogen content in titanium from 0.002 to 0.03% (by mass)

even increases the fatigue limit by 10-15%. The authors attribute the increase in fatigue limit to a rise in the static strength of the titanium as a result of injection of hydrogen, and to the hardening effect of hydrides segregated in the testing process due to the slight rise in specimen temperature. The hardening effect of hydrides under the conditions of cyclic testing prevails over their activity as stress concentrators.

3. INFLUENCE OF HYDROGEN ON THE PROPERTIES OF WELDED JOINTS

Numerous studies published in recent years indicate convincingly that hydrogen exerts its most damaging influence on the properties of welded joints. Increased hydrogen contents contribute to the appearance of porosity in the metal of the seam and the zone around the seam and to the formation of cracks that lower the strength of the welded joints and, in some cases, even lead to total failure of the welded joint.

In metals that absorb hydrogen endothermically, rapid crystallization of the molten metal and rapid cooling of the seam metal and the zone around it result in the formation of heavily supersaturated hydrogen solutions in the metal. If the hydrogen concentration in the molten metal is above a certain critical limit, the hydrogen supersaturation that takes place during cooling may result in formation of pores.

In metals that absorb hydrogen endothermically, pores are formed in the seam metal as a result of seeding and growth of bubbles of hydrogen, which is liberated on cooling of the metal as a result of the decrease in its solubility, in the liquid metal of the welding tool [28, 46, 218, 220-227]. Some of these bubbles escape, while others are trapped inside the metal, causing porosity in the seam.

A.A. Alov [28] notes that the shapes of these pores may vary. Usually, they have an elongated "caterpillar" shape, but globular pores are also encountered. The development of gas pores takes place in two stages: first a seed is formed, and then it grows into a visible macropore. Since a large work must be performed for spontaneous formation of a seed, pores appear basically on nonspontaneous centers [28, 29]. The latter may take the form of shrinkage porosity, oxide films, and breaks in the solidity of the metal. Pores germinate preferentially in the region of reciprocal crystallization at the interface between the solid and transitional solid-liquid zones. The pore develops initially in the form of a narrow canal between adjacent dendrites. On reaching the crystallization front, the canal broadens.

Hydrogen also contributes to the development of cracks in welded joints. The mechanism by which hydrogen influences cracking is quite complex and has not been studied at all. Cracks may form in welded joints directly during the welding process, in the cooling phase after welding, and even long after welding.

While pores are formed during cooling of the molten metal in metals that absorb hydrogen endothermically, they form on rapid heating in metals that absorb it exothermically.

Figure 44 illustrates the influence of the rate of direct electrical heating of thin technical titanium bars with various contents of hydrogen on the tendency to blistering. If we remember that the heating rate of the metal in the zone around the weld does not exceed 500 deg/sec, we must take 0.01% (by mass) as the admissible hydrogen concentration in the basic metal.

Hydrogen causes cold cracks to develop in welded joints in titanium [218-221, 222-227]. These cracks appear a certain time after welding, with an incubation period that may run to several months. Table 4 presents the results of Ye.A. Guseva's studies [222] of the cracking tendency of welded joints in titanium and VT5 alloy, which were made on special specimens.

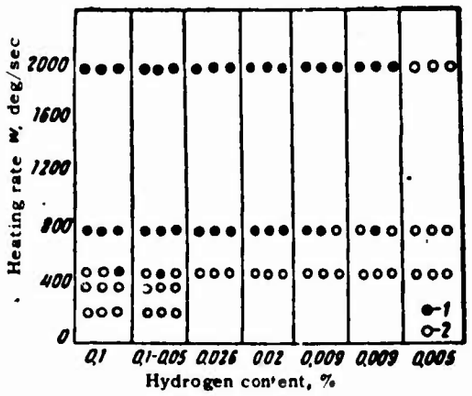

Fig. 44. Influence of rate of direct electrical heating on the blistering tendency of thin technical titanium bars. 1) Blistering; 2) no blistering.

TABLE 4

Influence of Hydrogen Content in Seam Metal on its Cracking Tendency [222]

Material	Impurity contents in fused metal, % (by mass)			Time to formation of crack, days
	H_2	N_2	O_2	
VT1	0,0117	0,032	0,33	16
	0,0096	0,039	0,27	57
	0,0083	0,020	0,13	256
	0,0029	0,032	0,21	365
VT5	0,020	0,034	0,16	55
	0,0104	0,033	0,21	75
	0,0071	0,017	0,21	89

The data given in Table 4 indicate that the time to cracking is sharply reduced with increasing hydrogen contents.

With the special specimens, it was established in the same paper [222] that structural transformations take place over a long

period at room temperature in the seam metal and in the zone around it, and lead to an increase in the volume of the metal that is larger the higher the hydrogen content. The author assumes that these volume changes are due to precipitation of titanium hydride from a hydrogen-supersaturated solid solution. In combination with macroscopic stresses of the first kind, the structural stresses of the second kind that then arise lead to the appearance of microcracks in the welded joints, and these then develop with the passage of time. The microcracks often appear in the zone around the weld rather than in the seam metal.

Since lamellar titanium hydride segregations have tensile strengths that are considerably lower than that of titanium, the first few microcracks resulting from internal stresses appear along the titanium/hydride interface. Subsequent propagation of these cracks also occurs preferentially along the hydride lamellae. Thus the fracture surface passes along the hydride segregations.

It is reported in [129] that the formation of cold cracks in titanium welded joints is promoted by a hydride transformation that takes place with an increase in specific volume and results in considerable local stresses of the first and second kinds, which favor brittle failure. The massiveness of the hydride transformation and, consequently, the tendency to formation of cold cracks increase with increasing hydrogen content.

Due to the very fast cooling of the metal under the conditions of welding, the hydride transformation takes place at temperatures near room temperature. At this temperature, relaxation of internal stresses is difficult, and for this reason the hydride transformation taking place in welding promotes cracking more strongly than when titanium products are cooled after annealing.

The distribution of the hydrides has a substantial influence on the tendency to cold cracking [225]. Slow cooling of the metal after the last heat treatments promotes the formation of brittle hydride-phase segregations along the grain boundaries. This distribution of the hydrides accelerates the formation of cold cracks and increases the sensitivity of the alloys to stress concentration at these points.

The level of the basic material's plastic properties has substantial influence on the tendency to cold cracking. Due to the high sensitivity to stress concentration, high-strength and low-plasticity alloys are more inclined to crack than low-strength, high-plasticity types.

It is shown in [138] that the cold cracks that appear in titanium and α-alloys some time after welding are also observed in many cases in the absence of a hydride phase. Thus, the hydride transformation in the seam metal and the zone around the weld is not the only cause of cracking in welded joints. It may be due to reversible hydrogen brittleness. Actually, the appearance of cold cracks is observed not only in titanium and the α-titanium alloys, but also in (α + β) titanium alloys at hydrogen concentrations quite far below the solubility limit.

It was observed in [218] that hydrogen greatly shortens the service life of the weld-seam material under alternating loads. Regardless of hydrogen content, specimens of the basic material withstood 10^7 cycles without failure. Welded specimens broke after a much smaller number of cycles. The number of cycles to failure of the welded specimens was smaller the higher the hydrogen content. As was indicated above, this pattern is not observed for sheet or forged material.

The difference observed in the behavior of sheet or forged material and weld-joint material is apparently due to structural differences (the former are deformed materials, while the weld seam has a cast structure), as well as rather large internal stresses in the welded joints.

Published data suggest that the hydrogen in welded joints is most detrimental to the properties of the metals. The strong tendency to cracking in welded joints that hydrogen causes is associated not only with the formation of heavily supersaturated solutions of hydrogen in the seam metal and the zone around the seam and with a shift of the hydride transformation toward lower temperatures, but also with internal stresses. The latter set up a directional flow of hydrogen to stretched positions in the lattice, and the progressive segregation of hydrogen at these places may weaken cohesive forces and generate cracks.

The above implies two directions that might be taken by countermeasures against cold cracking in welded joints. Firstly, it is necessary to try to eliminate all sources of hydrogenation during the welding process. Secondly, the weldments must be heat-treated to relieve internal stresses. The stronger the tendency of the alloy to form cold cracks, the shorter must be the time between the welding and heat-treating operations [138]. Since the tendency to cold cracking due to hydrogen becomes stronger as the seam metal loses plasticity, it is necessary to protect this metal from contamination by nitrogen and oxygen.

Part Three

INFLUENCE OF HYDROGEN ON THE STRUCTURE AND PROPERTIES OF METALS AND THEIR ALLOYS

Chapter 1

BERYLLIUM, MAGNESIUM, AND ALUMINUM

1. INTERACTION OF BERYLLIUM, MAGNESIUM AND ALUMINUM WITH HYDROGEN

It was assumed until recently that beryllium did not react directly with hydrogen on heating to 1273°K [149], and that the solubility of hydrogen in solid beryllium was negligibly small [150]. Blanchard and Bochirol [365] detected marked solubility of hydrogen in solid beryllium. Beryllium containing 0.32 and 1.52% of BeO was degasified in vacuum at 998°K during 4 hours and then held in a hydrogen atmosphere at pressures of 300-760 mm Hg (0.04-0.1 Mn/m^2) in the temperature range from 773 to 1023°K for 2-3 hours. After the metal had cooled, the hydrogen content in the specimens was determined by degasification. An anomalously high hydrogen absorption was detected at temperatures around 873°K. At a pressure of 0.1 Mn/m^2 (760 mm Hg), it is 0.8 $cm^3/100$ g. The activation energy of hydrogen absorption by beryllium is 36-43 kcal/g-atom (150-180 kj/g-atom), depending on the purity of the metal, for the 898-1023°K temperature range.

It is assumed that although the compounds BeH or BeH_2 may form in an electric discharge between beryllium electrodes in a hydrogen atmosphere, they would hardly form on direct reaction of beryllium with molecular hydrogen [149].

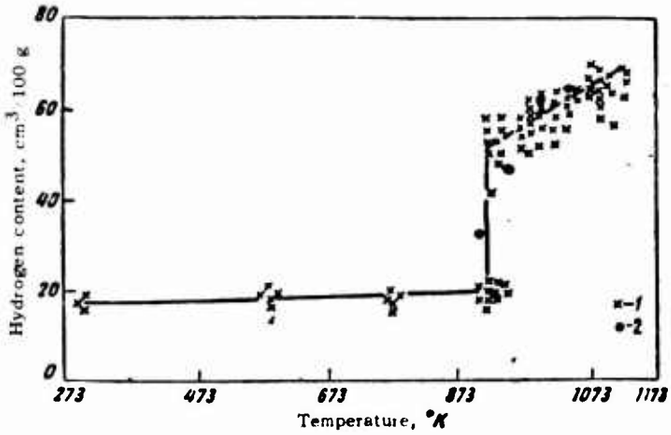

Fig. 45. Solubility of hydrogen in magnesium as a function of temperature at a pressure of 0.1 Mn/m^2. 1) According to M.V. Sharov and V.V. Serebryakov; 2) according to Koeneman and Metcalfe.

Indirect methods of preparing beryllium hydride BeH_2 are described in [5]. Beryllium hydride BeH_2 is a solid nonvolatile white substance. It is quite stable up to temperatures of the order of 353°K. It decomposes readily at 393°K.

According to published data [4, 5], magnesium has practically no reaction with molecular hydrogen at temperatures below 373-433°K. Not even sprayed magnesium, which has an active, expanded surface, adsorbs molecular hydrogen. However, ionized hydrogen is readily adsorbed by magnesium. It is then easily desorbed on heating to 473-573°K.

At high enough temperatures, magnesium and its alloys absorb hydrogen quite readily. The solubility of hydrogen in magnesium increases with rising temperature. The first published data on the solubility of hydrogen in magnesium [4, 5] are not entirely reliable, principally because of inadequacies of the method used to determine hydrogen content.

The most accurate data on the solubility of hydrogen in molten and solid magnesium were obtained in the study of M.V. Sharov and V.V. Serebryakov [188], using a method developed by A.P. Gudchenko [186, 187] to determine hydrogen content.

The data obtained by these authors on the solubility of hydrogen in magnesium are given in Fig. 45. They can be represented approximately by the straight line satisfying the equation

$$\lg C_0 = -\frac{1120}{T} + 2{,}576,$$

where C is the solubility at a hydrogen pressure of 1 atmosphere (0.1 Mn/m^2). For an arbitrary pressure p, the equation assumes the form

$$\lg C/p^{1/2} = -\frac{1120}{T} + 1{,}136,$$

From this it follows that the heat of solution of hydrogen in liquid magnesium is 10.32 kcal/g-atom (43 kj/g-atom).

The solubility of hydrogen in magnesium was recently studied by Koeneman and Metcalfe [181], who used a Sieverts apparatus. They found that the solubility of hydrogen in magnesium is subject to Sieverts' law for temperatures of 913, 948 and 998°K. At 1048°K, Sieverts' law holds only at low pressures. The corrected results obtained by the authors for the solubility of hydrogen in magnesium appear in Fig. 45.

The values found by the authors for the solubility of hydrogen in solid magnesium are substantially higher than those obtained in earlier investigations.

The solubility of hydrogen in magnesium depends substantially on the contents of alloying elements and impurities. Thus, for example, the solubilities of hydrogen in alloys of magnesium with aluminum in the solid state are as follows [278]:

Al content, %.....	0	3	6	10	20	30
Solubility, cm^3/100 g of metal...	19	22	23	20.5	18	15.3

A detailed study of the solubility of hydrogen in the magnesium alloy ML5 was made in [189]. The results can be described by the following equations:

a) for the solid alloy

$$\lg C = -\frac{47}{T} - 0{,}198 + \frac{1}{2}\lg p;$$

b) for the liquid alloy

$$\lg C = -\frac{680}{T} + 0{,}948 + \frac{1}{2}\lg p,$$

where C is the hydrogen content in cm^3/100 g of metal; p is the hydrogen pressure in mm Hg.

In view of the small size of the hydrogen atom, it may be assumed that hydrogen forms interstitial solid solutions in magnesium.

On direct interaction of magnesium with hydrogen, hydrides form only at rather high pressures. However, magnesium hydrides can be obtained indirectly [5]. The structure of magnesium hydride has not been precisely established. It is supposedly a polymorphous compound in which the magnesium atoms are linked by "hydrogen bridges."

It was established in [180] that the compound SiH_2 forms along grain boundaries in alloys of magnesium with silicon that have been saturated with hydrogen. This is confirmed by the fact that on degasification of magnesium-silicon alloys, both hydrogen and silicon are evolved, a fact that can be used to purify magnesium of silicon. The amount of degassed silicon and hydrogen conforms to the atomic ratio 1:2, which, in turn, corresponds to the formula SiH_2. It is shown in [177, 178] that zirconium hydrides form in alloys of magnesium with zirconium on saturation with hydrogen.

Sublimated aluminum films adsorb a certain amount of hydrogen at temperatures from 90 to 293°K. Insignificant absorption takes place even at 273°K. The rate of reaction of hydrogen with aluminum increases with rising temperature, and in the liquid state aluminum absorbs hydrogen readily, owing to the high diffusion rates of hydrogen in liquid aluminum.

Data obtained by various authors on the solubility of hydrogen in liquid aluminum at a pressure of 0.1 Mn/m^2 are shown in Fig. 46a.

It is assumed that the data of Ransley and Neufeld are most reliable. In the temperature range from 660 to 850°C, their results can be described by the equation

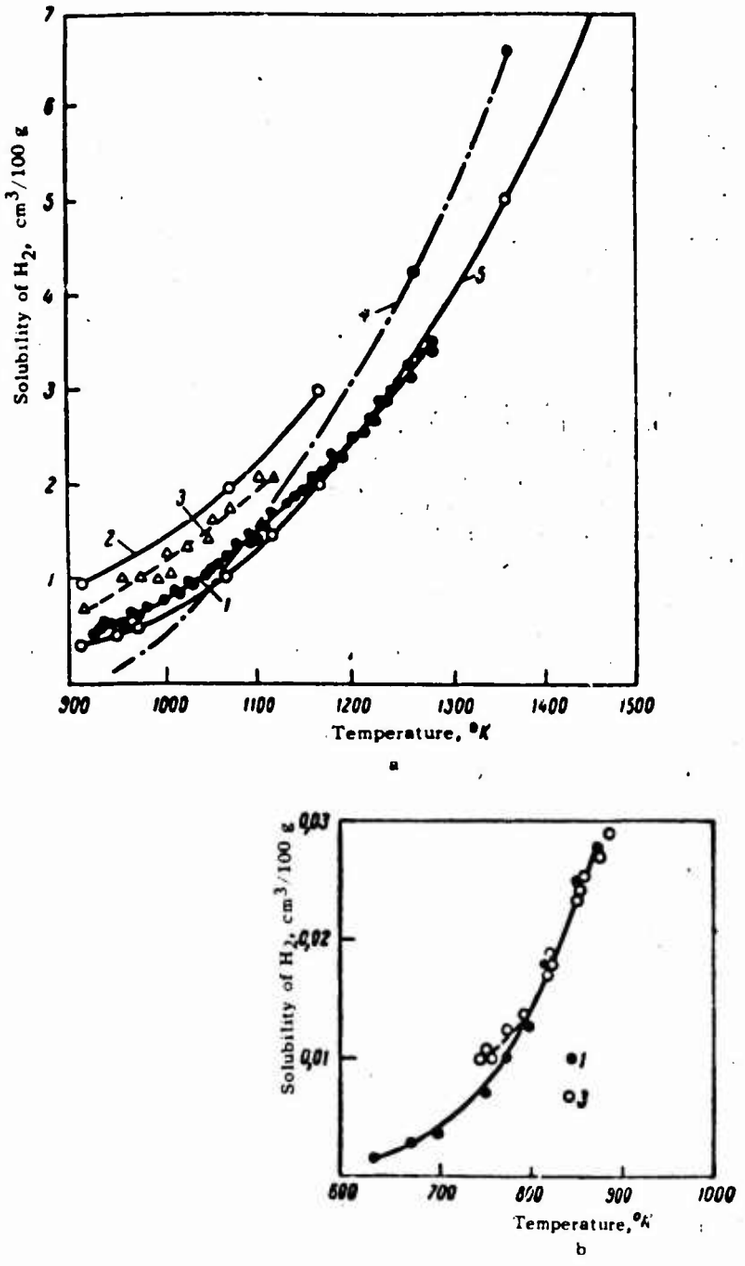

Fig. 46. Solubility of hydrogen in aluminum as a function of temperature at a pressure of 1 atmosphere excess (0.1 Mn/m^2). a) In liquid aluminum; b) in solid aluminum; 1) Eichenauer and Pebler; 2) Baukloh and Osterlen; 3) Ransley and Neufeld; 4) Röntgen and Braun; 5) Röntgen and Möller.

$$\lg C/p^{1/2} = -\frac{2760}{T} + 1{,}356,$$

from which it follows that the heat of solution of hydrogen in liquid aluminum is 25 kcal/g-atom (10.5 kj/g-atom).

The solubility of hydrogen in solid aluminum can be described by the equation

$$\lg C/p^{1/2} = -\frac{2080}{T} - 0{,}652,$$

from which it follows that the heat of solution of hydrogen in solid aluminum is 19 kcal/g-atom (80 kj/g-atom).

Ransley and Neufeld established that hydrogen dissolves in aluminum in the atomic form in accordance with Sieverts' law. In aluminum, the hydrogen atoms may be ionized to protons, but the possibility of such ionization has not been taken into account in any of the papers. Water vapor does not react with solid aluminum. It is reported in [173] that attempts to introduce hydrogen into solid aluminum by heating it in steam at 900°K for two days were not crowned with success. In [49], on the other hand, it was found that on heating in steam, bubbles may form at the surface of aluminum of high purity. Annealing of aluminum at 773°K does not cause formation of bubbles if the dew point of the surrounding air is below 278°K. Very small silicon additives aggravate the tendency of aluminum to form bubbles during annealing at 773°K, although they have no influence at lower temperatures (573°K). Introduction of beryllium in quantities greater than 0.003% prevents bubble formation completely. The oxide film formed on annealing of aluminum in dry air at 723-773°K prevents the formation of bubbles, while the film formed at lower temperatures does not affect this process.

However, steam reacts readily with liquid aluminum according to the scheme

$$3H_2O + 2Al \rightleftarrows Al_2O_3 + 6H.$$

Molecular hydrogen penetrates solid aluminum in very small quantities because of the slight dissociation of the hydrogen molecules into atoms. The partial pressure of atomic hydrogen at a molecular-hydrogen pressure of 1 atmosphere excess (0.1 Mn/m^2) is only 10^{-12} atmosphere excess (10^{-13} Mn/m^2) at 773°K.

The hydrogen liberated in the reaction of aluminum with water vapor may give rise to atomic-hydrogen pressures many times greater than the equilibrium value. Hence the hydrogen formed in the reaction of aluminum with steam diffuses effectively into solid aluminum. Reaching pores (cavities), the atomic hydrogen recombines to form hydrogen molecules. The hydrogen pressure in these pores may exceed the yield point of the aluminum [161].

Molten aluminum readily absorbs hydrogen on heating in an oil-fired furnace, and in larger quantities as the temperature rises, as follows from the data given below [173]:

Temperature, °K.....	1023	1073	1123	1173
Hydrogen content, cm^3/g.....	0.20	0.36	0.44	0.6

V.P. Ivanov and A.G. Spasskiy [172] assume that the contradictory results as to the solubility of hydrogen in aluminum that

have been obtained by various authors can be explained by the presence of oxides in the metal, the content of which may vary greatly between melts. It was shown in [170-172] that if aluminum or aluminum alloys are purified of oxides, for example by introduction of 0.3% of dehydrated manganese chloride at 993-953°K, they become immune to hydrogen absorption. While the hydrogen content in unrefined alloys increases from 0.2-0.45 to 0.45-1.15 cm^3/100 g of metal when steam is bubbled through it, it is impossible to saturate melts with hydrogen when they have been thoroughly purified of oxides; the hydrogen content in these melts did not exceed 0.10 cm^3/100 g after steam had been blown through them at 1003-1073°K for 1-2 hours. Nor were the melts saturated with hydrogen on reheating in electric and gas-fired furnaces to 1173-1123°K. The gas content at 973°K was again found to be less than 0.1 cm^3/100 g. According to [170-172], the true solubility of hydrogen in aluminum at 973°K and atmospheric pressure is only 0.05-0.06 cm^3/100 g.

The authors of [172] give the following representation of the role taken by oxide inclusions in the gasification of aluminum. If the melt contains no oxides or contains oxides that are not active with respect to hydrogen, only a solution of hydrogen in aluminum will be formed on reaction of aluminum with molecular hydrogen. If the melt contains oxides that are active with respect to hydrogen, hydrogen will be adsorbed by the oxides from the liquid solution, with formation of compounds of the type $(Al_2O_3)xH$. The equilibrium between the liquid solution and the gaseous phase will be upset, the hydrogen will begin to pass into the liquid solution, to be adsorbed from it again by the oxides. This process will continue until total equilibrium is established in the gaseous phase/liquid solution/oxides system. The net result will be that the aluminum oxides cause a high degree of gasification of the melt, exceeding by tens of times the equilibrium solubility of hydrogen in aluminum.

If the aluminum is in a water-vapor (steam) atmosphere, the aluminum oxides will adsorb it and be converted to the hydroxide. Elimination of chemically bound water from the hydroxide takes place in the temperature range from 773 to 1073°K. The water vapor reacts with molten aluminum to form aluminum oxides and hydrogen, of which some goes into the gaseous phase, while some is dissolved in the liquid aluminum, also forming complex compounds of the $(Al_2O_3)xH$ or $[Al_2O_3)xH_2O]yH$ type unless dehydration has been complete. These complexes are highly stable and are responsible for a high degree of gas saturation.

Unfortunately, V.P. Ivanov and A.G. Spasskiy determined the hydrogen content in the aluminum only from the appearance of the first bubble (A.P. Gudchenko's method). Thus their results can be explained by difficulty of formation of the first bubble in oxide-free aluminum because of the absence of nonspontaneous seeding centers, so that it appears at a pressure considerably lower than in aluminum containing oxides. This gives the false impression that the hydrogen content is lower in aluminum without oxide films than in aluminum that has been contaminated by such films. Hence the results of A.G. Spasskiy and coauthors cannot be regarded as reliable until they are checked using other methods to determine

hydrogen.

Hydrides are not formed on reaction of aluminum with molecular hydrogen. The hydride AlH_3, which is a highly unstable compound, has been obtained indirectly; it can exist only in ether solution [5].

2. INFLUENCE OF HYDROGEN ON THE PROPERTIES OF BERYLLIUM

As follows from the data given above, formation of hydrides in beryllium is excluded under actual production conditions, so that we do not observe hydride brittleness in it. Beryllium oxide BeO is a highly stable compound that is not reduced by hydrogen at even the highest temperatures [154]. Hence the development of hydrogen embrittlement in beryllium is also excluded. In view of the negligibly low solubility of hydrogen in beryllium, we should hardly expect the development of reversible hydrogen brittleness of the second kind in it.

Thus, hydrogen does not represent a hazard for beryllium in many of its applications. Blowing hydrogen through liquid beryllium does not change its properties and has no influence on the temperature of the transition from viscous to brittle failure [150]. After beryllium specimens had been held at 1173°K in a hydrogen atmosphere for several hours, no lowering of plasticity was detected [365].

When beryllium is used to make components for nuclear reactors, hydrogen (chiefly in the form of tritium) is formed in it due to neutron bombardment [152, 153]. Under such bombardment, helium is formed in addition to tritium, often in large quantities. Pores and cracks appear in the beryllium as a result.

The formation and growth of gas pores in beryllium under neutron bombardment was studied by Hickman and Chute [368], who used an electron-microscope technique. It was found that the pores form for the most part on segregations of a second phase, perhaps on compounds formed by impurity iron with the beryllium. Thus the distribution of these segregations determines the distribution of the pores. The pore sizes vary from 150-200 Å to 8-10 μ.

It was shown in this study that irradiation with doses up to $2.3 \cdot 10^{20}$ neutrons/cm^2 at temperatures up to 773°K results in an increase in yield point and an almost total loss of plasticity. Bombardment at higher temperatures, 823-973°K, causes no change in the mechanical properties of beryllium at room temperature.

Redding and Barnes [152] injected hydrogen into beryllium in the form of deuterium from a cyclotron. Cavities, which they interpreted as hydrogen-filled pores, were detected in the beryllium after such bombardment.

The consequences of cyclotron bombardment of beryllium with protons were studied by Ells and Evans [369]. Helium is not formed in such bombardment, and hence the intrinsic effect of hydrogen on the structure and properties of the beryllium was studied in this case. The work was done with beryllium purified by

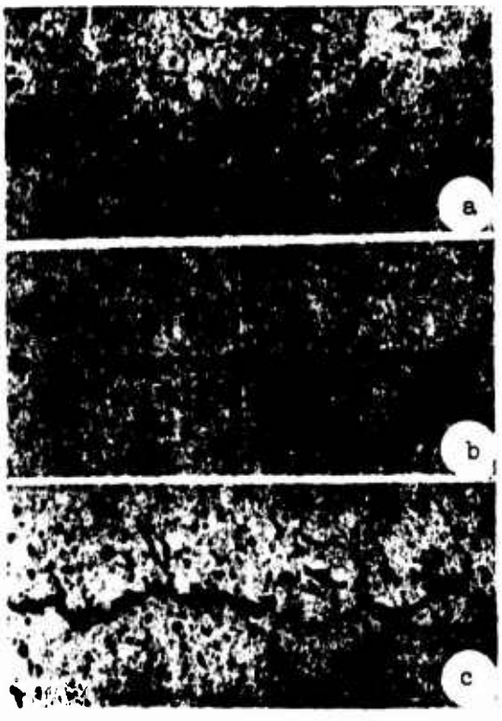

Fig. 47. Microstructure of bombarded beryllium. a) Cast beryllium, annealing at 573°K, 1 hour; b) cast beryllium, annealing at 1273°K; c) extruded beryllium.

zone melting. The beryllium specimens were bombarded with 7-Mev protons, with their temperatures held below 223°K. The protons penetrated to a depth of 0.047 cm. The hydrogen content in the hydrogenated layer was 0.25-0.5 cm^3/100 g [0.02% (atomic)].

The irradiated specimens were polished and etched in a 10% glycerine solution of hydrofluoric acid. Pores were detected in the bombarded specimens on metallographic examination. These pores did not appear immediately after bombardment, but only after a certain type of heat treatment. In cast material, for example, pores appear only after annealing at 573°K for at least an hour. In material with fine-grained structure and a high oxygen content, pores are formed after an hour's annealing only at temperatures above 773°K. Hydrogen pores form preferentially at grain boundaries. In low-temperature annealing, the pores are very fine; as the annealing temperature is raised they become larger, and at temperatures above 1273°K most of the pores disappear, both at the grain boundaries and inside the grains.

In hot-extruded beryllium, which has a finer grain than the cast material, pores form both inside the grains and at their boundaries. At higher temperatures, 1073-1273°K, the pores merge to form cracks (Fig. 47). Metallographic examination showed that these cracks form along grain boundaries.

In beryllium, hydrogen bubbles are formed at considerably lower temperatures than helium bubbles and grow faster. This indicates that hydrogen diffuses considerably faster than helium in beryllium.

3. INFLUENCE OF HYDROGEN ON THE PROPERTIES OF MAGNESIUM

The data given above on the interaction of magnesium with hydrogen indicate that formation of hydrides in this metal is excluded under the actual conditions of production and use of magnesium, so that no hydride brittleness appears (with the exception of alloys of magnesium with zirconium). Nor do we observe hydrogen embrittlement in magnesium and its alloys, since magnesium oxides are not reduced by hydrogen even at their melting points.

The most harmful effect of hydrogen in magnesium is associated with the decrease in hydrogen solubility as the metal solidifies from the melt, causing porosity in the metal. The factors that govern the development of porosity in lightweight alloys and countermeasures against it are examined in papers by Soviet scientists [64, 183, 186, 189, 279-286]. The porosity of magnesium alloys has been most thoroughly studied by M.V. Sharov and coauthors.

It is proposed in [278] that, as a rule, the formation of bubbles in the liquid metal does not result in porosity. In this case the bubbles float up easily and are eliminated from the melt. Evolution of gas is most dangerous during freezing of the alloy, when the forming crystals interfere with the buoyancy of the bubbles.

The rate of gas evolution depends on the amount of gas that must be liberated in the crystallization interval from the liquidus point to the solidus, and on its ability to form supersaturated solutions. The gas porosity naturally decreases with decreasing difference between the liquid and solid-phase solubilities and with increasing tendency to formation of supersaturated solutions. Thus, as was noted above, raising the aluminum content in magnesium to 6% increases the solubility of hydrogen in the solid state, but increasing it further lowers this solubility. For this reason, the rate of gas evolution first falls and then rises as the aluminum content in magnesium is increased.

The extent of hydrogen supersaturation of the metal depends not only on cooling rate, but also on composition. Figure 48 presents a three-dimensional diagram illustrating the variation of hydrogen supersaturation of magnesium-aluminum alloys as a function of cooling rate and aluminum content [278]. The data shown on the diagram indicate that supersaturation of the solid metal by hydrogen decreases with increasing aluminum content. The decline of supersaturation with increasing aluminum content in magnesium-aluminum alloys is found to be decisive, and gas-shrinkage porosity becomes more severe with increasing aluminum content.

An undulating distribution of gas-shrinkage porosity is observed in many cases. Gas-shrinkage porosity extends throughout the entire volume of a casting, except for the peripheral layers,

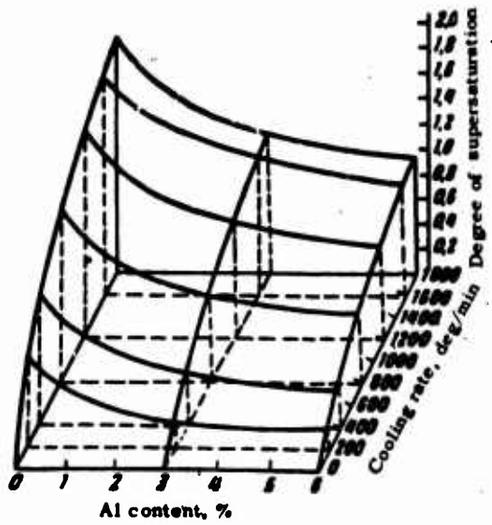

Fig. 48. Change in degree of hydrogen supersaturation in magnesium-aluminum alloys as a function of their composition and of cooling rate.

where the higher cooling rate results in formation of supersaturated hydrogen solutions.

M.V. Sharov and Ye.L. Bibikov [278] recommend the following countermeasures against gas-shrinkage porosity:

1) reducing the hydrogen content in the metal to the corresponding solubility at the solidus temperature and a partial pressure of 0.10 Mn/m^2;

2) increasing the solubility of hydrogen in the solid metal at the solidus temperature;

3) relatively rapid cooling, which ensures formation of supersaturated hydrogen solutions in the solid metal.

It was shown in the work of M.V. Sharov et al. that the hydrogen content in the liquid metal can be lowered by degasifying the melt with chlorine, helium or argon. Allowing the liquid metal to stand before pouring also degasifies it. Solubility in the solid metal at the solidus temperature can be adjusted by alloying; here, for example, 0.1% Ca gives good results. Supersaturated solutions of hydrogen in magnesium alloys may be formed on chill-mold casting if the hydrogen content does not exceed 20-22 cm^3/100 g.

An investigation of gas-shrinkage porosity in ML5 alloy [189] showed that the use of massive, slowly cooling air gates may prevent the formation of gas-shrinkage porosity if the solubility of the hydrogen does not exceed its solubility limit in the liquid state. Under these conditions, the hydrogen will move

by diffusion from the casting into the air gate, where its solubility is higher because of the higher temperature.

Finished pieces with microporosity are characterized by permeability to gases and very low mechanical properties. Microporosity lowers impact strength and the fatigue characteristics particularly sharply [374]. Figure 49 shows the influence of hydrogen on the mechanical properties of magnesium alloy ML5 (Mg + 9% Al) in the quenched state. These data indicate that hydrogen has no marked influence on the properties of ML5 if the content of the gas is not above the solubility limit. At hydrogen contents above this limit, both the strength and plastic properties of ML5 alloy decline sharply.

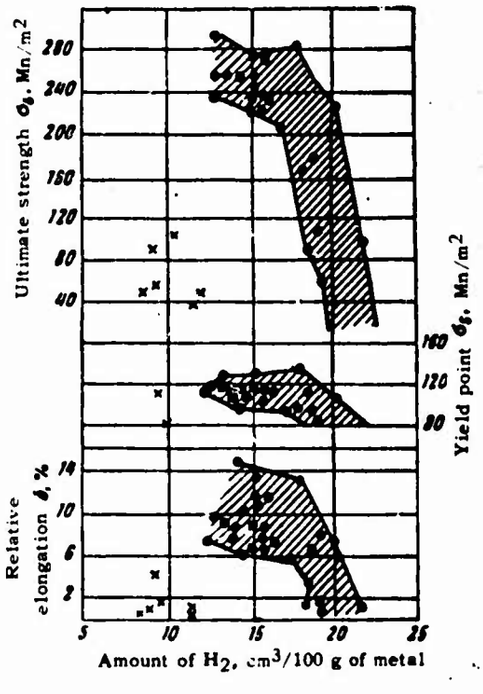

Fig. 49. Influence of hydrogen on the mechanical properties of ML5 alloy in the quenched state.

In annealed ML5 alloy, the decline of the mechanical properties begins at lower hydrogen concentrations than in the quenched state. It appears that annealing promotes escape of hydrogen from the supersaturated solution, so that microscopic discontinuities form.

It was shown in [151, 177, 178] that during prolonged homogenizing of alloys of magnesium with zirconium in moist carbon dioxide, or in quick annealing in a hydrogen atmosphere, the ε-hydride of zirconium is formed. The hydride segregations are germinated preferentially along grain and subgrain boundaries, as well as at dislocations. Segregation of hydrides at the grain

boundaries inhibits grain growth.

It was shown in [126] that in creep tests run on homogenized Mg + 0.6% Zr alloy, the creep rate is proportional to the first power of the stress for small applied stresses and to the thirtieth power for large stresses. An explanation given for this result in [178] is as follows: at small stresses, when the process takes a long time, hydrides are segregated from the supersaturated solution and inhibit the development of creep, while under large stresses the time to failure is so short that there is no time for solution decay.

The properties of the alloy Mg + 0.5% Zr were studied in [177] in connection with the conditions of work in nuclear reactors. Tensile tests were made at a speed of 0.01%/hr at 773°K in a CO_2 atmosphere with 0.02% (by mass) of water vapor present as an impurity. It was shown that under these conditions, the alloy is saturated with hydrogen and that hydride segregations form in it along $\langle 11\bar{2}0 \rangle$ directions, if possible perpendicular to the direction of action of the applied tensile stresses. As a result of hydrogen saturation, microcracks form along these directions and brittle failure of the alloy occurs in accordance with the specific hydrogen distribution.

Although the steam content in the gas cooling the reactor is considerably lower than 0.02% (by mass), a considerable quantity of hydrogen is taken up over five years of operation, and a drop in plasticity is possible if the hydrides are distributed in the manner observed.

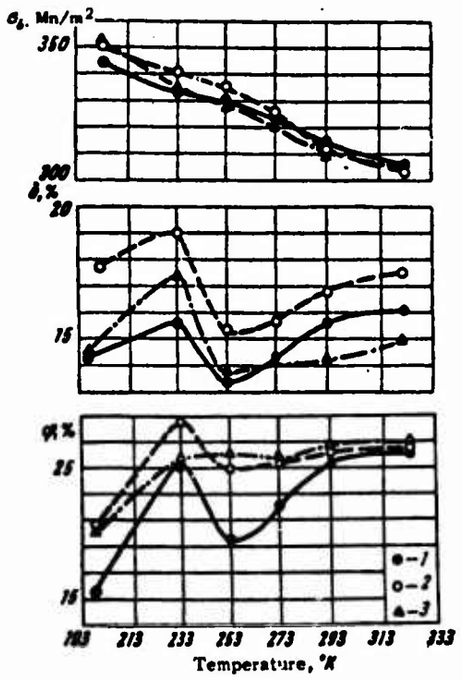

Fig. 50. Influence of test temperature on the mechanical properties of MA2-1 alloy extruded rod at various deformation speeds, mm/min: 1) 0.4; 2) 4; 3) 20.

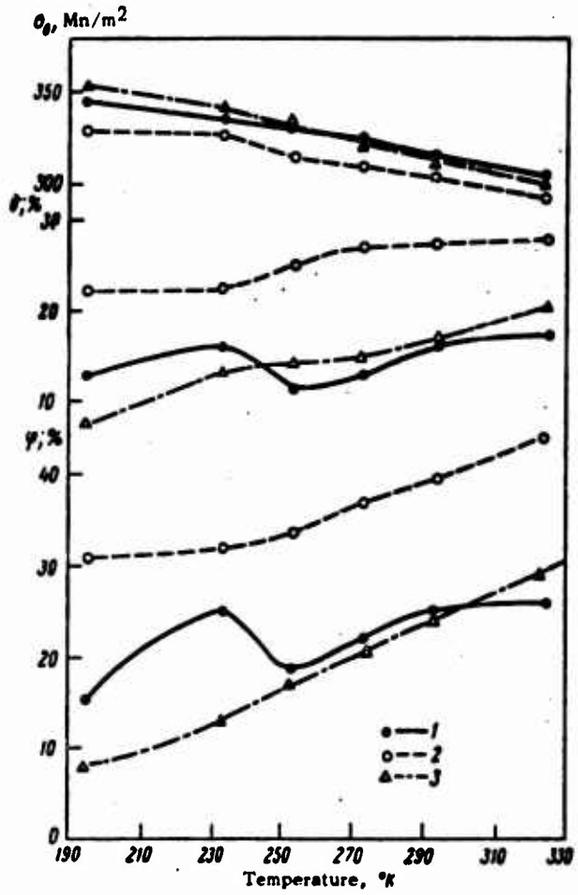

Fig. 51. Influence of test temperature on the mechanical properties of MA2-1 alloy at a deformation rate of 4 mm/min. 1) Extruded rod; 2) vacuum annealing at 573°K; 3) annealing at 573°K in air.

In view of the high solubility of hydrogen in magnesium and its alloys, reversible hydrogen brittleness of the second kind may arise in them.

This hypothesis is confirmed by data that we obtained for the magnesium alloy MA2-1. Extruded rods 20 mm in diameter containing 16 cm^3/100 g of H_2 were taken for the investigation. Mechanical tensile tests showed that the plasticity trough characteristic of reversible hydrogen brittleness is observed for extruded MA2-1 alloy in the temperature range from 243 to 293°K (Fig. 50). This trough is most conspicuous at a deformation rate of 0.4 mm/min. With increasing speed of deformation, it becomes smaller, and the necking curve shows no sign of it at 20 mm/min. The decrease in necking and elongation at temperatures below 233°K is associated with transition of the magnesium to the brittle state for other reasons.

Mechanical-test specimens were prepared from rods of MA2-1 alloy and were subjected to vacuum annealing at 573°K for 10 hours, with the result that their hydrogen content was reduced by

half. No reversible hydrogen brittleness was observed in these specimens (Fig. 51). Necking and elongation were increased by factors of 1.5-2 over those for the extruded material.

To evaluate the role of the heat treatment itself in this plasticity increase, an MA2-1 alloy blank was annealed in an air furnace under exactly the same conditions as were used in vacuum annealing, and specimens were lathed out of the center for mechanical tests. The plastic properties of these specimens were found to be very low. Thus, vacuum annealing may be a highly effective method of increasing the plasticity of magnesium and magnesium alloys.

4. INFLUENCE OF HYDROGEN ON THE PROPERTIES OF ALUMINUM

As in the metals examined above (beryllium and magnesium), no hydride brittleness is observed in aluminum or aluminum alloys, because no aluminum hydrides are formed under the conditions of their production and use. Nor do we observe hydrogen embrittlement, since aluminum oxides are not reduced by hydrogen, even at the melting point of aluminum.

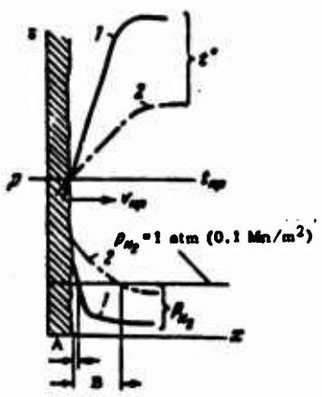

Fig. 52. Temperature and equilibrium partial pressure distribution diagram for dissolved hydrogen across section of freezing metal: 1) high cooling rate; 2) low cooling rate.

As in the case of magnesium, the most detrimental influence of hydrogen on the properties of aluminum and its alloys is associated with the appearance of porosity. The mechanism by which pores form in aluminum alloys is in many respects similar to the mechanism for magnesium alloys. Among the many published papers, those of M.V. Sharov and A.P. Gudchenko are of the greatest interest [184-191].

Thus, aspects of the appearance of porosity at various cooling rates were studied in [276].

With rapid cooling, a steep temperature gradient is set up in the liquid phase next to the crystallization front, with the result that the equilibrium partial pressure of the dissolved hydrogen at the crystallization front rises sharply (Fig. 52). Hence

conditions for the formation of bubbles will be created only in a thin layer of liquid metal (layer A) directly adjacent to the crystallization front, where the internal hydrogen pressure is higher than the external pressure.

When this layer of liquid metal is relatively thin and the crystallization front is advancing rapidly, there is no time for formation of bubbles, since this process involves diffusion of hydrogen and considerable time is required for that. Such high crystallization rates are observed in semicontinuous casting of small ingots. A.P. Gudchenko showed that all of the hydrogen is retained in the supersaturated solid solution when flat aluminum ingots are cast from metal containing even 0.95-1.2 $cm^3/100$ g of H_2.

At comparatively low crystallization rates, the thickness of the liquid-metal layer at the crystallization front, where seeding of bubbles is a possibility, may be quite large (layer B in Fig. 52) due to the shallower temperature gradient. Under these conditions, bubbles will form, since the volume of the hydrogen-supersaturated liquid metal is quite large and the rate of advance of the crystallization front is rather slow.

Until recently, it was a rather general belief that on entering the melt, hydrogen increases the probability of hot cracking in continuously cast ingots and in shaped castings. But this conviction was based on the traditional attitude toward hydrogen as a harmful impurity in metals. Systematic studies by G.A. Korol'kov and I.I. Novikov [440] have shown that this is not always the case. After steam treatment, the hot shortness of the alloys V95, Al + 4.5% Cu, and Al + 0.8% Si dropped sharply, that of D16 alloy was moderately reduced, and that of alloys AMts and grade A00 aluminum showed practically no change. It was found in this same study that hot shortness is reduced when hydrogen reduces linear shrinkage in the effective crystallization range. Hydrogen bubbles liberated during crystallization inhibit shrinkage purely mechanically. The wider the crystallization range, the greater the number of hydrogen bubbles left in the metal and the stronger the effect of hydrogen in reducing the tendency to hot shortness. This is why vacuum annealing of the metal tends to aggravate hot shortness.

This influence of hydrogen on the tendency of metals to hot shortness cannot be universal. The influence of hydrogen on the tendency of the ingot or shaped casting to form hot cracks must be determined by at least two factors: the useful effective reduction of linear shrinkage and the detrimental lowering of the alloy's plasticity in the solid and solid-liquid states.

As in the case of magnesium, gas-shrinkage porosity in aluminum alloys can be reduced by eliminating hydrogen from the melt. M.V. Sharov [184] analyzed the theory of degasification phenomena in light alloys as it applies to aluminum alloys and showed that elimination of hydrogen from the melt is possible as a result of its liberation in the form of bubbles and by diffusive elimination of atomic hydrogen into the environment.

Methods of degasifying aluminum alloys based on the bubble

mechanism of eliminating hydrogen from the melt, such as freezing or melting in a vacuum, have not been developed very extensively, since the former is wasteful and the latter expensive.

Diffusive elimination of hydrogen from the melt is possible if the reaction between the melt surface and moist air is eliminated and conditions that facilitate diffusion of hydrogen from the melt are created. Such conditions obtain when the alloys are melted under fluxes. The liquid flux protects the melt from reaction with moist air and eliminates from the surface the oxide film that impedes escape of hydrogen from the melt. It is shown in [282, 284] that the degasifying ability of fluxes is enhanced considerably if they include fluorides of alkali or alkaline-earth elements. However, this treatment does not secure adequate density of the castings, since as much as 0.4 $cm^3/100$ g of H_2 remains in the metal.

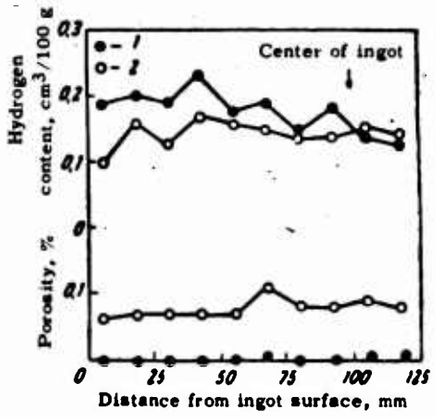

Fig. 53. Distribution of hydrogen content and porosity over cross section of ingot 200 mm thick (99.2% Al). 1) Immediately after casting; 2) after 12 hours of heating at 853°K.

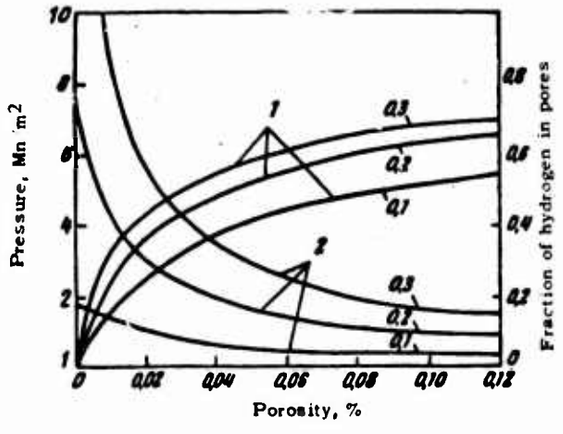

Fig. 54. Hydrogen pressure in pores and distribution of hydrogen between solution and pores at 853°K as functions of porosity (the numerals on the curves indicate hydrogen content, $cm^3/100$ g). 1) Fraction of H_2 in pores; 2) H_2 pressure in pores.

Hydrogen content can be lowered substantially by increasing the holding time of the melt under the flux to 2 hours and replacing the flux at periodic intervals [186]. However, this method of countering gas porosity is not very elegant.

Degasification is accomplished most effectively by passing active and inert gases – chlorine, argon, nitrogen, helium – through the melt. Little is gained by the use of inert gases; chlorination is most effective. Chlorination can lower the hydrogen content in the metal to 0.05-0.07 $cm^3/100$ g. However, this method has a number of shortcomings, most important among which are the toxicity of chlorine and the enlargement of the cast grain.

Chlorides of such metals as zinc, manganese, and aluminum, which, unlike chlorine, are nontoxic, are also used for degasification. However, they are less effective than chlorine and are quite hygroscopic.

It is reported in [191] that aluminum alloys can be degasified successfully using hexachloroethane. Hexachloroethane is nonhygroscopic, inexpensive, and readily available. Hexachloroethane treatment of aluminum alloys results in a substantial decrease in the hydrogen content in the metal.

Studies conducted in recent years [419] have shown that when there is no coarse interdendritic porosity from the crystallization process, minute spherical cavities 1-2 μ in diameter form in the metal. This secondary porosity appears as a result of the tendency of hydrogen to escape supersaturated solid solutions. Secondary porosity is observed in aluminum at hydrogen concentrations as low as 0.1-0.15 $cm^3/100$ g.

Secondary porosity may be absent in the ingot immediately after pouring, but appear after subsequent heating to high enough temperatures (Fig. 53). Under plastic deformation, these pores are flattened and distorted, and the hydrogen leaves for solid solution, but the pore seeds remain and the pores reappear on later heating of the deformed metal. Reconstitution of a system of crushed pores inherited from previous heat treatment is an easier process than the germination of new pores.

The pore system changes on heating: pores at grain boundaries expand, pores inside the grains are resorbed, and the network of uniformly distributed fine pores is replaced by larger pores, up to 10 μ in diameter, which are distributed along grain boundaries. If the pores are close enough to the surface of the metal, they disappear as a result of diffusion of hydrogen from the metal through the surface. In the process of pore growth, the hydrogen pressure in them diminishes (Fig. 54).

It was shown in [136] that porosity may appear in aluminum and its alloys with magnesium on proton bombardment. It was observed that the pores form both along the grain boundaries and inside the grains. The grain-boundary pores are larger than the internal ones. The pore diameters did not exceed 5 μ for the materials selected in the hydrogen concentration range studied (up to

28 cm^3/100 g).

If the temperature of the bombarded specimens is below 313°K, breaks in continuity appear even at an H_2 content of 1.1 cm^3/100 g. Pores were observed at grain boundaries even at 0.18 cm^3 of H_2/100 g. With increasing hydrogen content, the number of cavities increases. As specimen temperature rises during bombardment, the pores become larger.

When bombarded specimens containing more than 14 cm^3/100 g of H_2 are subsequently annealed at 573°K, the intragranular pores first increase in size and then begin to disappear. The pores at the grain boundaries consolidate very rapidly and become cracks if annealing is continued long enough.

In specimens containing from 6.6 to 13.2 cm^3/100 g of H_2, the pores enlarged only along the grain boundaries, but continuous cracks were not formed along these boundaries. The pores inside the grains vanish completely after 20 hours of annealing.

Annealing at 773°K produces the same effect, but in a shorter time. After 1 hour of annealing at this temperature, cracks were detected along the grain boundaries in specimens containing more than 0.001% H_2, while the pores vanished completely in specimens with 0.0002% H_2.

It was found that the pores formed during proton bombardment have no substantial influence on the processes that take place during recrystallization, but do inhibit grain growth. To some degree, magnesium reduces the number of pores formed in aluminum under proton bombardment.

Reference is made by Kolobnev and Al'tman [463] to a lowering of the mechanical properties of aluminum alloys as a result of development of porosity. Eastwood [373] reports that the mechanical properties of nitrogen-degasified aluminum alloys with 2.5 and 8% of Cu and aluminum with 13% Zn are higher than without degasification.

Opie and Grant [370] studied the mechanical properties of an alloy of aluminum with 5% Si and established that within its solubility range, hydrogen has no influence on the properties of this alloy, but that the gas porosity due to hydrogen sharply lowers ultimate strength and elongation. These authors submit the hypothesis that the gas porosity may take the form of an interdendritic network invisible to the unaided eye but capable of lowering the mechanical properties sharply.

It is reported in [173] that the presence of 0.005% (by mass) of H_2 in aluminum results in the appearance of a distinct yield point on the tension curves.

The influence of gas-shrinkage porosity on the mechanical properties of aluminum and its alloys can be judged from the results obtained by M.V. Sharov and M.F. Oding [287], in a study of the influence of degasification on the structure and properties of AL8 alloy. It was shown in this work that treatment of the melt

with 1% zirconium chloride at temperatures of 1023 and 1073°K causes a substantial rise in the ultimate strength and yield point, and particularly in elongation.

TABLE 5

Mechanical Properties of AL8 Alloy in Initial State and After Degasification

Treatment of melt	Grains per mm^2	Gas porosity, points	Mech. properties (averages)		
			σ_b	$\sigma_{2,0}$	δ
			Mn/m^2	Mn/m^2	%
Initial state	50	4—5	300	172	10
Chlorine treatment	74	1	380	195	32
$ZrCl_4$ treatment	500	2	404	213	27,6
Chlorine and $ZrCl_4$ treatment	75	1	384	205	34,8

The properties of alloy AL8 improve on treatment of the melt with zirconium chloride for two reasons: degasification and grain refinement. To separate the effects of these two factors, the influence of chlorination on the properties of AL8 alloy was studied in the same project. Chlorination causes little change in grain size and, at the same time, results in very thorough degasification of the alloy.

The results of the study, which appear in Table 5, indicate that chlorination raises both the strength and plasticity properties of the alloy substantially. Thus, degasification alone, without marked grain refinement, improves the mechanical properties of the alloy appreciably. However, the yield point rises only insignificantly.

Increased hydrogen content is a cause of porosity in weld seams. Investigation [176, 141-143, 288] has shown that seam porosity in arc welding of aluminum results from hydrogen that has entered the liquid metal as a result of reaction between moisture and the aluminum. It is noted in [288] that a high degree of porosity appears when the metal contains more than 0.002% (by mass) of bound hydrogen. On the other hand, considerably larger contents of free hydrogen do not cause porosity under similar conditions.

In the opinion of G.D. Nikoforov [141-143], most of the hydrogen is introduced into the seam metal from the surface of the welding rod, which is many times larger than the area of the basic metal participating in formation of the seam. Hence the most effective measures against porosity are as follows:

1) increasing the diameter of the welding rod, which reduces the relative importance of its surface;

2) use of rational surface treatment on the welding rod, which reduces the amount of hydrogen transferred from it into the tool.

A.A. Alov reports that in addition to the above, countering gas porosity requires that the appearance of pore seeds and their

subsequent development into macroscopic bubbles be inhibited. This requires an effort to refine the dendrites and create a more nearly equilibrium structure in the metal.

Aluminum alloys containing more than 4-5% Mg are particularly inclined to porosity under the conditions not only of casting, but also of welding [141-143]. Pores are formed in welding alloys of the AMg6 type as a result of reaction of the molten metal with moisture present in the particles of oxide film that fall into the tool on fusion of the base and electrode materials.

It should be noted in conclusion that the question as to the possibility of reversible hydrogen brittleness developing in aluminum has not been cleared up. It is reported in [408] that hydrogen brittleness of the type observed in steel was not detected in aluminum. However, no reference is made to either the deformation rates used, or the hydrogen contents, or the test temperature. The above-noted possibility of formation of secondary porosity on heating of aluminum ingots due to segregation of hydrogen from supersaturated solid solution permits the assumption that similar hydrogen segregation may take place in cracks germinated during plastic deformation by the dislocation mechanism. If, in addition, hydrogen is transported by dislocations to a region of dislocation pileup, the hydrogen pressure in the germinating crack will be higher than in a secondary pore. It follows from this that the development of hydrogen brittleness of the second kind is possible in aluminum under certain conditions.

Manuscript Page No.

Transliterated Symbols

128 кр = kr = kriticheskiy = critical

Chapter 2

URANIUM

1. INTERACTION OF URANIUM WITH HYDROGEN

Among the metals of Subgroup IIIB of the Periodic Table, the influence of hydrogen on mechanical properties has been studied quite thoroughly only for uranium. Uranium absorbs hydrogen in an endothermic reaction, and the amount of hydrogen absorbed by it diminishes with increasing temperature. Studies [4, 5, 9] have shown that the solubility of hydrogen in uranium is described approximately by Sieverts' law, which assumes the following form for the various modifications of uranium:

for α-uranium: $\lg C/p^{1/2} = -\frac{338}{T} - 0{,}688;$

for β-uranium: $\lg C/p^{1/2} = -\frac{892}{T} + 0{,}408;$

for γ-uranium: $\lg C/p^{1/2} = -\frac{277}{T} - 0{,}052;$

for liquid uranium:

$$\lg C/p^{1/2} = -\frac{587}{T} + 0{,}426.$$

Here C is the concentration in parts by weight per million; p is the pressure in mm Hg.

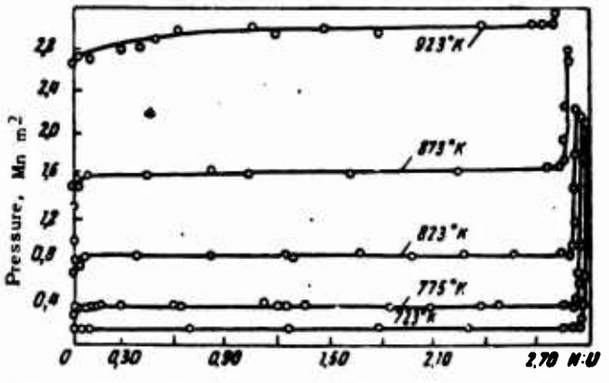

Fig. 55. Isotherms of interaction of uranium with hydrogen at various temperatures as a function of pressure.

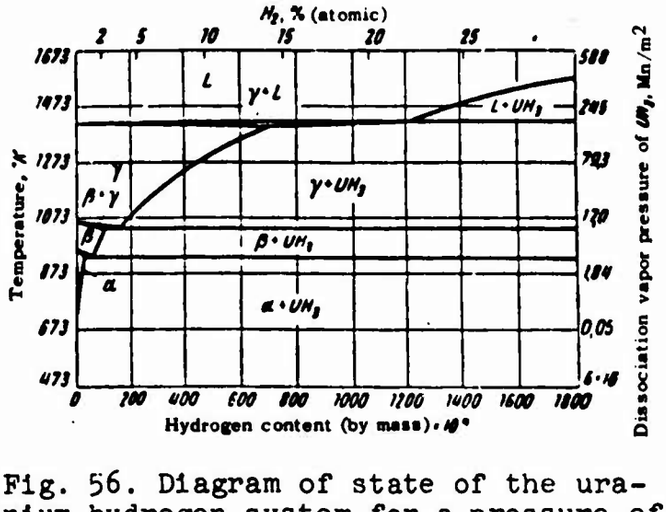

Fig. 56. Diagram of state of the uranium-hydrogen system for a pressure of 0.1 Mn/m^2.

These equations are valid for single-phase regions. As the hydrogen content is increased above a certain limit, a two-phase region, in which pressure does not change with increasing hydrogen concentration in the metal, makes its appearance (Fig. 55).

A diagram of state of the uranium-hydrogen system based on the results published in [363, 364, 375] appears in Fig. 56. This diagram has been constructed basically from the inflection points of the isotherms illustrating the variation of equilibrium hydrogen pressure in the uranium-hydrogen system as a function of hydrogen concentration in the metal.

These data indicate that the solubility of hydrogen in α-uranium is negligibly small. In the high-temperature β- and γ-modifications, hydrogen is much more soluble. Thus, for example, the solubility of hydrogen in the α-modification of uranium [9] in % (by mass) is as follows: $0.6 \cdot 10^{-7}$ at 373°K; $0.2 \cdot 10^{-5}$ at 473°K; $0.2 \cdot 10^{-4}$ at 573°K and $0.2 \cdot 10^{-3}$ at 873°K.

Davis found that the solubility of hydrogen in the β- and γ-phases follows Sieverts' law, something that is not observed for α-uranium. On extrapolation to zero pressure, the straight lines illustrating solubility as a function of the square root of pressure intersect the axis of ordinates above zero solubility. Davis showed that this anomaly is due to impurities.

2. INFLUENCE OF HYDROGEN ON THE PROPERTIES OF URANIUM

Analysis of the uranium-hydrogen phase diagram shows that the dominant form of hydrogen brittleness in uranium is hydride brittleness. In quantities from 0.0001 to 0.0005% (by mass), hydrogen is a normal impurity in uranium. Even at these very low concentrations, it is present in the form of the hydride UH_3 [363]. Segregations of uranium hydride usually form along grain boundaries, growing in size and diminishing in number with decreasing cooling

rate. At cooling rates above 40 deg/sec in the temperature range from 548-648°K, uranium hydride is segregated in the form of a very fine network along the grain boundaries, and it is difficult to detect it in the structure on examination under the optical microscope. At lower cooling rates, the uranium hydride segregations become quite large and are easily detected in microstructural analysis at ordinary powers in the form of grayish-brown needle-shaped inclusions. These inclusions also form along grain boundaries, but do not present a continuous network of the kind observed when cooling is rapid.

Because of the negligibly small solubility of hydrogen in the α-phase, the hydride brittleness of uranium appears at very low hydrogen concentrations, giving rise to complications in cold pressworking of uranium and its use in nuclear reactors [382].

A survey of studies of the influence of hydrogen on the properties of uranium that have been made by various investigators in the USA is given in [382]. The first mention of hydrogen brittleness in uranium is found in the work of Henks, Taub and Doll, who observed that annealing of cold-worked uranium in a salt bath at 873°K for 30 min does not bring about any increase in plasticity. At the same time, vacuum annealing at the same temperature for 30 min raises plasticity by a substantial margin. Mass-spectroscopic analysis indicated that the hydrogen content in the uranium after salt-bath annealing was 0.00007-0.00015% (by mass), while that after vacuum annealing was 0.00003-0.00005% (by mass).

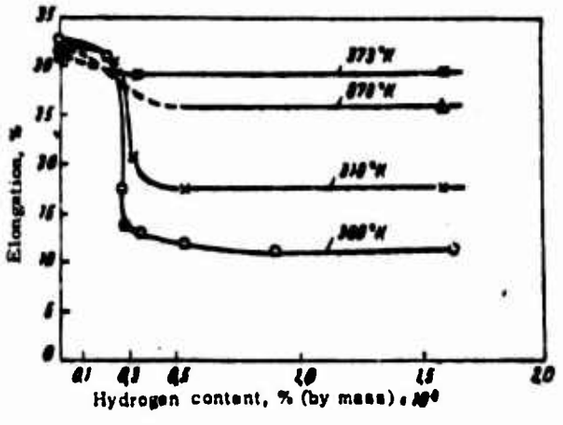

Fig. 57. Influence of hydrogen on elongation of uranium at various test temperatures.

Weber showed that annealing in air, in a salt bath, or in unpurified argon or helium results in a decrease in the elongation of the vacuum-annealed uranium. Gas analysis showed that the plasticity drop in uranium is due to hydrogenation in the annealing process. A large part of the hydrogen can be eliminated from uranium by repeated vacuum annealing for half an hour at 873°K; its plasticity is then restored.

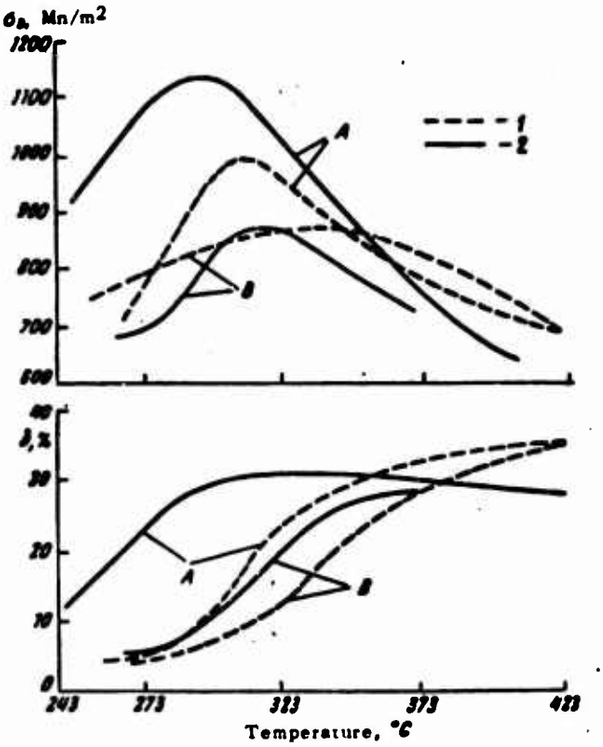

Fig. 58. Influence of test temperature on the mechanical properties of uranium after vacuum annealing (A) and annealing in a hydrogen atmosphere (B). 1) Data of Marsh et al.; 2) data of Davis.

Davis studied the influence of test temperature on the mechanical properties of uranium with various hydrogen contents. To introduce hydrogen, the specimens were annealed at 873 and 973°K in a hydrogen atmosphere at various pressures. Tension tests were run at a speed of 2.5%/min. The studies showed that hydrogen lowers the elongation of uranium more strongly as the temperature is lowered (Fig. 57). Although brittleness intervenes at room temperature at contents of 0.00003% (by mass) of H_2, and at 0.00004% (by mass) at 318°K, it is not observed even at 0.0015% (by mass) at 373°K.

Hydrogen has a strong influence on the temperature of the viscous-to-plastic failure transition in uranium. The fracture of uranium without hydrogen at room temperature is of the mixed type. Marsh, Mühlenkamp and Menning showed that increasing the hydrogen content from 0.00008 to 0.00047% raises the cold-shortness threshold and causes brittleness in uranium at room temperature (Fig. 58).

The results of Davis (Fig. 58) are not quite in agreement with the results obtained by Marsh, Mühlenkamp and Menning, which can be explained by the differences in the impurity contents in the uranium and in the technology of preparing the starting material.

The manner in which various forms of uranium hydride segregations and their distribution influence the properties of uranium was studied in [372]. The investigations were conducted on uranium rods containing less than 0.013% (by mass) of impurities. Various microstructures were produced in the rods by various types of heat treatment. Specimens with a normal hydrogen content [of the order of 0.0003% (by mass)] were heat treated, as were vacuum-annealed specimens containing approximately 0.00003% (by mass) of H_2. In the latter group of specimens, the structure differed only in having a smaller quantity of hydrides, owing to their smaller hydrogen contents. The hydrides in the starting material were intermediate in size.

These studies showed that fine hydride segregations along the grain boundaries raise ultimate strength and yield point in recrystallized and unrecrystallized uranium that has been quenched from the β-region. At the same time, fine hydride segregations in the form of a continuous network along grain boundaries lower elongation more sharply than do coarse segregations. The temperature of the viscous-to-brittle transition is higher for uranium with the fine hydride network along the grain boundaries than for uranium with coarse hydride segregations at a given hydrogen concentration in the uranium. However, this shift is not particularly large in practice.

It was observed in the same study that a rise in ultimate strength is observed at temperatures below 303°K owing to precipitation of fine hydride segregations. This strength increase is observed in unrecrystallized uranium that has been quenched from the β-region, as well as in recrystallized and quenched metal. The authors also observed that an increase in hydrogen content in uranium refines the grain.

In the discussion to [372], Gorham and Weber note that the properties of quenched uranium may be influenced by decay of supersaturated hydrogen solutions formed as a result of quenching under the influence of applied stresses. Thus, for example, irreversible brittleness of the second kind should be superimposed on hydride brittleness of the first kind. The brittleness of the second kind, which is due to segregation of hydrides under the influence of applied stresses, should be intensified with rising temperature up to a certain limit. In fact, the elongation of quenched uranium alloys with 0.0003% H_2 first rises with increasing temperature, since the tendency to hydride brittleness of the first kind decreases with increasing temperature, and then declines, since hydride brittleness due to supersaturated-solution decay is beginning to manifest.

Unfortunately, the mechanical tests in the work cited were not conducted with a variety of deformation speeds, so that the hypotheses advanced concerning the mechanism of brittleness in quenched uranium that is contaminated by hydrogen require experimental confirmation.

Davis is of the opinion that impurities are the decisive factor in hydrogen brittleness in α-uranium. However, these ideas, like those set forth in Cotterill's survey [9], require rigorous

experimental proof.

It is pointed out in [375] that the detrimental influence of hydrogen on the properties of uranium is not limited to hydrogen brittleness. It also causes porosity in castings. Hydrogen has a tendency in uranium to diffuse from the interior of the metal toward the surface and break up protective coatings.

Chapter 3

TITANIUM AND ITS ALLOYS

1. KINETICS OF INTERACTION OF TITANIUM AND ITS ALLOYS WITH HYDROGEN

Titanium that has been annealed in a high vacuum begins to absorb hydrogen even at room temperature [192, 193]. As the temperature rises, the rate at which titanium absorbs hydrogen increases. For extremely pure iodide titanium annealed in a vacuum at high temperature, the highest rate of absorption is observed at temperatures around 573°K [194]. For technically pure titanium, the maximum of hydrogen absorption rate is shifted to higher temperatures, of the order of 973-1073°K. The rate of hydrogen absorption by titanium increases with diminishing size of the macroscopic and microscopic granules. It has been shown that oxygen and nitrogen present in titanium lower the rate at which it absorbs hydrogen. The rate of absorption is lowered particularly sharply by an oxide film on the surface of titanium.

The hydrogen-absorption process depends substantially on the ratio of surface to volume. Sponge titanium, with its enormously branched surface, absorbs hydrogen many times more rapidly than dense titanium [201].

At very high initial hydrogen pressures, the rate of its absorption by the alloys is lower as compared with moderate pressures. There is reason to assume that this is due to the formation of a hydride film, diffusion through which is difficult, on the surfaces of the titanium alloys.

Titanium alloys absorb hydrogen less rapidly than does technically pure titanium [195, 196] (Fig. 59).

All Soviet titanium alloys can be listed in the following order of decreasing hydrogen absorption rate: VT1, VT15, VT5, VT3-1, VT3, VT5-1, VT10, VT6. The farther to the right the alloy is in this series, the slower is the rate of its interaction with hydrogen. Of all of the alloys investigated, VT6 interacts most slowly with hydrogen. There is no doubt that the processes of hydrogen absorption by titanium alloys are determined in many respects by the coefficients of diffusion of hydrogen in titanium in the presence of the alloying components. We may therefore assume that the rate of diffusion of hydrogen in titanium will be lowered substantially in the simultaneous presence of magnesium and aluminum or aluminum and vanadium.

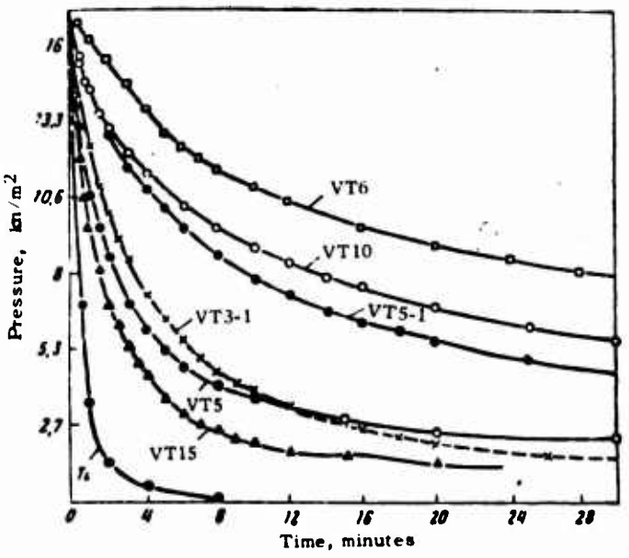

Fig. 59. Kinetic curves of absorption of hydrogen by titanium and Soviet titanium alloys at 973°K and a pressure of 17 kn/m² (100 mm Hg).

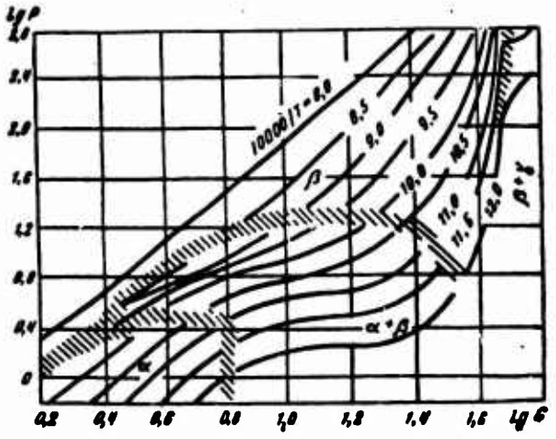

Fig. 60. Isotherms of equilibrium hydrogen pressure in the Ti-H system [pressure in mm Hg; H in % (atomic)].

A quite definite equilibrium hydrogen pressure is established in a closed system for each temperature and each fully defined hydrogen concentration in titanium and titanium alloys.

The higher the hydrogen concentration in the titanium, the higher will be its equilibrium pressure over the titanium. Figure 60 presents isotherms of equilibrium hydrogen pressure above titanium-hydrogen alloys according to A.D. McQuillan [197].

. Generalizing the results of [197, 200], we can arrive at the following formulas linking the equilibrium hydrogen pressure p above highly purified titanium with the temperature and the concentration C of the hydrogen in the metal:

for the α-phase

$$p = 9{,}62 \cdot 10^{8} C^{2} e^{-\frac{10900}{T}};$$

for the β-phase [$C \leq 10\%$ (atomic)]

$$p = 44{,}7 \cdot 10^{8} \cdot C^{2} e^{-\frac{14000}{T}};$$

for titanium hydride

$$\lg p = -\frac{1280}{T} + 0{,}5 \lg T + 4{,}69.$$

In one of our own papers [198], we indicated that interstitial impurities, specifically oxygen and nitrogen, displace hydrogen from titanium and raise its equilibrium pressure above the metal. This made it possible to propose an original indirect method of determining oxygen in titanium from the equilibrium pressure of hydrogen injected into it.

In the two-phase region, hydrogen is redistributed between the α- and β-phases until the equilibrium hydrogen pressures arrive at the same value in each of the phases. As a result of this redistribution, the hydrogen is concentrated preferentially in the β-phase.

Titanium does not react only with molecular hydrogen. Hydrogen may penetrate into titanium as a result of reaction with water vapor, hydrocarbons, ammonia, and other hydrogen-containing substances.

The interaction of titanium with water vapor can be described by the following scheme:

$$Ti + H_2O \rightarrow TiO_2 + [H] + H_2.$$

On interaction with titanium, therefore, water vapor decomposes to form an oxide film on the specimen surface and hydrogen, which is distributed between the gaseous phase and the solid titanium in accordance with the Sieverts distribution law. In this case the rate of hydrogen absorption by the titanium will be lower than for absorption of pure hydrogen, since the oxide film on the specimen surface sharply inhibits the diffusion of hydrogen into the interior of the metal. Moreover, oxygen diffuses into the metal, forming an oxygen-rich layer that also retards the diffusion of hydrogen into the metal.

It was shown in [201] that titanium sponge reacts reversibly with water vapor and air up to temperatures of the order of 573-673°K. At higher temperatures, titanium sponge enters into a chem-

ical reaction with water vapor and possibly with oxygen, and the reaction becomes irreversible. An electrode pressed from titanium sponge begins to react chemically with water vapor at lower temperatures, of the order of 373°K, because of its fresh surfaces.

Titanium also absorbs hydrogen from a number of other hydrogen-containing gases. This must be remembered in processing and use of titanium and its alloys. Thus, for example, when a gas flame is used to heat titanium, special precautionary measures must be taken to exclude reaction of the titanium with hydrogen.

2. DIAGRAM OF STATE OF THE TITANIUM-HYDROGEN SYSTEM

Many studies have been devoted to the phase diagram of the titanium-hydrogen system. An exhaustive survey of the literature published on this problem up to 1946 will be found in [2]. However, the early studies of this system are not quite reliable due to the low purity of the titanium used, and particularly the high oxygen and nitrogen contents.

Figure 61 shows the Ti-H diagram of state according to the most reliable sources [202-204].

It follows from the diagram of state that hydrogen broadens the β-phase region and narrows the α-phase region. Eutectoid decay of the β-phase into α- and γ-phases takes place in the titanium-hydrogen system. The diagram shows two lines of β-phase eutectoid decay corresponding to heating (A_c) and cooling (A_r). The eutectoid point occurs at 36.6-38.0% (atomic) of H_2 [1.21-1.26% (by mass)]. The α- and β-phases are interstitial solid solutions of hydrogen in α- and β-titanium, respectively.

The solubility of hydrogen in α-titanium drops off sharply with temperature from 7.9% (atomic) [0.18% (by mass)] at 573°K to 0.1% (atomic) [0.002% (by mass)] at room temperature, with the decline particularly steep in the 573-398°K temperature range [68].

A quite detailed determination of the solubility of hydrogen in titanium in the 373-573°K temperature range was made by Koster, Bangert, and Evers [206], who measured internal friction. According to their results, the maximum solubility of hydrogen in titanium is somewhat lower than indicated by earlier data [0.13 instead of 0.18% (by mass) of H_2]. The solubility of hydrogen in α-titanium diminishes smoothly without any discontinuities.

McQuillan [207] gives the following equation determining the solubility of hydrogen in α-titanium:

$$\lg C = 6{,}829 - \frac{1{,}95 \cdot 10^3}{T},$$

where C is the hydrogen concentration in % (by mass), divided by 10^4; T is absolute temperature.

McQuillan [202] also showed that the positions of the phase regions in the titanium-hydrogen phase diagram depends substan-

tially on the purity of the titanium. For magnesium-thermal titanium, the two-phase (α + β) region is broadened, while the position of the boundary between the β/β + γ phase regions undergoes almost no change.

The influence of oxygen and nitrogen on the solubility of hydrogen in titanium at temperatures above eutectoid was studied in [234]. To plot the solubility line, the hydrogen-saturated specimens were annealed at 400°C for 64 hours, and then cooled to the necessary temperature, at which they were held for 20 hours, and quenched in water.

It follows from these data that oxygen and nitrogen produce no essential change in the solubility of hydrogen in titanium at room temperature (Fig. 62). However, at temperatures above 348°K, both of these elements increase the solubility of hydrogen in titanium to some degree. The isothermal sections of the titanium-oxygen-hydrogen diagram of state that we obtained are illustrated by Fig. 63.

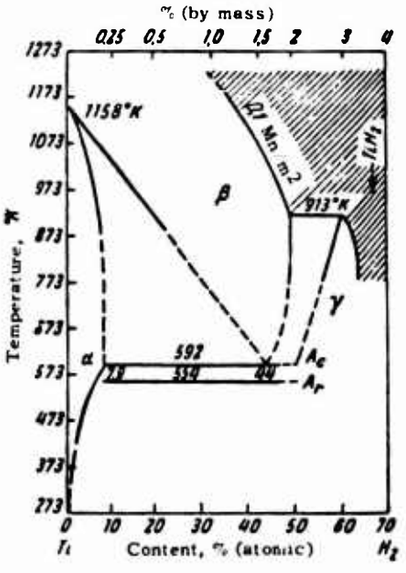

Fig. 61. Diagram of state of titanium-hydrogen system.

As we noted above, hydrogen is in a partially ionized state in titanium. Ionized hydrogen atoms form a proton gas, which is apparently in dynamic equilibrium with the unionized hydrogens. The unionized hydrogen atoms form interstitial solid solutions with the titanium. The crystal lattice of α-titanium has two kinds of spaces that may be occupied by the interstitial atoms: tetragonal spaces with a radius of 0.034 nm and octahedral spaces with a radius of 0.062 nm.

Since the radius of the hydrogen atom is 0.041 nm, it can occupy only the octahedral spaces. Here, however, concurrently with the decrease in system free energy due to chemical interaction,

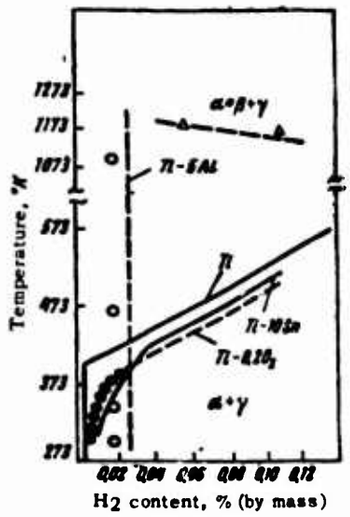

Fig. 62. Sclubility of hydrogen in the α-phase in unalloyed iodide titanium and alloys of titanium with 0.2% O_2 (0.2% N_2), 5% Al, 10% Sn [42].

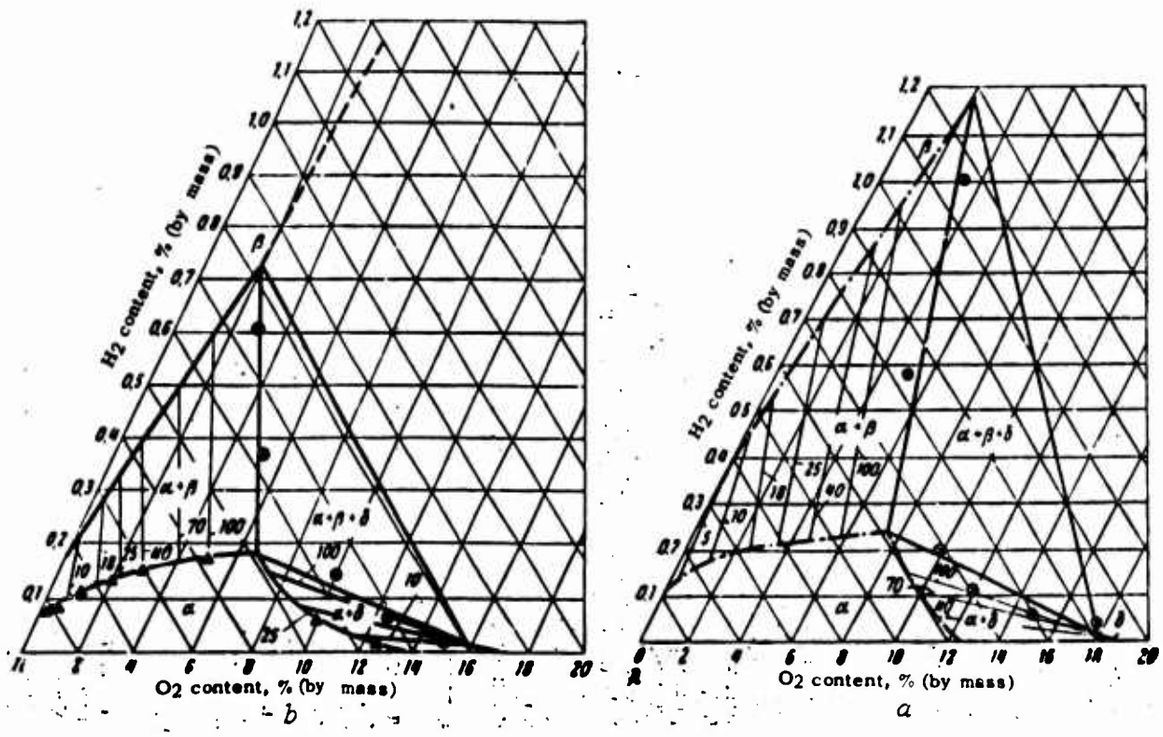

Fig. 63. Isothermal sections of titanium-oxygen-hydrogen phase diagram at 973 (a) and 1073°K (b) (the numerals on the curves indicate the equilibrium H_2 pressure in mm Hg).

there is an increase in this energy due to the great vibrational freedom of the hydrogens in such spaces. For this reason, hydrogen has low solubility in the α-phase. Even at relatively low hy-

drogen concentrations, the solid solutions of hydrogen in α-titanium become thermodynamically unstable.

In the body-centered lattice of the β-modification of titanium, lattice spaces with a radius of 0.044 nm conform almost exactly to the atomic radius of hydrogen, and no increase in free energy due to free vibrations of the atom in the interstices takes place. Hence hydrogen is easily soluble in the β-phase and stabilizes it.

The γ-phase is a titanium hydride representing an interstitial phase of variable composition. Opinions as to the nature of this phase and its homogeneity region are quite contradictory. In [210], it is suggested that two phases coexist in the region of high hydrogen concentrations: γ and δ. However, the existence of the δ-phase cannot be regarded as definitely proven, since magnesium-thermal titanium with considerable quantities of impurities was used in all of the studies in which it was detected. To solve this problem it will be necessary to carry out a detailed study on iodide titanium.

The absorption of hydrogen by titanium is accompanied by an increase in volume due to the lower density of titanium hydride. The density of titanium decreases linearly on hydriding from 4.506 to 4.27 g/cm^3 as the hydrogen content rises from 0 to 40% (atomic). The density of titanium hydride with the composition $TiH_{1.63}$ is 3.912 g/cm^3, i.e., approximately 13% lower than that of titanium. The density of $TiH_{1.75}$ is 15.5% lower than that of titanium.

The first x-ray diffraction studies of the titanium-hydrogen system had indicated that titanium hydride has a face-centered cubic lattice. In more recent studies [208, 212-214], however, it has been established that titanium hydride has a tetragonal lattice rather than the cubic one assumed previously. The tetragonal lattice is confirmed by the fact that titanium hydride shows strong optical anisotropy on examination in polarized light.

3. INFLUENCE OF HYDROGEN ON THE STRUCTURE AND PROPERTIES OF TITANIUM

Hydrogen brittleness may manifest in titanium during fast and slow deformation. The hydrogen brittleness that develops in titanium at high deformation rates is associated with the segregation of lamellar hydrides. Since hydrogen has extremely low solubility in α-titanium at temperatures around and below room temperature, hydride brittleness dominates in α-titanium and masks all other forms.

Technically pure titanium of moderate strength (σ_b = 450 Mn/m^2) and a small hydrogen content [~0.002% (by mass)] is not a cold-short metal, unlike other hexagonal metals, and this is explained in terms of the very high tensile limit of technical titanium. Cold shortness is not a property inherent to pure titanium. Titanium becomes cold-short under the influence of impurities present in it, primarily hydrogen. The transition temperature of titanium from brittle to viscous fracture rises with in-

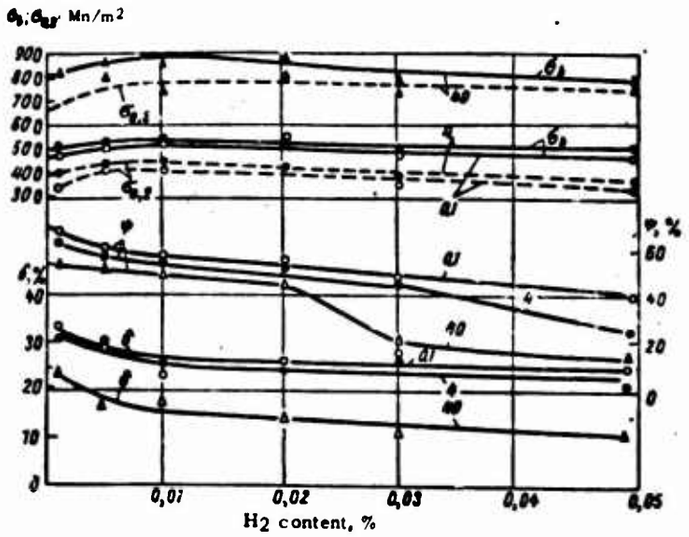

Fig. 64. Influence of hydrogen on the mechanical properties of titanium during tests at various stretching speeds (numerals on curve).

creasing hydrogen content in it. This effect can be explained by the fact that hydrogen lowers the tensile limit of titanium and therefore facilitates brittle failure.

Hydrogen increases the notch sensitivity of titanium, which is characterized by the relative change in the mechanical properties of notched as compared to smooth specimens. Hence the hydrogen embrittlement of titanium has its strongest effect on impact strength. At the same time, hydrogen causes practically no change in the lattice parameters of α-titanium and therefore has little influence on mechanical properties in standard tensile tests run on smooth specimens. If the hydrogen content exceeds a certain limit (Fig. 64), the hydrogen brittleness at high deformation rates manifests not only in impact-strength tests, but also in fast tensile tests.

The change in the properties of titanium on saturation with hydrogen is accompanied by a change in microstructure. The microstructure of titanium that has been saturated to varying degrees with hydrogen is shown in Fig. 65 for comparison with that of titanium that has been subject to vacuum extraction for 6 hours at 1173°K. The initial material has a polyhedral structure with no segregations of a second phase. As the titanium is saturated with hydrogen, lamellar segregations of titanium hydride make their appearance, and the quantity increases with increasing hydrogen content. At low hydrogen contents, titanium hydride is segregated along definite crystallographic directions, and at high concentrations in the form of compact segregations with coarse shapes.

The hydrogen brittleness of titanium depends substantially on its impurity content. While the impact strength of magnesium-

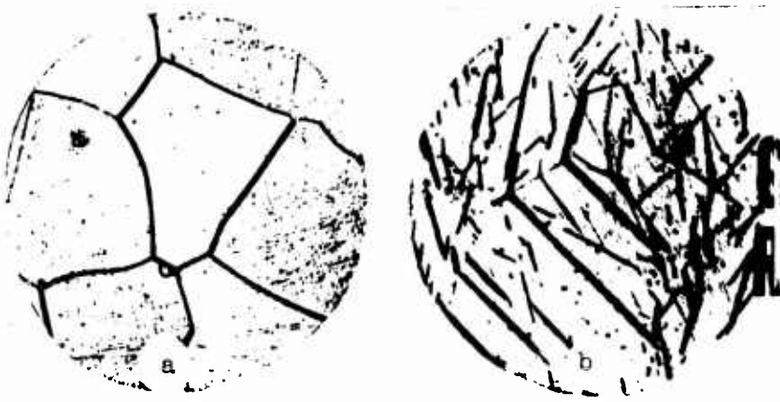

Fig. 65. Change in microstructure of titanium as a function of hydrogen content: a) 0.002% H_2; b) 0.05% H_2.

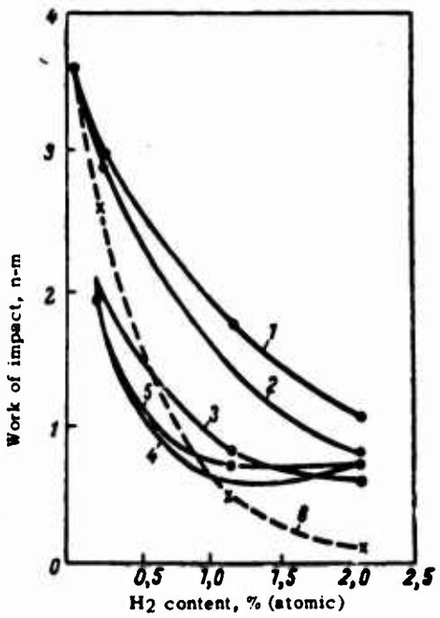

Fig. 66. Impact strength of technical titanium at room temperature as a function of hydrogen content after quenching from 673°K (1), after aging at room temperature for 1 day (2), 1 week (3), 1 month (4), 6 months (5), and after slow cooling (6).

thermal titanium declines relatively slowly as the hydrogen content is increased to 0.01%, that of iodide titanium drops sharply even when minute quantities of hydrogen are introduced. Sodium-thermal titanium shows a tendency to hydrogen brittleness at H_2 contents greater than 0.009% [455].

Lenning, Craighead and Jaffee [68] observed that hydrogen lowers the toughness of slowly cooled alloys, in which the solid solution has decayed completely, to the greatest degree, and af-

fects quenched alloys to a lesser degree. Hydrogen-saturated quenched titanium specimens may age at room temperature, with the result that impact strength drops sharply (Fig. 66).

Despite the sharp rise in the notch sensitivity of titanium in the presence of hydrogen in single tensile or impact tests, hydrogen has practically no influence on the sensitivity of titanium to stress concentrators under the conditions of alternating cyclic load application [215, 216]. Hydrogen lowers the fatigue strength of titanium [159, 229] and increases its creep rate when a load is first applied at room temperature.

The hypothesis that in titanium, as in (α + β) titanium alloys, hydrogen brittleness should develop not only at high, but also at low deformation rates was advanced in [251]. The hydrogen brittleness that develops at low deformation rates should manifest in a temperature range corresponding to a definite value of the hydrogen diffusion coefficient.

It should be noted in this connection that unusual behavior of titanium at elevated temperatures had been observed even earlier [45]. The relative elongation of titanium rises by a factor of 1.5-2 when the temperature is raised to 523°K, but it diminishes at higher temperatures and reaches a minimum at 723-773°K. At still higher temperatures, the elongation increases rapidly.

Unfortunately, the studies of the influence of temperature on the mechanical properties of titanium were conducted during the first few years of its technical application, before attention was drawn to the metal's hydrogen brittleness. It is therefore difficult to judge from the published data the part played by hydrogen in this plasticity loss.

We conducted a special study devoted to the influence of hydrogen on the mechanical properties of titanium in the 473-873°K temperature range. It was observed in this investigation that reversible hydrogen brittleness is superimposed on the elongation decrease in the presence of hydrogen in the temperature range from 673-773°K at low stretching speeds.

The mechanism by which hydrogen influences the properties of titanium at 573-773°K is not entirely clear. These temperatures are too high for the existence of Cottrell hydrogen atmospheres, which are due to elastic, geometric, or electrical interaction. A possibility that is not excluded, however, is chemical interaction between oxygen atoms on the dislocation line and hydrogen atoms.

As regards the nature of the property change, the processes taking place in titanium during slow stretching in the temperature range from 673-773°K are similar to strain aging. Only further experiments can decide how extensive this similarity is.

It has been observed that hydrogen causes cracking and sharply reduces plasticity and impact strength in particular in welded joints. Daley and Hartbower [217] reported that at hydrogen contents above 0.013% (by mass) in the seam metal, its impact strength

at room and subzero temperatures drops sharply.

S.M. Gurevich [47] showed that increasing the hydrogen content of the seam metal in arc welding of type VT1 technical titanium from 0.01 to 0.05% (by mass) causes an impact-strength decrease from 6 to 1.5 kg-m/cm^2 (from 6000 to 1500 nm/m^2) if the tests are conducted at room temperature. The other mechanical properties change very little. Thus, for example, elongation decreases from 22 to 18% and the bending angle of welded joints with 0.05% H_2 is only 10% lower than that for the basic metal with 0.01% H_2.

The works cited above [225-227] not only refined the mechanism of formation of blisters and cracks in weld seams, but also made it possible to indicate maximum permissible hydrogen contents. According to the data given in these studies, technical titanium welds well, no blisters or pores are formed, and the impact strength of the weld seam is close to that of the basic metal at hydrogen contents smaller than 0.01% (by mass) of H_2. Vacuum annealing of the sheets before welding raises the room- and subzero-temperature impact strengths to an even greater degree. Use of vacuum-annealed electrode wire for consumable-electrode arc welding also raises the impact strength of the seam metal.

Since titanium reacts vigorously with hydrogen, oxygen and nitrogen at high temperatures, the inert gases used for shielding in welding of titanium must be as pure as possible. To retain satisfactory plasticity in the weld seam and the zone around it, the relative humidity of the helium or argon must not exceed 5% [221].

4. INFLUENCE OF α-STABILIZERS ON THE TENDENCY OF TITANIUM TO HYDROGEN BRITTLENESS

The elements that stabilize the α-phase of titanium include impurity elements, oxygen and nitrogen, as well as one of the most

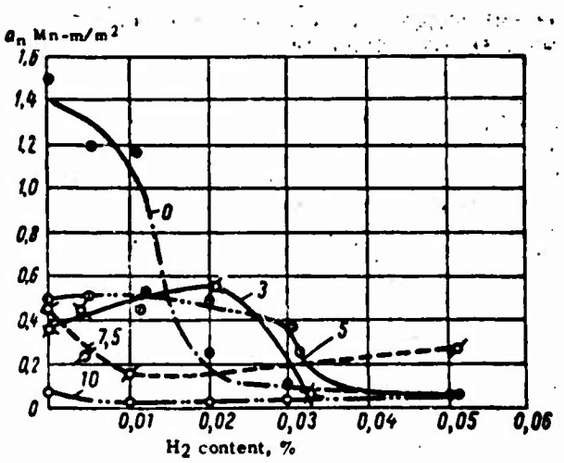

Fig. 67. Influence of hydrogen on impact strength of alloys of titanium with aluminum [the numerals on the curves refer to aluminum content in % (by mass)].

common and important alloying elements used with titanium: aluminum. With titanium, oxygen and nitrogen form interstitial solid solutions, while aluminum forms substitutional solutions.

Studies published in [232-234, 236] have shown that oxygen and nitrogen do not affect the nature of hydrogen brittleness in titanium. Oxygen and nitrogen cause no substantial change in the quantity of hydride segregations in titanium at room temperature, since the solubility of hydrogen in titanium at this temperature does not change appreciably on injection of nitrogen or oxygen. However, to the extent that the oxygen and nitrogen as such lower the plasticity of titanium substantially, the plasticity of technical titanium at room temperature and a given hydrogen concentration is lower the greater the contents of nitrogen and oxygen. At temperatures above 348°K, both of these elements increase the solubility of hydrogen in titanium slightly, and the detrimental influence of hydrogen is manifested at hydrogen concentrations higher than in the case of iodide titanium.

Aluminum lessens the tendency of titanium to hydrogen brittleness [234]. This favorable effect of aluminum is particularly clearly manifest in the manner in which impact strength varies as a function of hydrogen content (Fig. 67). The favorable effect of aluminum is explained by the fact that, in contrast to oxygen and nitrogen, aluminum increases the solubility of hydrogen in α-titanium at room temperature by a substantial margin (see Fig. 62).

It was shown in [234] that the alloy Ti + 10% Sn shows hydrogen embrittlement at H_2 contents higher than 0.015%, i.e., at concentrations somewhat higher than in technically pure titanium. This is because tin also raises the solubility of hydrogen in titanium at elevated and room temperatures (see Fig. 62). A certain number of point segregations were detected along grain boundaries in vacuum-annealed Ti + 10% Sn alloy. The nature of these segregations remained unclear, but it was established that they are unrelated to hydrogen.

5. INFLUENCE OF HYDROGEN ON THE STRUCTURE AND PROPERTIES OF INDUSTRIAL α-ALLOYS

The general nature of the influence of hydrogen on the structure and properties of industrial α-titanium alloys is the same as for technical titanium. The α-titanium alloys differ from titanium only in the concentration beginning at which impact strength begins its sharp decline. As we noted earlier, tin and particularly aluminum counter the tendency of titanium to hydrogen brittleness, a fact explained by the increase in the solubility of hydrogen in α-solid solution and inhibition of the hydrogen-diffusion process in titanium in the presence of tin and aluminum. Aluminum is an indispensable component of the α-alloys, and hence all of the α-titanium alloys presently in use are less inclined to hydrogen brittleness than is titanium.

The mechanisms of hydrogen brittleness in titanium and α-titanium alloys are similar. On saturation with hydrogen, titanium-hydride segregations appear in the structure of titanium and the α-alloys, and the amount increases with increasing hydrogen con-

tent in the alloy. It is these titanium hydride segregations that are the cause of hydrogen brittleness in titanium and α-titanium alloys.

The hydrogen brittleness of typical α-titanium alloys in the annealed state rises with increasing speed of the tensile-machine crossbar. Hydrogen brittleness of α-alloys and titanium is especially conspicuous in tests run on notched specimens at high tensile-machine speeds and in impact tests.

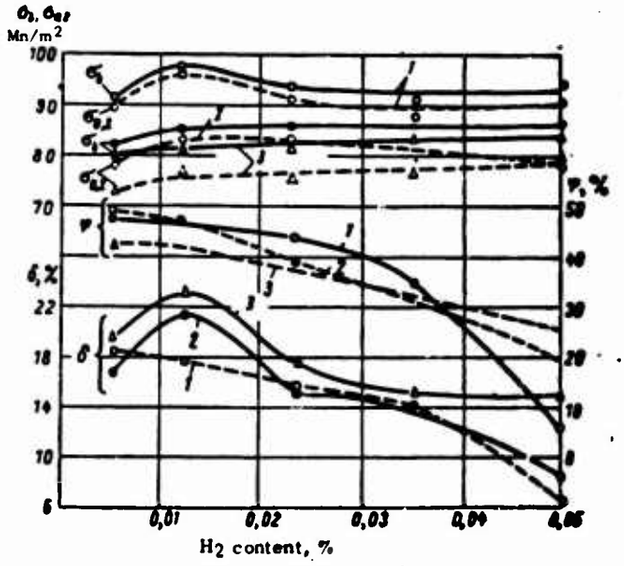

Fig. 68. Influence of hydrogen on the mechanical properties of VT5-1 alloy in tensile tests at various speeds, mm/min: 1) 35; 2) 4; 3) 0.1.

The influence of hydrogen on the mechanical properties of the α-titanium alloy VT5-1 at various stretching speeds is shown in Fig. 68. At all of the stretching speeds studied, the ultimate strength and yield point of the VT5-1 alloy are somewhat higher at low hydrogen contents and then decrease. However, the strength properties obtained as a result of mechanical tests on smooth specimens at room temperature cannot be used as a basis for inferences as to the hydrogen-brittleness tendency of the alloy. The plastic properties of titanium and its alloys, and the necking ratios in particular, vary to a considerably greater extent as functions of hydrogen content. Transverse necking and elongation show maxima at 0.015% (by mass) of H_2 and then drop off sharply, with plasticity declining faster at high stretching speeds. The impact strength of the alloy diminishes at H_2 contents greater than 0.030% (by mass).

A detailed study of the hydrogen brittleness of a foreign titanium alloy with 5% Al and 2.5% Sn was made in Haynes's paper [240]. The relationships that he obtained agree with those described above for the Soviet alloy VT5-1. Brittle failure of the

Ti-5Al-2.5Sn alloy in tensile tests is observed at 0.05% (by mass) of H_2, and at 0.035% (by mass) of H_2 in impact testing. The long-term strength of the alloy at room temperature decreases if the hydrogen content exceeds 0.025% (by mass).

Until recently, it was quite generally thought that brittle failure of hydrogen-saturated specimens did not occur on slow application of the stresses for α-alloys, but this is not the case. Thus, for example, the α-alloys VT10 and VT4 are inclined to hydrogen brittleness at both fast and slow stretching speeds on the machine. Hydrogen brittleness was also observed at low deformation rates in the alloys Ti-4%Al-7%Cu; Ti-12%Sn-7%Cu [241].

Low-testing-speed hydrogen brittleness is most strongly developed in the quenched α-alloys. Hydrogen brittleness was studied in [243] in the α-alloys VT5 and VT5-1, which were cooled at various rates from 873°K after homogenization at this temperature. The specimens were heated at a comparatively low temperature, so that the polymorphic transformation would not take place during cooling and the various cooling rates would not affect the sizes of the macro- and micrograin.

The influence of hydrogen on the mechanical properties of VT5-1 alloy in the quenched state and after cooling with the furnace is shown in Fig. 16 (see page 56). Hydrogen causes a decrease in necking and elongation in VT5-1; here, in the quenched state, this plasticity loss is most pronounced at H_2 contents greater than 0.03% (by mass) in mechanical testing at slow speeds, while in the annealed state it is more conspicuous at high deformation rates. The experimental facts described above can be explained by formation of hydrogen-supersaturated solid solutions during quenching. At high enough hydrogen concentrations in the alloys, the excess hydride segregations are preserved in addition to the supersaturated solid solutions.

The excessive hydride segregations, which are usually lamellar, cause hydrogen brittleness in α-alloys at high stretching speeds, while the hydrogen-supersaturated solid solutions decay under the prolonged action of applied stresses, which also causes brittleness of the material.

This does not exclude the possibility of development of processes in the α-alloys that cause hydrogen brittleness even without the formation of hydride-phase segregations, processes similar to those that arise in hydrogen-saturated (α + β) titanium alloys, steels and other materials that are inclined to hydrogen brittleness at low stretching speeds.

Although the α-alloys are inclined to hydrogen brittleness at both high and low deformation rates, only the brittleness that appears at high speeds, especially under impact loads, is extremely dangerous, since these alloys are usually used in the annealed state. Welded joints are an exception; here, due to the rapid cooling, supersaturated hydrogen solutions may form and then decay with segregation of hydrides not only on application of external load, but even under the influence of internal macroscopic stresses of the first kind. The volume changes due to seg-

regation of hydrides, combined with the macroscopic stresses, may in time cause cracking and failure of the welded joint. The premature failure of α-alloy welded joints is similar in nature and mechanism of development to the phenomena observed in welded joints in technical titanium, which we examined earlier.

6. INFLUENCE OF β-STABILIZERS ON THE TENDENCY OF TITANIUM TO HYDROGEN BRITTLENESS

The introduction of β-stabilizers into titanium alloys in sufficient quantities results in the appearance of the β-phase in the structure. The thermodynamic properties of hydrogen solutions in the β-phase differ from those of the hydrogen-saturated α-phase. Since the dimensions of the interstices in the body-centered lattice of the β-phase conform more closely to those of the hydrogen atom than do the interstices in the α-phase hexagonal lattice, the solubility of hydrogen in the β-phase is very high. Thus, up to 0.5% (by mass) [19.4% (atomic)] of H_2 dissolves in the β-titanium alloy VT15 (3.5% Al; 7.5% Mo; 11% Cr). Thus, hydrides appear in the β-phase only at very hydrogen concentrations.

In alloys with a structure composed of α- and β-phases, hydrogen is distributed nonuniformly between them. The hydrogen concentrations determined by (11) are established in the phases. According to [244, 245], the heat of solution of hydrogen in the β-phase is about -27,500 kcal/g-atom, while that in the α-phase is -21,500 (-115 and -88 kj/g-atom, respectively) at the alloying-element concentrations encountered in industrial alloys, so that (11) assumes the form

$$\frac{C_\beta}{C_\alpha} = e^{\frac{1500}{T}},$$

if we assume that the ratio of the entropy factors is close to unity. It follows from this that at room temperature the hydrogen content in the β-phase is approximately 150 times that of the α-phase. As the temperature rises, the ratio of concentrations in the β- and α-phases diminishes, amounting to only 4.5 at 1000°K.

Huber [246] confirmed autoradiographically that the hydrogen in (α + β) alloys is concentrated in the β-phase. L.S. Moroz and Yu.D. Khesin [253] arrived at the same conclusion on the basis of x-ray structural analysis of the (α + β) alloy Ti + 2% Mn + 1.3% Fe + 0.8% Cr + 1.2% Mo + 1.2% V. Quantitative determinations of hydrogen content in the β-phase [247-250] by electrolytic phase separation in a nonaqueous electrolyte and subsequent x-ray structural or gas analysis of the precipitated β-phase indicated that as the average hydrogen content is increased from 0.005 to 0.050% (by mass) of H_2, its concentration in the β-phase rises from 0.121 to 0.491% (by mass) for VT3-1 alloy and from 0.123 to 0.405% for VT8 after isothermal annealing. In aged alloys in the same average hydrogen content range, its concentration in the β-phase changes from 0.158 to 0.687% (by mass) for VT3-1 alloy and from 0.177 to 0.600% for VT8 alloy.

It was established in [251] that in alloys of the Ti-Mo and

Ti-Al-V systems, hydrogen dissolves quite readily in the α- and β-phases at high temperatures. When the temperature is lowered slowly, the hydrogen is redistributed between the β- and α-phases, with the result that the hydrogen content in the β-phase is increased substantially in alloys of the Ti-Mo and Ti-Al-V systems.

The appearance of the β-phase in the structure of the alloys results in substantial changes in their tendency to hydrogen brittleness. The greater the amount of β-phase in the alloy, the higher will be the total solubility of hydrogen and, consequently, the weaker will be the tendency to hydride brittleness. In most industrial (α + β) alloys, the total solubility in the β- and α-phases is so high that hydride brittleness appears at hydrogen concentrations above those encountered under industrial conditions.

But this does not mean that (α + β) alloys are less inclined to hydrogen brittleness than α-titanium alloys. Detailed studies [61, 238, 252-258] have shown that hydrogen causes embrittlement in (α + β) titanium alloys under prolonged action of stresses, for example, at very low specimen stretching speeds (0.5-0.012 mm/min). Hydrogen embrittlement in slow tensile testing is manifested more distinctly on notched than on smooth specimens. Hydrogen brittleness of (α + β) titanium alloys is observed in a definite temperature range. At temperatures that are too low, plasticity is recovered. Raising the test temperature also weakens the tendency to hydrogen brittleness, but raises the rate of deformation at which it is observed.

Thus, to determine the tendency of (α + β) alloys to hydrogen brittleness, tension tests must be conducted at slow speeds and preferably at low temperatures. Otherwise the data obtained on the brittleness sensitivity of the alloys may be spurious.

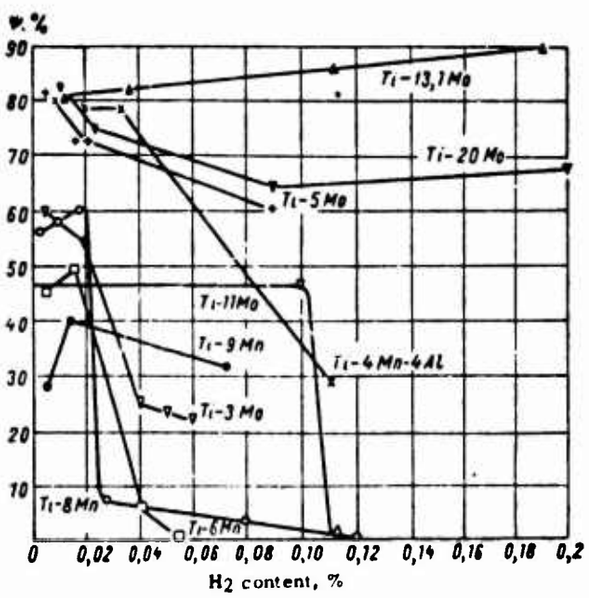

Fig. 69. Influence of hydrogen on necking of alloys in the Ti-Mo and Ti-Mn systems.

The influence of a β-stabilizing element on hydrogen embrittlement was first studied in detail by Jaffee, Lenning and Craighead [258], who used alloys of the Ti-Mn and Ti-Mo systems prepared from purest iodide titanium as their specimens. The alloys were quenched from 973 to 1023°K in water, with the result that the β-solid solution alone was fixed at room temperature in the alloys Ti + 9% Mn; Ti + 13% Mo and Ti + 20% Mo. The alloys Ti + + 3% Mn; Ti + 6% Mn; Ti + 5% Mo and Ti + 10.9% Mo had a two-phased (α + β) structure. The influence of hydrogen on the necking of the Ti-Mn and Ti-Mo alloys is shown in Fig. 69. The tests were run at a stretching speed of 0.1 mm/min at 298°K.

The alloys Ti + 3% Mn and Ti + 6% Mn are embrittled at approximately the same hydrogen content as technically pure titanium alloy Ti8Mn [0.02-0.03% (by mass) H_2].

The alloys with molybdenum are less sensitive to hydrogen embrittlement. In alloys represented solely by the β-phase, no hydrogen embrittlement is observed at all at room temperature in the hydrogen-content range studied [from 0.0015 to 0.075% (by mass) for the Ti-Mn alloys and from 0.0015 to 0.2% (by mass) for the Ti-Mo alloys].

It was established that the influence of hydrogen on the temperature of the transition from brittle to viscous failure is stronger the less there is of the β-stabilizing element in the alloy: in the β-alloy Ti + 20% Mo, hydrogen has practically no effect on the brittle-to-viscous transition temperature.

There are data indicating that molybdenum reduces hydrogen brittleness not only in binary alloys, but also in complex alloys, for example the alloy of titanium with 7% Al and 3% Mo. Lenning, Berger and Jaffee [259] also investigated the influence of additives that stabilize the β-phase on the permissible content of hydrogen in α-titanium alloys. It was observed, for one thing, that injection of 2% Mo makes it possible to preserve a rather high impact strength in alloys containing more than 0.2% H_2.

The influence of the amount of β-phase on the tendency of (α + β) alloys to hydrogen brittleness was studied in the paper of L.S. Moroz and Yu.D. Khesin [253]. The alloy chosen for the studies was Ti + 2% Mn + 1.3% Fe + 0.8% Cr + 1.2% Mo and 1.2% V. This alloy was quenched from two temperatures, 823 and 933°K, with the result that 20 and 50% of the β-phase, respectively, were fixed in its structure. Determination of the alloy's mechanical properties with smooth specimens and slow stretching indicated that the alloy with more of the β-phase was less inclined to hydrogen brittleness than that with the smaller quantity.

The influence of β-stabilizing elements on the hydrogen embrittlement of titanium was also investigated by Jaffee and Williams [260]. Alloys with β-isomorphic stabilizers (Mo, V, Nb and Ta) and β-eutectoid stabilizers (Mn, Cr and Fe) were studied in this paper. The alloys were prepared from three grades of the initial titanium: iodide (0.03% O_2), magnesium-thermal (0.108% O_2), and magnesium-thermal with additional oxygen injected (0.27% O_2). The alloys were injected with 0.02, 0.03, 0.04, 0.06 and 0.08% H_2.

They were tested for impact strength, tensile strength at high and low stretching speeds, and long-term strength. Since the object of the work was not to establish the true tolerances of hydrogen content, but to evaluate the relative tendencies to hydrogen embrittlement, the tension tests were run on smooth specimens. Use of these specimens made it possible to eliminate the effects associated with the varying influence of alloying elements on the notching tendency of titanium.

The results of extensive investigations of the influence of β-stabilizers on the hydrogen embrittlement of titanium showed that the trend to reversible hydrogen brittleness diminishes with increasing quantity of β-phase.

All of the β-stabilizers investigated can be arranged in the following order of increasing tendency to hydrogen embrittlement: molybdenum, niobium, chromium, vanadium, manganese and iron. Tantalum does not appear in this series, since Ti-Ta alloys behaved as α-alloys at all of the tantalum and hydrogen concentrations studied.

It was shown in [260] that aluminum lowers the tendency of (α + β) alloys to hydrogen embrittlement, since it raises the solubility of hydrogen in the α-phase, with the result that the β-phase is less saturated with hydrogen. Oxygen, on the other hand, sharply increases the tendency to hydrogen embrittlement, lowering the maximum concentrations at which brittleness is observed. Thus, in Ti + 4% Mo alloy prepared from iodide titanium, hydrogen brittleness is observed at 0.06-0.08% (by mass) H_2, and in the same alloy with 0.200% O_2 at 0.02-0.04% (by mass) H_2.

The authors propose classifying all (α + β) alloys into the following groups on the basis of tendency to hydrogen embrittlement:

a) alloys with high solubility of hydrogen in the β-phase. As a rule, these alloys contain considerable concentrations of molybdenum, which strongly increases the solubility of hydrogen in the β-phase;

b) alloys with high tolerance for hydrogen content because of its high solubility in the α-phase. These alloys contain 4% and more of Al. The total permissible quantity of hydrogen depends on the nature of the β-stabilizer used in the alloy with aluminum. Tin has an effect similar to that of aluminum but weaker;

c) alloys with low solubility of hydrogen, which is therefore segregated in these alloys in hydride form. These alloys behave like α-alloys and show hydrogen brittleness under impact loading. They include the alloys Ti + 4% Ta, Ti + 8% Ta, Ti + 4Nb and Ti + + 2% Fe;

d) alloys with relatively low solubility in both the α- and β-phases, which are inclined to reversible hydrogen brittleness only at low hydrogen concentrations, before the hydrides appear in the structure.

7. HYDROGEN BRITTLENESS OF INDUSTRIAL (α + β)-ALLOYS IN THE ANNEALED STATE

The influence of hydrogen on the structure and properties of industrial (α + β) titanium alloys differs from its effect on the structure and properties of α-titanium alloys and pure titanium. Hydrogen does not lower the impact strength of industrial (α + β) alloys substantially over a broad concentration range and has almost no influence on the other mechanical properties in mechanical tension tests on smooth specimens under conditions that are standard for most materials. To illustrate this relationship, Fig. 70 shows the influence of hydrogen on the impact strength of Soviet industrial (α + β) alloys [195]. For comparison, the same diagram shows the influence of hydrogen on the impact strength of technically pure titanium and α-alloys. On the basis of the nature of the impact-strength variation, all of these alloys can be classified into two groups: all α-alloys (VT1, VT5, VT5-1) belong to one group, and the (α + β) alloys to the other (VT3, VT3-1, VT6, VT8).

The impact strength of the first group of alloys diminishes sharply on introduction of comparatively small hydrogen concentrations (0.01-0.03%). The impact strength of alloys of the second group, on the other hand, shows no appreciable change over a rather broad hydrogen concentration interval, and only on introduction of 0.2-0.25% (by mass) does it begin to drop off sharply. The impact strength of the β-titanium alloy VT15 decreases at still higher hydrogen concentrations [of the order of 0.3% (by mass)]. The impact strength of VT4 alloy, which is sometimes classified as an (α + β) alloy, varies as a function of hydrogen content in the same manner as that of the α-alloys, while the impact strength of VT10, which is regarded as an α-alloy with intermetallide hardening, varies in much the same way as that of the (α + β) alloys on introduction of hydrogen. Impact strength begins to diminish at the hydrogen concentration at which hydrides appear in the structure of the alloy. The drop in impact strength is a consequence of hydride brittleness.

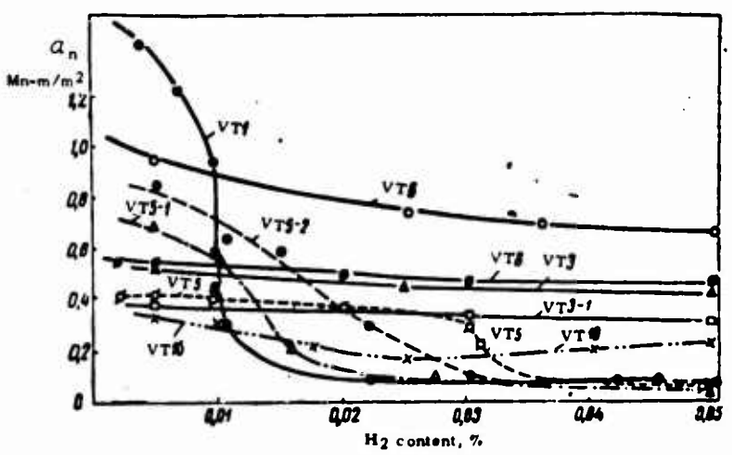

Fig. 70. Variation of impact strength of technically pure titanium and titanium alloys as a function of hydrogen content.

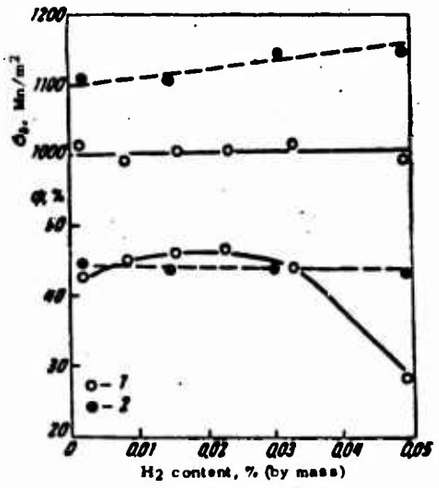

Fig. 71. Influence of hydrogen on the mechanical properties of VT3-1 alloy at deformation rate of 0.4 mm/min. 1) 1958-1959 data; 2) 1964 data.

The influence of hydrogen on the mechanical properties of Soviet (α + β) titanium alloys – VT3-1, VT6, and VT8 – at various stretching speeds was studied in [238, 239]. The tests were made on forged bars 14 × 14 mm in cross section. The forging blanks for the mechanical-test specimens had been annealed in vacuum at 1173°K for 6 hours, followed by saturation with hydrogen at the same temperature and cooling to room temperature with the furnace. These studies indicated that the strength characteristics of (α + + β) titanium alloys rise rapidly with increasing stretching speed. At any stretching speed, the strength properties of all of the alloys studied increase to some degree with increasing hydrogen content. The elongation and necking of the alloys first show practically no change with increasing hydrogen content, but they decrease at hydrogen contents above a certain concentration (0.03% for VT3-1 alloy, 0.02% for VT8, and 0.10% for VT6), although this decrease is observed only in slow tensile tests.

The hydrogen embrittlement of Soviet (α + β) alloys was also investigated in [248, 256, 261, 272]. The data obtained in these studies basically confirm the results of our own investigations, which were described above.

When we repeated these studies in 1964, we detected neither brittle failure nor plasticity loss in VT3-1, even at 0.1% (by mass) of H_2. It was also observed in a study of the properties of VT3-1 after isothermal annealing that at concentrations below 0.1% (by mass), hydrogen has no appreciable effect on its plasticity in tests run on smooth specimens at room temperature (Fig. 71). Thus we observe a certain disagreement between the results obtained in 1964 and those that we obtained in 1958-1959.

This discrepancy may be a consequence of two factors: a) titanium sponge now contains fewer impurities than it did in 1958-

1959; b) the composition of VT3-1 alloy was recently modified; the aluminum content was increased and iron and silicon are now injected among the alloying elements. Indeed, it was found in [260] that oxygen strengthens the tendency of the (α + β) alloys to hydrogen brittleness, while aluminum reduces it. The improvement of the titanium sponge and the increased aluminum content in VT3-1 alloy have depressed the temperature at which hydrogen brittleness develops to below room level.

It was shown in [290], with reference to VT3-1 with 0.03% (by mass) of H_2 that had been subjected to isothermal annealing after hydrogenation that troughs appear at subzero temperatures on the curves illustrating the variation of plasticity with temperature, and become more pronounced the slower the deformation (see Fig. 19). At low enough test temperatures, plasticity is restored. Consequently, hydrogen brittleness is a danger only in a certain temperature range, which depends on rate of deformation.

8. INFLUENCE OF HEAT TREATMENT ON THE HYDROGEN BRITTLENESS OF (α + β) ALLOYS.

Heat treatment has appreciable influence on hydrogen embrittlement in (α + β) alloys. This question was investigated by Burte et al. [254] on the alloy Ti3Mn complex. Specimens of this alloy were given various types of heat treatment, with the result that materials with four strength levels were obtained. Heat treatment consisted in quenching followed by aging. It was found that hydrogen lowers plasticity particularly sharply in the strongest material. The detrimental influence of hydrogen is weakened as the ultimate strength decreases, and below 840 Mn/m^2 it is almost absent. These data were confirmed in a later study of Burte [257], typical results from which appear in Fig. 72.

Fig. 72. Influence of ultimate strength of titanium alloys on maximum permissible hydrogen content.

TABLE 6

Influence of Temperature of Final Heat Treatment of Alloy on Permissible Hydrogen Concentration

Heat treatment	Ultimate strength, Mn/m²	H_2 tolerance, % (by mass)
Quenching from 973°K	1100	Above 0,026
Aging 8 hr at 873°K	850	0,014—0,026
Aging 4 hr at 813°K	970	0,009—0,014
Aging 48 hr at 703°K	1240	0,0025—0,009

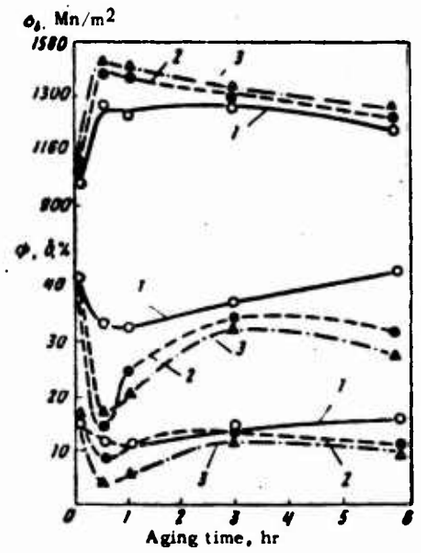

Fig. 73. Influence of holding on the mechanical properties of VT3-1 alloy with aging at 773°K: 1) 0.002% H_2; 2) 0.03% H_2; 3) 0.05% H_2.

Analyzing the results of their own work and preceding studies, Williams, Schwartzberg and Jaffee [264] conclude that hydrogen embrittlement is determined in the final analysis not by ultimate strength, but by the temperature of the final heat treatment: the lower this temperature, the lower must be the maximum permissible hydrogen content. This conclusion is nicely confirmed by the data shown in Table 6.

It follows from these data that there is no relation between ultimate strength and maximum permissible hydrogen content, but a rigorous one between the temperature of the final heat treatment and the hydrogen tolerance. Unfortunately, this relationship was not investigated in detail, since the authors did not feel that such a relationship existed.

Hydrogen embrittlement of the alloy Ti-4Al-4Mn was studied in [265] after 6% stretching and aging at temperatures from 273 to 353°K. It was found that if the aging time was shorter than 1

hour, brittle fracture is not observed at low deformation speeds at any of the hydrogen concentrations studied. After aging from 1 to 10 hours, specimens of the alloy containing 0.025-0.04% H_2 showed brittle failure, but if the aging time exceeded 10 hours, the plasticity of the alloy was recovered.

We have observed that hydrogen causes a sharp decrease in the plasticity of VT3-1 alloy after brief aging at 773°K (Fig. 73). Loss of plasticity in (α + β) alloys is observed after brief aging at elevated temperatures even in the absence of hydrogen. This plasticity decrease is explained by the fact that the ω-phase is segregated primarily on the decay of the metastable β-phase. During aging, the ω-phase is gradually transformed to the stable α-phase, a process accompanied by an increase in the plasticity of (α + β) alloys. In view of the above, the data in Fig. 73 can be explained by hydrogen increasing the amount of ω-phase formed during brief aging. For this reason, (α + β) alloys may not be used after short aging.

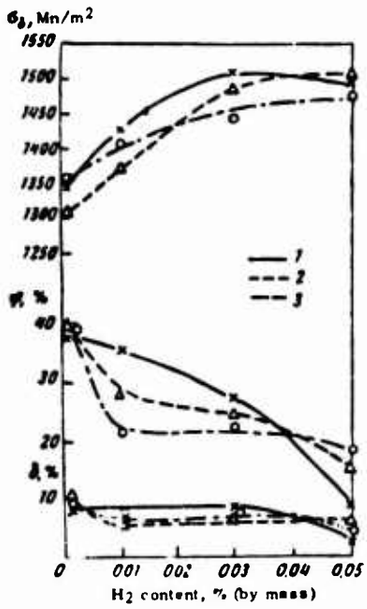

Fig. 74. Influence of hydrogen on the mechanical properties of VT3-1 alloy immediately after quenching and 40 and 90 days later. 1) Freshly quenched state; 2) after 40 days; 3) after 90 days.

It was reported in a recently published paper by Daniels, Quigg and Troiano [266] that the hydrogen embrittlement of the (α + β) alloy Ti-4Al-4Mn depends substantially on the structure of the alloy. It shows the least inclination to hydrogen embrittlement after quenching, a somewhat stronger tendency after quenching and aging, and the strongest tendency after annealing.

Different results were obtained in [262], which was devoted to study of the influence of hydrogen on the structure and properties of the (α + β) alloys VT3-1, VT6, and VT8 in the quenched

state.

Figure 74 shows, by way of example, the influence of hydrogen on the mechanical properties of VT3-1 alloy in mechanical testing at moderate stretching speed (4 mm/min) immediately after aging and 40 and 90 days afterward. It is seen from these data that hydrogen has a much stronger influence on the properties of VT3-1 in the quenched state than in the annealed state. First of all, hydrogen strengthens the quenched alloys considerably. The ultimate strength rises from 1345 Mn/m^2 for the alloy without hydrogen to 1507 Mn/m^2 at an H_2 content of 0.05%. Necking decreases steadily, and a particularly severe loss of plastic properties is observed when more than 0.03% H_2 is introduced.

In agreement with microstructural studies, the above-described influence of hydrogen on the mechanical properties of VT3-1 and VT6 alloys in the quenched state can be explained in terms of the hydrogen increasing the amount of β-phase at a given heating temperature in the (α + β) region by virtue of its β-stabilizing effect and, consequently, increasing the amount of the martensitic phase on quenching. The increase in the amount of martensitic phase in the alloy's structure is what causes the moderate but palpable rise in the strength of the alloys in the quenched state.

The solubility of hydrogen in the α'-phase would tend to be closer to that in the α-phase than that in the β-phase. Indeed, segregation of hydrides is clearly in evidence in the structure of quenched VT3-1 alloy with 0.05% H_2. It is segregation of hydrides that causes the sharp drop in the plastic properties of VT3-1 in tests at a speed of 4 mm/min, at which these alloys do not embrittle in the annealed state.

The strength properties of VT3-1 increase in the process of aging after quenching, and necking and elongation decrease. The loss of plasticity begins even at an H_2 content of 0.015% (by mass) and is particularly sharp at 0.05% H_2. A similar pattern is also observed for VT6 alloy.

The property instability of quenched VT3-1 and VT6 alloys is practically never observed unless hydrogen has first been introduced. This property instability can be attributed to decay processes developing in hydrogen-supersaturated solutions. Submicroscopic segregations of titanium hydride or some other hydrogen-containing phase that also leads to brittle failure are formed as a result of this decay. The experimental data indicate that the maximum permissible hydrogen contents in heat-treated titanium alloys will not be the same as those for annealed alloys.

9. INFLUENCE OF HYDROGEN ON THE LONG-TERM STRENGTH AND THERMAL STABILITY OF (α + β) ALLOYS

It was observed in the first studies of hydrogen brittleness in (α + β) titanium alloys that the harmful effects of hydrogen come into evidence very strongly in long-term strength tests.

In one of the very first papers on hydrogen brittleness in

titanium, Burte [254] observed that hydrogen causes embrittlement in alloys tested at high stretching speeds at room temperature after holding under load at elevated temperatures. Since ($\alpha + \beta$) alloys do not embrittle in the testing process at high stretching speeds, the plasticity decrease was attributed to the influence of prior holding at elevated temperatures under stress. It was established in subsequent studies that this embrittlement is associated with a decrease in the thermal stability of ($\alpha + \beta$) alloys in the presence of hydrogen.

Williams, Jaffee, and Bently [267] investigated the influence of hydrogen on the thermal stability of the ($\alpha + \beta$) titanium alloy Ti-140A. Thermal stability was determined by tensile-testing specimens at room temperature after holding at elevated temperatures with and without stressing. It was found that after holding at 588-698°K, hydrogen-containing specimens of Ti-140A alloy show lowered plasticity, with the embrittlement more pronounced the higher the treatment temperature (within the range studied). Application of a stress aggravates embrittlement even more. These same authors found that vacuum annealing raises the thermal stability of Ti-140A alloy sharply. The favorable influence of vacuum annealing is due to removal of hydrogen, which accelerates the decay of supersaturated solid solutions.

It has been observed in a number of studies that hydrogen lowers the thermal stability of the Soviet alloys VT3 and VT3-1. It is reported in [7] that if VT3 alloy is annealed for several tens of hours at 723-773°K, its impact strength falls sharply. This effect is even more pronounced if hydrogen is present in the alloy. While the impact strength drops from 8 to 2.5 kg-m/cm^2 (from 8000 to 2500 Mn/m^2) after 723°K annealing of VT3 alloy that has been thoroughly degasified by vacuum annealing, the impact strength of hydrogen-saturated VT-3 drops in some cases from 8000 to 50 Mn/m^2.

It was reported in [269] that hydrogen lowers the thermal stability of VT3-1 alloy, which differs from VT3 only in having 2% Mo added to it. Since molybdenum stabilizes the β-phase, the thermal-stability decrease of VT3-1 alloy in the presence of hydrogen is less strongly manifest than that of VT3.

Investigation of the microstructure of VT3 alloy indicates that a $TiCr_2$ phase is precipitated from supersaturated solutions in the process of isothermal annealing at temperatures above the eutectoid transformation, and this results in a sharp drop in impact strength. If, however, the alloy is saturated with hydrogen, a phase containing hydrogen is segregated in addition to the $TiCr_2$. This phase might possibly be titanium hydride, although the possibility of formation of a more complex phase is not excluded. The greater the amount of hydrogen in VT3, the more conspicuous the second-phase segregations become in its structure. The microstructure also changes similarly on isothermal annealing of VT3-1 alloy.

Thus the decrease in thermal stability of VT3-1 alloy in the presence of hydrogen is explained by acceleration of eutectoid β-phase decay by the hydrogen. The decay products, segregating along

the grain boundaries, render plastic deformation difficult, and hence impact strength and necking decrease. The higher the temperature of isothermal annealing, the greater the quantity of decay products and the lower the plasticity of the alloy.

TABLE 7

Influence of Hydrogen on the Long-Term Strength of VT3-1 Alloy

Heat treatment	Test temperature, °K	0.002% H_2			0.05% H_2		
		σ Mn/m²	Time, hr	Remarks	σ n/mm²	Time, hr	Remarks
Isothermal annealing	673	750	200	Withstood tests	750	200	Withstood tests
	723	600	150	Same	600	150	Same
		750	56	Failed	750	45	Failed
	773	400	210	Withstood tests	400	210	»
		450	326	Same	450	87	»
Simple annealing	673	750	336	» »	750	336	Withstood tests
	723	700	234	» »	60	817	Same
	773	400	210	Failed	400	140	Failed

The influence of hydrogen on the thermal stability of Soviet (α + β) titanium alloys was also studied in [247, 249, 256, 261]. These studies confirmed the hypothesis [7] that hydrogen accelerates eutectoid decay of the β-phase in VT3 alloy at hydrogen contents above 0.015% (by mass). But at very high hydrogen contents [above 0.12% (by mass)], stabilization of the β-phase was observed, so that the β-phase no longer decayed during isothermal annealing. The same authors indicated that hydrogen has very little influence on the thermal stability of VT3-1 alloy.

We recently made a study of the influence of hydrogen on the long-term strength of VT3-1 alloy of modified composition (Table 7). It was observed that after simple annealing, VT3-1 alloy has a lower long-term strength than after isothermal annealing. Injection of 0.05% H_2 into VT3-1 alloy lowers long-term strength.

It must be noted, however, that hydrogen in quantities below 0.05% H_2 does not cause a catastrophic collapse of long-term strength. In no case did VT3-1 alloy with 0.05% H_2 fail before 100 hours under a load corresponding to the lower-limit stress given in the technical specifications.

These data stand in contradiction to earlier results. As we noted above, it was observed in [269], which dates from 1959, that the introduction of 0.05% (by mass) of H_2 into VT3-1 alloy causes a sharp drop in plasticity after 100 hours of annealing at 773°C without application of any external stresses.

In recent foreign sources [268, 456], hydrogen was again observed to have no appreciable influence on the long-term strength and thermal stability of alloys in which a sharp drop in these characteristics had been observed earlier. Thus, for example, [268] failed to find any substantial effect of hydrogen on the thermal stability of the alloy Ti + 2% Al + 2% Mn. During prolonged holding in the 573-623°K temperature range, the alloy embrittles to the same degree irrespective of its hydrogen content. Application of stresses intensifies embrittlement of the alloys with and without hydrogen also to the same degree.

The decrease in the detrimental effect of hydrogen on thermal stability and long-term strength in (α + β) titanium alloys is apparently due to improvement of the quality of titanium sponge, particularly as regards reducing its content of interstitial impurities, notably oxygen and nitrogen.

10. HYDROGEN BRITTLENESS OF THE β-ALLOYS

It is now generally accepted that titanium alloys with a structure represented by the β-phase are not inclined to hydrogen brittleness. Indeed, Jaffee, Lenning and Craighead [258] failed to detect a drop in the plasticity of the alloys Ti + 13% Mo and Ti + 20% Mo, after quenching to the β-phase, even at 0.2% (by mass) of H_2, in tensile tests at a speed of 0.1 mm/min at 298°K (see Fig. 69). According to the same source, the alloy Ti + 9% Mn, also quenched for the β-phase, shows no tendency to hydrogen brittleness in the hydrogen concentration range from 0.0015-0.075% under the same mechanical testing conditions.

L.S. Moroz and Yu.D. Khesin [253] showed that a foreign β-titanium alloy containing 3% Al, 13% V, 11% Cr is not inclined to hydrogen brittleness at room temperature after quenching from the β-region. We obtained similar data for the Soviet β-titanium alloy VT15 [289] (Fig. 75).

Although the plastic properties of VT15 alloy are lowered somewhat as hydrogen content rises, no catastrophic loss of plasticity occurs at either high or low stretching speeds, even at 0.2% H_2, in contrast to the α- and (α + β)-alloys.

Impact strength decreases slightly with increasing hydrogen content, but remains rather high. Only at hydrogen contents above 0.25% (by mass) does a sharp drop in the impact strength of quenched VT15 alloy take place. The first hydride segregations appear at considerably higher hydrogen concentrations [above 0.5% (by mass)].

We should, however, expect β-titanium alloys to be inclined to hydrogen brittleness in a certain temperature range. Alloy VT15, like other metals with a body-centered cubic lattice, goes over into the brittle state at sufficiently low temperatures. In mechanical tensile tests at a speed of the order of 6 mm/min, the temperature of the transition from plastic to brittle is about 203°K.

It should be noted in this connection that the data given

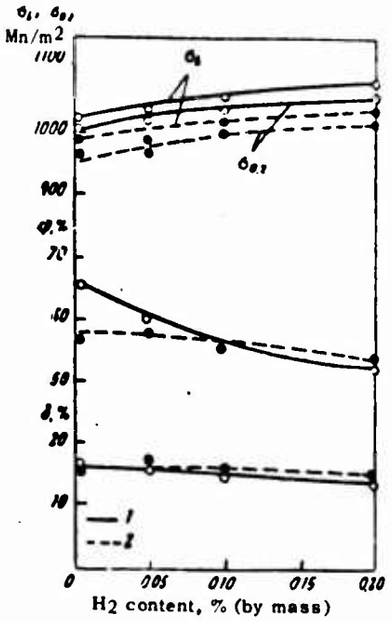

Fig. 75. Influence of hydrogen on the mechanical properties of VT15 alloy in the quenched state in tensile tests at room temperature with various rates of deformation, mm/min: 1) 4; 2) 0.4.

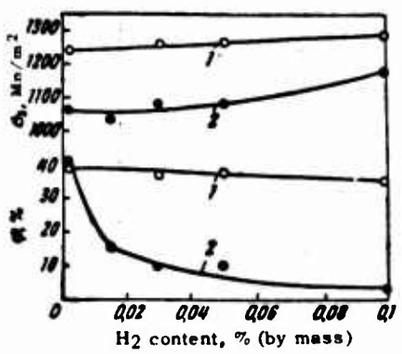

Fig. 76. Influence of hydrogen on the mechanical properties of VT15 alloy at 255°K and various stretching speeds, mm/min: 1) 20; 2) 0.4.

above were obtained as a result of mechanical tests only at room temperature. Such data cannot be regarded as sufficient proof that β-titanium alloys have no tendency to hydrogen brittleness at all.

Actually, mechanical tests made at 255°K showed [290] that even the first hydrogen concentration injected into the alloy [0.015% (by mass)] causes a sharp drop in transverse reduction at low deformation speed (Fig. 76). While VT15 alloy that has first been vacuum-annealed and then quenched from 1053°K in water has 50% necking at 255°K, the alloy with 0.015% (by mass) of H_2,

treated by the same formula, has 15% necking. Cracks appear on the surfaces of hydrogenated specimens before failure during stretching at low speed, but they do not advance through the entire cross section of the specimen. Figure 77 shows the typical appearance of the surface of a VT15-alloy specimen near the point of failure in slow deformation.

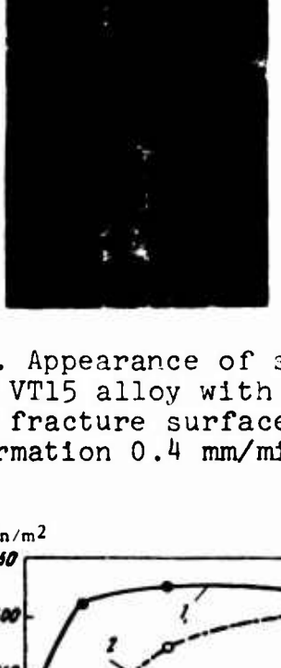

Fig. 77. Appearance of specimens of VT15 alloy with 0.10% H_2 near fracture surface. Rate of deformation 0.4 mm/min.

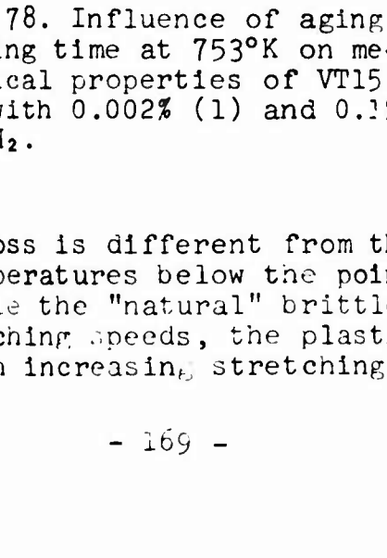

Fig. 78. Influence of aging holding time at 753°K on mechanical properties of VT15 alloy with 0.002% (1) and 0.1% (2) H_2.

This plasticity loss is different from the brittleness that the alloy shows at temperatures below the point of transition to the brittle state. While the "natural" brittleness of VT15 alloy manifests at all stretching speeds, the plasticity of the alloy increases at 255°K with increasing stretching speed. With the ten-

sile-machine crossbar moving at 20 mm/min, transverse necking decreases only slightly with increasing hydrogen content, but even at 0.1% (by mass), the typical pattern of brittle failure is not observed. The specimen breaks with the formation of a neck showing an area reduction of the order of 35%. As in the ($\alpha + \beta$)-titanium alloys, the hydrogen brittleness of VT15 alloy is manifest in a certain temperature range, which depends on hydrogen content and speed of deformation (see Fig. 20).

The influence of aging time at 723°K on the mechanical properties of VT15 alloy with 0.002%, 0.05 and 0.1% of H_2 after quenching from 1053°K is illustrated by Fig. 78. During aging, the alloy hardens rapidly with a simultaneous substantial decrease in its plasticity. Hydrogen lowers the ultimate strength of the aged alloy by a considerable margin. At the same time, VT15 alloy with hydrogen shows elongation and necking figures that exceed those for the hydrogen-free alloy by factors of 1.5-2, for all of the aging procedures investigated.

The microstructure of quenched VT15 alloy is represented by the β-solid solution without any segregations of a second phase. Aging results in decay of the metastable β-solid solution that has been fixed by quenching, with formation of dispersed α-phase segregations; the number of α-phase segregations decreases with increasing hydrogen content. The decrease in the amount of hardening-phase segregations is what causes the decrease in the aging effect with increasing hydrogen content in the alloy. Thus, as a β-stabilizer, hydrogen increases stability of the phase and therefore lowers the rate of its decay and reduces the amount of the hardening α-phase. For this reason, hydrogen at concentrations greater than 0.03% lowers the strength of aged VT15 alloy to a marked degree, with a simultaneous increase in plasticity.

In attempting to determine the hydrogen diffusion coefficient in VT15 alloy, we encountered yet another effect. It was found in layer-by-layer analysis of hydrogenated specimens that peaks corresponding to anomalously high hydrogen contents were observed periodically on the monotonic curve characterizing the decrease in hydrogen concentration with increasing distance from the hydrogenated surface. These peaks could be explained only in terms of the notion that hydrogen diffuses considerably more rapidly along grain boundaries than through the body of the grain at low temperatures.

This implies that the hydrogen concentration along the grain boundaries will be considerably higher than the average for low-temperature hydrogenation. It can be inferred indirectly that the hydrogen concentration along the grain boundaries after etching of VT15 alloy may be close to the solubility limit, i.e., of the order of 0.5% (by mass), while its average concentration after etching is only 0.02-0.03% (by mass). This segregation of hydrogen along grain boundaries may make the material brittle at average hydrogen concentrations that are considered safe.

Thus, the tendency to hydrogen brittleness is determined not only by the average concentration of hydrogen in the metal, but also by its distribution. Obviously, the lower the hydrogenation

temperature, the greater will be the segregation of hydrogen along grain boundaries and the higher should the tendency to hydrogen brittleness become. Segregation of hydrogen along grain boundaries has not yet received the attention that it merits, since it has been assumed that hydrogen diffuses equally easily along the boundaries of the grains and through them. However, this conclusion is valid only for rather high temperatures.

Considerable segregation of hydrogen along grain boundaries is also quite possible in cathodic hydrogenation of iron, nickel and other metals.

11. MAXIMUM PERMISSIBLE HYDROGEN CONCENTRATIONS IN TITANIUM AND ITS ALLOYS

On the basis of a number of studies devoted to the influence of hydrogen on the embrittlement of titanium and its alloys, it has been established that hydrogen embrittlement is especially conspicuous if the hydrogen content exceeds a certain limit. This limit was naturally taken as the maximum permissible hydrogen content.

As a result of numerous studies devoted to the hydrogen brittleness of technical titanium, it may be assumed that the hydrogen content in this metal should not exceed 0.010% (by mass) if hydrogen brittleness is to be avoided. In α-titanium alloys, due to the favorable influence of aluminum and tin, it appears that higher hydrogen contents may be tolerated – up to approximately 0.02% (by mass).

A maximum hydrogen content of 0.0125% (by mass) has been established for deformable (α + β)-titanium alloys used in the aviation industry on the basis of a number of studies carried out in the USA.

No marked hydrogen embrittlement has been observed in the Soviet alloys VT3-1 (modified composition) and VT6 throughout the entire concentration range studied [from 0.0 to 0.1% (by mass) of H_2]. However, hydrogen lowers the thermal stability of VT3 and VT3-1 alloys. For this reason, the hydrogen content in VT3 should not exceed 0.015% (by mass), and that in VT3-1 0.03%. Hydrogen embrittlement of the (α + β) alloy VT8 is observed at hydrogen contents above 0.02% (by mass), and in VT4 above 0.015%.

It is shown in [228] that up to 0.025% (by mass), hydrogen does not influence the plastic properties of the alloys AT3, AT4 and AT6 in tensile tests at both high and low speeds. Up to this concentration, the thermal stability of AT3 and AT4 remains high. Injection of 0.015% H_2 into AT6 causes a marked deterioration of thermal stability.

AT8 alloy is most sensitive to hydrogen. Injection of 0.015% H_2 causes a sharp drop in the plasticity of this alloy in tensile testing at high and low speeds.

Data given in [289, 290] indicate that if VT15 alloy is used at temperatures above 283°K, hydrogen in amounts not exceeding

0.015% (by mass) does not lower the plasticity of the metal in the quenched state to any substantial degree and does not markedly affect its properties after quenching and aging. The same source indicates that sheets of this alloy must be plated with titanium to prevent selective (grain-boundary) absorption of hydrogen during etching.

It should be noted in closing that the maximum permissible hydrogen contents that have now been established are not absolute. When α-, (α + β)- and β-titanium alloys work at low temperatures, they must have hydrogen contents below 0.015%. The tolerances for hydrogen in titanium must be substantially lower for coarse-grained than fine-grained material. When titanium and its alloys are used in welded joints, the hydrogen content must be below these values by factors of 1.5-2, since the stress field in the seam and the zone around it promote directional migration of hydrogen atoms and the development of premature failure of the weldments.

In accordance with the above, the norms that have been established for permissible hydrogen content in titanium and its alloys must be reviewed to take the structure and field of application into account.

Chapter 4

ZIRCONIUM AND ITS ALLOYS

1. KINETICS OF INTERACTION OF ZIRCONIUM WITH HYDROGEN

Zirconium reacts quite actively with hydrogen even at very low temperatures. Zirconium powder can absorb hydrogen even at room temperature [4, 5]. The activation energy of the zirconium-hydrogen reaction is found to be 17.6 kcal/g-atom (74 kj/g-atom). Oxide films sharply reduce the rate of absorption of hydrogen by zirconium. The retarding effect of the oxide film is determined not by its thickness, but by the nature of the oxide. The thin oxide film formed at room temperature inhibits absorption of hydrogen by zirconium more strongly than the thick layer formed at high temperature. Oxygen and nitrogen in solid solution have little influence on the rate of interaction of zirconium with hydrogen.

Zirconium and its alloys can be saturated with hydrogen in reactions with water and water vapor at high pressure [242, 320]. Zirconium and its alloys operate under such conditions in water-cooled nuclear reactors. The reaction of zirconium with water or water vapor [steam] can be described by the scheme

$$Zr + 2H_2O \rightleftarrows ZrO_2 + 2H_2.$$

The hydrogen formed in this reaction is absorbed by the metal. It has been observed that the amount of absorbed hydrogen is proportional to the quantity of corroded metal. Since hydrogen embrittles zirconium severely even at very low contents, it was feared that zirconium and its alloys could not be used in water-cooled reactors. However, experience showed that the amount of hydrogen absorbed by zirconium in the corrosion process is small under normal conditions, and this provided an assurance that although hydrogen saturation of zirconium is undesirable, its detrimental effect will not be felt if the reactors are not designed for excessively long periods of operation.

The conditions under which zirconium-alloy fuel jackets may absorb larger quantities of hydrogen were defined more precisely in [315]. Reference [316] studied the hydrogen saturation of joints made in the alloy zircalloy-2 using eutectic solders with copper, nickel and iron during corrosion in water at 633°K with and without secondary attack by hydrogen. These studies showed that joints enriched in nickel absorb considerably more hydrogen than joints made from solders with iron or copper.

Studying the influence of various alloying elements on hydrogen absorption by zirconium during corrosion in hot water, Wanklin and Hobkinson [317] also observed that zirconium alloyed with nickel is rapidly saturated by hydrogen.

These studies made it necessary to review the composition of zircalloy-2, one of whose alloying elements is nickel. As a result of these investigations, two modifications of zircalloy-type alloys were proposed [320]: zircalloy-2 without nickel (1.2-1.7% Sn; 0.12-0.18% Fe; 0.05-0.15% Cr; Ni $\leqslant$ 0,007%) and zircalloy-4 (1,2—1,7% Sn; 0,18—0,24% Fe; 0,07—0,13% Cr; 0,007% $\leqslant$ Ni).

2. DIAGRAM OF STATE OF THE HYDROGEN-ZIRCONIUM SYSTEM

Although many researchers have studied the zirconium-hydrogen system since 1891, reliable data have been obtained only recently. The results of early studies of this system, a survey of which can be found in the monograph [2], are highly contradictory, since they were done on zirconium containing large quantities of impurities, which were, moreover, present in various proportions.

Further, the early studies did not give sufficient attention to precautions that would ensure establishment of the most complete equilibrium possible in the zirconium-hydrogen system. Also, it was only recently found that zirconium contains a large quantity (up to 5%) of its analogue, hafnium, and that the early studies had been made essentially on zirconium-hafnium alloys.

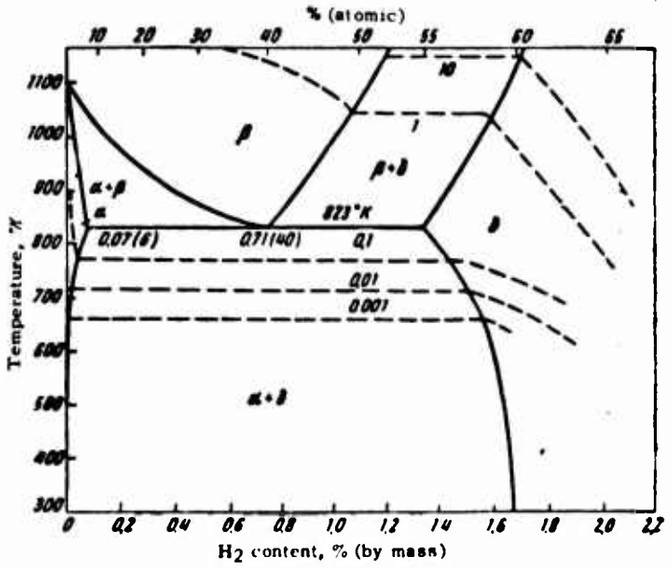

Fig. 79. Phase diagram of zirconium-hydrogen system. The dashed curves indicate equilibrium hydrogen pressure isobars and the numerals the hydrogen pressures in Mn/m^2.

The phase diagram that we have constructed for the zirconium-hydrogen system from the results of the most dependable studies

[291-293, 300, 321] appears in Fig. 79. The high-temperature part of the diagram was studied by Ells and McQuillan [292], who investigated equilibria in the zirconium-hydrogen system by a method that McQuillan and others had previously used successfully to study the titanium-hydrogen system. This method involves measurement of the equilibrium hydrogen pressure as a function of hydrogen concentration above the zirconium-hydrogen alloys in a closed space. The boundaries of the phase regions are determined from the sharp changes in the trends of isotherms or isobars.

These studies showed that the phase diagram of the zirconium-hydrogen system is similar to the titanium-hydrogen diagram. As in titanium, hydrogen stabilizes the β-phase of zirconium, shifting the two-phase α + β region toward lower temperatures. At a low enough temperature, eutectoid decay of the β-phase takes place in the system.

It was at first assumed that the solubility of hydrogen in α-zirconium was very high, but these data were not subsequently supported. Actually, as was shown by Gulbransen and Andrew [297], the solubility of hydrogen in α-zirconium is very low. These data were confirmed in the work of S.M. Schwartz and M.W. Mallett [298] and Lubowitz [321]. According to these sources, the solubility of hydrogen in α-zirconium diminishes sharply with decreasing temperature and amounts to only about 0.003% (by mass) at 473°K and 0.0008% at room temperature. The very low solubility of hydrogen in α-zirconium at room temperature was confirmed by B.I. Bruk and G.I. Nikolayeva [304], who studied the zirconium-hydrogen system using tritium.

Interstitial impurities (oxygen, nitrogen and carbon) lower the solubility limit [310]. It is assumed that by occupying octahedral spaces in the crystal lattice, the interstitial atoms inhibit the implantation of hydrogen atoms regardless of the spaces that they occupy – whether tetrahedral or octahedral. The dimensions of the atoms increase from oxygen to carbon, and thus carbon lowers the solubility of hydrogen to a greater degree than oxygen.

The solubility of hydrogen can be represented as a function of temperature in the 578-859°K range by the equation

$$\lg C = -1880/T + 5{,}18,$$

from which the heat of solution of hydrogen in α-zirconium is found to be 8.6 kcal/g-atom (36 kj/g-atom).

The solubility of hydrogen in β-zirconium is considerably higher than that in α-zirconium. Thus, according to [295], the solubility of hydrogen in β-zirconium in the 1123-1148°K temperature range is 51.2-52.5% (atomic) [1.14-1.19% (by mass)]. A.S. Meyerson and O.P. Kolchin found that the solubility of hydrogen in β-zirconium at 1273°K and atmospheric pressure is 39.8% (atomic).

In contrast to the earlier works, in which the authors had found several hydride phases, Ells and McQuillan found only one hydride (the δ-phase on Fig. 79). The existence of only one hy-

dride in the zirconium-hydrogen system has been confirmed by x-ray structural analyses conducted at room and high temperatures [293, 294], by precision heat-capacity determination [300] and by dilatometry. The homogeneity region of the hydride lies between 60 and 67% (atomic) at room temperature and between 66 and 62% (atomic) at 873°K.

Beck [322] recently made a thorough x-ray structural study of zirconium alloys with hydrogen in the range of high concentrations. Many investigators had found another γ-hydride phase in this region in addition to the δ-phase. Only Bogan and Bridge, who made an x-ray structural analysis at elevated temperatures, failed to detect it. Beck showed that the γ-phase is a metastable phase that dissociates comparatively easily on heating and appears again on cooling below the eutectoid line. However, it is not a product of eutectoid decay. The γ is a metastable phase that forms instead of the stable α-phase on decay of the δ-phase as the temperature is lowered below the solubility line. Thus γ is a phase intermediate between the α- and δ-phases, and corresponds to ZrH in composition. This phase has a tetragonal body-centered lattice with two zirconium atoms per elementary cell and the hydrogen in tetrahedral spaces.

Recent studies in the hydrogen-rich region indicated only a single stable phase, the δ. Beck assumes that there must be two stable hydride phases, δ and ε. The transition from the δ- to the ε-phase begins, in his opinion, at 62.5% (atomic) H_2, and takes place in a very narrow concentration range, of the order of 0.1% (atomic). The ε-phase has a body-centered tetragonally distorted cubic structure, with the degree of the tetragonal distortion rising with increasing hydrogen content.

Beck's data are in good agreement with the results obtained by Lubowitz [321] in his study of the zirconium-hydrogen system in the range of high hydrogen concentrations.

The zirconium hydride ZrH_2 is a brittle black powder. Its density is farther below that of zirconium the higher the hydrogen content. The density of the zirconium hydride $ZrH_{1.92}$ is 5.47 g/cm³, i.e., 15.4% below the density of zirconium (6.49 g/cm³). According to Sieverts and Gotta [306], the heat of formation of the hydride with the composition $ZrH_{1.92}$ is 40.5 kcal/g-atom (170 kj/g-atom). Calculations based on the highly interesting thermodynamic theory of the solubility of hydrogen in zirconium that was proposed in [308] give 41.4 kcal/g-atom (174 kj/g-atom).

3. INFLUENCE OF HYDROGEN ON THE STRUCTURE AND PROPERTIES OF ZIRCONIUM AND ITS ALLOYS

As we noted above, the solubility of hydrogen in zirconium and in industrial alloys based on it (the zircalloys) is negligibly small. Hence the dominant form of hydrogen brittleness in zirconium and its alloys should be hydride brittleness of the first kind. Since the solubility of hydrogen in zirconium and zirconium alloys increases sharply with rising temperature, we may expect them to show irreversible hydrogen brittleness of the second kind, developing at low deformation speeds in hydrogen-super-

saturated solid solutions.

Actually, even the very first studies [323, 324, 328] showed that hydrogen has no substantial influence on the strength characteristics of zirconium, but does lower its impact strength substantially at low temperatures. Hydrogen brittleness appears at a content as small as 0.001% H_2. At hydrogen concentrations from 0.001 to 0.01% (by mass), zirconium becomes brittle if it is heated above 588°K and then cooled at a rate slower than a certain critical rate. Hydrogen brittleness does not develop in quenched zirconium at these hydrogen contents. Hydrogen brittleness appears after aging at temperatures below 533°K. The loss of impact strength that takes place is associated with decay of the supersaturated solution, which is accompanied by formation of dispersed zirconium-hydride segregations. This is consistent with the fact that the solubility of hydrogen in zirconium at room temperature does not exceed 0.0008%.

Hydrogen brittleness is the more pronounced the higher the hydrogen content, and at concentrations higher than 0.01% quenching is no longer capable of fixing the supersaturated solution of hydrogen in the α-phase and thus preventing the drop in impact strength at room temperature.

In [325], the influence of hydrogen on the properties of iodide zirconium at room temperature and at the temperature of liquid nitrogen (77°K) was made on specimens prepared from 12.7-mm hot-rolled slabs. The slabs were heated at 673°K for 3 hours, after which they were either quenched in ice water or cooled with the furnace. The results obtained in this study indicated that the ductility of zirconium drops sharply with increasing hydrogen content. Hydrogen lowers the plasticity of zirconium more sharply in the annealed than in the quenched state. Thus, quenching makes it possible to improve the plastic properties of zirconium when it contains hydrogen. However, at hydrogen contents above 0.005%, the plasticity increase as a result of quenching the zirconium is moderate.

It must be noted that the plasticity of quenched zirconium specimens containing amounts of hydrogen above equilibrium solubility is higher at 76°K than at 293°K. This indicates that hydride brittleness of the second kind has developed in the quenched specimens. The same results justify advancing the hypothesis that hydride brittleness of the second kind, like reversible brittleness, should develop in a definite temperature range. At excessively low temperatures, the decay processes are slowed down to the extent that they have ceased altogether in tensile tests at the standard speeds.

We studied the influence of hydrogen on the mechanical properties of domestic zirconium. Iodide zirconium that had been remelted in a vacuum-arc furnace with a consumable electrode was used for the studies. Rods with a 14 × 14-mm cross section were forged out of the ingot at 1033°K and cut up into blanks. These blanks, which were to be used to make mechanical-testing specimens, were subjected to vacuum annealing at 1073°K for 6 hours and were saturated with hydrogen. They were heated at 673°K for 1

hour and then quenched in water or cooled slowly with the furnace. The test results for the annealed zirconium are shown in Fig. 80. Hydrogen lowers the plastic properties of zirconium more strongly after slow cooling than after quenching.

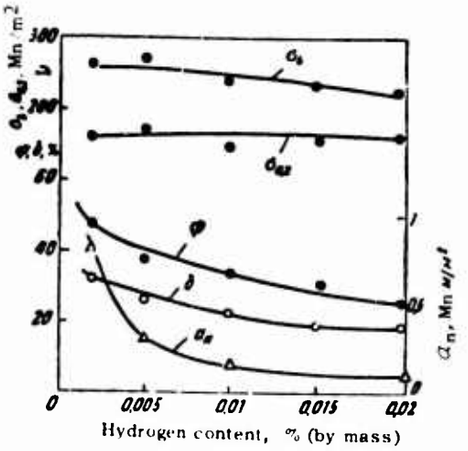

Fig. 80. Influence of hydrogen on the mechanical properties of domestic zirconium.

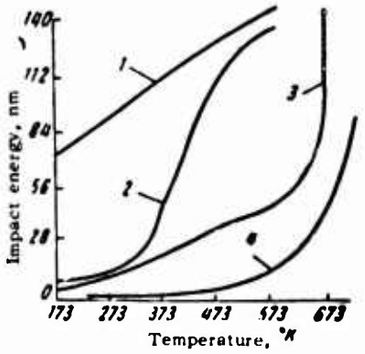

Fig. 81. Influence of test temperature on work required to break zirconium alloy with 1.5% Sn and various hydrogen contents, % (by mass): 1) <0.001; 2) 0.0045; 3) 0.026; 4) 0.06.

Thus, we can convert some of the hydrides into solid solution and thereby raise the ductility of zirconium by heating it above the solubility line and quenching it in water. However, quenching would hardly be a practicable method of countering hydrogen brittleness. Hydrogen may be segregated in hydride form from the supersaturated solution even at room temperature, because of the high diffusion rate of hydrogen atoms in zirconium. These segregations will lower the plasticity of the zirconium. A similar effect is also observed in titanium.

Hydride brittleness is observed not only in zirconium, but also in zirconium alloys. Figure 81 shows the effect of test tem-

perature on the work to failure of a zirconium alloy with 1.5% Sn and various hydrogen contents in impact tests of notched specimens. These data indicate that hydrogen raises the temperature of the ductile-to-brittle transition. Thus, for example, at H_2 contents below 0.001% (by mass), the temperature of the transition to brittleness lies below 173°K, while at 0.06% (by mass) of H_2, the transition temperature is 673°K.

The authors of [457] studied the influence of hydrogen on the mechanical properties of zirconium and the following alloys based on it: zircalloy-2; the high-strength alloy 3Z1 (Zr + 1.25% Al + 1% Sn + 1% Mo) and the alloy Zr + 2.5% Nb, which is used to make pipes. The alloys contained as impurities, in % (by mass): 0.08-0.11 O_2, 0.006-0.015 C, 0.0015-0.0025 N_2. The alloy Zr + + 2.5% Nb was investigated in the quenched and aged state, and all the other alloys after complete annealing.

The studies were made on smooth and notched specimens, the latter with a theoretical stress concentration coefficient of 8.

The study was concerned with the structure and properties of alloys containing up to 0.05% (by mass) of H_2. Microstructural analysis showed that in unalloyed zirconium and zircalloy-2, practically all of the hydrogen was bound into hydrides. The hydride lamellae were segregated basically along grain boundaries and in smaller quantities inside the grains, along definite crystallographic planes. No hydride segregations were observed in the alloy Zr + 1.25% Al + 1% Sn + 1% Mo, even at 0.05% (by mass) of H_2. The authors of [457] explain this in terms of all of the hydrogen in the alloy being concentrated in the β-phase, in which it dissolves readily. In the alloy Zr + 2.5% Nb with 0.05% (by mass) of H_2, only small amounts of hydrides were detected.

In tests on smooth specimens, the ultimate strength and yield point of zirconium are practically independent of hydrogen content, but they show a decrease in tests on notched specimens. Ultimate strength and yield point show an increase with increasing hydrogen content in zircalloy-2 when the tests are run on smooth specimens. For notched specimens, the ultimate strength of zircalloy-2 decreases with increasing hydrogen content, while the yield point shows practically no change. The elongation of zirconium and zircalloy-2 decreases with increasing hydrogen concentration (Table 8).

It was found in [457] that zirconium and zircalloy-2 are not inclined to accelerated static fatigue in the presence of up to 0.05% (by mass) of H_2. Grain-size increase, 20% cold deformation, corrosion in steam at 673°K, and quenching from 873°K do not lower the fatigue strength of zircalloy-2. Failure under static load occurs in zirconium and zircalloy-2 only at stresses near the ultimate strength. The alloys Zr + 1.25% Al + 1.0% Sn + 1.0% Mo and Zr + 2.5% Nb, on the other hand, are highly sensitive to notching and premature failure under static load (Fig. 82).

The hydrogen-brittleness mechanism of zirconium and its alloys is determined by the shape of hydride segregations and their distribution in the matrix.

The shape and manner of distribution of the hydrides from decay of supersaturated hydrogen solutions in α-zirconium was studied in [311-313].

TABLE 8

Influence of Hydrogen on the Mechanical Properties of Zirconium and Zircalloy-2 in Tensile Tests

H_2 content, % (by mass)	Description of specimens	σ_b, Mn/m²	$\sigma_{0,2}$, Mn/m²	δ, %
	Zirconium			
—*	Smooth	358	135	32,5
0,02		362	149	27,3
0,05		340	153	24,0
—*	Notched	388	202	—
0,02		365	202	—
0,05		378	191	—
	Zircalloy-2			
—*	Smooth	318,5	225	41,5
0,02		331	224	34,5
0,05		445	278	33,0
—*	Notched	452	312	—
0,02		437	294	—
0,05		413	333	—

* Vacuum-annealed specimens.

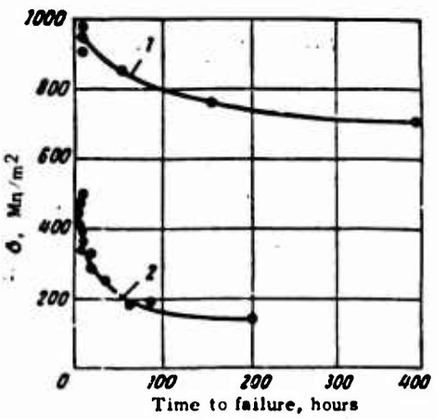

Fig. 82. Long-term strength of alloy Zr + 1.25% Al + 1% Sn + 1% Mo with 0.05% H_2 in tests on smooth (1) and notched (2) specimens.

Fig. 83. Shapes of hydride segregations in zirconium.

The most thorough investigation of the habit of the hydride segregations was made by Bailey, who used transmission electron microscopy, electron diffraction, and x-ray structural methods of analysis [314]. These studies showed that it is not the stable δ-hydride with face-centered cubic structure, but the metastable γ-hydride with tetragonal lattice (a = 4.617 Å, c = 4.888 Å) that is precipitated from the supersaturated hydrogen solution in α-zirconium. Bailey established that zirconium hydride is segregated after slow cooling in the form of lamellae that are quite large

in two dimensions and small in the third. The following relationships are observed between the crystal structures of the hydride lamellae and the matrix:

$$(\bar{1}100)_\alpha \parallel (111)_\gamma \text{ and } (11\bar{2}0)_\alpha \parallel (110)_\gamma.$$

The habit planes of the hydride lamellae are $\{11\bar{2}0\}$ and $\{10\bar{1}0\}$, with the $\{11\bar{2}0\}_\alpha$ planes parallel to $\{110\}_\gamma$ and $\{10\bar{1}0\}$ almost parallel to $\{131\}$.

On abrupt quenching, zirconium hydride segregates in the form of needles with their axes pointing in the $<11\bar{2}0>$ direction. The habit planes of these acicular segregations are the $\{10\bar{1}0\}_\alpha$ planes, which are parallel to $\{111\}_\gamma$. No dislocations or grain boundaries are necessary for germination of hydrides. If they are present, however, the hydrides form preferentially on them. No hydride segregations have been detected along twinning planes.

When first germinated, the acicular segregations are coherently related to the matrix. The needles grow rapidly in the $<11\bar{2}0>$ directions, i.e., along their own axes. In growth in directions normal to the needle axes, certain planes of the segregations lose coherence. Segregation growth in the directions normal to the axis is also accompanied by formation of dislocation loops or dislocation segments in the basal plane due to the difference between the interatomic distances along the $<10\bar{1}0>$ directions in the matrix and the hydrides (Fig. 83). At moderate cooling rates, we observe both forms of hydride segregation: lamellar and acicular.

The influence of hydrides on the formation of microscopic cracks in zirconium was studied by Young and Schwarz in [327] with the electron microscope. They established that intensive twinning with limited slip takes place in impact (or high-speed tensile) tests of zirconium that has been saturated with hydrogen. The converse picture was observed in slow tensile tests.

As a rule, the twins propagate as far as the hydride segregations, and then minute microscopic cracks were frequently observed on the other side of the hydride lamellae, at a point directly opposite the end of the twin. When the twins approached the hydride lamella from both sides, small pores were observed at the point of juncture between the twin and the hydride. Even after impact testing, vacuum-annealed zirconium showed very few microcracks. The number of microcracks in the zirconium increased with increasing rate of deformation and with increasing number of twins.

It follows from the experimental data cited above that the formation of microcracks is related to interruption of twinning bands by the hydride lamellae that have been segregated out.

The interaction of the acicular hydride particles with dislocations in quenched zirconium specimens with various hydrogen contents was studied in [424]. Tensile tests in the temperature range from 120-240°K showed that the critical cleavage stress increases to several times its initial value as hydrogen content rises. This increase in the critical cleavage stresses is due to the fact that

the finely dispersed acicular hydride segregations act effectively as barriers to moving dislocations.

Chapter 5

VANADIUM, NIOBIUM AND TANTALUM

1. INTERACTION OF METALS OF SUBGROUP VB WITH HYDROGEN

Unlike the transition metals of Subgroups III-IVB, metals of Subgroup VB react less actively with hydrogen and absorb smaller quantities of it. Compact vanadium does not react with hydrogen at elevated temperatures. However, if vanadium is activated by repeated alternating heating in a hydrogen atmosphere at 1073-1373°K and degasification in vacuum at the same temperature, it absorbs hydrogen readily thereafter, sometimes as much as 100 volumes per volume of the metal [4, 5]. Activated vanadium absorbs hydrogen also at lower temperatures, but the absorption rate diminishes sharply as the temperature goes down.

Hydrogen dissolves in vanadium with evolution of heat, and hence its solubility in vanadium increases with diminishing temperature (see Fig. 2); the heat of solution of hydrogen in vanadium is 7.7 kcal/g-atom (32 kj/g-atom) [4]. According to Sieverts, the highest content of hydrogen in vanadium corresponds to the formula $VH_{0,71}$ [1,37% (by mass) of H_2], or 157 cm^3 to 1 g of vanadium. According to a later study [359], the maximum hydrogen content in vanadium corresponds to the formula $VH_{0.9}$. As hydrogenation progresses, the density of vanadium drops by 6-13%, depending on hydrogen content [357, 360]. Sieverts and Gotta [360] assume that only solid solutions are formed on reaction of vanadium with hydrogen. The monograph [362] cites unpublished data of Mallett and Bridge according to which vanadium hydride was prepared as follows. Iodide vanadium was activated in a high vacuum for 3 hours at 1173°K and then cooled to 573°K and held for 5 hours at a pressure of 1 atmosphere (0.1 Mn/m^2) in hydrogen obtained by thermal decomposition of uranium hydride. The resulting product corresponded to the formula $VH_{0.97}$, which indicates 48.4% (atomic) of H_2. X-ray structural analysis indicated that the product is a phase with a tetragonal crystal lattice. Due to blurring of the lines on the x-ray pattern, the parameters of this phase could be determined only approximately (a = 3.02 A and c = 3.36 A).

In a later study of the dissociation vapor pressure of hydrogen in the vanadium-hydrogen system, Kofstad and Wallace [361] failed to detect any second phase below 33% (atomic) of H_2 in the temperature range from 438 to 729°K. The deviation from the Sieverts law, which is particularly marked at low temperatures and high hydrogen concentrations, is explained by the authors as due to the ability of the hydrogens to locate in two positions: in normal interstices of the vanadium lattice and in extraordinary

positions due to defects caused by deformation of the lattice on injection of the hydrogen atoms. X-ray diffraction studies conducted later [459] indicate that the vanadium hydride V_2H, which has a tetragonally distorted body-centered lattice with an axis ratio $c/a = 1.1$, is formed in the vanadium-hydrogen system below 423°K. At room temperature, the solubility of hydrogen in vanadium is 2% (atomic) [0.039% (by mass)], and the two-phase region extends from 2 to 30% (atomic). A diagram of state of the vanadium-hydrogen system (Fig. 84) was constructed in [468] on the basis of x-ray structural analysis.

In many respects, niobium reacts with hydrogen in the same way as vanadium. Like vanadium, compact niobium does not usually react with hydrogen at temperatures below 523°K, unless it is activated by heating to high temperatures in a hydrogen atmosphere. After activation of niobium, hydrogen is absorbed, although slowly, even at room temperature [329]. As the temperature rises, the hydrogen absorption rate in niobium increases. The amount of absorbed hydrogen decreases with increasing temperature (see Fig. 2). The process of hydrogen absorption by niobium is exothermic, i.e., it is accompanied by liberation of heat. The heat of solution of hydrogen in niobium changes from 16 to 23.3 kcal/g-atom (from 67 to 97.5 kj/g-atom) as the hydrogen concentration rises.

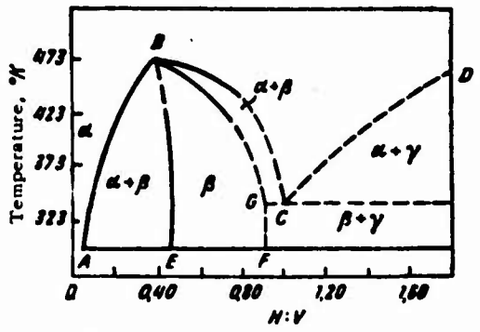

Fig. 84. Phase diagram of vanadium-hydrogen system.

The reaction of niobium with hydrogen is reversible, and the hydrogen can be eliminated from the niobium by vacuum annealing. It is reported in [51] that vacuum annealing for 2 hours at 1273°K is sufficient to eliminate hydrogen from niobium quite thoroughly.

A detailed study of the niobium-hydrogen system was made in [335]. The work was done on niobium that had been refined by electron-beam melting and had a small content of the basic impurities: (0,04% O_2; 0,004% N_2, 0,01—0,1% Ta). The hydrogen for the work was obtained by decomposition of titanium hydride. Figure 85 shows the equilibrium hydrogen pressure as a function of its content in the niobium. At small hydrogen contents and high temperatures, the variation of the equilibrium hydrogen pressure as a function of the atomic ratio N_H/N_{Nb} (N is the number of atoms) at room temperature is expressed by straight lines in logarithmic coordinates. At high enough hydrogen concentrations in the low-temperature region, the relation between log p and log N_H/N_{Nb} is not linear, indicating transition to a two-phase region. At temperatures above 723°K, the solubility of hydrogen in niobium is proportional to the square root of pressure throughout the concentration range [329, 330]. The existence of only one hydride, NbH, has been definitely established in the niobium-hydrogen system. The stoichiometric hydride cannot be prepared in direct reactions of compact niobium

with hydrogen. Thus, Coy and Douglas [334] report that they succeeded in preparing a hydride of the composition $NbH_{0.89}$. Niobium hydride is a dark gray powder with a density lower than that of niobium (6.0-6.6 and 8.57 g/cm^3, respectively). The hydride forms from niobium and hydrogen with evolution of 9.2 kcal/g-atom of heat (38 kj/g-atom).

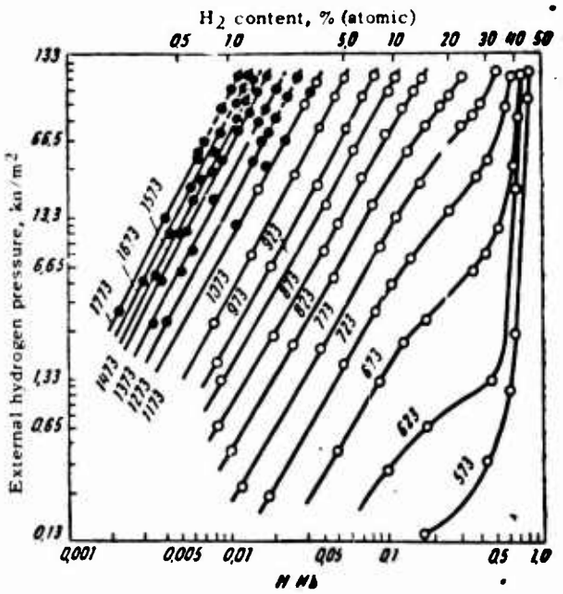

Fig. 85. Equilibrium hydrogen pressure isotherms in the niobium-hydrogen system.

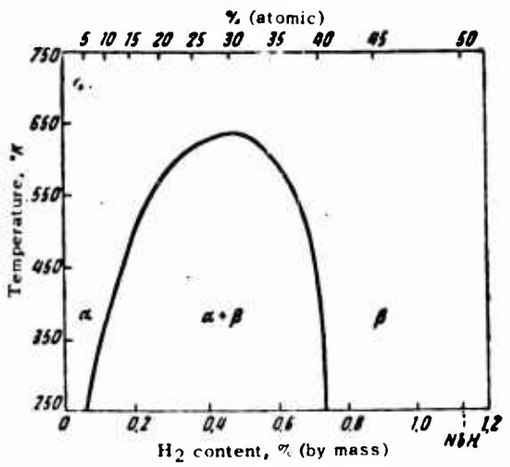

Fig. 86. Phase diagram of niobium-hydrogen system.

On the basis of data on the hydrogen equilibrium pressure as a function of its content in niobium [335], and the results of x-ray structural analysis published in [338-340, 344], the phase di-

agram of the niobium-hydrogen system may be represented by the diagram of Fig. 86. At low temperature, the niobium-hydrogen system is represented by three phase regions: the solid solution of hydrogen in niobium (α-phase), the two-phase α + β region, and the homogeneity region of the hydride NbH (β-phase). With rising temperature, the two-phase (α + β) region becomes smaller, to vanish above 650°K.

The single-phase structure peculiar to pure niobium is replaced by two phases at high enough hydrogen concentrations [341, 345]. Segregations of the hydride phase appear in the structure of the metal in the form of transgranular plates, networks along grain boundaries, or isolated inclusions. According to the results of microstructural analysis, the solubility of hydrogen in niobium corresponds to approximately 0.06% (by mass).

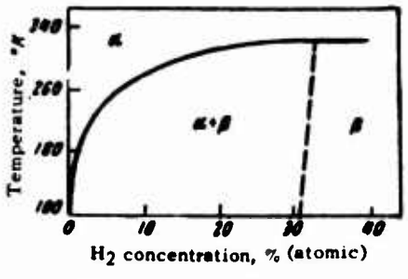

Fig. 87. Phase diagram of tantalum-hydrogen system.

Tantalum reacts quite vigorously with hydrogen. After brief degasification in vacuum at 1273-1373°K, tantalum in the form of dense specimens 15-40 μ in thickness absorbs hydrogen readily. The rate of the reaction of tantalum with hydrogen increases with rising temperature [332]. At lower temperatures, the reaction kinetics of tantalum with hydrogen is not parabolic, although this law is observed at higher temperatures. This type of reaction between tantalum and hydrogen is explained by formation of tantalum hydride at lower temperatures. The rate of reaction of tantalum with hydrogen increases with increasing pressure.

Tantalum absorbs hydrogen with evolution of heat, and therefore the solubility of hydrogen in this metal decreases with rising temperature (see Fig. 2). The highest concentration of hydrogen in tantalum corresponds to the formula $TaH_{0.76}$. Solution of hydrogen in tantalum causes an increase in its volume. A preparation of the composition $TaH_{0.76}$ has a density of 15.1 g/cm^3, i.e., 9% lower than the density of pure tantalum (16.6 g/cm^3) [4, 5].

Hydrogen dissolved in tantalum can be eliminated by vacuum annealing at temperatures above 1273° [4, 5]. At low pressures, the kinetics of the reaction of hydrogen with tantalum depends strongly on the surface state of the specimens. If there is a dense oxide film on the surface of the tantalum, it will not react with hydrogen below 673°K.

The existence of only two phases has been established in the tantalum-hydrogen system [323]: the α-solid solution of hydrogen in tantalum and the β-solid solution based on tantalum hydride Ta_2H.

On the basis of their own studies, which were made by the x-ray structural and conductivity methods on very pure tantalum,

and on the basis of data obtained by other authors, Watt, Wallace and Craig constructed a phase diagram of the tantalum-hydrogen system (Fig. 87). According to this diagram, the solubility of hydrogen in tantalum, which amounts to more than 40% (atomic) at temperatures above 323°K, drops off sharply as the temperature is lowered and becomes negligibly small below 120°K. Segregations of the hydride Ta_2H appear as a result of the decrease in solubility in the tantalum structure. The lattice constant of tantalum increases when hydrogen is dissolved.

2. INFLUENCE OF HYDROGEN ON THE PROPERTIES OF VANADIUM

Since vanadium absorbs hydrogen with evolution of heat and thus the solubility of hydrogen in the metal increases on cooling, there should be no gas porosity due to hydrogen in vanadium ingots. The hydrogen pressure in cavities in vanadium is negligibly small, and there is therefore no brittleness due to molecular hydrogen. Hydrides form in direct reaction between vanadium and hydrogen, and hence hydride brittleness may develop in the metal. However, when hydrogen is introduced into vanadium in concentrations below the solubility limit, the distortions in the vanadium lattice become so large that brittleness appears, resembling the cold shortness due to such interstitial impurities as oxygen and nitrogen [348, 353, 362].

Reference [362] presents data obtained by Braun, according to which ductile vanadium becomes brittle after cathodic saturation. Hydrogen brittleness appears at H_2 contents greater than 0.01% (by mass), while the solubility of hydrogen in vanadium is 0.039% (by mass).

Cathodic hydrogen saturation of vanadium takes place in various acidic media, e.g., in solutions containing up to 40% by volume of H_2SO_4, up to 5 of H_3PO_4, or up to 1 of HCl. Braun submits the following example: a compact specimen of vanadium containing 0.077% O_2, 0.082% N_2 and 0.0021% H_2 as impurities was subjected to cathodic saturation for 16 hours at a current of 18 amp in a 10% sulfuric acid solution, with the result that the hydrogen content in the vanadium rose to 0.29% (by mass). The vanadium with this hydrogen content was so brittle that it could be crushed.

It is reported in the same source that hydrogen can be eliminated from vanadium by vacuum annealing, a process in which its content is reduced to 0.0016% (by mass), and the ductility of the metal restored. Arc remelting in an inert-gas atmosphere eliminates hydrogen from the metal. A vanadium specimen that had been saturated with hydrogen to a content of 0.014% (by mass) contained 0.0045% (by mass) of H_2 after arc remelting in an inert-gas medium.

It is indicated in [362] that vanadium can be saturated by hydrogen to concentrations at which hydrogen brittleness appears by etching in solutions of acids and by heat treatment in an atmosphere containing hydrogen or some other hydrogen-containing gas.

Reference [454] reports that the ductile-to-brittle transi-

tion occurs in vanadium in the hydrogen concentration range from 0.008-0.06% (by mass).

A systematic study of the influence of hydrogen on the structure and properties of vanadium was made by Roberts and Rogers [348]. The work was done on 99.2% pure vanadium with the following impurities in %: 0.2 C; 0.01 Si; 0.01 Fe; 0.015 Ca; 0.02 O_2; 0.01 N_2 and 0.003 H_2. The specimens were wires 0.89 mm in diameter produced by cold drawing of rods 12.7 mm in diameter. The wire specimens were given recrystallizing annealing in a vacuum at two temperatures (45 min at 1073°K and 60 min at 1273°K). Annealing at 1073°K produced uniform, slightly elongated grains with diameters of the order of 1-2 μ. The structure obtained after annealing at 1273°K was uniform but highly heterogranular: the grain diameters varied from 1 to 150 μ.

The specimens were saturated by hydrogen in an iron retort at a temperature of the order of 773°K in a current of dry hydrogen. The temperature and time of saturation were varied so as to obtain predetermined hydrogen concentrations in the metal. The wire specimens were tensile-tested at a deformation rate of 1.3 mm/min at various temperatures.

Specimens of unhydrogenated vanadium showed ductile fracture with formation of a cup or cone. The failure of hydrogenated fine-grained specimens was ductile at 433°K, but brittle at room temperature. Hydrogenated specimens showed more ductile fracture at the temperature of liquid nitrogen than at room temperature.

Studies [348] made on vanadium foil 0.025 mm thick with a distinct texture showed that the foil broke at a 45° angle to the direction of rolling at a 0.1% (by mass) [4.6% (atomic)] content of H_2 and without orientation at 0.15% (by mass) [6.9% (atomic)]. It follows from these data that failure takes place along {100} cleavage planes in heavily textured hydrogenated foil.

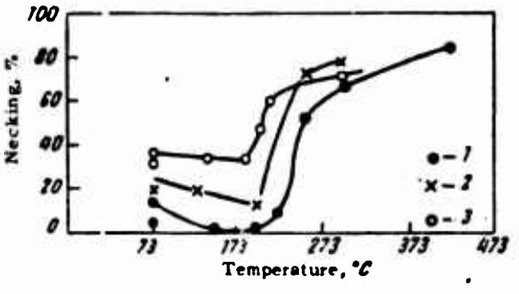

Fig. 88. Influence of test temperature on necking of vanadium containing 0.008% (by mass) of H_2 at various deformation speeds, min^{-1}: 1) $5 \cdot 10^{-2}$; 2) 100; 3) $19 \cdot 10^3$.

Small, distinctly outlined pits are observed along the margins of the fracture on electron-microscope examination at a power of 10,000; they may have appeared as a result of at least partial propagation of the failure along grain boundaries. In a micro-

structural investigation of fine-grained specimens, Roberts and Rogers detected a second phase. This phase forms veins of irregular shape, extending lengthwise along the wire, apparently along grain boundaries. The authors of this study conclude that this may be vanadium hydride VH. No second phase was detected in coarse-grained specimens. The studies showed that the ductility of hydrogenated coarse-grained specimens without the second phase is the same as that of hydrogenated fine-grained specimens with segregations of the second phase. Thus, the second phase influences ductility only slightly if at all. In this connection, it seems doubtful that the phase detected in [348] is indeed vanadium hydride, since metallic hydrides lower ductility substantially.

To account for the hydrogen brittleness of vanadium, Roberts and Rogers cite unpublished data of Mallett, according to which it may be assumed that the hydrogen atoms in a preparation with the composition $VH_{0.92}$ are positioned along {100} planes formed by vanadium atoms. Thus, the oriented failure of vanadium is explained by assuming that the hydrogen atoms promote splitting along {100} planes and that the crack propagates along these planes. However, there is no information at all as to whether such preferential segregation of hydrogen along {100} planes is preserved in vanadium at lower hydrogen concentrations.

We assume that at low hydrogen concentrations and rather low temperatures, the brittleness of vanadium is reversible hydrogen brittleness of the second kind. Indeed, as we indicated earlier, hydrogen brittleness appears in vanadium in a definite temperature interval. It is more pronounced at room temperature than at the temperature of liquid nitrogen or at 437°K. Baldwin [380] arrived at similar conclusions from a study of the variation of ductility in vanadium containing 0.008% (by mass) of H_2 as a function of deformation rate and temperature (Fig. 88). Additional data favoring this hypothesis will be given above [sic], when we examine the influence of hydrogen on the properties of niobium-vanadium alloys.

3. INFLUENCE OF HYDROGEN ON THE PROPERTIES OF NIOBIUM

As we noted above, hydrides are formed in the niobium-hydrogen system, so that we should expect hydride brittleness of the

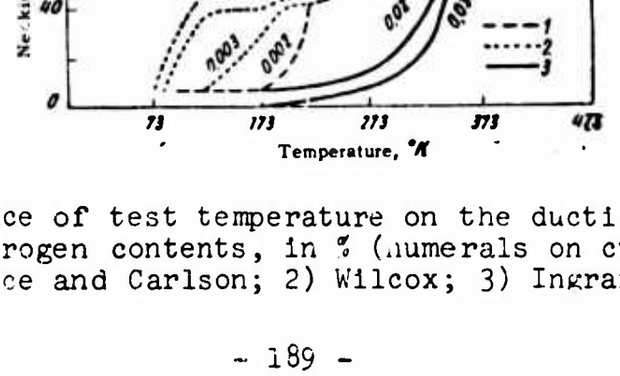

Fig. 89. Influence of test temperature on the ductility of niobium with various hydrogen contents, in % (numerals on curves). 1) According to Eustice and Carlson; 2) Wilcox; 3) Ingram.

first kind at sufficiently high hydrogen contents. Since hydrogen severely distorts the niobium lattice, large internal stresses should arise and cause brittleness at high deformation rates. The solubility of hydrogen in niobium is very high, and we should therefore expect development of reversible hydrogen brittleness at low deformation speeds.

Figure 89 illustrates the influence of hydrogen on the plastic properties of niobium in tensile tests at low temperatures [336, 342, 343, 347], from which we see that the temperature of the transition from the plastic to the viscous state rises with increasing hydrogen content.

The data of various authors are not in complete quantitative agreement. The reason for these discrepancies may consist in varying degrees of purity of the niobium. The highest hydrogen concentration at which niobium retains sufficient plasticity at room temperature varies, according to different authors [334, 341, 347] from 0.012 to 0.05% (by mass). However, all sources note that brittle failure of niobium occurs at room temperature at hydrogen concentrations with which there are no hydride segregations in the structure.

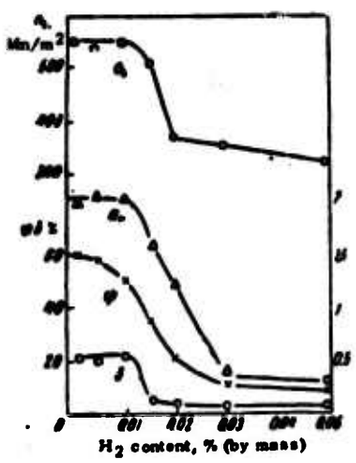

Fig. 90. Influence of hydrogen on the mechanical properties of niobium at a deformation rate of 0.4 mm/min.

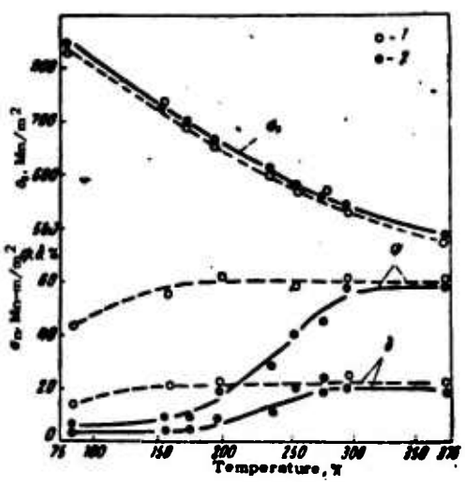

Fig. 91. Influence of test temperature on mechanical properties of niobium with various hydrogen contents at deformation rate of 0.4 mm/min: 1) 0.0001; 2) 0.005.

It was reported in [346], a study made on niobium that had been electron-beam remelted, that hydrogen has practically the same influence on the mechanical properties of deformed and recrystallized niobium. This indicates low sensitivity of the hydrogen brittleness of niobium to structure.

We studied the influence of hydrogen content and test temperature on the properties of domestic niobium. The work was done

on niobium rods that had been arc-remelted. The average impurity contents in the original material were as follows, in %: 0.05 C; 0,02 O_2; 0,016 N_2; 0,08 Zr; 0,06 Si; 0,1 Ti; 0,06 Fe; 0,4 Ta.

Mechanical tensile tests were run at a speed of 0.4 mm/min. The influence of hydrogen content on mechanical properties in tests run at room temperature is illustrated by Fig. 90. These data indicate that at H_2 contents above 0.015%, all of the mechanical properties of the niobium are lowered.

The influence of test temperature on the mechanical properties of niobium with 0.0001 and 0.005% H_2 in tests at a deformation speed of 0.4 mm/min is shown in Fig. 91. These data indicate that with decreasing temperature, the strength properties of niobium rise. The plasticity of niobium with a small hydrogen content remains high, even at comparatively low temperatures. Injection of hydrogen into the niobium, even in small quantities, results in a sharp decrease in plasticity.

Microstructural investigation of niobium [347] has shown that at temperatures above 123°K, pores form near the fracture surface and increase in number as hydrogen content increases. At a test temperature of 88°K, a large number of twins is observed at the fracture surface, except for specimens with 0.0001% H_2 tested at a stretching speed of 6 min^{-1}. At this temperature, teeth appear at the beginning of the tension curves, and the authors associate them with twinning. Such tension curves were observed at temperatures below 123°K.

Only indirect inferences can be drawn concerning the hydrogen brittleness of niobium. It is nevertheless clear that it is not hydride brittleness, since the first hydride segregations appear at much higher concentrations. The loss of plasticity in hydrogenated specimens may be due to reversible hydrogen brittleness. However, recovery of plasticity at rather low temperatures is characteristic for this type of brittleness, and such recovery was observed in none of the sources cited. It should, however, be noted that the low-temperature brittleness of niobium has not been studied thoroughly enough. The intervals on the temperature scale at which the metal's properties have been studied have been too broad.

A number of facts indicating interaction between hydrogen atoms and dislocations in niobium appears to us to confirm the reversibility of the metal's low-temperature hydrogen brittleness. As we noted above, convincing evidence of the existence of such interaction in niobium was obtained in a study of the recovery of yield point and dynamic elastic modulus in hydrogenated niobium specimens subjected to alternating tension and relaxation [355]. The interaction of hydrogen with dislocations in niobium is also confirmed by the stepwise nature of plastic deformation in coarse-grained niobium at room temperature with hydrogen contents above 0.0089% (by mass). This is also attested to by the ultimate-strength and yield-point maxima at 223°K in niobium containing 0.003% H_2. A similar peak has been observed in steel at higher temperatures. According to Nabbarro, the peak in steel results from carbon-atom mobility becoming comparable with the rate of mo-

tion of dislocations at a certain temperature. The net result is that impurity atmospheres follow dislocations, retarding their motion and increasing resistance to plastic deformation. Cottrell derived an empirical equation for the deformation rate at which resistance to deformation should rise:

$$\dot{\varepsilon} = 10^9 D.$$

Wilcox, Brisbane and Klinger [347], combining this equation with the equation for the diffusion coefficient of hydrogen in niobium,

$$D = 0{,}0215 \exp\left(-\frac{9370}{RT}\right),$$

find that at a deformation rate of 0.005 min^{-1}, dislocation capture of impurity atmospheres should be observed at 178°K instead of the experimentally found 223°K.

The temperature of initial hydrogen-atmosphere capture by impurity atoms can also be evaluated from Eq. (24) (see page 80). If we assume that, as for titanium, the coefficient A is $6 \cdot 10^{-21}$ erg-cm, we find that at a deformation speed of 0.005 min^{-1}, the temperature of impurity-atmosphere capture by dislocations for $\rho = 10^8$ cm^{-2} and, consequently, also the maximum development of hydrogen brittleness in niobium, should be observed around 200°K. Remembering that (41) was derived for high temperatures, the agreement between the experimental and calculated temperatures of hydrogen-atmosphere capture must be regarded as satisfactory.

4. HYDROGEN BRITTLENESS OF VANADIUM-NIOBIUM ALLOYS

The influence of hydrogen on the mechanical properties of vanadium-niobium alloys, which form a continuous series of solid solutions, was investigated in [342].

The alloys were prepared from iodide vanadium containing, in %: 0,01 C; 0,001 H; 0,00055 N; 0,015 O_2; 0,02 Cr and 0,02 Fe, and niobium containing, in %: 0,004 C; 0,001 H_2; 0,011 N_2; 0,003 O_2; 0,001 Fe; 0,014 Ta and 0,01 Zr. The alloys were smelted out in an arc furnace under an inert atmosphere. They were rolled into slabs for fabrication of bending specimens and into rods for tensile-test specimens. The bending-test specimens had the dimensions 6.35 × 1.6 × 30 mm; the gauge length of the tensile specimens was 3.2 mm in diameter and 25.4 mm long. All specimens were ground, polished, and then given recrystallization annealing at temperatures from 1393 to 1573°K, depending on alloy composition, for 12 hours in sealed ampules with a helium atmosphere. The size of the recrystallized grain varied from 0.5 mm for pure vanadium to 0.04 mm for the alloy Nb + 10% V; the pure niobium had an unrecrystallized structure, since the 1573°K temperature at which it was annealed was below the recrystallization point.

Specimens prepared by the above method contained from 0.008 to 0.0012% (by mass) of H_2. To obtain other hydrogen concentrations, the specimens were either annealed in vacuum at a pressure of 10^{-5} mm Hg for 8 hours at 1173°K or saturated with hydrogen at

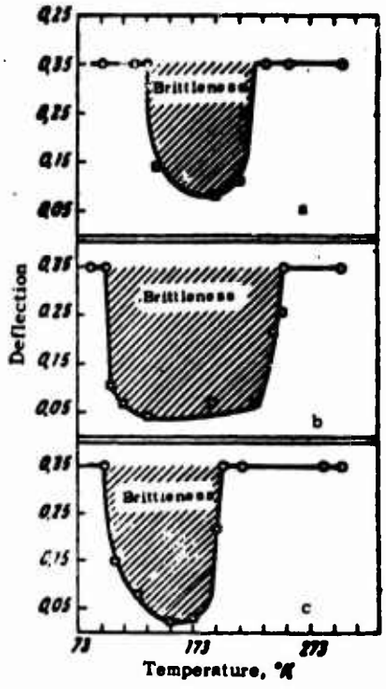

Fig. 92. Maximum bending deflection as a function of temperature for alloys of vanadium with niobium containing 0.001% (by mass) of H_2: a) 40% V + 60% Nb; b) 70% V + 30% Nb; c) 100% V.

1073°K. In vacuum-annealed specimens, the hydrogen content was below 0.00011% (by mass).

The bending tests were conducted at steadily increasing load, so that the deflection increased at a rate of 0.254 mm/min. The deflections at which numerous cracks appeared or the specimen broke were determined in this study. If the specimen bent to 90° without cracking or failure, it was regarded as plastic. The tensile tests were conducted with the machine's crossbar moving at 0.2 mm/min.

The bending tests showed that all alloys were plastic after vacuum annealing all the way down to the lowest temperature tested (77°K). Alloys containing 0.001% (by mass) of H_2 showed brittle failure in a certain temperature range (Fig. 92). The hydrogen-brittleness temperature range of alloys of vanadium with niobium depends on composition (Fig. 93); it extends from 173 to 113°K for pure vanadium. With increasing niobium content, the brittleness temperature range broadens as far as the composition V + 40% Nb; on a further increase in niobium content, it becomes smaller, and alloys containing more than 60% Nb show no inclination to hydrogen brittleness over the entire temperature range at the hydrogen concentrations studied (0.001%). The investigations also showed that vanadium and vanadium-rich alloys are more sensitive to hydrogen brittleness than niobium and niobium-rich alloys.

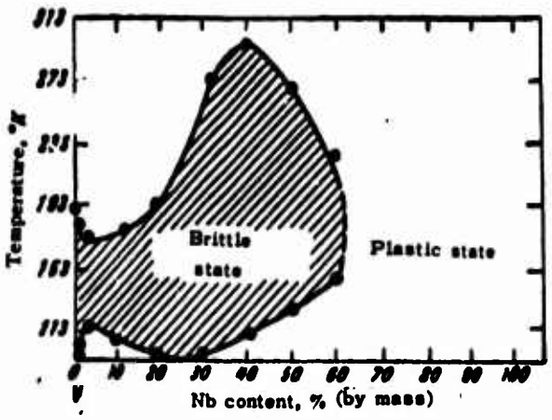

Fig. 93. Temperature range of hydrogen brittleness in alloys of vanadium with niobium.

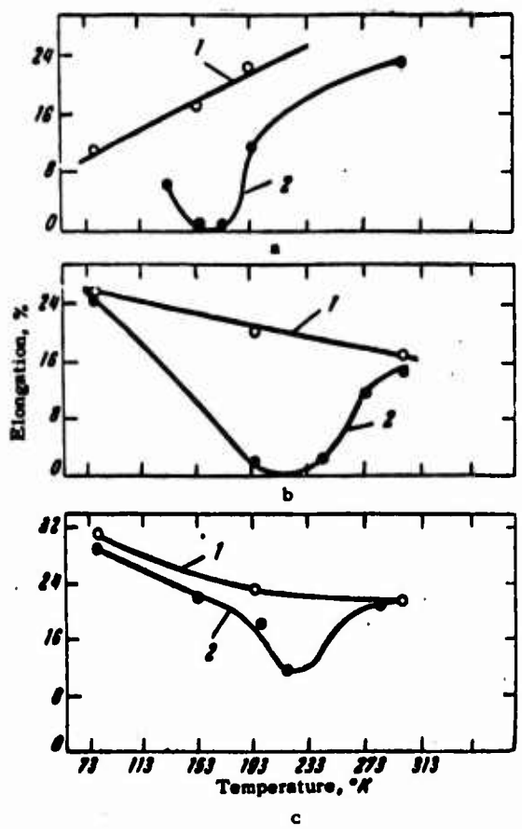

Fig. 94. Uniform elongation of vanadium-niobium alloys as a function of temperature with 0.001 and 0.0001% (by mass) of H_2: a) V + 1.5% Nb; b) V + 30% Nb; c) V + 70% Nb; 1) vacuum annealing; 2) 0.001% H_2.

The upper temperature threshold of hydrogen brittleness rises with increasing hydrogen content. For the alloy of vanadium with

30% Nb, it is 258°K at 0.001% (by mass) of H_2. An increase in hydrogen content to 0.002% (by mass) raises the upper brittleness threshold to room temperature.

Introduction of 0.001 and 0.002% (by mass) of H_2 into the alloys 30% V + 70% Nb and 18% V + 82% Nb does not cause hydrogen brittleness. At H_2 concentrations above 0.003% (by mass), brittleness does appear, with its temperature interval broadening as the hydrogen content rises.

Niobium containing 0.005% (by mass) of H_2 is also inclined to hydrogen brittleness under the test conditions selected. At this concentration, the temperature of the ductile-to-brittle transition is near 243°K.

Hydrogen brittleness also appears in alloys of vanadium with niobium in tensile tests at slow speeds. In this type of test, hydrogen brittleness also manifests in a certain temperature range, which depends on the composition of the alloys. Increasing the niobium content in the alloys leads to increased plasticity of hydrogenated specimens, as is illustrated by Fig. 94.

Vacuum-annealed niobium retains its high plasticity down to the temperature of liquid nitrogen. Introduction of 0.002% (by mass) of H_2 into it results in a sharp transition from ductile to brittle. The temperature of the transition in tensile tests is 203°K.

5. INFLUENCE OF HYDROGEN ON THE PROPERTIES OF TANTALUM

It follows from the tantalum-hydrogen diagram of state (see Fig. 87) that either reversible hydrogen brittleness of the second kind or brittleness of the first kind, which we have identified as cold shortness due to dissolved hydrogen, may develop in tantalum at temperatures above 323°K. At temperatures below 150°K, only hydride brittleness of the first or second kind should appear, depending on experimental conditions. And, finally, any form of brittleness may appear in the 150-323°K temperature range, depending on hydrogen concentration and experimental conditions.

It has long been known that hydrogen causes brittleness in tantalum [2, 4]. It was observed that tantalum may, despite its high corrosion resistance, undergo hydrogenation in aggressive media up to the concentrations at which it becomes brittle [377]. Alloying with O_2, C, Fe, Si, Ni, Nb, Ti and W does not protect tantalum from hydrogenation in use in corrosive media, nor does it prevent the development of hydrogen brittleness [377]. The most effective way to protect tantalum is to provide a contact with platinum. At a 10,000:1 ratio of the contacting tantalum and platinum surfaces, holding in concentrated hydrochloric acid at 423°K does not cause hydrogen brittleness, even after 10,000 hours.

Hydride brittleness is the dominant form at room temperature. The habit of the hydride segregations and their influence on the failure mechanism in tantalum was studied by Bakish [381]. The investigations were made on highly purified tantalum (99.9% Ta; 0.03% C and 0.03% Fe). The hydrogen was injected into the tantalum

by annealing in a hydrogen atmosphere at 973°K and by cathodic saturation at room temperature in an electrolyte composed of 90% HNO_3 (70%) + 10% HF (48%) at a current density of about 0.08 amp/cm^3 [sic].

Microstructural analysis showed that the product of the interaction of tantalum with hydrogen (the author calls it β-tantalum hydride TaH; it is apparently, however, Ta_2H) is segregated along {100} planes. Segregation of the hydrides severely distorts the tantalum lattice, warping the specimens.

After tantalum has been annealed in a hydrogen atmosphere, the specimens show brittle failure in bending. Failure takes place by cleavage along the {100} and {110} planes, but cleavage along {100} plane appears to predominate. In specimens that have been electrolytically saturated with hydrogen, cleavage takes place preferentially along {110} and less often along {100} planes.

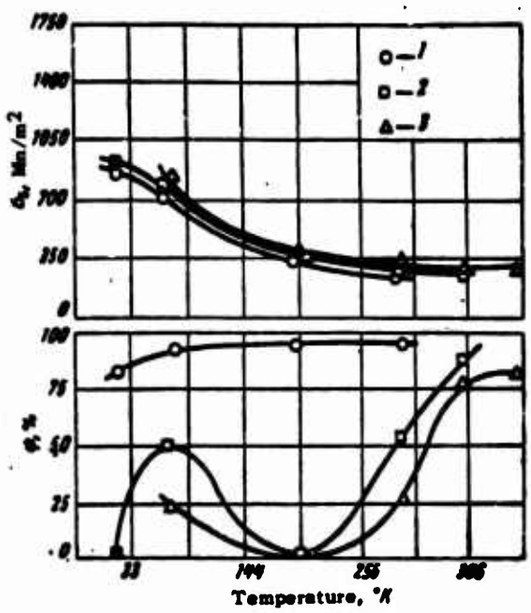

Fig. 95. Influence of test temperature on mechanical properties of recrystallized tantalum without hydrogen (1), with 0.014 (2) and 0.027 (3) % H_2.

The influence of hydrogen on the mechanical properties of tantalum at low temperatures was studied in [346]. Tantalum ingots 12.7 mm in diameter were prepared for the investigation by electron-beam melting. In a Sieverts apparatus, from 0.015 to 0.059% (by mass) of H_2, which corresponds to 2.7 and 10.5% (atomic), were injected into these ingots. After hydrogenation, the ingots were set down into rods 0.35 mm in diameter. Specimens were cut out of these rods and subjected either to tempering to relieve stresses or to recrystallization annealing. The heat treatment was conducted in a hydrogen atmosphere in the Sieverts apparatus in order to prevent losses of hydrogen during degasification. Micro-

structural examination of the original and hydrogenated specimens showed no second phase.

Studies were made on smooth and notched specimens. The notch was half the specimen radius deep; it was V-shaped with a 60° angle and a 0.15-mm radius of curvature. This notch provided a theoretical stress-concentration factor of three. The smooth specimens were tensile-tested at a machine crossbar speed of 0.15 mm/min and the notched specimens at 0.127 mm/min.

The results obtained in this study (Fig. 95) showed that hydrogen brittleness develops in tantalum in a definite temperature range. The upper temperature range of brittleness is shifted toward higher temperatures as hydrogen content increases. At low temperatures, plasticity is recovered, the more strongly the lower the hydrogen content.

No substantial differences were observed in the behavior of deformed and recrystallized tantalum. This indicates that the tendency of tantalum to hydrogen brittleness has little dependence on structure.

Since this brittleness manifests at low deformation speeds and the hydrogen concentration is below the solubility limit, this brittleness should be classified as reversible. At temperatures below 273°C, the hydrogen brittleness of tantalum containing 10.5% (atomic) of H_2 should be at least partially reversible due to hydride segregation.

The influence of hydrogen on the behavior of tantalum in fatigue tests was studied in [397]. The studies were conducted on tantalum containing the following impurities, in %: 0,005 C; 0,007 O_2; 0,0005 H_2, 0,003 N_2; 0,08 Nb, 0,01 Fe. Some of the specimens were annealed in a hydrogen atmosphere at 873°K for 3 hours, with the result that the hydrogen content reached 0.0295% (by mass). Hydride segregations extending along the rod axis were observed in the hydrogenated tantalum. The fatigue tests were conducted under the conditions of symmetrical tension and compression at a frequency of 2000 cycles/min at 195°K. It was observed that the lifetime of the hydrogenated specimens was considerably shorter than that of the unhydrogenated ones.

Chapter 6

CHROMIUM, MOLYBDENUM AND TUNGSTEN

1. INTERACTION OF CHROMIUM, MOLYBDENUM AND TUNGSTEN WITH HYDROGEN

Unlike the majority of transition metals, chromium and molybdenum and tunsten in particular absorb comparatively small quantities of hydrogen. Finely divided chromium does not absorb hydrogen at 473-1023°K in direct treatment with molecular hydrogen [4, 5]. The absorption of hydrogen by chromium is an exothermic process, and therefore the solubility of hydrogen in chromium increases with rising temperature (see Fig. 2).

On the basis of calorimetric data of Sieverts and Gotta, Smith [2] advanced the hypothesis that the solubility of hydrogen in chromium should pass through a maximum at 573°K. The heat of solution of hydrogen in chromium is 3.8 kcal/g-atom (16 kj/g-atom) for the preparation $CrH_{0.26}$ [351].

Considerably larger amounts of hydrogen dissolve in chromium in electrolytic processes [up to 0.45% (by mass)]. Chromium precipitated electrolytically from aqueous solutions at room temperature contains up to 60 volumes of hydrogen per volume of metal, and as much as 300 volumes when deposited at 323°K [4, 5]. On heating in vacuum at around 333°K, most of the hydrogen is driven out of the chromium, but complete elimination requires vacuum annealing at temperatures above 873°K. When hydrogen dissolves in chromium, the constants of the latter's lattice are increased and its density is reduced. The density of the preparation $CrH_{0.26}$ is 6.77 g/cm^2, i.e., 5.85% below that of pure chromium (7.19 g/cm^3).

Two hydride phases can be produced on electrolysis: CrH and CrH_2. The hydride CrH has a structure of the wurtzite type, while that of CrH_2 is of the fluorite type. According to [354], both hydrides have broad homogeneity regions. Chromium hydrides are unstable and decompose even at room temperature.

Pure molybdenum films adsorb hydrogen very actively at temperatures from 90 to 293°K [4, 5]. Molybdenum does not absorb hydrogen at room temperature, but it does at elevated temperatures, although in smaller quantities than in the case of chromium [351].

The solubility of hydrogen in molybdenum shows an unusual dependence on temperature. It increases with rising temperature to 1073°K and then diminishes. Thus, the process of hydrogen absorption by molybdenum is exothermic below 1073°K and endothermic above that point. Hydrogen absorbed by molybdenum at elevated tem-

peratures is readily desorbed on cooling. Solution of hydrogen in molybdenum in the 673-1373°K range proceeds with absorption of 12.5 kcal/g-atom (52.5 (kj/g-atom) of heat [354]. The formation of molybdenum hydrides was not detected under the conditions studied.

Tungsten is among the elements that absorb hydrogen very actively as a result of activated adsorption [4, 5]. The amount of gas adsorbed at a given temperature increases with rising pressure, and decreases with increasing temperature at constant pressure. At temperatures above 673°K, the adsorbed hydrogen is desorbed.

At the same time, tungsten does not absorb hydrogen at temperatures below 1473-1573°K. Absorption of hydrogen by tungsten has been studied for the most part at temperatures that must be regarded as low for this metal. It is quite possible that tungsten absorbs appreciable quantities of hydrogen at higher temperatures. Indeed, Langmuir [386] reports marked absorption of hydrogen by tungsten at 2773°K. Reliable data on the formation of tungsten hydrides are not available.

2. INFLUENCE OF HYDROGEN ON THE PROPERTIES OF CHROMIUM, MOLYBDENUM AND TUNGSTEN

All metals of Subgroup VIa have a strong tendency to cold shortness and are sensitive to stress concentrators. The ductile-to-brittle transition temperature for these metals is higher than for other metals at a given degree of purification. This is accounted for by the small interatomic distances in these metals, as a result of which the solubility of interstitial impurities is negligibly small. For this reason, hydrogen causes brittleness in these metals at negligibly small concentrations.

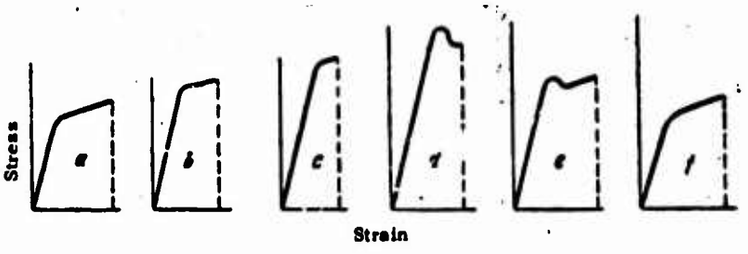

Fig. 96. Nature of tension curves of molybdenum after various heat treatments.

Cathodic absorption of hydrogen increases hardness and brittleness in chromium [4, 5] and results in a sharp decrease in the plasticity of molybdenum in bending tests [387, 389].

In [390], a detailed study was made of the influence of hydrogen on the yield point of molybdenum. The investigation was made on molybdenum with the following impurity contents in the initial state, in %: 0,013 C; 0,0114 O_2; 0,004 N; 0,03 Fe. Tensile specimens were made up from wire 0.5 mm in diameter. The wire was given re-

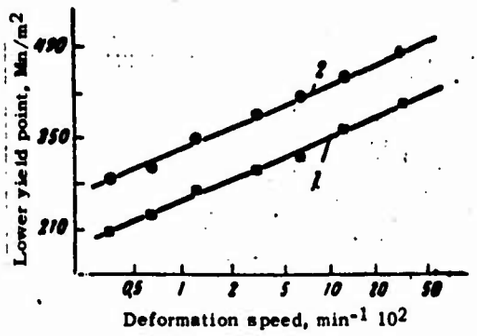

Fig. 97. Yield point of molybdenum as a function of deformation rate. 1) Slow cooling; 2) quenching and aging at 298°K (25°C) for 36 hours.

crystallization-annealing in a hydrogen atmosphere. After annealing, the specimens had a uniform structure with a grain diameter of 0.05 mm and the contents of hydrogen, oxygen and nitrogen in the molybdenum had decreased to 0.002, 0.0052 and 0.002%, respectively.

The specimens were then annealed for 1 hour at 2823°K in a hydrogen atmosphere or in vacuum, followed by slow cooling in the hydrogen atmosphere or by quenching.

The specimens were then aged in an oil bath at 298, 323, 373 and 403°K for times up to 200 hours, after which they were tensile-tested at room temperature. The construction of the clamps protected the wire specimen from bending and shearing.

The nature of the tension curves changes considerably after aging (Fig. 96). After slow cooling, molybdenum does not show a distinct yield point (curve *a*). Immediately after quenching, a faint yield plateau can be detected (curve *b*). Molybdenum has less elongation in the quenched state than after annealing. Aging results in an even sharper drop in elongation. After brief aging, the yield plateau disappears (curve *c*); with increasing aging time, a yield peak with sharp and lower limits appears on the tension curve (curve *d*). At deformation rates slower than $8 \cdot 10^{-5}$ sec^{-1}, no yield plateau is observed, and the tension curve has the same shape as for quenched specimens, except that the conventional yield point is higher for the aged specimens. Increasing the aging time lowers the yield point and restores ductility (curve *e*). At later aging stages, the yield peak vanishes and plasticity is fully restored (curve *f*).

Yield point is expressed as a function of deformation-speed logarithm by a straight line within the deformation-speed range studied (Fig. 97). The ultimate strength and elongation also depend substantially on rate of deformation. Annealing has no influence on the level of the yield point. Quenching in water raises the yield point by approximately 35 Mn/m^2. At all aging temperatures, the yield point first rises to 420 Mn/m^2 with in-

creasing aging time and then decreases to the figure characteristic for the annealed metal (Fig. 98). The yield-point maximum is attained the more rapidly the higher the temperature.

The logarithm of the aging time at which the maximum yield point is reached is a linear function of the inverse absolute temperature, and the activation energy of the aging process can be found from the slope of the line. This energy is found to be 9.5 kcal/g-atom (40 kj/g-atom).

At a given aging time, the yield point depends linearly on the logarithm of deformation speed. This relation is illustrated by Fig. 97, which presents data for molybdenum that was quenched in water and aged 36 hours at 298°K. Completely brittle failure is not observed after aging under any set of conditions; appreciable plastic deformation preceded failure in all cases. A region of relative brittleness corresponds to aging in a certain range of holding times. Failure of the specimens is plastic for short or long aging. In relatively brittle failures, the ultimate strength and yield point practically coincide, while in plastic failure the yield point is quite far below the ultimate strength.

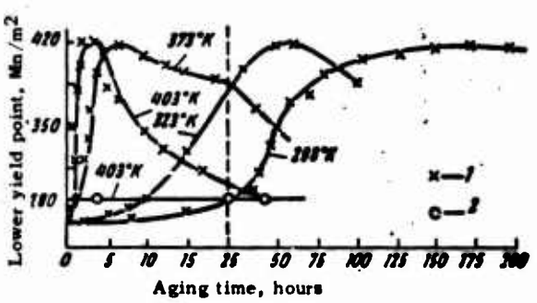

Fig. 98. Yield point of molybdenum as a function of aging time at various temperatures. Deformation speed $1.1 \cdot 10^{-4}$ sec^{-1}. 1) Mo + + H_2; 2) Mo annealed in vacuum.

The results obtained for specimens that had been hardened in hydrogen and aged under the same conditions were similar, except that the yield points were lower. Such changes were not observed on aging in the vacuum-hardened specimens.

Analysis of the experimental data obtained in the study led the author to the conclusion that the changes in properties that take place on aging are governed by interstitial introduction of hydrogen into the molybdenum lattice during hardening and its redistribution during aging. Immediately after hardening, the hydrogen is distributed statistically, while during aging it diffuses to dislocations, forming Cottrell atmospheres on them, to grain boundaries, and to other interfaces.

The time τ necessary for formation of sufficient dense Cottrell atmospheres can be evaluated from

$$\tau = \frac{1}{2D\rho},$$

where ρ is the dislocation density; D is the diffusion coefficient of the impurity atoms.

Hill gives the following equation for the coefficient of diffusion of hydrogen in molybdenum at 848-1253°K:

$$D = 0{,}059e^{-\frac{14700}{RT}}.$$

If we assume that this equation applies for the temperature range studied and $\rho = 10^6$ cm^{-2}, we obtain 108 and 0.25 hours, respectively, for temperatures of 298 and 403°K. These values agree satisfactorily with the aging times at which the yield-point maximum is reached (about 100 and 2 hours, respectively). The activation energy of the aging process coincides quite closely with that for diffusion of hydrogen in molybdenum. Thus, hydrogen in molybdenum forms impurity atmospheres on dislocations, and these atmospheres increase the resistance to plastic deformation. At a high enough deformation speed, the dislocations are torn out of the hydrogen atmospheres surrounding them, producing the yield peak. However, this peak is not sharp. It may be assumed on this basis that the dislocations are not entirely freed of their hydrogen atmospheres in molybdenum; they trail the dislocations, lagging a certain distance behind them and thus retarding their motion. This assumption by the authors of the study under consideration is consistent with the dislocation mechanism of hydrogen brittleness set forth above. The drop in yield point on prolonged aging is apparently due to desorption of hydrogen from the molybdenum.

Although hydrogen is absorbed by tungsten in negligibly small quantities, it also lowers its plasticity by the Rebinder effect.

Chapter 7

NICKEL, PALLADIUM AND PLATINUM

1. INTERACTION OF NICKEL, PALLADIUM AND PLATINUM WITH HYDROGEN

All of the metals considered in this chapter react quite vigorously with hydrogen. Nickel adsorbs hydrogen readily at low temperatures. As the temperature rises, the amount of adsorbed hydrogen decreases, and physical adsorption virtually disappears above 373°K. Absorption of hydrogen by nickel begins at temperatures around 473°K. The Sieverts law is observed at pressures above 100 mm Hg (0.013 Mn/m^2). The solubility of hydrogen in nickel increases with increasing temperature (see Fig. 1).

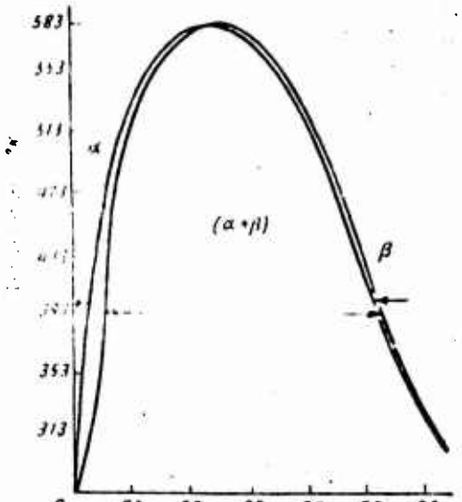

Fig. 99. Phase diagram of palladium-hydrogen system.

The amount of hydrogen absorbed by nickel may vary as a function of the state of the metal and the method of saturation (from 0.2 volume of hydrogen to one volume of metal for cast nickel to 200 volumes for nickel reduced from the oxides).

According to [394], the solubility of hydrogen in nickel of 99.5% purity at temperatures from 673 to 873°K and low pressures may be described by the equation

$$\lg C = 1{,}732 + 0{,}5 \lg p - \frac{645}{T}.$$

The heat of solution of hydrogen in nickel is 5.9 kcal/g-atom (24.7 kj/g-atom) [394] and 3.5 kcal/g-atom (14.5 kj/g-atom) according to Sieverts.

In molten nickel, the solubility of hydrogen rises from 40.6 cm^3/100 g at 1728°K to 48.6 cm^3/100 g at 1963°K. The heat of solution is 4.8 kcal/g-atom (20 kj/g-atom) [52].

Hydrogen that has been introduced into nickel electrolytically is quite easily removed from it. At room temperature in air, a considerable part of the hydrogen has been removed after 60-70 hours. Nickel hydrides can be obtained easily by indirect methods [5]. It is shown in [396] that nickel hydride is formed along grain boundaries when the metal is electrolytically saturated with hydrogen.

The palladium-hydrogen system is one of the most thoroughly studied. Palladium interacts vigorously with hydrogen. At low temperatures, it adsorbs hydrogen readily, and enormous quantities are absorbed at room temperature (more than 1000 volumes of hydrogen to a volume of the metal). The amount of hydrogen absorbed by palladium drops sharply with increasing temperature (see Fig. 2). Absorption of hydrogen by palladium is accompanied by evolution of 4.2 kcal/g-atom of heat (17.5 kj/g-atom). Hydrogen is driven out of the palladium by heating in vacuum. Heating to temperatures of the order of 573°K is sufficient for quite complete elimination of hydrogen from palladium.

The amount of hydrogen absorbed is proportional to the square root of pressure only at temperatures above 873°K. At lower temperatures, the absorption isotherm has three branches, indicating the existence of three phase regions in this system: α, $\alpha + \beta$ and β. The existence of these phase regions has been confirmed by x-ray structural analysis methods [398, 399]. The diagram of state of the palladium-hydrogen system constructed on the basis of these data appears in Fig. 99. Both phases of this system have face-centered cubic lattices whose constants depend on the composition of the phases.

On cathodic polarization, palladium is readily saturated to concentrations corresponding to the formulas Pd_2H, PdH and even $PdH_{2.2}$. The hydrogen occupies octahedral spaces in the face-centered lattice of palladium.

Platinum also absorbs hydrogen very actively. However, the solubility of hydrogen in platinum is moderate (0.067 cm^3/100 g at 682°K and 0.93 cm^3/100 g at 1615°K). Platinum also dissolves hydrogen in the molten state. Absorption of hydrogen by platinum is described satisfactorily by the Sieverts law. A distinctive property of this system is the high permeability of platinum for hydrogen. Unlike compact platinum, platinum black and platinum sponge absorb large quantities of hydrogen, basically, it appears, due to physical surface absorption. Platinum does not form hydrides with hydrogen.

2. INFLUENCE OF HYDROGEN ON THE PROPERTIES OF NICKEL, PALLADIUM AND PLATINUM

As we noted above, hydrogen forms hydrides and solid solutions with nickel. We may therefore expect hydride brittleness and reversible brittleness to develop in nickel, the latter coming into evidence at low deformation speeds.

It has in fact been observed [396] that when hydrides form on the surfaces of specimens during electrolytic hydrogenation, the specimens show brittle fracture. This is explained by the instability of the nickel hydrides and their decomposition into nickel and hydrogen. Since nickel hydride is formed preferentially along grain boundaries, its decomposition results in formation of cracks along the grain boundaries due to the high pressures developed.

At higher oxygen contents, nickel is inclined to hydrogen embrittlement [400, 401]. It is reported in [400] that annealing nickel specimens with 0.024% O_2 in a hydrogen atmosphere at 1073-1173°K causes severe embrittlement of the specimens. At the same time, similar annealing of nickel with 0.004% (by mass) of O_2 causes no appreciable change in its mechanical properties.

It is indicated in [403] that hydrogen brittleness in nickel may be due to molecular hydrogen. The work was done on nickel containing less than 0.0004% (by mass) of O_2. The nickel was treated with hydrogen at 873°K under pressures of 0.1, 70 and 100 Mn/m^2. Some of the specimens were tensile-tested at room temperature immediately after hydrogen saturation, and the others after vacuum annealing at 923°K.

The results obtained in this study indicated that annealing in hydrogen at 873°K at 0.1 Mn/m^2 for 250 hours does not produce brittleness. At a pressure of 70 Mn/m^2, hydrogen causes a sharp plasticity loss after as little as one hour of holding at 873°K. Subsequent heating in a vacuum at 923°K restores plasticity.

Microscopic studies have shown that although no visible changes can be detected in grain-boundary structure after prolonged treatment with hydrogen at pressures of 0.1 and 70 Mn/m^2, the specimens do fail along grain boundaries. After exposure to hydrogen under a pressure of 100 Mn/m^2 for 125 hours, disintegration is observed along grain boundaries.

Thus, reversible changes take place in the structure of nickel at moderate pressures and irreversible changes when the pressure is high enough. In either case, however, the brittleness is due to the high hydrogen pressure in pores.

The authors of the paper make reference to the uniqueness of these results. Brittleness due to prolonged treatment of hydrogen at high pressure and elevated temperatures is also observed in steels. In steels, this effect is associated with the formation of methane along grain boundaries. Such a reaction is excluded in nickel. Thus, it was first shown in [403] that the pressure in the pores due to hydrogen alone causes failure along grain bound-

aries without the application of tensile stresses.

The most convincing data on the tendency of nickel to hydrogen brittleness at low deformation speeds were obtained by Troiano et al. [75, 95, 274]. The study was made on specimens that had been saturated with hydrogen electrolytically in a 2n aqueous solution of H_2SO_4 doped with 250 mg of As per liter in the form of sodium arsenide. Smooth specimens were saturated at a current density of 3.4 amp/cm^2, and notched ones at 1.9 amp/cm^2. To prevent losses of hydrogen from the specimens, they were cadmium-plated immediately after saturation.

Mechanical tensile tests carried out on a hydraulic machine indicated that the plasticity of nickel and nickel alloys that have been electrolytically saturated with hydrogen decreases with decreasing deformation speed, while the plasticity of unhydrogenated specimens rises by a small margin. Figure 100 shows, by way of example, the influence of deformation speed on necking in nickel and an alloy of nickel with 28% Fe at room temperature. As in other metals, this brittleness manifests in a certain temperature range. At a deformation speed of 1.25 mm/min, this range extends from 83 to 533°K, with the plasticity minimum observed at 477°K.

It was shown in the same study that hydrogen has no influence on the ultimate strength of nickel and nickel alloys in tests on smooth specimens, but if the tests are conducted on notched specimens, the ultimate strength increases with increasing hydrogen content, passes through a maximum, and then diminishes. It was observed that the tendency of nickel to hydrogen brittleness decreases with increasing chromium and iron content.

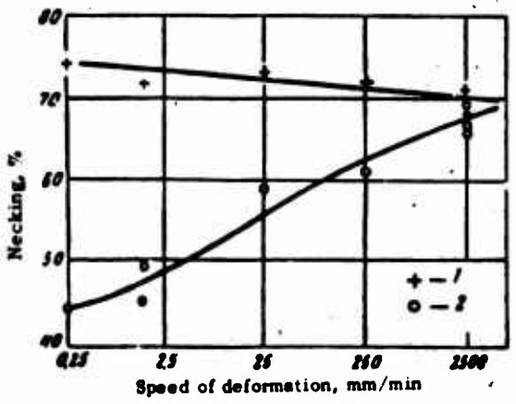

Fig. 100. Influence of deformation speed on necking in nickel. 1) Without hydrogen; 2) hydrogenated.

A later detailed investigation of hydrogen brittleness in nickel was made by Boniszewski and Smith [102], who investigated highly purified nickel containing less than 0.001% of impurities. The studies were made on sheet specimens that were annealed after

fabrication in an atmosphere of dry hydrogen for 1 hour at 873°K. The nickel took up practically no hydrogen in this annealing; hydrogen was injected into the specimens electrolytically. The specimens were electrolytically polished before cathodic hydrogenation, leaving a thickness of 0.2 mm. The conditions and composition of the bath were adjusted so that no nickel hydride would form on the specimen surfaces.

Hydrogenation was carried out in 1n H_2SO_4 solution prepared from analytically pure acid and distilled water of high purity, at temperatures of 364-367°K and a current density of 50 ma/cm^2. The anode was a platinum spiral. The authors place special emphasis on the need to have the saturating equipment in a clean atmosphere; dust and gases from volatile laboratory materials contaminate the bath and nickel hydrides appear on the surfaces of the specimens. If etching is carried out properly and the above precautions are taken, the metal does not crack during hydrogenation, as verified by mechanical tests of the specimens after degasification.

The hydrogen was distributed nonuniformly over the cross-sections of the specimens, but the concentration gradient was small. Actually, cracks were germinated inside the specimen, and not on its surface, in all of the tensile tests.

The mechanical tensile tests were carried out on an Instron machine in the temperature range from 77 to 293°K at deformation speeds from $3.33 \cdot 10^{-4}$ to $8.33 \cdot 10^{-1}$ sec^{-1}. Ultimate strength is independent of hydrogen content, but the true breaking stresses undoubtedly decrease with increasing hydrogen content, since the necking of the hydrogenated specimens was considerably less than that of the hydrogen-free specimens. It was also observed in the investigations of Boniszewski and Smith that the ductility of hydrogen-saturated nickel decreases with diminishing deformation speed.

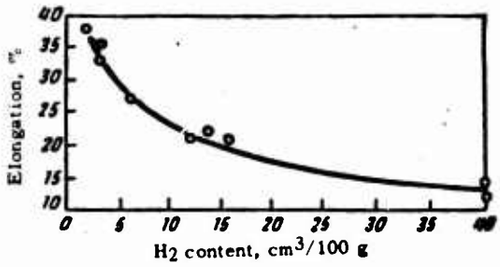

Fig. 101. Influence of hydrogen content on relative elongation of nickel.

At all deformation speeds, hydrogen-free nickel specimens show ductile failure with formation of a neck, which degenerates into two converging wedges at the moment of failure. Hydrogenated specimens have brittle failure at slow deformation speeds, with the fracture surface passing along grain boundaries. The higher the deformation speed, the greater the permanence of viscous fail-

ure, but wedge failure is not observed even at the highest speed studied (0.833 sec^{-1}). In hydrogenated specimens, in addition to the basic crack leading to failure, we observe secondary cracks that appear after 10% elongation.

Figure 21 (see page 62) illustrates the influence of test temperature on the elongation of nickel containing 40 $cm^3/100$ g of H_2 at two stretching speeds. At very low temperatures (below 143°K), hydrogen-saturated specimens show ductile failure, but at higher temperatures hydrogen brittleness develops. As follows from dislocation theory, the hydrogen brittleness is less strongly in evidence at a deformation speed of $1.67 \cdot 10^{-3}$ sec^{-1} than at $3.33 \cdot 10^{-4}$ sec^{-2} [sic]. The greatest brittleness is observed at temperatures from 193 to 223°K.

Figure 101 illustrates the influence of hydrogen on the elongation of nickel under the mechanical testing conditions described above. As follows from these data, hydrogen brittleness disappears completely only at low hydrogen concentrations, of the order of 1.7 $cm^3/100$ g [0.01% (atomic)].

It was reported in [75] that nickel and monel metal are inclined to static hydrogen embrittlement. This phenomenon was observed at temperatures of 450-533°K in a rather broad range of stresses. This embrittlement is quite similar to that observed in steel. However, due to the low mobility of hydrogen in metals with the face-centered lattice, delayed failure is observed at temperatures above room level.

The variation of resistivity in the tension process indicated that there is no incubation period for crack formation. This is due to the nonuniform distribution of hydrogen in the metal. As in steels, the crack develops intermittently, with periods of almost instantaneous growth alternating with total cessation of crack development.

The influence of hydrogen on the mechanical properties of palladium and platinum has been studied much less thoroughly. Saturation of palladium with hydrogen increases hardness and lowers all of the other mechanical properties in tensile tests. It is reported in [154] that prolonged hydrogen treatment of platinum lowers its ductility.

Chapter 8

COPPER, SILVER AND GOLD

1. INTERACTION OF COPPER, SILVER AND GOLD WITH HYDROGEN

At low temperatures, copper adsorbs hydrogen by physical adsorption and chemosorption. As the temperature rises, the amount of hydrogen adsorbed by copper decreases. At elevated temperatures, copper absorbs hydrogen. Depending on the degree of dispersion and the preparation of the copper, it absorbs from 0.3 to 5.6 $cm^3/100$ g [4, 5] at room temperature. The solubility of hydrogen in copper increases with increasing temperature (see Fig. 1). In the molten metal, the solubility of hydrogen rises from 5.6 $cm^3/100$ g at 1373°K to 9.0 $cm^3/100$ g at 1573°K [52].

The solubility of hydrogen in copper rises substantially on transition from the solid to the liquid state. In an atmosphere of dry hydrogen, solid copper dissolves 0.00018% (by mass) of H_2 at temperatures near the melting point, but 0.00054% in the molten state [423]. The solubility of hydrogen in copper is subject to the Sieverts law. Data on the possibility of copper-hydride formation on direct reaction of the metal with hydrogen are contradictory. Copper hydride can be obtained comparatively easily by indirect methods.

Silver does not adsorb hydrogen; it also absorbs only small amounts [4] (0.006 $cm^3/100$ g at 673°K and 0.046 $cm^3/100$ g at 1173°K). The solubility of hydrogen in solid silver is proportional to the square root of pressure. The lattice parameters of silver do not change when hydrogen dissolves in it.

Gold does not adsorb hydrogen, either at room or at subzero temperatures. Sieverts states that gold dissolves practically no hydrogen up to 1573°K. However, N.A. Galaktionova [4] cites data of Trowbridge according to which molten gold can dissolve from 37 to 46 volumes of hydrogen per volume of metal.

No experimental data are available for gold and silver that would definitely establish the existence of their hydrides.

2. INFLUENCE OF HYDROGEN ON THE PROPERTIES OF COPPER, SILVER AND GOLD

Since hydrides are not formed in these metals in a direct reaction with hydrogen, the development of hydride brittleness is excluded.

The most important effect of hydrogen on the properties of copper and silver consists in gas porosity in castings and hydrogen embrittlement. In gold, due to the negligibly low solubility of hydrogen, these phenomena apparently do not occur.

In copper, hydrogen causes porosity in ingots [283]. Comparatively coarse pores, distended in the direction toward the center of the ingot, are formed by hydrogen directly, while fine scattered porosity uniformly distributed through the entire volume is due to the combined action of oxygen and hydrogen. As the metal freezes, these gases react with one another to form water vapor. This vapor cannot diffuse out of the interior of the metal and therefore causes porosity in the ingot. It is reported in [283] that 0.0001% (by mass) of H_2 (1 cm^3/100 g) reacts with oxygen to form an amount of water vapor such that the porosity in the ingot represents 44% of its volume.

The most dangerous form of hydrogen brittleness in copper is hydrogen embrittlement [211, 263, 296, 349]. It is observed when the metal contains cuprous oxide. It is therefore assumed that the reaction $Cu_2O + H_2 \rightarrow 2Cu + H_2O$ takes place at high temperature. It follows from this reaction that 1 gram-molecule of cupric [sic] oxide (143.14 g), which has a density of about 6.2 g and occupies a volume of 23.1 cm^3, should be converted to 127 g of copper with a density of 8.96 g/cm^3 (the volume of this copper is 14.2 cm^3) and 18 g of water vapor. Thus, 18 g of water vapor must be accommodated in a volume smaller than 9 cm^3, giving rise to a high water-vapor pressure in cavities and cracks. Under high pressure, the water vapor causes products to decrepitate and blister.

The temperature and pressure of the water vapor may be such that partial condensation begins. Baker [425] refers to three typical conditions that may prevail in cavities:

1. The amount of water may be such that it is vaporized completely at a temperature below the critical point when the copper is heated. In this case there will be no sharp increase in pressure with rising temperature.

2. The amount of water may be such that as the temperature rises, the decrease in the density of the water and increase in the water-vapor density bring about a critical state at a certain temperature. In this case, the water-vapor pressure in the cavities will also rise continuously with rising temperature.

3. The amount of water may be larger than that necessary to create critical conditions. In this case, the water occupies the entire volume of the cavity before the critical temperature is reached. Since water is practically incompressible, a further increase in temperature causes a sharp rise in the pressure in the cavities.

To temperatures below the critical point (647°K), the embrittlement of copper should be less sharply evident than at higher temperatures, and this is confirmed experimentally. Harper et al. [420, 421] do not agree with Bekker [sic]. They indicate that the water-vapor pressure in cavities cannot reach the critical point

under real conditions.

It was observed in [420, 421] that two processes take place when copper is annealed in a hydrogen atmosphere: formation of water vapor and deoxidation. At both low and high temperatures, total deoxidation takes place more rapidly than intergranular failure along grain boundaries due to formation of water vapor. Thus the brittleness of copper is observed in a definite temperature range.

Ashton heated annealed copper wire 0.85 mm in diameter in a hydrogen atmosphere at 1123°K for various times and then tensile-tested them at room temperature to obtain the following results:

Annealing time, minutes	Initial state	1	5	10	20	60
Terminal elongation, %	32	6	6	10	10	12

His data indicate that copper embrittles in short-term annealing, but that increasing the annealing time restores ductility. This justifies the conclusion that some mechanism operates during annealing to permit slow healing of pores and cracks.

The investigations of Teppl [sic] indicated that neither the content of oxygen nor its physical state in the copper is a decisive factor determining the embrittlement of copper during annealing. The conditions of development of hydrogen brittleness are determined primarily by the specimen holding time and temperature and the hydrogen concentration in the atmosphere.

Above 973°K, hydrogen penetrates into the specimens and heating for half an hour is sufficient, even with a content of 0.5% H_2 in the atmosphere, to produce visible defects on the sheet surfaces. As the temperature is lowered, the maximum permissible hydrogen content – that which does not produce rejects during annealing – increases, and at ordinary copper-annealing temperatures (673-773°K), a 10% H_2 content in the atmosphere is not detrimental to the surface quality of sheets or their properties, even after holding for two hours.

The studies showed that up to temperatures of the order of 873°K, the presence of water vapor aggravates embrittlement of copper, while the reverse picture is observed at higher temperatures.

In [349], it is stated on the basis of thermodynamic analysis of the reaction $Cu_2O + H_2 \rightarrow 2Cu + H_2O$ that this reaction cannot take place in solid copper. Hence the author assumes that the decrepitation of copper as a result of injection of hydrogen into it is due to large internal stresses.

In the same study, ingots intended for the fabrication of wire and containing 0.018% O_2 were held at 1123°K in a hydrogen flame for 1.5 hours. After the first few hot-rolling passes, a large number of macroscopic cracks appeared on the ingot. However, despite these cracks from the early stages of hot rolling, rods could be cold-rolled to a diameter of 5 mm. Wire obtained in this

way was of better quality than might have been expected if hydrogen embrittlement had developed sufficiently. Defects were observed on the surface of the wire, but they did not propagate along its entire length.

The failure mechanism of copper after treatment in a hydrogen atmosphere was studied in [469]. The investigations were made on copper containing 0.04% of impurities (0.0003% O_2). The specimens were annealed in atmospheres of hydrogen and dry nitrogen and in a vacuum. Hydrogen annealing was carried out at 973°K for 3 hours. Tensile tests were performed on a Baldwin and Southwork [sic] machine at room temperature with the crossbar moving at 2.54 mm/min.

One of the specimens that had been treated in hydrogen was stretched to failure; stretching of the other specimens was terminated at various stages in the development of the neck, corresponding to cross-sectional area reductions of 63.5, 74.5 and 80.4%. The specimens were then cut along the axis and their microstructure studied in the longitudinal section.

These investigations showed that copper fails as a result of the appearance of cavities in the metal; they grow with increasing applied stresses until they have merged into a germinating crack. The crack propagates in a zigzag fashion until the cross section of the specimen has been weakened to the point that the top separates from the bottom along a conical surface.

As a rule, the cavities in hydrogen-treated copper are germinated at the point of intersection of three or two grains or at a twin that has formed during annealing. The number of cavities increases sharply as the neck develops. While the number of cavities ranges from one per 1 mm^2 at the moment of necking, it runs into the hundreds per 1 mm^2 by the time of failure, i.e., the number of cavities in the volume of the metal has increased a thousandfold. Numerous cavities appear along grain boundaries parallel to the tension axis.

During creep, cavities appear, as a rule, at boundaries perpendicular to the tension axis. At the time of necking, the dimensions of the cavities are of the order of 1-2 μ, but they gradually approach 10-20 μ.

In specimens that have been annealed in dry nitrogen and in hydrogen, the cavities are germinated not along grain boundaries, but inside the grain; nevertheless, the total number of cavities at corresponding stages in tension is only slightly smaller than in specimens that were annealed in hydrogen. In unhydrogenated specimens, cavities appear as a result of the effort of the metal to relieve stresses where the strain nonuniformity is greatest. Since the number and volume of the pores are almost the same in hydrogenated and unhydrogenated specimens, it may be assumed that the energies of their formation at grain boundaries in the former case and inside the grain in the latter are quite similar.

It is reported in [403] that the hydrogen brittleness of copper, like that of nickel, may be due to a high molecular-hydrogen

pressure in the pores. A study was made of copper containing 0.02-0.03% O_2. The copper specimens were held in hydrogen at 873°K under pressures of 0.1 and 70 Mn/m^2 for various times, after which they were tensile-tested at room temperature. Some of the specimens were annealed in a vacuum at 923°K after hydrogenation, in order to eliminate the hydrogen. The results obtained in this study indicate that prolonged action of molecular hydrogen under high pressure leads to brittleness in copper. In contrast to nickel, irreversible structural changes take place in copper at a hydrogen pressure of 70 Mn/m^2, and vacuum annealing does not restore its plasticity. Microstructural analysis showed that hydrogen treatment at a pressure of 70 Mn/m^2 causes disintegration along grain boundaries; this weakens the cohesive forces between grains and results in brittle intergranular failure when the specimens are stretched.

The high sensitivity of copper to brittle failure under these conditions as compared with nickel is apparently due to differing degrees of purity of the metals. The copper contained a large quantity of oxygen, and it is possible here that a water-vapor pressure was added to the hydrogen pressure in the pores.

It was found in [415] that a distinct plasticity trough is observed in oxygen-free copper in the 773-973°K temperature range. The author explains this trough by fixation of supersaturated hydrogen solutions in copper and their decay on heating above 773°K with formation of molecular hydrogen. This hydrogen is accumulated in various types of cavities, chiefly along grain boundaries, where the pressure rises to contribute to brittle failure.

After vacuum annealing, in which hydrogen is efficiently removed, the plasticity trough is less distinct and has been shifted toward lower temperatures.

The influence of hydrogen on the properties of silver and gold has not been as thoroughly studied. It is reported in [53, 426] that hydrogen embrittlement may develop in silver. After annealing in a hydrogen atmosphere at temperatures above 773°K, silver becomes brittle and blisters appear on its surface in some cases. Brittleness is also detected when hydrogenated silver specimens are heated in an air atmosphere.

REFERENCES

1. Smittel's, K., Gazy i metally [Gases and Metals]. Metallurgizdat, Moscow-Leningrad, 1940.

2. Smith, D.P., Hydrogen in Metals, Chicago-Illinois, 1948.

3. Kherd, D., Vvedeniye v khimiyu gidridov [Introduction to Hydride Chemistry]. IL, 1953.

4. Galaktionova, N.A., Vodorod v metallakh [Hydrogen in Metals]. Metallurgizdat, 1959.

5. Mikheyeva, V.I., Gidridy perekhodnykh metallov [Hydrides of Transition Metals]. Izd. AN SSSR, 1960.

6. Smialowski, M., Hydrogen in Steel, Oxford, London, Warsaw, 1962.

7. Livanov, V.A., Bukhanova, A.A., Kolachev, B.A., Vodorod v titane [Hydrogen in Titanium]. Metallurgizdat, 1962.

8. Karpenko, G.V., Kripyakevich, R.I., Vliyaniye vodoroda na svoystva stali [Influence of Hydrogen on the Properties of Steel]. Metallurgizdat, 1962.

9. Kotterill, P., Vodorodnaya khrupkost' metallov [Hydrogen Brittleness of Metals]. Metallurgizdat, 1963.

10. Yavoyskiy, V.N., Batalin, G.N., Trudy nauchno-tekhnicheskogo obshchestva chernoy metallurgii [Transactions of the Ferrous Metallurgy Scientific-Technical Society]. Vol. IV, Metallurgizdat, 1955.

11. Wagner, Heller, Z. phys. Chem., B., 1940, 46, No. 4, page 242.

12. Hill, M.L., Hydrogen Embrittlement in Metal Finishing, Reinhold Publishing Corporation N.Y., London, 1962, pages 72-92.

13. Fedorov, S.N., Kunin, L.L., Sachkova, L.M., Trudy komissii po analiticheskoy khimii [Transactions of the Commission on Analytical Chemistry]. Izd. AN SSSR, 1960, 10, pages 46-48.

14. Lakomskiy, V.I., Avtomaticheskaya svarka [Automatic Welding], 1962, No. 7, pages 50-57.

15. Krasnikov, I.A., ZhETF, 1939, 9, No. 10, pages 1194-1203.

16. Krasnikov, I.A., Izv. AN SSSR, OTN, 1946, No. 1, pages 133-140.

17. Eichenauer, W., Hattenbach, K., Pebler, A., Z. Metallkunde, 1961, Vol. 52, No. 10, pages 682-684.

18. Yavoyskiy, V.N., Batalin, G.I., Stal', 1954, No. 6, pages 487-494.

19. Yavoyskiy, V.N., Chernegi, D.F., Stal', 1956, No. 9, pages 790-793.

20. Kohen, A., Specht, W., Z. Physik, 1930, 62, No. 1-2, pages 1-31.

21. Svenson, B., Ann. Phys., 1933, 18, No. 5, pages 299-302.

22. Wucher, G., Compt. rend., 1949, 229, pages 175-177.

23. Bastien, P.G., Phys. Met. of Stress Corrosion Fracture AIME Symposium, 1959, Interscience Publishers, N.Y.

24. Klyachko, Yu.A., Izmanova, T.A., Kunin, L.L., Khimicheskaya nauka i promyshlennost', 1958, No. 1, page 127.

25. Rudee, M.L., Huggins, R.A., Phys. status Solidi, 1964, 4, No. 3, pages K101-K103.

26. Alov, A.A., Voprosy teorii svarochnykh protsessov [Problems of the Theory of Welding Processes]. Mashgiz, 1959.

27. Cottrell, A.H. and Bilby, B.A., Proc. Phys. Soc., 1949, 62A, No. 1, pages 49-62.

28. Alov, A.A., Osnovy teorii protsessov svarki i payki [Fundamentals of the Theory of Welding and Soldering Processes]. Mashinostroyeniye, 1964.

29. Alov, A.A., Bobrov, G.V., Shmakov, V.M., Svarochnoye proizvodstvo, 1961, No. 3, pages 9-10.

30. Van Byuren, Defekty v kristallakh [Defects in Crystals]. IL, 1962.

31. Cottrell, A.H., Hunter, S.C., Nabarro, F.R.N., Phil. Mag., 1953, 44, page 1063.

32. Suzuki, H., Rep. Tohoku Univ. Res. Inst., 1952, A4, page 455.

33. Snoek, J.L., Physika, 1941, 8, page 711.

34. Grdina, Yu.V., Izvestiya vuzov. Chernaya metallurgiya, 1959, No. 5, pages 69-72.

35. Weiner, L.C., Gensamer, M., Acta Metall., 1957, 5, No. 12, pages 692-694.

36. Rogers, H.C., Trans. Met. Soc. AIME, 1959, 215, page 666.

37. Rogers, H.C., Acta Metall., 1954, 2, No. 1, page 167.

38. Heller, W.R., Stress Corrosion Cracking and Embrittlement. J. Wiley and Sons, N.Y., 1956, pages 163-175.

39. Baranov, S.M., Collection "Metallovedeniye i termoobrabotka" [Physical Metallurgy and Heat Treatment]. Mashgiz, 1961, pages 138-145.

40. Braun, M.P., Krukovskaya, G.N., Collection "Struktura i svoystva litykh splavov" [Structure and Properties of Cast Alloys], No. 1, Izd. AN USSR, 1962, pages 82-94.

41. Werner, J.E., Davis, H.M., Trans. Am. Soc. Metals, 1961, 53, pages 853-869.

42. Heller, W.R., Acta Metall., 1961, 9, pages 600-613.

43. Glikman, L.A., Kolgatin, N.N., Teodorovich, A.P., Deryabina, V.I., Metallovedeniye [Physical Metallurgy]. Sudpromgiz, 1959, No. 3, pages 58-73.

44. Troiano, A.R., Metal Prog., 1960, 77, No. 2, pages 112-117.

45. Moroz, L.S., Chechulin, B.B., Polin, I.V., et al., Titan i yego splavy [Titanium and its Alloys]. Sudpromgiz, 1960.

46. Lushkov, N.L., Razduy, F.I., Shleyzman, V.M., Vodorod v svarnykh shvakh i bor'ba s nim [Hydrogen in Weld Seams and Countermeasures Against it]. Sudpromgiz, 1959.

47. Gurevich, S.M., Mishchenko, S.V., Avtomaticheskaya svarka, 1956, No. 5, pages 1-12.

48. Shorshorov, M.Kh., Povorov, G.V., Amfiteatrova, T.A., Svarochnoye proizvodstvo, 1957, No. 4, pages 1-5.

49. Kavasima, Namiko, Jamada et al., Light Metals (Japanese), 1964, 14, pages 231-238.

50. Haynes, R., J. Inst. Metals, 1960, 88, No. 12, pages 509-512.

51. Zakharova, G.V., Zhorova, L.P., Tsvetnyye metally, 1963, No. 5, pages 53-58.

52. Weinstein, M., Elliott, J.F., Trans. Metall. Soc. AIME, 1963, 227, pages 285-286.

53. Hondros, E.D., J. Inst. Metals, 1960, 88, No. 6, pages 275-276.

54. Bradford, S.A., Carlson, O.N., Trans. Metall. Soc. AIME, 1962, 224, No. 8, pages 738-741.

55. Wasilewski, R.J., Kehl, G.L., Metallurgia, 1954, XI, 50, No. 301, pages 225-230.

56. Someno, M., Nagasaki, K., Sinku Kagaku, Vacuum chem., 1960, 8, No. 4, pages 145-148.

57. Eichenauer, Met. Sci. Rev. Met., 1960, 57, 409.

58. Lieser, K.H., Witte, H., Z. phys. Chem., 1954, 202, page 321.

59. Someno, M., Nippon Kinzoku Gakkaisku, 1960, 24, page 249.

60. Geleznuas, V.L., Cohn, P.K., Prill, R.H., J. Electrochem. Soc., 1963, 110, No. 7, pages 799-804.

61. Moroz, L.S., Khesin, Yu.D., Izv. AN SSSR, OTN, 1960, No. 1, 111-122.

62. Stroh, A.N., Advances in Phys., 1957, 6, page 418.

63. Stroh, A.N., Proc. Roy. Soc., 1955, 231A, page 548.

64. Klyachko, Yu.A., Legkiye metally [Light Metals], 1934, No. 7, pages 24-30.

65. Klyachko, Yu.A., Izmaylova, F.A., Stal', 1957, No. 6, pages 507-511.

66. Klyachko, Yu.A., Larina, O.D., Stal', 1961, No. 7, pages 604-607.

67. Ryabov, R.A., Gel'd, P.V., Gol'tsov, V.A., Izvestiya vuzov, Chernaya metallurgiya, 1963, No. 4, pages 98-102.

68. Lenning, G.A., Craighead, C.M., Jaffee, R.I., J. Metals, 1954, 6, No. 3, page 367.

69. Mallett, M.W., Albrecht, W.H., J. Electrochem. Soc., 1957, 104, No. 3, pages 142-146.

70. Gulbransen, E.A., Andrew, K.F., J. Metals, 1955, 7, No. 1, pages 136-144.

71. Mallett, M.W., Trzeciak, M.J., Trans. Am. Soc. Metals, 50, pr. No. 36.

72. Liu, T.S., Steinberg, M.A., Trans. Am. Soc. Metals, 1958, 50, pages 455-477.

73. Livanov, V.A., Bukhanova, A.A., Kolachev, B.A., Trudy MATI [Transactions of the Moscow Aviation Engineering Institute], 1961, No. 50, pages 61-70.

74. Haynes, R., J. Inst. Metals, 1961, 90, No. 3, pages 80-87.

75. Mihelich, J.L., Troiano, A.K., Nature, 1963, 197, No. 4871, pages 996-997.

76. Borelius, G., Lindblom, J. Ann. Phys., 1927, 82, page 201.

77. Hendricks, C.B., Ralston, R.R., J. Am. Chem. Soc., 1929, 51, No. 11, page 3278.

78. Ham, W.R., J. Chem. Phys., 1933, 1, page 476.

79. Euringer, G., Z. Phys., 1935, 96, No. 1-2, page 37.

80. Smithells, C.J., Ransley, C.E., Proc. Roy. Soc., 1936, A157, page 292.

81. Gubanov, A.I., FTT, 1964, 6, No. 4, pages 1023-1029.

82. Hill, M.L., Johson, E.W., Acta Metall., 1955, 3, page 566.

83. Ransley, C.E., Talbot, D.E.J., Z. Metallkunde, 1955, 46, page 328.

84. Edwards, A.G., Brit. J. Appl. Phys., 1957, 8, page 406.

85. Grimes, H.H., Acta Metall., 1959, 7, No. 12, pages 782-786.

86. Eichenauer, W., Pebler, A., Z. Metallkunde, 1957, 48, page 373.

87. Moroz, L.S., Khesin, Yu.D., Mingin, T.E., Chernetsov, V.I., Collection "Metallovedeniye" [Physical Metallurgy]. Sudpromgiz, 1957, page 175.

88. Barnett, W.J., Troiano, A.R., J. Metals, 1957, 9, No. 2; (11), pages 486-494.

89. Scott, T.E., Troiano, A.R., Nature, 1960, 185, No. 4710, pages 372-373.

90. Troiano, A.R., Corrosion, 1959, 15, No. 4, pages 2071-2127.

91. Potak, Ya.M., Breslavtseva, O.P., Survey entitled "Nekotoryye problemy prochnosti tverdogo tela" [Certain Problems in the Strength of Solids]. AN SSSR, 1959, pages 152-164.

92. Rostoker, W., Steel, 1956, 139, No. 20, pages 138-144.

93. Bastein, P., Amiot, P., Compt. Rend., 1955, 211, No. 24, pages 1760-1762.

94. Frohmberg, R.D., Barnett, W.J., Troiano, A.R., Trans. Am. Soc. Metals, 1955, 47, pages 892-925.

95. Blanchard, P., Troiano, A.R., Mem. Sci. Rev. met., 1960, 57, pages 409-422.

96. Potak. Ya.M., Khrupkiye razrusheniya stali i stal'nykh detaley [Brittle Failure of Steel and Steel Parts]. Oborongiz, 1955.

97. Kripyakevich, R.I., Collection entitled "Voprosy mashinovedeniya i prochnosti v mashinostroyenii" [Problems of Mechanical Engineering and Strength in Machine Building], 1960, VI, No. 5, Izv. AN USSR, Kiev, pages 70-74.

98. Moroz, L.S., Mingin, T.E., Collection "Metallovedeniye," Sudpromgiz, 1958, No. 2, pages 3-24.

99. Moroz, L.S., Mingin, T.E., Collection "Metallovedeniye," Sudpromgiz, 1959, No. 3, pages 51-57.

100. Bastein, P., Amiot, P., Compt. rend., 1954, 238, No. 23, pages 2238-2239.

101. Yagunova, V.A., Popov, K.V., Collection "Issledovaniya po zharoprochnym splavam" [Studies of High-High-Temperature-Strength Alloys]. Izd. AN SSSR, 1962, No. VIII, pages 199-202.

102. Boniszewski, I., Smith, G.C., Acta Metall., 1963, 11, No. 3, pages 165-178.

103. Zappfe, C.A., Sims, C., Trans. Am. Inst. Min. (Metall) Engrs., 1941, 149, page 225.

104. Zappfe, C.A., Metal Prog., 1951, 60, No. 21.

105. Besnard, S., Ann. chem., 1961, 6, page 245.

106. Sleeswyk, A.W., Acta Metall., 1958, 6, page 598.

107. Talbot-Besnard, S., Acta Metall., 1963, No. 12, pages 1373-1375.

108. De Kacinczy, F., Acta Metall., 1959, 7, page 706.

109. Van Ooijen, D.J., Fast, J.D., Acta Metall., 1963, page 211.

110. De Kacinczy, F., Jernkantor Ann., 1956, 140, page 347.

111. De Kacinczy, F., J. Iron Steel Inst., 1964, 177, page 85.

112. Garofalo, F., Chou, Y.T., Ambegaokas, V., Acta Metall., 1960, 8, No. 8, pages 504-512.

113. Petch, N.J., Phil. Mag., 1936, 21-22, page 331.

114. Zwicker, U., J. Less-Common Metals, 1959, 1(3), pages 165-184.

115. Hill, M.L., Johnson, E.W., Trans. Am. Inst. Min. (Metall.) Engr., 1959, 215, page 717.

116. Popov, K.V., Yagunova, V.A., FMM, 1959, 8, No. 2, pages 187-192.

117. Bast'yen, P., Amio, P., IV Mezhdunarodnyy neftyanoy kongress [Fourth International Petroleum Congress]. Gostoptekhizdat, 1956, Vol. VIII, pages 124-136.

118. Plusquellec, J., Bastein, P., Azou, P., 6-e colloq. metallurg., Relations entre défauts échelle atom et propertiétes macroscopiques [Sixth Metallurgical Congress; Relations Between Atomic-Scale Defects and Macroscopic Properties], Saslay, 1962, pages 119-128.

119. Cadoff, J.B., Winter, J., U.S. Govt. Res. Repts., 1961, 35, No. 4, page 460.

120. Pugh, Trans. Am. Inst. Min. (Metall.) Engrs., 1957, 209, page 1243.

121. Sklyuyev, P.V., Kvator, L.I., Shapiro, V.Ye., Stal', 1956, No. 10, pages 809-915.

122. Rebinder, P.A., VI s"yezd russkikh fizikov [Sixth Congress of Russian Physicists]. Gosizdat, 1928, pages 28-30.

123. Rebinder, P.A., Yubileynyy sbornik AN SSSR, posvyashchennyy 30-letiyu Velikoy Oktyabr'skoy sotsialisticheskoy revolyutsii [Anniversary Collection of the Academy of Sciences USSR Devoted to the 30th Anniversary of the Great October Socialist Revolution], AN SSSR, Moscow-Leningrad, 1947, page 553.

124. Likhtman, V.I., Shchukin, Ye.D., UFN, 1958, 66, page 213.

125. Rostoker, U., Mak-Kogi, D., Markus, G., Khrupkost' pod deystviyem zhidkikh metallov [Brittleness Under the Action of Liquid Metals]. IL, 1962.

126. Greenfield, P., Smith, C.C., Taylor, A.M., Trans. Am. Inst. Min. (Metall.) Engrs., 1961, 221, No. 5, pages 1065-1073.

127. Petch, N.H., Stables, P., Nature, 1952, 169, pages 842-843.

128. Morlet, J.G., Johnson, H.H., Troiano, A.R., J. Iron and Steel Inst., 1958, 5, pages 37-44.

129. Shorshorov, M.Kh., Nazarov, G.V., Belov, V.V., Collection "Titan i yego splavy" [Titanium and its Alloys], No. X, Issledovaniye titanovykh splavov [Investigation of Titanium Alloys]. Izv. AN SSSR, 1963, pages 284-292.

130. Savitskiy, V.G., Popov, K.V., Izvestiya Sib. otd. AN SSSR, 1960, No. 8, pages 138-143.

131. Moroz, L.S., Mingin, T.E., Metallovedeniye i termicheskaya obrabotka metallov, 1962, No. 4, pages 2-6.

132. Shorshorov, M.Kh., Izv. AN SSSR, OTN, 1962, No. 4, page 521.

133. Shurakov, S.S., Collection "Metallovedeniye" [Physical Metallurgy]. Sudpromgiz, 1957, page 100.

134. Makarova, A.M., Avtomaticheskaya svarka, 1960, No. 2, page 9.

135. Prokhorov, N.N., Tekhnologicheskaya prochnost' metallov pri svarke [Technological Strength of Metals in Welding]. Profizdat, 1960.

136. Ells, C.E., Evans, W., Trans. Am. Inst. Min. (Metall.) Engrs., 1963, 222, No. 4, pages 438-442.

137. Mikhaylov, A.S., Krylov, B.S., Metallovedeniye i termicheskaya obrabotka metallov, 1962, No. 4, pages 48-54.

138. Mikhaylov, A.S., Krylov, B.S., Titan i yego splavy [Titanium and its Alloys], No. X, Issledovaniye titanovykh splavov [Investigation of Titanium Alloys]. Izd. AN SSSR, 1963, pages 144-150.

139. Kotfila, R.I., Erbin, E.F., Metal. Prog., 1954, 66(4), page 128.

140. Popov, L.Ye., Butkevich, L.M., Kozhemyakin, V.Ye., Aleksandrov, N.A., FMM, 1963, 16, No. 3, pages 457-462.

141. Nikiforov, G.D., Makhortova, A.G., Svarochnoye proizvodstvo, 1961, No. 3, pages 5-9.

142. Nikiforov, G.D., Silant'yeva, S.A., Kainova, G.Ye., Svarochnoye proizvodstvo, 1963, No. 1, pages 26-29.

143. Nikiforov, G.D., Silant'yeva, S.A., Svarochnoye proizvodstvo, 1962, No. 12, pages 1-5.

144. Cottrell, C.L.M., J. Iron and Steel Inst., 1953, 174,

pages 17-24.

145. Cottrell, C.L.M., J. Iron and Steel Inst., 1954, 176, page 213.

146. Cottrell, C.L.M., Brit. Weld. J., 1954, 1, No. 4, page 177.

147. Cottrell, C.L.M., Bradstreet, N., Brit. Weld. J., 1954, 1, No. 7, page 322.

148. Darvin, G.E., Buddery, J.H., Beryllium, London, 1960.

149. Berilliy i yego splavy [Beryllium and its Alloys]. Collection of papers edited by A.M. Bochvar and A.I. Trapeznikov. GONTI, 1931.

150. Cotterill, P., Goosey, R.E., Martin, A.J., Metallurgy of Beryllium, London, 1963, pages 220-236.

151. Harris, J.E., Partridge, P.G., Eeles, W.T., Rickards, G.K., J. Nucl. Mater., 1963, 9, No. 3, pages 339-347.

152. Rich, J.B., Redding, G.B., Barnes, R.S., J. Nucl. Mater., 1959, 1, No. 1, page 96.

153. Ells, J.B., Perryman, J., Nucl. Mater., 1959, 1, No. 1, page 73.

154. Slavinskiy, M.P., Fiziko-khimicheskiye svoystva elementov [Physicochemical Properties of the Elements]. Metallurgizdat, 1952.

155. Ells, C.E., Trans. Canad. Inst. of Mining and Metallurgy, 1960, 63, page 609.

156. Barnes, R.S., Redding, G.B., Cottrell, A.H., Phil. Mag., 1958, 3, No. 25, page 97.

157. Ells, C.E., J. Nucl. Mater., 5, 1962, page 147.

158. Sauerwald, Z. anorg. Chem., 1949, 258, No. 1-2, page 26.

159. Wood, R.A., Williams, D.N., Ogden, H.R., Defense Metals Inform. Center Memorandum, 1961, No. 124, 19 pages.

160. Magniy i yego splavy [Magnesium and its Alloys]. Collected papers, Oborongiz, 1941.

161. Cochran, C.N., J. Electrochem. Soc., 1961, 108, No. 4, pages 317-321.

162. Röntgen, R., Braun, H., Metallwirt., 1932, 11, page 471.

163. Röntgen, R., Möller, F., Metallwirt., 1934, 13, page 81.

164. Bircumchau, L., Trans. Faraday Soc., 1935, 31, page 1439.

165. Winterhager, H., Alum. arch., 1939, 12.

166. Baukloh, W., Redjali, Metallwirt., 1942, 21, No. 45-46, pages 683-688.

167. Ransley, C.E., Neufeld, H., J. Inst. Metals, 1948, 74, pages 599-617.

168. Dardel, Y., Trans. Met. Soc. AIME, 1949, 180, page 273.

169. Hofmann, W., Maatsch, J., Z. Metallkunde, 1956, 47, page 89.

170. Spasskiy, A.G., Lovtsov, D.P., Sb. trudov MITsMiZ [Collected Transactions of Moscow Institute of Nonferrous Metallurgy named for Z-], 1955, No. 5, pages 381-388.

171. Lovtsov, D.P., Liteynoye proizvodstvo, 1955, No. 12, pages 18-20.

172. Ivanov, V.P., Spasskiy, A.G., Liteynoye proizvodstvo, 1963, No. 1, pages 26-28.

173. Smallman, R.E., Williamson, G.K., Ardley, G., Acta Metall., 1953, 1, No. 2, page 126.

174. Foster, L.M., Gillespie, A.S., Jack, T.H., Hill, W.W., Nucleonics, 1963, 21, No. 4, pages 53-55.

175. Frolov, V.V., Svarochnoye proizvodstvo 1960, No. 9, pages 1-5.

176. Nikiforov, G.D., Makhortova, A.G., Svarochnoye proizvodstvo, 1961, No. 4, pages 6-10.

177. Day, J.H., J. Nucl. Mater., 1964, 11, No. 2, pages 249-251.

178. Harris, J.E., Partridge, P.G., J. Inst. Metals, 1964-1965, page 93.

179. Roginskaya, Ye.V., Uspekhi khimii, 1952, 21, No. 1, page 3.

180. Mannchen, W., Bornkessel, K., Z. Metallkunde, 1963, page 422.

181. Koeneman, J., Metcalfe, A.G., Trans. Am. Soc. Metals, 1959, 51, pages 1072-1081.

182. Winterhager, H., Aluminium archiv., 1938, 12, page 7.

183. Voronov, S.M., Gazy v alyuminiyevykh splavakh i metody degazatsii rasplava [Gases in Aluminum Alloys and Methods of Degasifying the Melt]. NKAP, 1938.

184. Sharov, M.V., Collection entitled "Legkiye splavy"

[Light Alloys]. Izd. AN SSSR, 1958, No. 1, pages 365-388.

185. Pemsler, J.P., Rapperport, E.J., Trans. Metall. Soc. AIME, 1964, 230, No. 1, pages 90-94.

186. Sharov, M.V., Gudchenko, A.P., Collection "Metallurgicheskiye osnovy lit'ya legkikh splavov" [Metallurgical Foundations of the Casting of Light Alloys]. Oborongiz, 1957, pages 306-340.

187. Gudchenko, A.P., Leont'yev, A.K., Trudy MATI [Transactions of the Moscow Aviation Engineering Institute], No. 49, 1961, pages 137-159.

188. Sharov, M.V., Serebryakov, V.V., Nauchnyye doklady vysshey shkoly, Metallurgiya, 1958, No. 2, page 37.

189. Sharov, M.V., Serebryakov, V.V., Trudy MATI, 1961, No. 49, pages 170-179.

190. Sharov, M.V., Nikishayeva, O.I., Nauchnyye doklady Vysshey shkoly. Metallurgiya, 1959, No. 1, pages 58-62.

191. Sharov, M.V., Nikishayeva, O.N., Trudy MATI, No. 49, 1961, pages 47-72.

192. Stout, W.L. and Gibbons, M.D., J. Appl. Phys., 1955, 26, No. 12, pages 1488-1492.

193. Abb, E.A., Plotnikov, R.I., Khutsishvili, L.Ya., ZhTF, 29, No. 8, 1959, pages 1146-1151.

194. Gulbransen, E.A., Andrew, K.F., J. Metals, I, 1949, No. 10, pages 741-749.

195. Livanov, V.A., Bukhanova, A.A., Kolachev, B.A., Nauchnyye doklady vysshey shkoly. Metallurgiya, 1958, No. 4, pages 248-254.

196. Schleicher, H.W., Zwicker, U., Z. Metallkunde, 1956, 47, No. 8, pages 570-576.

197. McQuillan, A.D., Proc. Roy. Soc., 1950, A204, No. 1078, page 302.

198. Livanov, V.A., Bukhanova, A.A., Kolachev, B.A., Trudy MATI, 1962, No. 55, pages 90-96.

199. Moroz, L.S., Mingin, T.E., DAN SSSR, 1965, 160, No. 2, pages 311-313.

200. Glebov, G.D., Pogloshcheniye gazov aktivnymi metallami [Absorption of Gases by Active Metals]. Gosenergoizdat, 1961.

201. Livanov, V.A., Bukhanova, A.A., Kolachev, B.A., Trudy

MATI, No. 43, 1960, pages 91-99.

202. McQuillan, A.D., Proc. Roy. Soc., 1950, A204, pages 309-323.

203. McQuillan, A.D., J. Inst. Metals, 1950, 78(3), page 249.

204. McQuillan, A.D., J. Inst. Metals, 1951, 79(5), page 371.

205. Elechenauer, W., Mem. Sci. Rev. Met., 1960, 57, page 943.

206. Koster, W., Bangert, L., Evers, M., Z. Metallkunde, 1956, 47, No. 8, pages 564-570.

207. McQuillan, A.D., Metallurgia of Titanium, N.Y., 1956.

208. Sidhu, S.S., Heaton, L., Zauberis, D.D., Acta Crystall., 1956, 9, page 607.

209. Yakimova, A.M., FMM, 1961, 12, No. 6.

210. Waag, R.M., Shipko, F.J., J. Am. Chem. Soc., 1956, 78, No. 20, pages 5155-5159.

211. Ransley, C.E., J. Inst. Metals, 1939, 65, page 147.

212. Sof'ina, V.V., Azarkh, Z.M., Orlova, N.I., Kristallografiya, 1958, 3, page 539.

213. Jaffe, L.D., J. Metals, 1956, 8, No. 7, 861. Trans. Met. Soc., AIME, 1956, 206, page 861.

214. Jakel, H.L., Acta Crystall., 1958, 11, pages 46-51.

215. Chechulin, B.B., Syshchikov, V.I., Collection Metallovedeniye [Physical Metallurgy]. Sudpromgiz, 1957, pages 196-205.

216. Berger, L.W., Titanium Abstract Bulletin, 1958, No. 11, page 503.

217. Daley, D.M.J., Hartbower, C.E., Welding J., 1956, 35, No. 9.

218. Gurevich, S.M., Avtomaticheskaya svarka, 1957, No. 1, pages 8-13.

219. Blackburn, P.E., Gulbranzen, E.A., J. Electrochem. Soc., 1960, 107, No. 12, pages 944-949.

220. Shorshorov, M.Kh., Nazarov, G.V., Svarka titana i yego splavov [Welding of Titanium and its Alloys]. Mashgiz, 1959.

221. Barrett, J.C., Lane, G.R., Huber, R.W., Welding J., 1953, 32, No. 6, pages 283s-291s.

222. Guseva, Ye.A., Svarochnoye proizvodstvo, 1958, No. 2, pages 10-14.

223. Voldrich, C.B., Welding J., 1953, 32, No. 6, pages 497-515.

224. Meredith, H.L., Handova, C.M., Welding J., 1955, 34, No. 7, pages 657-672.

225. Mikhaylov, A.S., Krylov, B.S., Metallovedeniye i termicheskaya obrabotka metallov [Physical Metallurgy and Heat Treatment of Metals], 1962, No. 4, pages 48-53.

226. Shorshorov, M.Kh., Nazarov, G.V., Collection "Titan i yego splavy," Issledovaniye titanovykh splavov ["Titanium and its Alloys," Investigation of Titanium Alloys], No. VII, Metallokhimiya i novyye splavy [Metallochemistry and New Alloys], AN SSSR, pages 226-238.

227. Shorshorov, M.Kh., Nazarov, G.V., Collection "Titan i yego splavy" [Titanium and its Alloys], No. X, Issledovaniye titanovykh splavov [Investigation of Titanium Alloys], AN SSSR, 1963, pages 278-283.

228. Yakimova, A.M., Collection "Titan i yego splavy." Issledovaniye titanovykh splavov [Titanium and its Alloys. Investigation of Titanium Alloys], No. VII, Metallokhimiya i novyye splavy [Metallochemistry and New Alloys], AN SSSR, 1962, pages 166-172.

229. Moroz, L.S., Khesin, Yu.V., Mingin, T.E., Chernetsov, V.I., Collection "Metallovedeniye" [Physical Metallurgy], Sudpromgiz, 1957, page 175.

230. Livanov, V.A., Bukhanova, A.A., Kolachev, B.A., Neverova-Skobeleva, N.P., Slavina, I.I., Sheynin, B.Ye., Shcherbina, L.V., Izvestiya vuzov, Tsvetnaya metallurgiya, 1964, No. 4, pages 124-130.

231. Kolachev, B.A., Livanov, V.A., Bukhanova, A.A., Metallovedeniye titana [Physical Metallurgy of Titanium]. Nauka, 1964, pages 88-94.

232. Borisova, Ye.A., Collection "Titan i yego splavy" [Titanium and its Alloys], 1960, No. III, AN SSSR, page 23.

233. Livanov, V.A., Bukhanova, A.A., Kolachev, B.A., Trudy MATI, 1961, No. 50, pages 82-92.

234. Lenning, G.A., Spretnak, J.W., Jaffee, R.I., J. Metals, 1956, II, Vol. 8, No. 10, pages 1235-1240.

235. Hempel, M., Hilenhagen, E., Arch. Eisenhüttenwesen, 1962, 33, No. 8, pages 567-581.

236. Berger, Z.W., Williams, D.N., Jaffee, R.I., Trans. Met. Soc. AIME, 1958, 212, No. 4, page 509.

237. Livanov, V.A., Bukhanova, A.A., Kolachev, V.A., Trudy MATI, 1961, No. 50, pages 83-103.

238. Livanov, V.A., Bukhanova, A.A., Kolachev, B.A., Trudy MATI, No. 43, 1960, pages 100-105.

239. Livanov, V.A., Bukhanova, A.A., Kolachev, B.A., Trudy MATI, 1961, No. 50, pages 52-61.

240. Haynes, R., J. Inst. Metals, 1961, 90, No. 3, pages 80-84.

241. Williams, D.N., Jaffee, R.I., J. Less-Common Metals, 1960, No. 1, pages 42-48.

242. Rubel, H., Debray, N., Rösler, H., Nucleonik, 1964, 6, No. 4, pages 159-168.

243. Kolachev, B.A., Livanov, V.V., Bukhanova, A.A., Gusel'-nikov, N.Ya., Izvestiya vuzov, Tsvetnaya metall., 1965, No. 2, 131-135.

244. McQuillan, A.D., J. Inst. Metals, 1941, 79(2), page 73.

245. McQuillan, A.D., J. Inst. Metals, 1952, 80(7), page 363.

246. Huber, C.Y., Gates, J.E., Young, A.P., Robereskin, M., J. Metals, 1957, 9, No. 7, (11), pages 918-923.

247. Blok, N.I., Glazova, A.M., Lashko, N.F., Yakimova, A.M., Izv. AN SSSR, OTN, 1958, No. 12, pages 96-99.

248. Kornilov, I.I., Glazunov, S.G., Yakimova, A.M., FMM, 1959, 8, No. 3, pages 370-378.

249. Yakimova, A.M., Collection "Titan v promyshlennosti" [Titanium in Industry]. Oborongiz, 1961, pages 131-134.

250. Blok, N.I., Glazova, A.M., Yakimova, A.M., Lashko, N.F., Collection "Titan v promyshlennosti" [Titanium in Industry]. Oborongiz, 1961, pages 135-141.

251. Livanov, B.A., Bukhanova, A.A., Kolachev, B.A., Gusel'-nikov, N.Ya., Collection "Titan i yego splavy" [Titanium and its Alloys]. Izd. AN SSSR, 1963, No. X, pages 307-316.

252. Jaffee, R.I., Lenning, G.A., Craighead, C.M., J. Metals, 1956, 8 (11), pages 907-913.

253. Moroz, L.S., Khesin, Yu.D., Collection "Nekotoryye problemy prochnosti tverdogo tela" [Certain Problems in the Strength of Solids]. Izd. AN SSSR, pages 140-151.

254. Burte, H.M., Erbin, E.F., Hahn, G.T., Seeger, J.W., Kotfila, R.J., Wruck, D.A., Metal Prog., 1955, 67(5), page 115.

255. Ripling, E.I., J. Metals, 1956, 8(5), pages 502-503.

256. Glazunov, S.G., Kornilov, I.I., Yakimova, A.M., Izv. AN SSSR, OTN, 1958, No. 9, pages 17-24.

257. Burte, H.M., Trans. Soc. Rheology, 1957, pages 119-151.

258. Jaffee, R.I., Lenning, G.A., Craighead, C.M., J. Metals, 1956, 8, No. 8 (11), pages 923-928.

259. Lenning, G.A., Berger, J.W., Jaffee, R.I., Fourth Summary Report and Contract, N.Y., 1955.

260. Jaffee, R.I., Williams, D.N., Trans. Am. Soc. Metals, 1959, 60, pages 820-840.

261. Yakimova, A.M., Collection "Titan i yego splavy" [Titanium and its Alloys]. Izd. AN SSSR, 1960, No. 3.

262. Kolachev, B.A., Livanov, V.A., Bukhanova, A.A., Gusel'nikov, N.Ya., Metallovedeniye i termoobrabotka, 1965, No. 5, pages 9-14.

263. Chaston, J.C., J. Inst. Metals, 1945, 71, page 23.

264. Williams, D.N., Schwartzberg, F.K., Jaffee, R.I., Trans. Am. Soc. Metals, 1959, 60, pages 802-804.

265. Blanchard, P.A., Quigg, R.I., Schaller, F.W., Steigerwald, E.A., Troiano, A.R., Wright Air Develop. Corp. Tech. Rep., 1959, pages 59-179.

266. Daniels, R.D., Quigg, R.I., Troiano, A.R., Trans. Am. Soc. Metals, 1959, 60, pages 843-860.

267. Williams, D.N., Jaffee, R.I., Bently, C.A., Metal Prog., 1956, 69, No. 6, pages 57-61.

268. Smith, A.J., Day, M.F., Grimmwade, M.F., Hopkin, L.M.L., J. Inst. Metals, 1960, 89, No. 3, pages 105-110.

269. Livanov, V.A., Bukhanova, A.A., Kolachev, B.A., Trudy MATI, 1961, No. 50, page 71.

270. Kornilov, I.I., Yakimova, A.M., Izv. AN SSSR, OTN, 1962, No. 4, pages 119-125.

271. Ostberg, G., J. Nucl. Mater., 1962, 5, No. 2, pages 208-215.

272. Yakimova, A.M., Metallovedeniye i termicheskaya obrabotka, 1964, No. 6, pages 18-22.

273. Gulyayev, V.N., Izv. AN SSSR, OTN, 1962, No. 6, pages 103-106.

274. Troiano, A.R., Trans. Am. Soc. Metals, 1960, 52, pages 54-80.

275. Williams, D.N., J. Inst. Metals, 1962-1963, 91, pages 147-152.

276. Gudchenko, A.P., Trudy MATI, No. 49, 1961, pages 120-136.

277. Sharov, M.V., Serebryakov, V.V., Nauchnyye doklady Vysshey shkoly, Metallurgiya, 1958, No. 3, page 25.

278. Sharov, M.V., Bibikov, Ye.L., Collection "Issledovaniye splavov tsvetnykh metallov" [Investigation of Alloys of Nonferrous Metals], No. 2, Izd. AN SSSR, 1960, pages 145-164.

279. Klyachko, Yu.A., Zavodskaya laboratoriya, 1937, No. 5, page 572.

280. Klyachko, Yu.A., ZhPKh, 1941, XIV, No 3, page 342.

281. Kolobnev, N.F., Al'tman, M.B., Gazovaya poristost' i metody bor'by s ney v alyuminiyevykh otlivkakh [Gas Porosity and Methods of Countering it in Aluminum Ingots]. Oborongiz, 1947.

282. Al'tman, M.B., Lebedev, A.A., Chukhrov, M.V., Plavka i lit'ye splavov tsvetnykh metallov [Smelting and Casting Nonferrous Alloys]. Metallurgizdat, 1963.

283. Plavka i lit'ye tsvetnykh metallov i splavov [Smelting and Casting Nonferrous Metals and Alloys], edited by A.D. Merfi. Metallurgizdat, 1959.

284. Livanov, V.A., Alekseyeva, T.V., Luzhnikov, L.P., Metallurg, 1939, No. 12, page 44.

285. Radin, A.Ya., Trudy pervoy konferentsii po teorii liteynykh protsessov [Transactions of the First Conference on the Theory of Foundry Processes]. Izd. AN SSSR, 1958, page 237.

286. Sharov, M.V., Bibikov, Ye.L., Nauchnyye doklady Vysshey shkoly, Metallurgiya, 1958, No. 4, page 101.

287. Sharov, M.V., Oding, M.F., Trudy MATI, No. 11, 1951, pages 19-58.

288. Kammer, P.A., Randall, M.D., Monroe, R.E., Groth, W.G., Weld. J., 1963, 42, No. 10, pages 433-441.

289. Kolachev, B.A., Livanov, V.A., Bukhanova, A.A., Gusel'nikov, N.Ya., Izvestiya vuzov, Tsvetnaya metall., 1965, No. 3, 131-135.

290. Kolachev, B.A., Livanov, V.A., Gusel'nikov, N.Ya., Bukhanova, A.A., Collection "Titan i yego splavy," Metallovedeniye titana [Titanium and its Alloys. Physical Metallurgy of Titanium]. Izd. AN SSSR, 1965.

291. Whithham, D., Mém. sci. rev. met., 1960, 57, No. 1, pages 2-15.

292. Ells, C.E., McQuillan, A.D., J. Inst. Metals, 1956-1957, 85, pages 85-89.

293. Vaughan, D.A., Bridge, J.R., J. Metals, 1956, 8 (11), No. 5, page 528.

294. Sof'ina, V.V., Azarkh, Z.M., Orlova, N.N., Kristallografiya, 1958, 3, No. 5, page 539.

295. Edwards, R.K., Levesgue, P., Cubicciotti, D., J. Am. Chem. Soc., 1955, 77, No. 5, pages 1307-1312.

296. Mattsson, E., Schückher, F., J. Inst. Metals, 1958-1959, 87, No. 8, pages 241-247.

297. Gulbransen, E.A., Andrew, K.F., Trans. Met. Soc. AIME, 1955, 203, page 136.

298. Schwartz, C.M., Mallett, M.W., Trans. Am. Soc. Metals, 1954, 46, page 640.

299. Jung-König, W., Richter, H., Zwicker, U., Metall, 1963, 17, No. 1, pages 1-7.

300. Douglas, T.B., J. Am. Chem. Soc., 1958, 80, No. 19, pages 5040-5046.

301. Kuczynski, G.C., Acta Metall., 1956, 4, page 58.

302. Espagno, L., Azou, P., Bastein, P., Compt. rend., 1959, 248, pages 2003-2005.

303. Gulbransen, E.A., Andrew, K.F., Trans. Amer. Inst. Min. (Metall.) Engrs., 1949, 185, pages 515-525.

304. Bruk, B.I., Nikolayev, G.I., DAN SSSR, 1957, 116, No. 1, 78-80.

305. Ormont, B.F., Struktura neorganicheskikh veshchestv [Structure of Inorganic Substances]. Gosteoretizdat, 1950.

306. Sieverts, A., Gotta, A., Z. anorg. chem., 1930, 187, page 155.

307. Greenwood, G.W., Boltax, J. Nucl. Mater., 1962, 5, page 134.

308. Martin, S.L., Rees, A.L.G., Trans. Faraday Soc., 1954, 50, pages 343-352.

309. Kreg, E.I., ZhPKh, 1937, 10, No. 10-11, page 1931.

310. Hall, M.N., Martin, S.L. and Rees, A.L.G., Trans. Fara-

day Soc., 1945, 41, page 306.

311. Langeron, I.P., Lehr, P., Rev. Metall., 1958, 60, page 901.

312. Kunz, F.W., Bibb, A.E., Trans. Amer. Inst. Min. (Met.) Engrs., 1960, 218, pages 133-135.

313. Westlake, D.G., Fischer, E.S., Trans. Amer. Inst. Min. (Metall.) Engrs., 1962, 224, page 254.

314. Bailey, J.E., Acta Metall., 1963, 11, pages 267-280.

315. Krenz, F.H., Biefer, G.J., Graham, N.A., Proceedings of 2nd International Conference on the Peaceful Use of Atomic Energy, N.Y., Vol. 5, 1958.

316. Glatter, J., Proceedings of 2nd International Conference on the Peaceful Use of Atomic Energy, Vol. 5, N.Y., 1958.

317. Wanklyn, J.N., Hobkinson, B.E., J. Appl. Chem., 1958, 8, page 572.

318. Kufstad, P.W.E., Wallace, A., Hydöne, J. Amer. Chem. Soc., 1925, 81, pages 5015-5019.

319. Khotkevich, V.I., Dun, D.L., Trudy fizicheskogo otdeleniya fiz. mat. f-ta Khar'kovskogo universiteta [Transactions of the Physical Division of the Physicomathematical Department of Khar'kov University], 1952, 3, page 87.

320. Kass, S., Kirk, W.W., Trans. Am. Soc. Metals, 1962, 55.

321. Lubowitz, G.G., J. Nucl. Mater., 1962, 5, No. 2, pages 228-233.

322. Beck, R.L., Trans. Am. Soc. Metals, 1962, 55, No. 1, pages 542-554.

323. Madzh, U.L., Collection "Tsirkoniy" [Zirconium]. IL, 1955, page 59.

324. Kalish, H.S., Materials and Methods, 1953, 37, No. 2, page 101; No. 5, page 174.

325. Muerlenkamp, G.T., Schwope, A.D., J. Inst. Metals, 1954, 82, page 600.

326. Forscher, F., J. Metals, 8, 1956, No. 5, page 536.

327. Young, A.P., Schwarz, C.M., Trans. Met. Soc. AIME, 1958, pages 309-310.

328. Borkov, N.V., Collection "Metallurgiya i metallovedeniye chistykh metallov" [Metallurgy and Physical Metallurgy of Pure Metals]. Gosatomizdat, 1951, No. 3, pages 46-63.

329. Sieverts, A., Moritz, H., Anorg. Allgem. chem., 1941, 247, page 124.

330. Smith, D.P., Eastwood, L.W., Gases in Metals, Cleveland, Ohio, 1953.

331. Albrecht, W.M., Mallet, M.N., Goode, W.D., J. Electrochem. Soc., 1958, 105, 4, pages 219-223.

332. Gulbransen, E.A., Andrew, K.K., J. Metals, 1956, 8, page 586.

333. Samsonov, G.V., Umanskiy, Ya.S., Tverdyye soyedineniya tugoplavkikh metallov [Solid [or Hard - Transl.] Compounds of High-Melting Metals]. Metallurgizdat, 1960.

334. Coy, H.E.M., Douglas, D.A., Columbium Metallurgy, Metall. Soc. Conferences, 1960, Vol. 10, pages 85-117.

335. Komjathy, S., J. Less-Common Metals, 1960, 2, pages 466-480.

336. Hahn, G.T., Gilbert, A., Jaffee, R.I., The Effect of Solutes on the Ductile-to-Brittle Transition in Refractory Metals, N.Y., 1962.

337. Hagen, H., Sieverts, A., Z. Anorg. Chem., 1930, 185, No. 3, page 230.

338. Albrecht, W.M., Goode, W.D., Mallet, M.W., J. Electrochem. Soc., 1959, 106, No. 11, page 981.

339. Brauer, G., Herman, R., Z. anorg. Chem., 1953, No. 274, pages 11-23.

340. Horn, F., Zieger, W., J. Am. Chem. Soc., 1947, 69, page 186.

341. Miller, Tantalum and Niobium, Metallurgy of the Rare Metals, No. 6, London, 1959.

342. Eustice, A.C., Carlson, O.N., Trans. Am. Soc. Metals, 1961, 53, page 501.

343. Ingram, A.G., Holden, F.C., Ogden, H.R., Jaffee, R.I., Trans. Am. Inst. Min. Metall. Engrs., 1961, 221, page 517.

344. Tzhebyatovskiy, V. and Stalinskiy, B., Byulleten' Pol'skoy Akademii nauk, 1953, No. 7, page 317.

345. Metallurgical Soc. Conference, Vol. 10, Columbium Metallurgy, No. 4, 1960.

346. Imgram, A.G., Bartlett, E.S., Ogden, H.R., Trans. Am. Inst. Min. (Metall.) Engrs., 1963, 227, pages 132-138.

347. Wilcox, B.A., Brisbane, A.B., Klinger, R.I., Trans. Am. Soc. Metals, 1962, 55, 179, pages 579-592.

348. Roberts, B.W., Rogers, H.C., J. Metals, 1956, 8, page 1213.

349. Nielson, O., Z. Erbergbau und Metallhüttenwesen, 1960, 13, No. 8, pages 381-387.

350. Hutting, G.T., Broadkorb, F., Z. anorg. chem., 1925, 144, pages 341-348.

351. Sieverts, A., Gotta, A., Z. Electrochem., 1926, 32, pages 105-109.

352. Martin, E., Metals and Alloys, 1929, 1, pages 831-835.

353. Loomis, B.A., Carlson, O.N., Reactive Metals, N.Y., London, 1959, pages 227-242.

354. Wessel, E.T., France, L.L., Begly, R.T., AIME Columbium Metallurgy Symposium, N.Y., 1960.

355. Wilcox, B.A., Huggins, R.A., J. Less-Common Metals, 1960, 2, No. 2-4, pages 292-303.

356. Cottrell, A.H., Phil. Mag., 1953, 44, page 829.

357. Kirschfeld, L., Sieverts, A., Z. Elektrochem. Soc., 1930, 36, pages 123-129.

358. Hagg, G., Z. phys. chem., 1931, 433, No. 11, page 454.

359. Nechay, Ye.P., Popov, K.V., FMM, 1962, 14, No. 2, pages 271-274.

360. Sieverts, A., Gotta, A., Z. anorg. Chem., 1928, 172, No. 1-3, pages 1-31.

361. Kofstad, P., Wallace, W.E., J. Am. Chem. Soc., 1959, 81, pages 5019-5022.

362. Rostoker, U., Metallurgiya vanadiya [The Metallurgy of Vanadium]. IL, 1959.

363. Katz, J.J., Rabinowitch, F., The Chemistry of Uranium, N.Y., 1951.

364. Mallett, M.W., Trzeciak, M.J., Trans. Am. Soc. Metals, 1958, 50, pages 981-989.

365. Blanchard, R., Bochirol, L., 5-e Colloque metallurg. Gaz dans métaux [5th Metallurgical Colloquium. Gases in Metals], Paris, 1962, pages 157-162.

366. Nechay, Ye.P., Popov, K.V., Issledovaniye staley i splavov [Investigation of Steels and Alloys]. Nauka,

1964, pages 227-229.

367. Korotkov, V.G., Rafinirovaniye liteynykh alyuminiyevykh splavov [Refining of Cast Aluminum Alloys]. Mashgiz, 1963.

368. Hickman, B.S., Chute, J. Austral. Inst. Metals, 1963, 8, No. 3, pages 298-307.

369. Ells, C.E., Evans, W., Trans. Am. Soc. Metals, 1962, 55, No. 1, pages 744-748.

370. Opie, W., Grant, N., Foundry, 1950, 78, No. 10, pages 104-109.

371. Shcherbakova, A.A., ZhPKh, 1956, 29, No. 6, pages 879-884.

372. Davis, W.D., Trans. Am. Soc. Metals, 1958, 50, pages 991-992.

373. Eastwood, L.W., Gases in Light Alloys, London, 1946.

374. Sharov, M.V., Morozov, B.S., Pletenev, V.M., Liteynoye proizvodstvo, 1953, No. 6, pages 16-19.

375. Mulford, R.N., Ellinger, F.N., Zacharaisen, W.H., J. Am. Chem. Soc., 1954, 76, No. 1, pages 297-300.

376. Hampel, C.A., Corrosion, 1958, 14, No. 12, page 557.

377. Bishop, C.R., Stern, M., J. Metals, 1961, No. 2, pages 144-145.

378. Clauss, A., Forestier, H., Compt. rend., 1958, 246, No. 23, pages 3241-3242.

379. Clauss, A., Compt. rend., 1962, 255, No. 21, pages 2760-2762.

380. Baldwin, W.W., The Metal Molybdenum, ASM, 1957, page 279.

381. Bakish, R., J. Electrochem. Soc., 1958, 105, No. 10, pages 574-576.

382. Owen, W.L., Metallurgia, 1962, 66, No. 393, pages 3-6.

383. O. Dette, J.H., Trans. Am. Inst. Min. (Metall.) Engrs., 1957, 209, page 924.

384. Kostron, H., Z. Metallkunde, 1952, 43, No. 8, pages 268-284; No. 11, pages 373-387.

385. Roberts, Proc. Roy. Soc., 1935, A152, page 445.

386. Langmuir, I., J. Am. Chem. Soc., 1919, 41, page 161.

387. Rengstorff, G.W., Fischer, R.B., J. Metals, 1952, 4, No. 2, page 157.

388. Adaryukov, I.Ye., Pevnyy, N.I., ZhFKh, 1937, 9, No. 4, page 592.

389. Perlmutter, D.D., Dodge, B.F., Industr. and Engineering Chem., 1958, 48, No. 5, page 885.

390. Lawley, A., Liebmann, W., Maddin, R., Acta Metall., 1961, 9, No. 9, pages 841-850.

391. Louthan, M.R., Marshall, R.P., J. Nucl. Mater., 1963, 9, pages 170-184.

392. Chadwick, J. Inst. Metals, 1963, 91, No. 12, pages 414-420.

393. Louthan, M.R., Trans. Am. Inst. Min. (Metall.) Engrs., 1963, No. 10, pages 1166-1170.

394. Armbruster, M.N., J. Am. Chem. Soc., 1943, 65, pages 1043-1054.

395. Popova, O.S., Sanzhirovskiy, A.T., DAN SSSR, 1961, 136, No. 3, pages 654-656.

396. Boniszewski, T., Smith, G.H., J. Phys. Chem. Solids, 1961, 21, page 115.

397. Wilcox, B.A., Trans. Metall. Soc. AIME, 1964, 230, No. 5, pages 1199-1202.

398. Linde, J.A., Borelius, G., Ann. Phys., 1927, 84, pages 777-774.

399. Krieger, F., Gehm, G., Ann. Phys., 1933, 16, pages 174-189.

400. Mito Satoru, J., Japan Inst. Metals, 1961, 25, No. 2, page 101.

401. Kurski Kazimerz, Rudy i metalenierelazne, 1962, 7, No. 2, page 42.

402. Sugeno, T., Kowaka, M., J. Appl. Phys., 1954, 25, No. 8, page 1063.

403. Moroz, L.S., Kolgatin, N.N., Teodorovich, V.P., Deryabina, V.M., FMM, 1963, 16, No. 5, pages 737-742.

404. Benson, N.D., McKeown, J., Mends, D.N., J. Inst. Metals, 1951-1952, 80, No. 3, page 131.

405. Greenwood, J.N., Miller, D.R., Suiter, J.W., Acta Metall., 1954, 2, page 250.

406. Reid, B.J., Greenwood, J.N., Trans. Met. Soc. AIME, 1958, 212, page 503.

407. Engl, J., Heidtkompt, G., Z. Physik, 1935, 95, No. 1-2, pages 30-41.

408. Mater. in Design Engng., 1959, 49, No. 6, pages 142, 144, 146.

409. Nadai, A., Manjoine, M.J., Proc. Am. Soc. Test. Mat., 1960, 40, page 822.

410. Leiris, H. de, Mencarelli, E., Bull. Assoc. techn. maritime et aeronaut, 1963, No. 63, pages 377-?16.

411. Hoffmann, W., Rauls, W., Arch. Eisenhüttenwesen, 1963, 34, No. 12, pages 925-931.

412. Wiester, Hans-Joachim, Dahl, Winfried, Hengstenberg, Helmut, Arch. Eisenhüttenwesen, 1963, 34, No. 12, pages 915-924.

413. Christensen, R.H., Appl. Mater. Res., 1963, 2, No. 4, pages 207-210, 247-248, 250, 252, 254.

414. Marshall, R.P., Acta Metall., 1961, 9, page 958.

415. Butamo, D.G., Tsvetnyye metally, 1964, No. 5, pages 70-74.

416. Bobylev, A.V., Chipizhenko, A.I., Tsvetnyye metally, 1945, No. 3, pages 62-65.

417. Howden, D.G., Milner, D.R., Brit. Weld., 1963, 10, No. 6, pages 304-316.

418. Butera, R.A., Kofstad, P., J. Appl. Phys., 1963, 34, No. 8, pages 2172-2174.

419. Talbot, D.E.J., Granger, D.A., J. Inst. Metals, 1963-1964, 92, No. 9, pages 290-296.

420. Harper, S., Callcut, V.A., Townsend, D.W., Eborall, M.A., J. Inst. Metals, 1961-1962, 90, No. 11, pages 414-422.

421. Harper, S., Callcut, V.A., Towsend, D.M., Eborall, M.A., J. Inst. Metals, 1961-1962, 90, No. 11, pages 423-430.

422. Chechulin, B.B., Bodunova, M.B., Metallovedeniye titana [Physical Metallurgy of Titanium]. Nauka, 1964, pages 196-203.

423. Phillips, J. Inst. Metals Lecture, 1947.

424. Westlake, D.G., Acta Metall., 1964, 12, No. 12, pages 1373-1380.

425. Baker, J., Inst. Metals, 1961-1962, 90.

426. Martin, D.L., Parker, E.R., Trans. Am. Inst. Min. Metall. Engrs., 1943, 152, page 269.

427. Ryabchikov, A.M., Ukr. fiz. zhurn., 1964, 9, No. 3, pages 303-308.

428. Leadbetter, M.J., Argent, B.B., J. Less-Common Metals, 1961, 3, page 19.

429. Sheely, W.F., J. Less-Common Metals, 1962, 4, page 487.

430. McHargue, C.J., McCoy, H.E., Trans. Metall. Soc. AIME, 1963, 227, No. 10, pages 1170-1174.

431. Dunm, B., Zeit. Phys., 1935, 94, page 434.

432. Ubbelohde, A.R., Proc. Roy. Soc., 1937, A159, page 295, page 306.

433. Mott, N.F., Jones, H., Theory of Properties of Metals and Alloys, Oxford, 1936.

434. Worsham, J.E., Wilkinson, M.K., Shull, C.A., J. Phys. Chem. Solids, 1957, 3, page 303.

435. Geller, W., Sun Tak-ho, Arch. Eisenhüttenwesen, 1950, 21, No. 2, page 423.

436. Yesin, O.A., Gel'd, P.V., Uspekhi khimii, 1953, 22, No. 1, page 171.

437. Gel'd, P.V., Ryabov, V.A., FMM, 1957, 5, No. 1, page 191.

438. Kun Chin-pin, Ke Tin-suy, FMM, 1957, 5, No. 1, pages 82-90.

439. Hewitt, J. Spec. Rept. Iron and Steel Inst., 1961, No. 73, pages 83-89.

440. Korol'kov, G.A., Novikov, I.I., Izv. AN SSSR, OTN, 1959, No. 2, pages 19-23.

441. Nekrasov, B.V., Kurs obshchey khimii [Textbook of General Chemistry]. Goskhimizdat, 1952.

442. Brophy, J.H., Rose, R.M., Wulff, J. Less-Common Metals, 1963, 5, No. 1, pages 90-91.

443. Barnes, R.S., J. Nucl. Mater., 1964, 11, No. 2, pages 135-148.

444. Barnes, R.S., Mazey, D.J., Phil. Mag., 1960, 5, page 1247.

445. Gulbransen, E.A., Andrew, K.F., J. Electrochem. Soc., 1954, 101, No. 11, pages 560-566.

446. Erickson, W.H., Hardie, D., J. Nucl. Mater., 1964, 11, No. 3, pages 341-343.

447. Sykes, C., Burton, H.H., Gegg, C.C., J. Iron. Steel Inst., 1947, 156, pages 155-180.

448. Stross, T.M., Tompkins, F.C., J. Chem. Soc., 1956, pages 230-234.

449. Barrer, R.M., Trans. Faraday Soc., 1940, 36, pages 1235-1248.

450. Chang, P.L., Benett, W.D., J. Iron Steel Inst., 1952, 170, pages 205-213.

451. Johnson, E.W., Hill, M.L., Trans. Met. Soc. AIME, 1960, 218, pages 1104-1112.

452. Bryan, M.L., Dodge, B.F., A.I.Ch.E. Journal, 1963, 9, No. 2, pages 223-228.

453. Lovtsov, D.P., Liteynoye proizvodstvo, 1955, No. 9, pages 15-19.

454. Magnusson, A.W., Baldwin, W.M., J. Mech. Phys. Solids, 1957, 5, page 172.

455. Beton, R.H., J. Inst. Metals, 1959, 88, No. 2, 93-95.

456. Fleitman, A.H., Trans. Am. Soc. Metals, 1958, 50, pages 991-992.

457. Weinstein, D., Holtz, F.C., ASM Transactions Quarterly, 1964, 57, No. 1, pages 284-294.

458. Forscher, F., Trans. Am. Inst. Min. (Metall.) Engrs., 1956, 206, 8, pages 536-543.

459. Kofstad, P., Butera, R.A., J. Appl. Phys., 1963, 34, pages 1517-1520.

460. Zanowick, R.L., Wallace, W.E., J. Chem. Phys., 1962, 36, page 2059.

461. Nechay, Ye.P., Vliyaniye vodoroda na sluzhebnyye svoystva stali [Influence of Hydrogen on the Service Properties of Steel]. Irkutsk, 1963, pages 131-139.

462. Tetelman, A.S., Robertson, W.D., Trans. Metall. Soc. AIME, 1962, 224, No. 4, pages 775-783.

463. Kolobnev, I.F., Al'tman, M.B., Gazy v alyuminiyevykh splavakh [Gases in Aluminum Alloys]. Oborongiz, 1948.

464. Belyayev, A.P., Gol'dshteyn, R.M., Tsvetnyye metally, 1956, No. 5, pages 61-63.

465. Presnyakov, A.L., Fizicheskaya priroda anomaliy plastichnosti u metallicheskikh splavov [Physical Nature of Plasticity Anomalies in Metallic Alloys], Alma-Ata, 1963.

466. Sokol'skaya, L.I., Gazy v legkikh metallakh [Gases in Light Metals]. Metallurgizdat, 1959.

467. Lakomskiy, V.I., Kalinyuk, N.N., Avtomaticheskaya svarka, 1963, No. 9, pages 31-35.

468. Maeland, A.J., J. Phys. Chem., 1964, 68, No. 8, 2197-2200.

469. Rogers, H.C., Trans. Metall. Soc. AIME, 1960, 218, No. 3, 498-506.